The Synthesis of Biologically Active Heterocycles: Development of Novel Imaging Agents for the Translocator Protein (18 kDa) and Poly(ADP-Ribose) Polymerase 1

Adele Blair, M.Sci.

A thesis submitted in part fulfilment of the requirements of the degree of Doctor of Philosophy

School of Chemistry

College of Science and Engineering

University *of* Glasgow
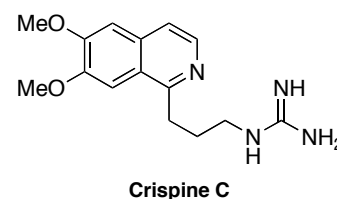
September 2014

Abstract

The Translocator Protein (18 kDa) (TSPO) resides mainly in microglia and is upregulated in response to neuronal injury and inflammation, rendering it an interesting target for imaging focal neuroinflammation in a range of diseases. A library of TSPO ligands based on PK11195 with positions suitable for [^{11}C]-, [^{18}F]- and [^{123}I]-labelling was prepared using three synthetic approaches. Implementation of a physicochemical study enabled selection of compounds most likely to be brain penetrant, and biological evaluation identified those with high binding affinities for the TSPO. From this, a lead candidate (compound **170**) was identified. Radiofluorination and *in vitro* autoradiography revealed the ability of this compound to image tumour tissue in a mouse model of glioblastoma.
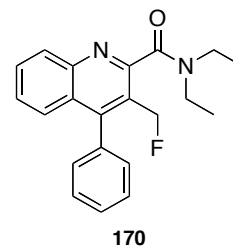
Poly(ADP-ribose) polymerase-1 (PARP-1) is an enzyme involved in the repair of DNA strand breaks, and widely regarded as a therapeutic target for cancer treatment. Many inhibitors of PARP-1 activity exist, *e.g.* olaparib. A programme of research focussing on the preparation of a potential PET imaging agent for measurement of PARP-1 activity, based on olaparib, was initiated. An expeditious seven step synthetic route was used to prepare a small library of compounds. Preliminary cell-free biological screening of these compounds indicated PARP-1 inhibitory potencies in the low nanomolar range demonstrating potential leads for development of a PET imaging agent, *e.g.* compound **223**.
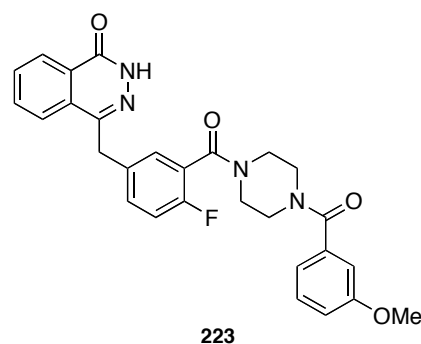
Extracts of *Carduus crispus* linn., traditionally used in Chinese folk medicine, yield a family of isoquinoline alkaloid natural products (Crispine A–E). Upon commencement of this project no reported synthesis of Crispine C existed in the literature. As such, a facile route utilising a key Pictet-Gams modification of the Bischler-Napieralski reaction for isoquinoline core formation was developed, enabling the first total synthesis of Crispine C to be achieved in seven steps and with an overall product yield of 25%.

Table of Contents

Acknowledgements

Author's Declaration

This thesis represents the original work of Adele Blair unless explicitly stated otherwise in the text. The research was carried out at the University *of* Glasgow in the Loudon Laboratory under the supervision of Dr. Andrew Sutherland during the period of October 2010 to September 2013. Portions of the work described herein have been published elsewhere as listed below.

A. Blair, L. Stevenson and A. Sutherland, *Tetrahedron Lett.*, 2012, **53**, 4084.

A. Blair, L. Stevenson, D. Dewar, S. L. Pimlott and A. Sutherland, *Med. Chem. Commun.*, 2013, **4**, 1461.

Abbreviations

Ac	acetyl
ADP	adenosine diphosphate
AIBN	azobisisobutyronitrile
Ala	alanine
aq	aqueous
Ar	aromatic
BBB	blood brain barrier
BDE	bond dissociation energy
BER	base excision repair
Boc	*tert*-butyloxycarbonyl
BOP	(benzotriazol-1-yloxy)tris(dimethylamino)phosphonium hexafluorophosphate
Bn	benzyl
br	broad
Bu	butyl
cat.	catalytic
CBR	central benzodiazepine receptor
Cbz	carboxybenzyl
cDNA	complementary deoxyribonucleic acid
CHI	chromatography hydrophobicity index
Ci	curie(s)
CI	chemical ionisation
CI	confidence interval
CNS	central nervous system
conc.	concentrated
cont.	continued
COSY	correlation spectroscopy
d	doublet
DC	decay corrected
DCE	dichloroethane
d.e.	diastereomeric excess
decomp.	decomposition
DEPT	distortionless enhancement by polarisation transfer

DIAD	diisopropyl azodicarboxylate
DIPEA	*N,N'*-diisopropylethylamine
DMA	*N,N'*-dimethylacetamide
DMAP	4-(dimethylamino)pyridine
DMEN	*N,N*-dimethylethylenediamine
DMF	*N,N'*-dimethylformamide
DMSO	dimethylsulfoxide
DNA	deoxyribonucleic acid
DPM	disintegrations per minute
dppf	(diphenylphosphino)ferrocene
DSB	double strand breaks
EDCI	ethyl 3-(3-dimethylaminopropyl)carbodiimide hydrochloride
e.e.	enantiomeric excess
EI	electron ionisation
EOB	end of bombardment
eq	equivalent(s)
ESI	electrospray ionisation
Et	ethyl
FAB	fast atom bombardment
g	gram(s)
GABA	gamma aminobutyric acid
Gly	glycine
h	hour(s)
HAB	high affinity binders
HBTU	*O*-benzotriazole-*N,N,N',N'*-tetramethyluroniumhexafluorophosphate
HOBt	hydroxybenzotriazole
HPLC	high performance liquid chromatography
HSA	human serum albumin
IAM	immobilised artificial membrane
IC_{50}	half maximal inhibitory concentration
IPA	isopropylalcohol
K_d	dissociation constant
kDa	kilodalton
K_i	inhibition constant
K_m	membrane partition coefficient
K_{222}	Kryptofix® 222

LAB	low affinity binders
lit.	literature
Log*D*	distribution coefficient
Log*P*	partition coefficient
m	multiplet
M	molar
MAB	mixed affinity binders
MBq	megabecquerel(s)
Me	methyl
Met	methionine
mg	milligram(s)
min	minute(s)
mL	millilitre(s)
mm	millimetre(s)
mM	millimolar
mmol	millimole(s)
Ms	methanesulfonyl
MS	molecular sieves
nM	nanomolar
Mp	melting point
MW	molecular weight
N	normal
n	number
NBS	*N*-bromosuccinimide
n.c.a	non-carrier added
nm	nanometer(s)
nM	nanomolar
nmol	nanomole(s)
NMP	*N*-methyl-2-pyrrolidone
NMR	nuclear magnetic resonance
[O]	oxidation
p-	para
PAR	poly(ADP-ribose)
PARP	poly(ADP-ribose) polymerase
PET	positron emission tomography
Petrol.	petroleum

Ph	phenyl
PhC	phosphatidylcholine
Phth	phthalimido
P_m	permeability
pM	picomolar
PPA	polyphosphoric acid
PPB	plasma protein binding
ppm	parts per million
Pr	propyl
q	quartet
QC	quality control
r.t.	room temperature
s	singlet
SAR	structure activity relationship
sec-	secondary
Ser	serine
SD	standard deviation
SM	starting material
SPECT	single photon emission computed tomography
SSB	single strand breaks
t	triplet
TBAB	tetra-*n*-butylammonium bromide
TBHDPB	tributylhexadecylphosphonium bromide
TCO	*trans*-cyclooctene
TFA	trifluoroacetic acid
TfO	triflate
THF	tetrahydrofuran
Thr	threonine
TLC	thin layer chromatography
TMHD	*N,N,N',N'*-tetramethylhexane-1,6-diamine
TMP	2,2,6,6-tetramethylpiperidine
TMS	trimethylsilyl
t_r	retention time
Ts	*para*-toluenesulfonyl
TSPO	Translocator protein (18 kDa)
Tyr	tyrosine

μg	microgram(s)
μL	microlitre(s)
μm	micrometer(s)
μM	micromolar
μmol	micromole(s)
UV	ultraviolet
μW	microwave
w/v	weight per volume

1 Introduction

1.1 Molecular Imaging

A recent definition of molecular imaging states that it is the real time characterisation and measurement of biological processes *in vivo*.[1,2] Nuclear imaging, a technique that falls into the molecular imaging category, provides a visualisation of the *in vivo* distribution of an administered radiotracer *via* external detection of the high-energy photons emitted during radionuclide decay. Adopting this method has enabled a continuously expanding range of molecular and cellular functions in both health and disease states to be studied non-invasively. Two techniques that employ this fundamental basis are single photon emission computed tomography (SPECT) and positron emission tomography (PET).

1.1.1 Single Photon Emission Computed Tomography (SPECT)

SPECT is a nuclear imaging technique that utilises radioisotopes, which decay *via* the emission of γ-radiation. A few of the most commonly employed radionuclides for SPECT imaging are listed in Table 1.[3] These radioisotopes display half-lives ranging from hours to days, and generally emit γ-rays of lower energy (~70 keV to 360 keV) compared to PET radioisotopes.[2]

Radionuclide	Emission route	Photon emission energies (MeV)	Half-life (h)
^{123}I	Electron capture	0.16	13.2
^{99m}Tc	Isomeric transition	0.14	6
^{111}In	Electron capture	0.17/0.25	67.9
^{67}Ga	Electron capture	0.09/0.19/0.30	78.3

Table 1. Radionuclides used for SPECT imaging

Utilising a radiotracer with a longer half-life makes SPECT imaging a more accessible modality, from studying longer biological processes to allowing for a more practical radiosynthesis. However, the compounding factor of this technique becomes apparent when considering the practical process of SPECT image acquisition. A SPECT study is

initiated by a radiotracer administered to the patient, which travels to the site of interest and emits high-energy photons during the decay process. Photon emission is directly detected using a gamma camera which rotates in a 360° revolution around the patient.[4] However, in order to obtain spatial resolution mechanical collimation is required. A lead collimator is positioned in front of the detector allowing only incident photons of defined perpendicular angle to the axis of rotation, and not those of an oblique angle, to pass through.[2] As a result, only 0.01% of signals are received by the detector and the necessary compromise between resolution and efficiency is a disadvantage of SPECT imaging.[3,5] Finally, a sodium iodide crystal within the detector then converts the photons to electrical signals which are used to create a 3D data set and subsequent image.[4]

1.1.2 Positron Emission Tomography (PET)

In contrast to SPECT, PET utilises radiotracers that are labeled with β^+-emitters, and a few of the most commonly employed radioisotopes are listed in Table 2.[3] These radionuclides have a considerably shorter half-life compared to those used for SPECT, and belong to elements more commonly found in nature. Generally, production of these radioisotopes requires an on-site cyclotron, the necessity of which renders PET a more expensive medical imaging technique. Furthermore, the significantly shorter half-life limits study length and applies greater pressure to the required radiosynthesis.

Radionuclide	Emission route	Maximum energy (MeV)	Half-life (min)
^{11}C	β^+	0.97	20.3
^{13}N	β^+	1.20	10
^{15}O	β^+	1.74	2
^{18}F	β^+	0.64	110

Table 2. Radionuclides used for PET imaging

During the decay process a nuclear proton is converted to a neutron, with subsequent emission of a positron and neutrino. This positron travels a short distance within the test object and undergoes annihilation with a surrounding electron to form two photons with energies of 511 keV that are simultaneously emitted at 180° to each other (Figure 1).[1,6] Spatial distribution is determined by acquisition of a large number of decay events and

subsequent image reconstruction.[3] This is referred to as electronic collimation and by removing the need for a lead collimator, it enables the collection of images of a much higher resolution and sensitivity compared to that of SPECT.[2]
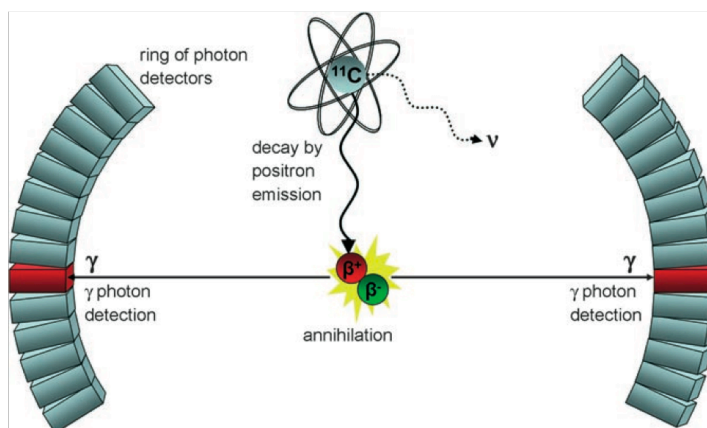
Figure 1. Positron decay and annihilation event[6]

(Reprinted with permission from *Angew. Chem. Int. Ed.*, 2008, **47**, 8998. Copyright 2008 John Wiley and Sons)

1.1.3 Clinical Application of PET and SPECT

An extensive range of diseases has been investigated using PET and SPECT imaging modalities.[7,8] One such example of the clinical utility of PET imaging is use of the radioligand [^{18}F]BAY-94-9172, which binds with high affinity to β-amyloid plaques. These plaques are known to accumulate in the brain of Alzheimer's sufferers and are used as an indicator of the neurodegenerative disease. The radiosynthesis of [^{18}F]BAY-94-9172 is illustrated in Scheme 1.[9] Starting from mesylate precursor **1**, a nucleophilic radiofluorination reaction in the presence of [^{18}F]potassium fluoride and Kryptofix®, followed by *N*-Boc deprotection provided [^{18}F]BAY-94-9172 (**2**) in a decay corrected radiochemical yield of 30%, in a preparation time of 90 minutes.
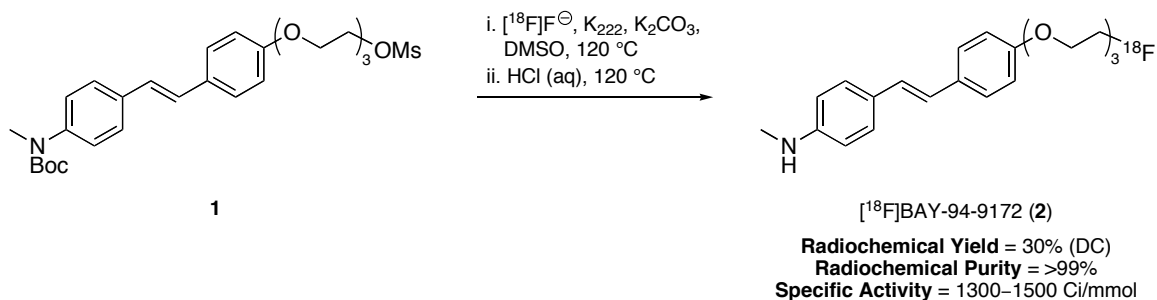
Scheme 1. Radiosynthesis of [^{18}F]BAY-94-9172 (**2**)

Typical PET images obtained through administration of this radioligand are shown in Figure 2.[1] The top row represents brain images obtained from a patient suffering from Alzheimer's disease, and the bottom row are that of a healthy 75 years old control patient. It is apparent that an accumulation of the radiotracer has occurred within the brain of the Alzheimer's patient, and much lower levels of radioactivity are detected in the brain of the control. This radioligand can therefore be used to monitor the development of this disease.
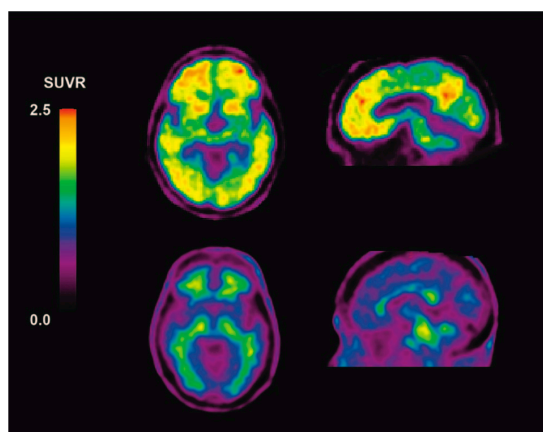
Figure 2. PET images of [^{18}F]BAY 94-9172 binding to β-amyloid plaques in an Alzheimer's disease patient (top row) and healthy control (bottom row)[1]

(Reprinted with permission from *Chem. Rev.*, 2008, **108**, 1501. Copyright 2008 American Chemical Society)

Another clinical application involves the use of SPECT imaging for the diagnosis of Parkinson's disease, a neurodegenerative condition that affects around 1 in 500 people in the UK.[10] Parkinson's disease is routinely diagnosed using [^{123}I]FP-CIT (also commonly known as DATScan™), a SPECT radiotracer with high affinity for presynaptic dopamine transporters. A typical radiosynthesis of this imaging agent is shown in Scheme 2.[11]

Starting from trimethylstannane precursor **3**, an oxidative iododestannylation reaction in the presence of [^{123}I]sodium iodide affords [^{123}I]FP-CIT (**4**) in good radiochemical yield of 64%.

3

[^{123}I]NaI, CH$_3$CO$_3$H

Radiochemical Yield = 64%
Radiochemical Purity = 98%

[^{123}I]FP-CIT (**4**)

Scheme 2. Radiosynthesis of [^{123}I]FP-CIT (**4**)

Once radioiodination has been achieved, the radioligand is administered to the patient and scanning ensues. A striking feature of Parkinson's disease is a reduction in the number of dopamine transporters within the brain, and this change can be observed in images acquired from a SPECT scan. Representative SPECT images obtained from a [^{123}I]FP-CIT scan of a healthy patient (a) versus a Parkinson's disease patient (b) is shown in Figure 3.[3] A comparison of the images highlights that a reduction in radioligand binding, correlating to a reduction in dopamine transporters is evident in the Parkinson's disease patient. This is therefore a powerful tool allowing for diagnosis and, monitoring progression of a disease.

Figure 3. SPECT images of [^{123}I]FP-CIT binding within an (a) normal and (b) Parkinson's disease patient[3]

(Reproduced from Ref. 3 with permission from The Royal Society of Chemistry)

1.2 Translocator Protein (18 kDa)

The Translocator protein (TSPO), formerly known as the peripheral benzodiazepine receptor (PBR), was discovered in 1977 by Braestrup and Squires while investigating

alternative binding sites for the benzodiazepine, diazepam.[12] On discovering that in addition to rat brain membrane, [^{3}H]diazepam bound to mitochondrial fractions from peripheral organs, the peripheral benzodiazepine receptor (PBR) was conceived. This descriptor was coined to differentiate it from the central benzodiazepine receptor (CBR) site on the GABA$_A$ receptor complex within the central nervous system (CNS).[13]

Since its discovery, a great deal of research has gone into characterising the TSPO. Intensive genetic studies have shown that the gene encoding the TSPO, *Bzrp*,[14] is a highly conserved primary coding sequence. The receptor has been cloned from various species, such as rodents and humans,[15,16] and the cDNA encoding this protein has shown to have up to 80% homology across different species.[17] Functional inactivation experiments have shown that an early embryonic lethal phenotype is the result of this type of study and explains this high level of sequence homology conservation.[18] The TSPO is evidently crucial for the development and functioning of an organism.

1.2.1 TSPO Distribution, Structure and Function

Anatomically the TSPO is widely expressed throughout the body and located within the peripheral organs.[19] It is particularly prevalent at higher levels in tissues involved in the synthesis and distribution of steroids.[20] In addition to the peripheral system, the TSPO can also be found in the CNS albeit at a much lower level of expression. Within the CNS, however, expression is not widespread and generally restricted to ependymal and glial cells.[21]

The TSPO is a tryptophan rich protein consisting of 169 amino acids.[17,22] It exists as a multimeric 140–200 kDa complex that exists primarily on the outer mitochondrial membrane (Figure 4).[14] The 18 kDa subunit has five transmembrane domains of α-helical secondary structure, which are connected by highly hydrophobic regions.[22,23] It has been proposed that several TSPO molecules arrange themselves in such a way as to form what has been described as a pore.[24] Protein density increases at contact sites between the inner and outer mitochondrial membrane and has therefore been classed as the mitochondrial permeability transition pore (MPTP).[22] This, coupled with the name of the protein, indicates that its functional role is in the transport of chemicals into the mitochondria. In addition to the 18 kDa subunit several other proteins are also associated with the TSPO at

these contact sites, including a 32 kDa voltage dependent anion channel (VDAC) and a 30 kDa adenine nucleotide translocator (ANT).[14]
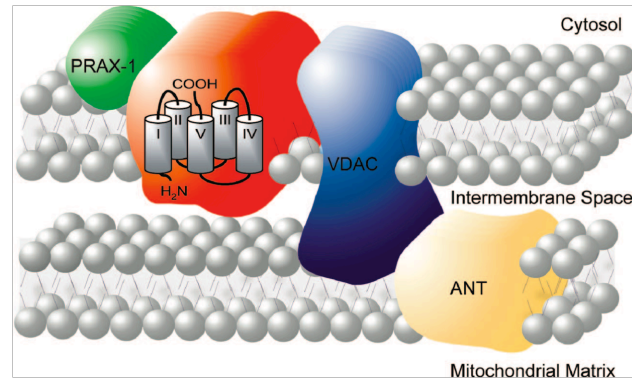
Figure 4. Structure of TSPO[22]

(Reprinted with permission from *J. Med. Chem.*, 2009, **52**, 581. Copyright 2009 American Chemical Society)

Many functions have been attributed to the TSPO, with steroid biosynthesis being the most extensively investigated.[14,18] In addition to steroidogenesis, the TSPO has also been associated with a wide range of cellular processes, *e.g.* oxygen sensing, protein transport, porphyrin transport and heme biosynthesis, ion transport, immunomodulation, cellular respiration and apoptosis.[17,25,26] However, as of yet, conclusive evidence for all proposed roles has not been presented. The role of the TSPO within the CNS is much less clear than that of the peripheral nervous system. One such proposal is that it contributes to three main functions: neurosteroid synthesis, regulation of the mitochondria and modulation of neuroinflammation in microglial cells.[17,27,28]

1.2.2 TSPO in Neuroinflammation

Within the CNS, the TSPO resides in glial cells including astrocytes and microglia.[28] Microglia are mesoderm-derived brain macrophages that represent the first-line of defense of the immune system, which predominantly exist in an inactive form but are activated in response to neuronal injury or inflammation.[28,29] When in this activated form, they undergo a morphological change from a macrophage to a phagocyte eliciting an immunological response.[30] Transformation into a phagocytic form is regarded as a protective role in the immunological response, however, it has also been proposed that activated microglia secrete neurotoxins such as nitric oxide and free radicals initiating a vicious cycle of

neuroinflammation.[31,32] An illustration of microglia activation and its associated processes in a disease state is illustrated in Figure 5.[33]
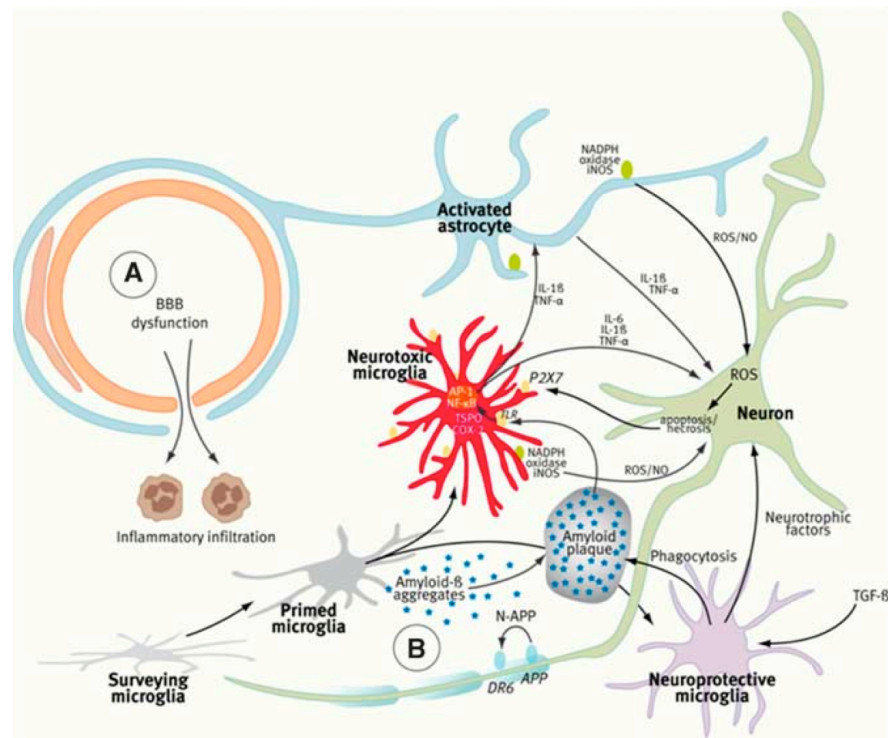
Figure 5. Process of neuroinflammation and the dual role of activated microglia in ischemic stroke and multiple sclerosis (**A**), and neurodegenerative diseases (**B**).[33] β-Amyloid plaques synonymous with Alzheimer's disease activate microglia triggering unselective neuronal death *via* secretion of inflammatory mediators. Conversely, a protective role is also suggested whereby phagocytosis eliminates them.
(Reprinted from A. H. Jacobs and B. Tavitian, *J. Cereb. Blood Flow Metab.*, 2012, **32**, 1393 under a Creative Commons license)

As previously mentioned, the TSPO resides in microglial cells and protein density is negligible in a healthy state. However, when detrimental changes within the CNS occur, there is a marked upregulation in protein expression by means of a mechanism still not fully understood.[28] The implication that the TSPO can be exploited as a sensitive biomarker for microglial activation has rendered it a very attractive diagnostic and therapeutic target for neuronal injury, neuroinflammation and neurodegenerative disorders such as Alzheimer's disease,[34] multiple sclerosis,[35] Parkinson's disease[36] and Creutsfeldt-Jakob disease.[37]

Traditionally, activated microglia are detected postmortem and achieved using histopathological techniques to excise and study diseased tissue of the central nervous system.[28] With recent advances in nuclear medicine and imaging modalities however, *in vivo* visualisation of activated microglia is now possible. The ability to non-invasively detect microglial activation provides a very attractive tool for the diagnosis and progression monitoring of neuroinflammation and diseases of the CNS.

1.2.3 TSPO Ligands and Radiotracers

Several endogenous ligands have been shown to occupy binding sites on the TSPO, *e.g.* cholesterol, porphyrin, heme and endozepines.[23] In addition, a substantial range of synthetic TSPO ligands with potential for PET and SPECT imaging applications have been developed. These compounds can be divided into seven distinct structural classes: benzodiazepines, quinoline carboxamides, indoleacetamides and indolylglyoxylamides, vinca minor alkaloids, oxodihydropurines, imidazopyridines and bioisosteric structures (imidazopyridazines and pyrazolopyrimidines), and phenoxyarylacetamides.[38]

1.2.3.1 Benzodiazepines

In 1950, one of the most widely recognised classes of medicinal agents was discovered, the benzodiazepines (Figure 6). 1,4-Benzodiazepines are prescribed for their antianxiety, anticonvulsant and anaesthetic properties, and it was the discovery that [³H]diazepam bound to peripheral tissue that led to the generation of a series of analogues intended as TSPO ligands. However, it became evident that the slightest of variations in structure affected selectivity, *e.g.* diazepam was equally potent for both the CBR and TSPO, while Ro5-4864 (an atypical benzodiazepine) and clonazepam was selective for the TSPO and CBR, respectively.[13] Despite this, the ability of Ro5-4864 to preferentially bind to the TSPO with high affinity encouraged research groups to investigate its potential as an imaging agent for the protein.
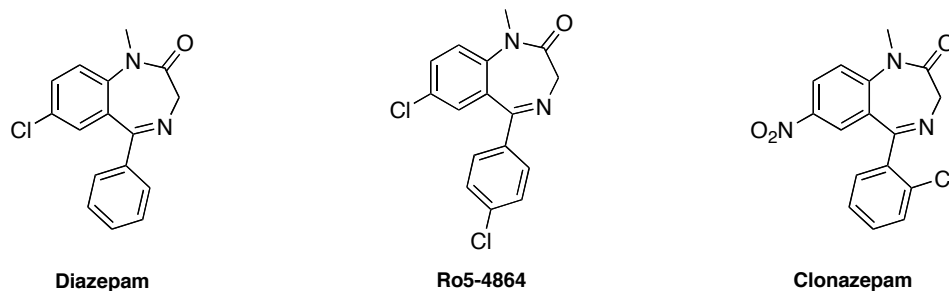
Figure 6. Benzodiazepines

Wieland and co-workers reported the radioiodination of a Ro5-4864 analogue in 1988 (Scheme 3).[39] Treatment of 4-iodoaniline (**5**) with boron trichloride and subsequent condensation with 4-chlorobenzonitrile afforded intermediate ketimine **6**, which was hydrolysed under acidic conditions affording 2-aminobenzophenone **7**. A cyclisation reaction with glycine ethyl ester hydrochloride generated the key 1,4-benzodiazepine core **8**, and a standard *N*-alkylation reaction using methyl iodide provided radiolabelling precursor **9**. Utilising an ammonium sulfate catalysed solid-phase halogen exchange reaction in the presence of [125I]sodium iodide, the synthesis of [125I]Ro5-4864 (**10**) was achieved in isolated radiochemical yields of 18–31% and high radiochemical purity.
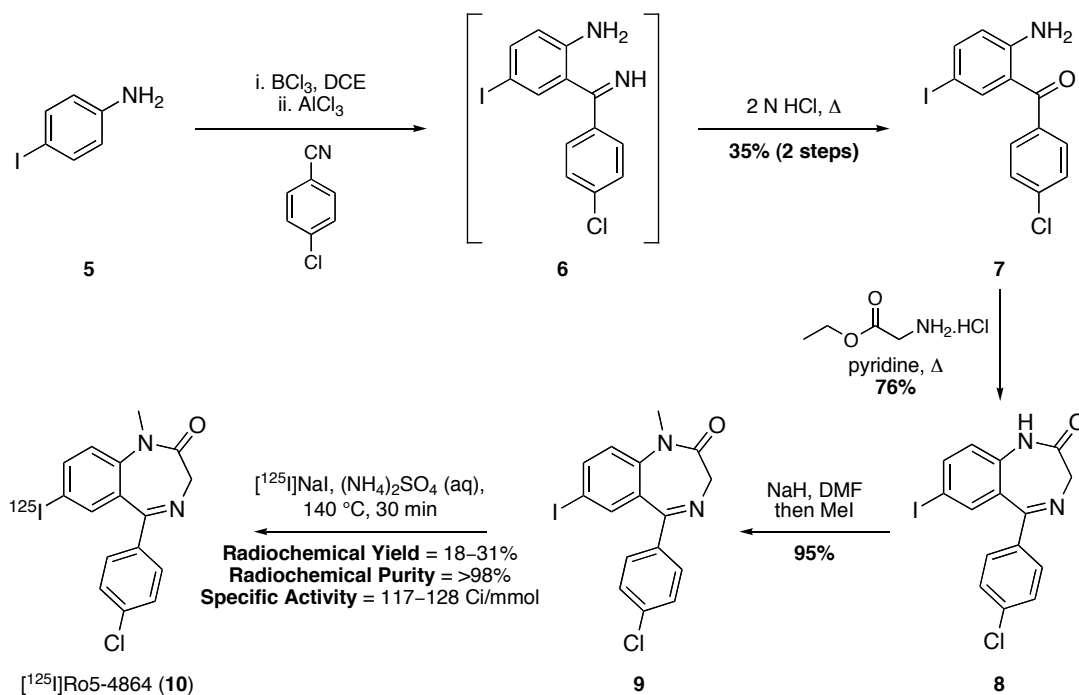
Scheme 3. Radiosynthesis of [125I]Ro5-4864 (**10**)

The [^{125}I]Ro5-4864 analogue was then investigated for its potential to act as a SPECT imaging agent, and results from an *ex vivo* autoradiography study indicated an accumulation of the radiotracer within tumour cells of C6 glioma rats.[39] [^{11}C]-Labelling of the *nor* derivative of Ro5-4864 has also been achieved.[40,41] A study by Young and co-workers utilising [^{11}C]Ro5-4864 concluded that, in contrast to the results of van Dort *et al.*, no accumulation of the radioligand in tumorous tissue of a human glioma model was observed.[41] This discrepancy in binding was subsequently reported by Krueger and co-workers in the same year, with a high binding affinity for the TSPO in rat (K_D = 1–9 nM) measured, but considerably lower affinity in humans (K_D = 54 nM).[15] As this compound requires the presence of additional mitochondrial protein components for binding,[23] and displays both temperature and species dependency,[42] it was naturally rendered an unsuitable imaging agent for the TSPO.

1.2.3.2 Quinoline Carboxamides

In 1984, a new class of TSPO ligand was discovered (Figure 7). The isoquinoline-3-carboxamide PK11195, a pharmacological antagonist named by French company Pharmuka, was the first non-benzodiazepine to be synthesised with high binding affinity (K_i = 9.3 nM) and selectivity for the TSPO.[43] Advantageously, PK11195 did not require the interaction of additional mitrochondrial proteins for binding, nor did it display species variation making it a more suitable ligand compared to the benzodiazepines.[42] Naturally, this led to the generation of large libraries of compounds bearing the key isoquinoline-3-carboxamide core, *e.g.* PK14105, and later potent quinoline-2-carboxamide TSPO ligands were reported, *e.g.* VC195 (K_i = 4.6 nM).[44]

PK11195   **PK14105**   **VC195**
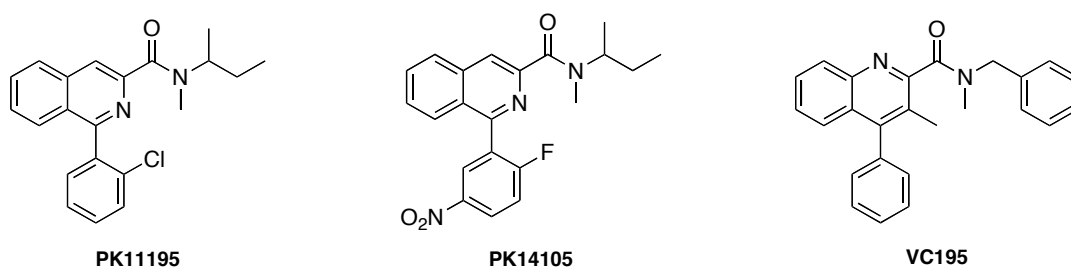
Figure 7. Quinoline carboxamide TSPO ligands

Given that PK11195 has a nanomolar binding affinity with the TSPO, several facile synthetic routes for the preparation of this ligand and its synthetic intermediates have been

published in the literature.[45,46,47] In addition, PK11195 has also been labeled with different radioisotopes, *e.g.* tritium for *in vitro* assays, carbon-11 and fluorine-18 for *in vivo* PET studies, and iodine-123/125 for SPECT studies.

Camsonne *et al.* reported the first radiosynthesis of PK11195 by methylation of the the the *N*-desmethyl precursor using [^{11}C]methyl iodide.[48] In 1986, Charbonneau *et al.* demonstrated that [^{11}C]PK11195 could be used to image TSPO binding sites within the heart and in doing so paved the way for it to be employed as a PET imaging agent.[49]

It is known that enantiomers of a molecule often behave differently in biological systems. Radiolabelling of PK11195 and its use in biological studies are generally performed using the racemate, and in 1994 Shah *et al.* embarked on an investigation to determine the effect each individual enantiomer had on binding with the TSPO.[50] The authors prepared (*S*)-PK11195 and (*R*)-PK11195 according to Scheme 4.[50] Starting from the carboxylic acid of 1-(2-chlorophenyl)isoquinoline-3-carboxylic acid (**11**), reaction with ethyl chloroformate followed by addition of (*S*)- or (*R*)-*sec*-butylamine afforded (*S*)- and (*R*)-**12**, respectively. *N*-Alkylation using [^{11}C]methyl iodide gave (*S*)- and (*R*)-PK11195 (**13**) in decay corrected radiochemical yields of 80%, within a reaction time of approximately 45 minutes. Having synthesised both enantiomers, the authors examined the binding of these compounds within ischaemic-lesioned rat brains. Preliminary results indicated that in healthy animals there was no apparent increase in uptake of one enantiomer over the other, however, in the disease model, a two-fold increase in uptake of the (*R*)-enantiomer was observed. This was particularly so in regions of the brain known to express greater levels of the TSPO, *e.g.* olfactory bulbs. The authors suggest that the slightly improved binding affinity of (*R*)-PK11195 may be due to the *sec*-butylamine group of the stereogenic centre sitting in a more favourable conformation aiding interaction with the protein's lipophilic binding domain.
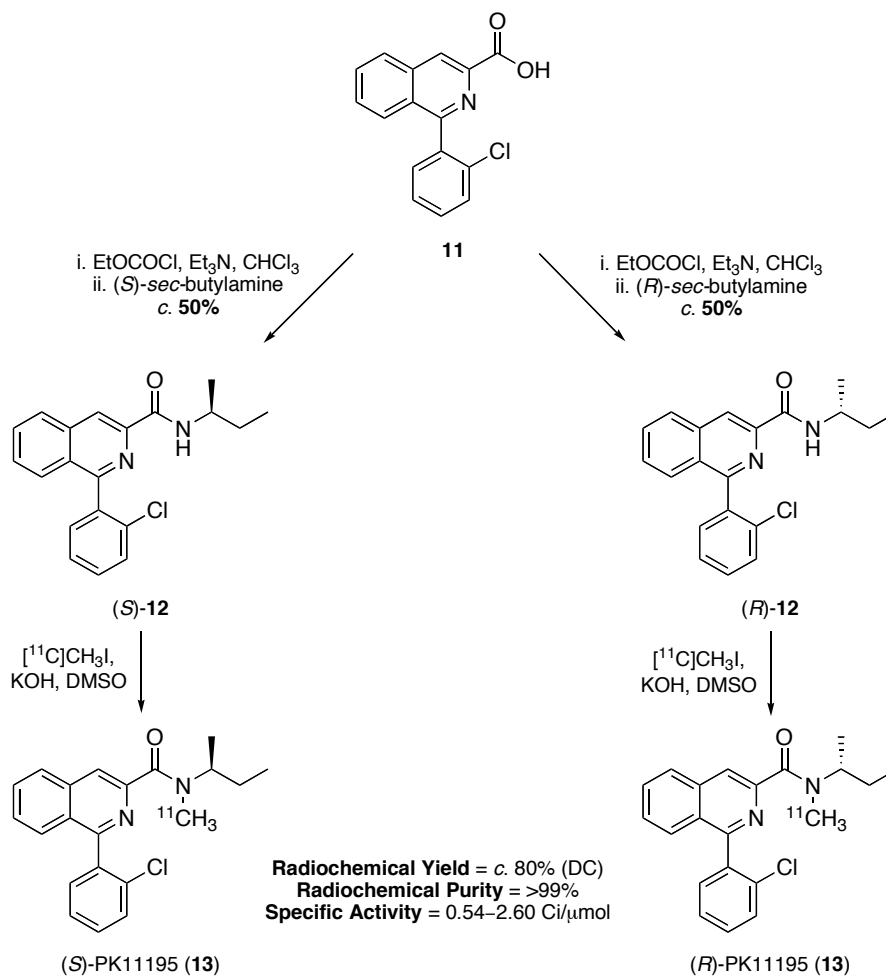
Scheme 4. Radiosynthesis of [^{11}C]PK11195 (**13**) enantiomers

In 2002, Rahman *et al*. reported a [^{11}C]-radiolabelled synthesis of racemic PK11195 and related analogues using [^{11}C]carbon monoxide and 1-(2-chlorophenyl)isoquinolin-3-yl triflate.[51] The authors proposed that radiolabelling the molecule at the carbonyl position using [^{11}C]carbon monoxide would yield a few key advantages over the conventional method of radioisotope incorporation using [^{11}C]methyl iodide. These advantages included, among others, a high specific activity due to reduction in isotopic dilution of the precursor compared to that for the *N*-alkylation method and a reduction in potential radiotracer metabolite interference.

The radiosynthesis of [^{11}C]PK11195 is illustrated in Scheme 5.[51] Starting from 2-chlorobenzophenone (**14**), reductive amination with ammonia gas followed by a sodium cyanoborohydride reduction of the resulting imine gave amine **15**. The amine was reacted with ethyl diethoxyacetate to give amide **16**, which was cyclised in the presence of concentrated sulfuric acid to form the isoquinoline core. The hydroxyl group of the isoquinoline core was then converted to the triflate, affording radiolabelling precursor **17**.

A palladium-mediated carbonylation reaction in the presence of $[^{11}C]$carbon monoxide and *N*-methyl-*sec*-butylamine afforded $[^{11}C]$PK11195 (**13**) in a decay corrected radiochemical yield of 55 ±1%, and an overall synthesis time of 35 minutes.
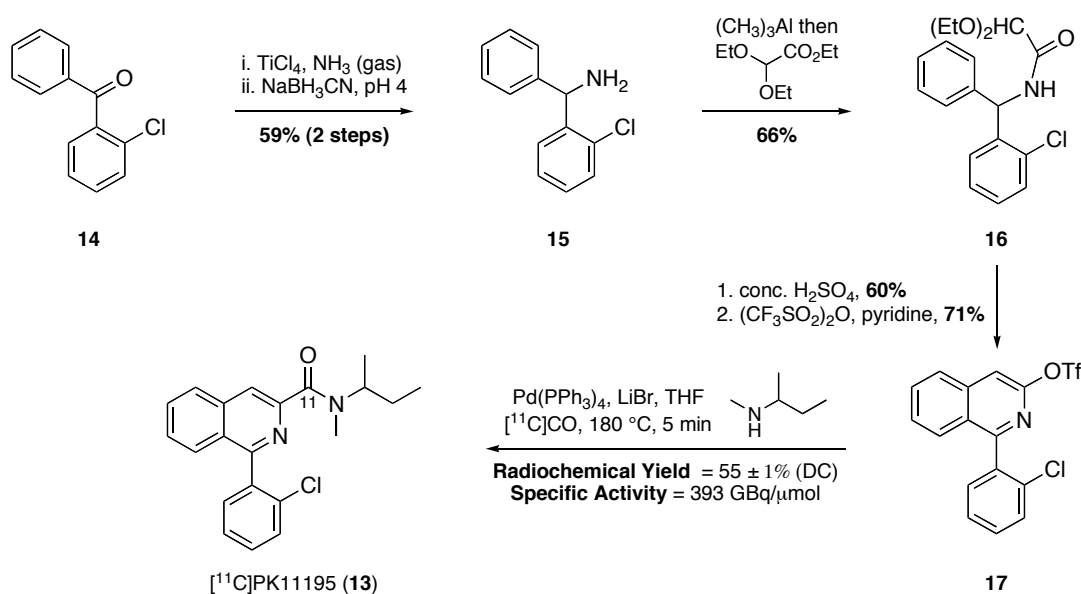
Scheme 5. Radiosynthesis of $[^{11}C]$PK11195 (**13**)

Recently, Pimlott *et al.* reported the synthesis of an $[^{123}I]$-labelled PK11195 analogue (Scheme 6).[52] Synthesis of the bromide precursor utilised for the radiolabelling procedure was described by Stevenson *et al.*[45] A palladium-catalysed coupling reaction of methyl 2-iodobenzoate (**18**) and amidoacrylate (**19**), followed by cyclisation and loss of the acetyl group afforded isoquinoline **20**. Bromination of the hydroxyl group gave **21**, and subsequent Suzuki-Miyaura cross-coupling reaction with 2-bromophenylboronic acid yielded biaryl **22**. Hydrolysis of the methyl ester group to give carboxylic acid **23** was achieved under basic conditions. This intermediate acid was then converted to the acyl chloride *in situ* and coupled with *N-sec*-butylamine affording amide **24**. *N*-alkylation using methyl iodide formed tertiary amide **25**, which was used to prepare the radiolabelling precursor. Trimethylstannane precursor **26** was prepared by a palladium(0)-catalysed procedure utilising hexamethylditin. Radioiodination was achieved by means of an electrophilic iododestannylation reaction in the presence of $[^{123}I]$sodium iodide and chloramine-T as the oxidant. Application of these reaction conditions afforded $[^{123}I]$PK11195 analogue (**27**) in an 83.9 ± 4.1% radiochemical yield, with high specific activity (25.5 ± 7.4 Ci/µmol) and radiochemical purity (>99%). The high isolated

radiochemical yields and high specific activity in particular make this an attractive route for the synthesis of a radioiodinated PK11195 analogue for SPECT imaging of the TSPO.
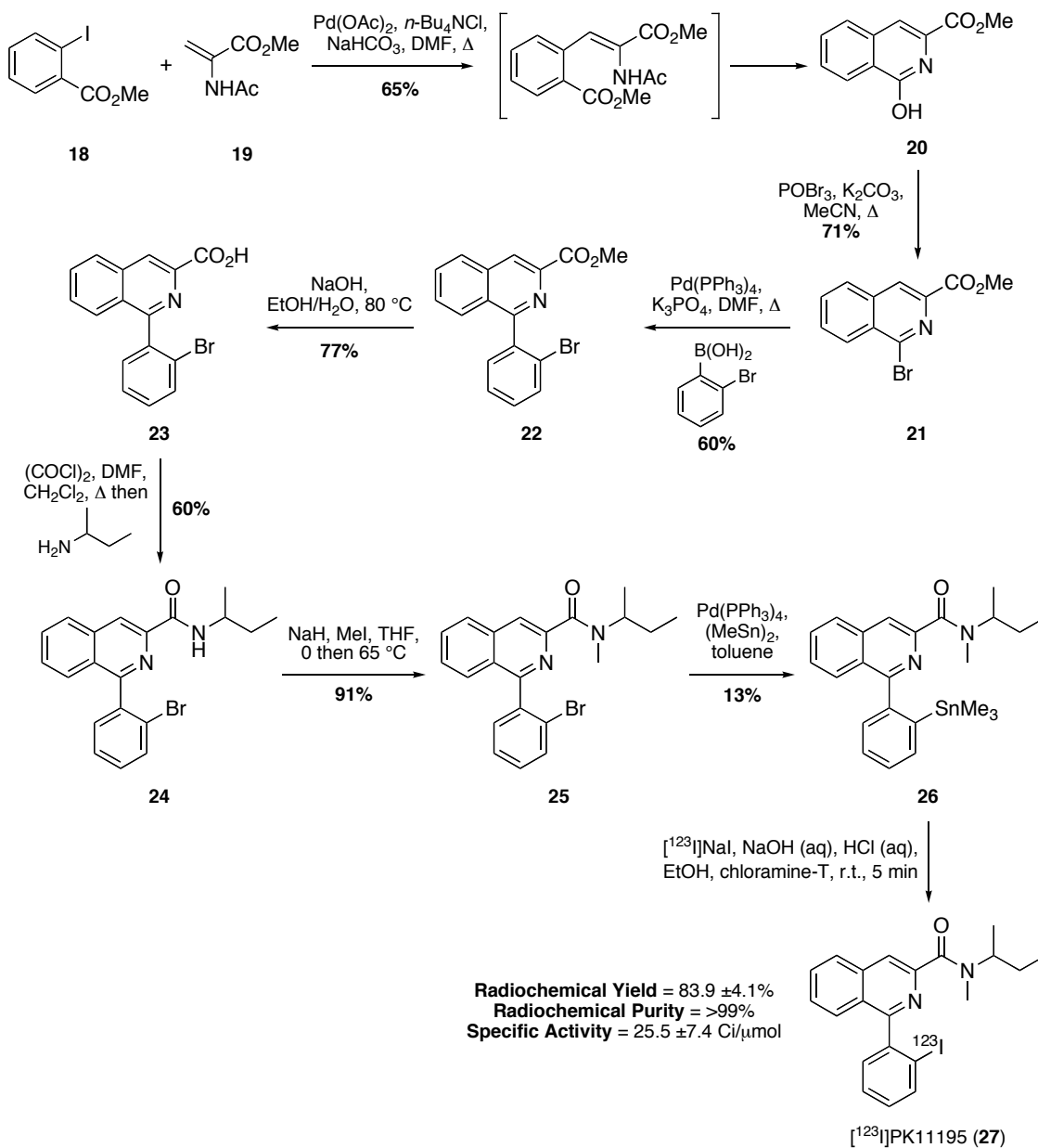
Scheme 6. Radiosynthesis of an [^{123}I]PK11195 analogue **27**

An [^{18}F]-analogue of PK11195 with potential for PET imaging was prepared and tested by Goodman and co-workers (Scheme 7).[53] Coupling of norephedrine hydrochloride (**28**) with benzoyl chloride **29** provided amide **30**. Cyclisation using a modified Pictet-Gams reaction afforded substituted isoquinoline **31**, which was converted to **32** under radical-promoted bromination conditions. The subsequent bromide was then used to prepare aldehyde **33** *via* an oxidative hydrolysis reaction using sodium periodate, which was further oxidised in the presence of silver nitrate to afford carboxylic acid **34**. Coupling of

the acid to methylamine gave secondary amide **35**, which was reacted with 3-triphenylmethoxypropylbromide to give **36**. Removal of the trityl group to give alcohol **37**, followed by treatment with *p*-toluenesulfonyl chloride afforded tosylate radiolabelling precursor **38**. An aliphatic radiofluorination reaction using [¹⁸F]potassium fluoride, Kryptofix® and potassium carbonate gave [¹⁸F]PK11195 analogue **39** in an 8% radiochemical yield (decay corrected) and 99% radiochemical purity. The total reaction time was approximately 90 minutes from end of bombardment.
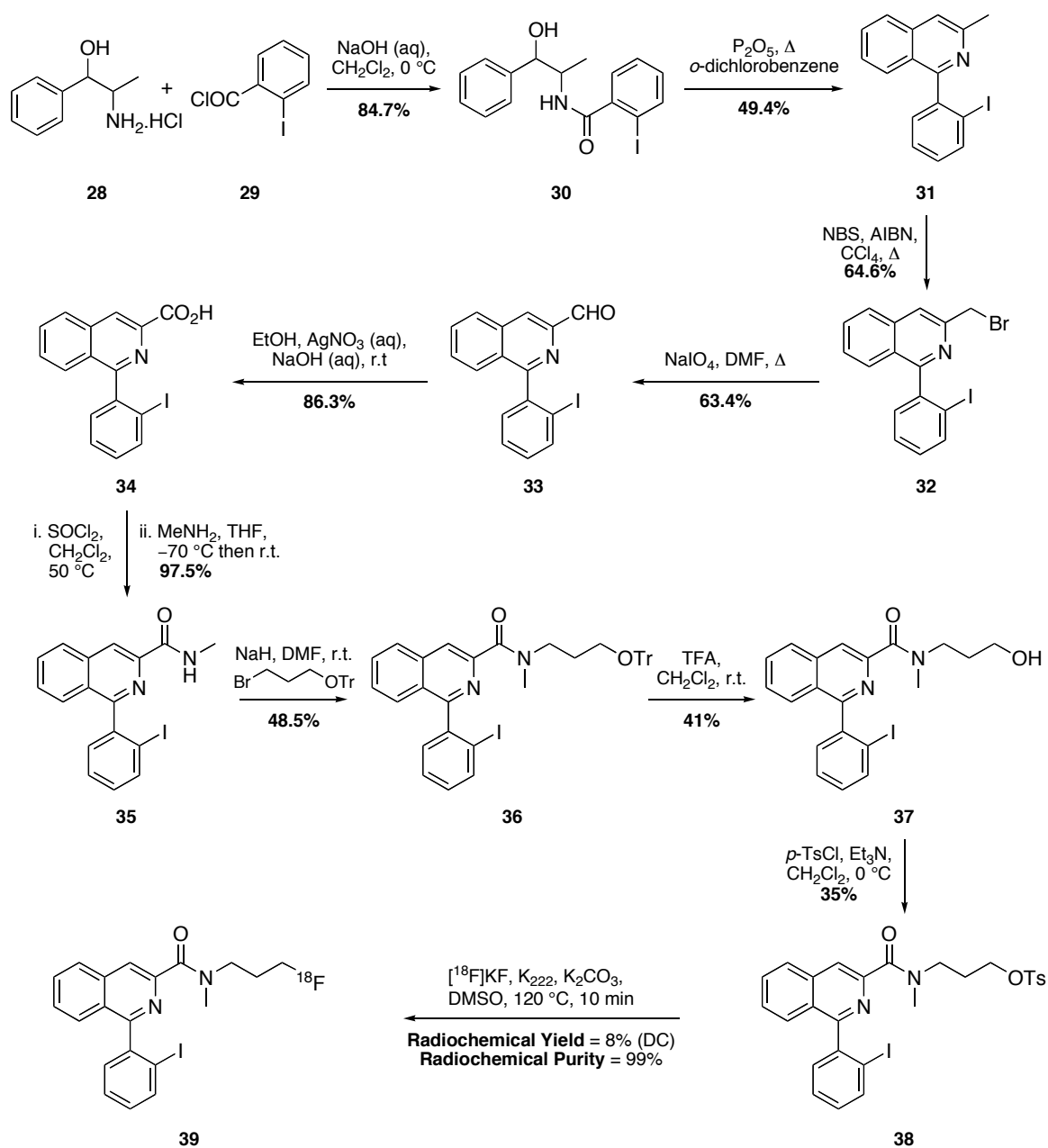
Scheme 7. Radiosynthesis of an [¹⁸F]PK11195 analogue **39**

[^{11}C]PK11195 has been extensively utilised as an imaging agent for the TSPO and a large volume of data focusing on animal models of health and disease is available in the literature. The results of a recent microPET study of [^{11}C]PK11195 binding in rats with temporal focal cerebral ischemia demonstrated an increase in binding potential of the radiotracer within the infarct at day 14, providing further validation of the radiotracer as an *in vivo* marker of activated microglia.[54] In addition, a considerable number of studies have been performed in humans examining its potential as an imaging agent for multiple sclerosis, Alzheimer's disease, ischemic stroke, Parkinson's disease, schizophrenia, and many more diseases.[42]

Despite the vast numbers of TSPO ligands and their radiolabelled versions that continue to be presented to literature, PK11195 is still widely regarded as the 'gold-standard' imaging agent and is routinely used in both research and clinical settings. Regardless of its status however, it does exhibit several undesirable properties making it a less than ideal radiotracer. The high lipophilicity of the compound results in substantial non-specific binding to additional fats and proteins. For example, it has been shown to bind reversibly and with low μM affinity to acute phase1 alpha-1 acid glycoprotein (AGP), a plasma protein found in concentrations of up to 1 mg/mL.[55] This reduces the concentration of free radiotracer available for blood brain barrier (BBB) penetration ultimately leading to poor signal to noise ratio.

1.2.3.3 Indoleacetamides and Indolylglyoxylamides

In the early nineties, Kozikowski and co-workers developed a new class of TSPO ligands that are now commonly referred to as the indoleacetamides.[56] As part of their studies they investigated the effects of varying alkyl chain length, inclusion of a halogen substituent on the phenyl rings, substitution of the indole and replacement of the amide functionality on binding to the TSPO. This intensive study provided FGIN-1-27 (Figure 8) with high binding affinity for the TSPO (K_i = 4.4 nM). Furthermore, it showed no affinity for GABA$_A$ receptors and demonstrated an ability to stimulate pregnenolone synthesis.[13,57,58] Tricyclic indoleacetamides have also demonstrated an affinity for the protein, *e.g.* SSR180575 (Figure 8) has a K_D of 3.0 nM. Similar to the FGIN-1 series this compound appears to have involvement in steroidogenesis.[22,59] However, despite displaying potent *in vitro* binding affinities, the high lipophilicities of these compounds limits their potential for *in vivo* imaging studies targeting activated microglia.
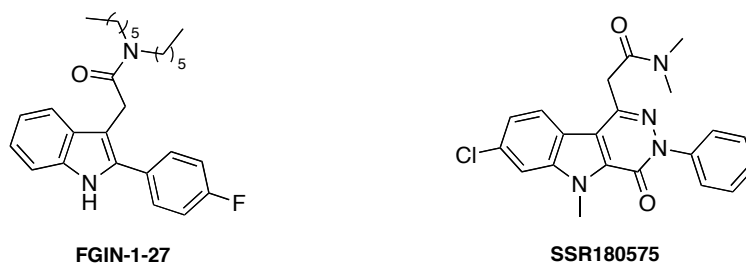
Figure 8. Indoleacetamide TSPO ligands

Analogues exhibiting a more appropriate lipophilicity were prepared by Tamagnan and co-workers in 2006.[60] Based on the indolylglyoxylamide core, the synthetic route depicted in Scheme 8 was used to generate a small library of TSPO ligands. Compound **44** was prepared starting from phenylhydrazine (**40**) and 3-bromoacetophenone (**41**). A Fisher indole synthesis afforded 2-(3'-bromophenyl)indole (**42**) which was converted to the corresponding iodo-compound **43** using a direct halogen exchange reaction. Acylation in the presence of diethylamine then gave compound **44**. A radioligand binding assay with the TSPO showed a binding affinity of 2.6 nM for **44**.
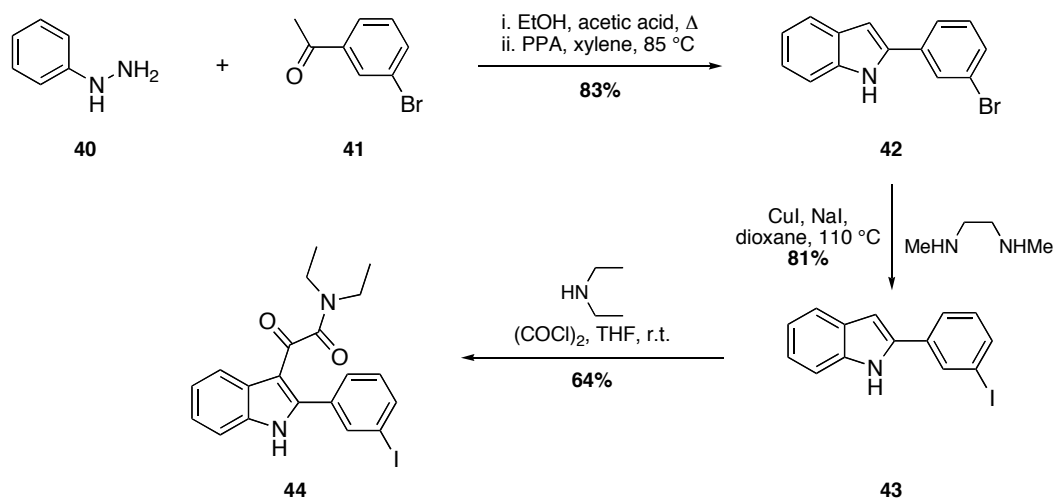
Scheme 8. Synthesis of indolylglyoxylamide TSPO ligand **44**

The Log$D$ value of **44** was measured at 2.18 and is within the acceptable range for successful blood brain barrier penetration, indicating a potential increase in uptake of the compound. In addition, the presence of the *meta*-iodo substituent provides a labeling position for future SPECT studies.

1.2.3.4 Vinca Minor Alkaloids

Vinpocetine (eburanamenine-14-carboxic acid ethyl ester) is a vinca alkaloid presenting neuroprotective properties that has been used for the treatment of acute and chronic stroke patients.[42,61] It is structurally related to the Vinca minor alkaloid, vincamine and has been radiolabelled by Farde and co-workers (Scheme 9).[62] The carboxylic acid group of the labeling precursor, apovincaminic acid (**45**) was subjected to an esterification reaction using [^{11}C]ethyl iodide to give [^{11}C]vincamine (**46**) in a decay corrected radiochemical yield of approximately 20%. Total radiosynthesis time was 30–35 minutes.

apovincaminic acid (**45**)

CH$_3$[^{11}C]CH$_2$I, TMP,
DMF, 100 °C, 10 min

Radiochemical Yield = ~20% (DC)
Specific Activity = 3.7 GBq/μmol (EOS)

[^{11}C]vincamine (**46**)

Scheme 9. Radiosynthesis of [^{11}C]vincamine (**46**)

As a semi-synthetic ligand it has a particularly low binding affinity for the TSPO with an *in vitro* IC$_{50}$ value of 0.2 μM.[61] However, it has been shown to block [^{3}H]PK11195 binding, demonstrating its potential as a TSPO ligand. A drawback of utilising [^{11}C]vinpocetine as an imaging agent for microglial activation is that in addition to occupying TSPO binding sites, it displays a similar binding affinity to other proteins, *e.g.* $\alpha_2\beta$-adrenergic receptors.[42] Despite the disadvantages associated with this radiotracer it has shown some success in a small clinical PET study of Multiple Sclerosis sufferers.[63] Preliminary findings indicated that uptake was greater for (**46**) compared to [^{11}C]PK11195 in all brain regions of interest.

1.2.3.5 Oxodihydropurines

TSPO ligands have also been modeled on purine, one of two nitrogenous bases that constitute the building blocks of nucleic acids. AC-5216 is one such example and offers the therapeutic advantage of TSPO-mediated antianxiety and antidepressant-like effects.[61]

The desmethyl precursor of [^{11}C]AC-5216 was synthesised and labeled according to the procedure illustrated in Scheme 10.[64] An amide coupling reaction between compound **47**

and *N*-ethyl benzylamine in the presence of BOP gave amide **48**. Base hydrolysis of the ethyl ester functionality then afforded carboxylic acid **49**, which was subjected to a Curtius rearrangement in the presence of diphenyl phosphorylazide to prepare the key dihydro-9*H*-purineacetamide core of **50**. Finally, alkylation of the desmethyl precursor using [^{11}C]methyl iodide produced [^{11}C]AC-5216 (**51**) in radiochemical yields of 60 ± 26% (within 15–20 minutes from end of bombardment), and high radiochemical purity (≥98%). Specific activities ranged from 85–130 GBq/μmol.
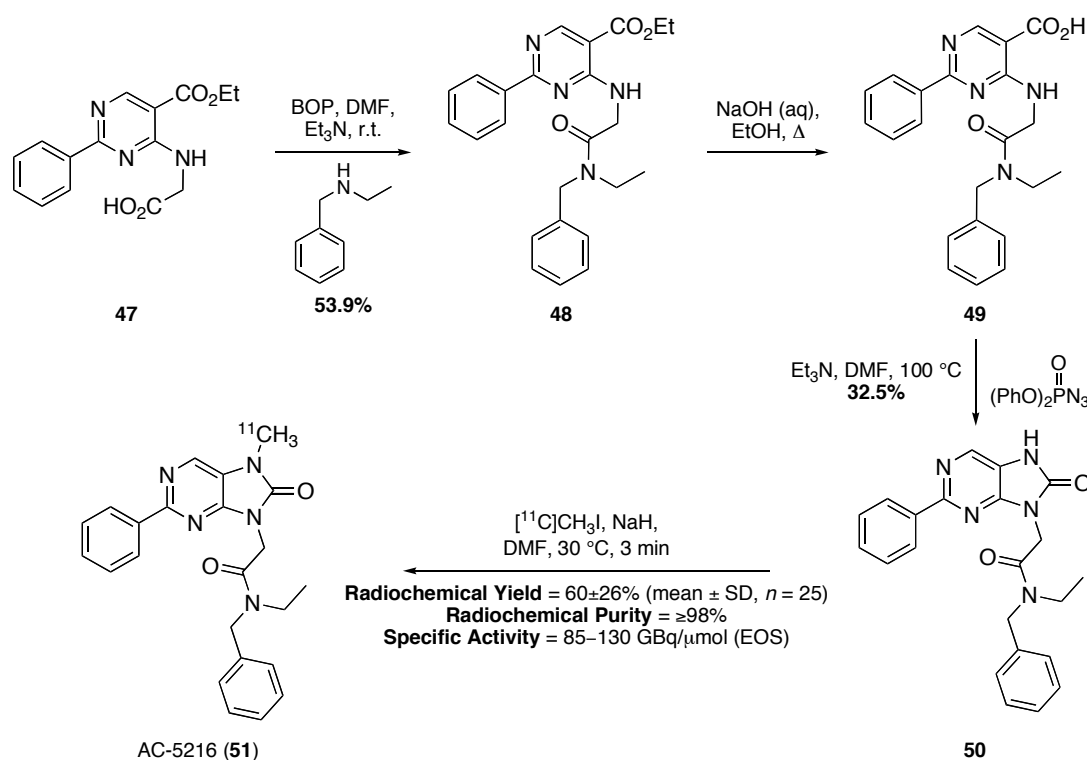
Scheme 10. Radiosynthesis of [^{11}C]AC-5216 (**51**)

This radiotracer has been extensively utilised, and successfully validated for use in PET imaging studies of both healthy and diseased animal models. In 2004, Oka and co-workers demonstrated that [^{11}C]AC-5216 bound with high affinity to rat C6 and human Hs683 glioma derived mitochondrial fractions (IC$_{50}$ 3.04 nM and 2.73 nM, respectively).[64] In addition, an investigation by Yanamoto examining uptake of the radiotracer by kainic acid-lesioned rats concluded that increased radioligand accumulation occurred, and that binding was specific.[65] The authors note that [^{11}C]AC-5216 has potential for imaging neuroinflammation.

1.2.3.6 Imidazopyridines and Bioisosteric Structures

The imidazopyridines and bioisosteric structures (imidazopyridazines and pyrazolopyrimidines) constitutes another class of TSPO ligands, some examples of which, followed by a selected radiosynthesis are illustrated below.

Two examples of compounds representing the imidazopyridine are shown in Figure 9. Alpidem, the first ligand of this structural class of TSPO binders, binds to both the TSPO and CBR with high affinity (K_i = 0.5–0.7 nM and 1–28 nM, respectively), and in addition to stimulating steroid biosynthesis has anxiolytic and anticonvlusant properties.[13,66] The fact that Alpidem presents a binding profile for two different sites led to the synthesis and testing of large compound libraries in search of a more appropriate ligand. CLINME is one such ligand, and has potential for both PET and SPECT applications.[67]
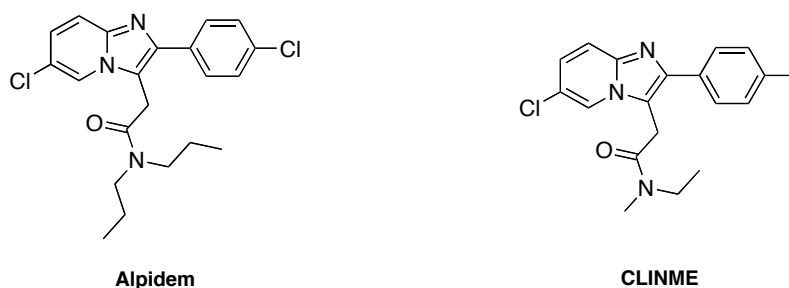
Figure 9. Imidazopyridine TSPO ligands

In 2008, Katsifis and co-workers reported the synthesis of a tosylate precursor and radiofluorination reaction for the preparation of [^{18}F]PBR111, a structural analogue of CLINME with high affinity for the TSPO (Scheme 11).[68] The imidazo[1,2-*a*]pyridine scaffold of **52** was prepared by an initial condensation reaction between 2-amino-5-chloropyridine and 2'-bromo-4-methoxyacetophenone. Treatment of this starting material with dimethylamine and formaldehyde resulted in formation of compound **53** *via* a Mannich condensation. Salt **54** was prepared by quaternisation of the tertiary amine using methyl iodide, which was converted to amide **55** *via* the nitrile intermediate. Demethylation of the methoxy group and amide hydrolysis in the presence of 48% hydrobromic acid afforded carboxylic acid **56**, which was subsequently coupled to diethylamine under standard amide coupling conditions to give compound **57**. Phenol **57** was then alkylated with 3-bromopropylacetate in the presence of the phase transfer catalyst tetrabutylammonium iodide to give phenol ether **58**, which was treated with caesium

carbonate providing alcohol **59**.   Finally, tosylation of the alchohol afforded radiofluorination precursor **60**. Incorporation of the radiolabel was then achieved under standard aliphatic radiofluorination conditions to afford [^{18}F]PBR111 (**61**) in a decay corrected radiochemical yield of 56–75% in 60–90 minutes.
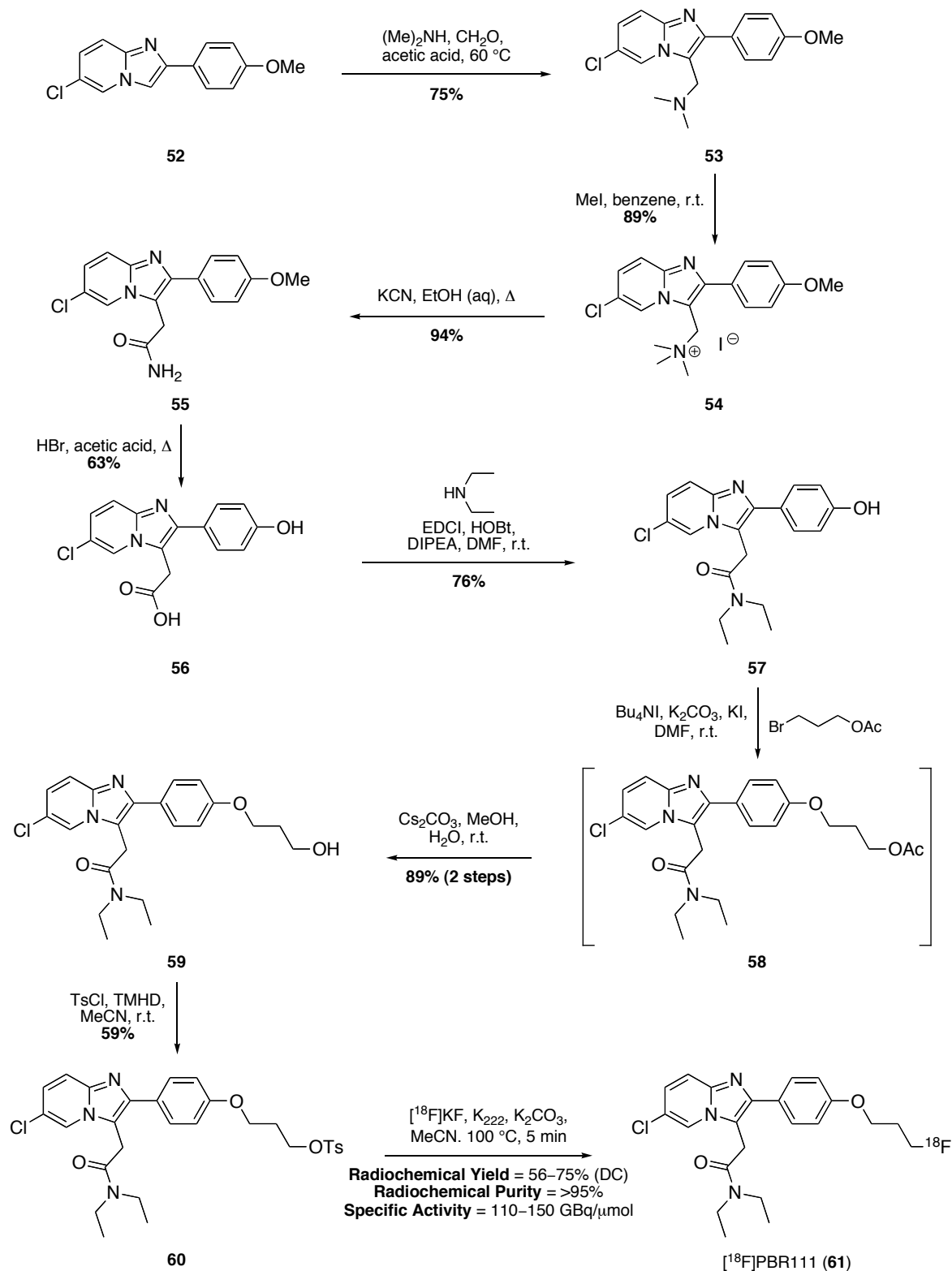
Scheme 11. Radiosynthesis of [^{18}F]PBR111 (**61**)

[^{18}F]PBR111 was then administered to rats and its biodistribution measured. The authors reported an increased uptake within the olfactory bulbs of the brain, which was successfully blocked using PK11195 and Ro5-4864 indicating specific binding with the protein. These results suggest that this radioligand has potential for imaging neuroinflammation.

The 2-arylpyrazolo[1,5-*a*]pyrimidin-3-ylacetamides are a class of compounds displaying high affinity and selectivity for the TSPO (Figure 10). Collectively they are bioisosteres of the imidazopyridines, but unlike Alpidem they exhibit much greater selectivity for the TSPO over the CBR. Initial work on this class of TSPO ligand was performed by Selleri *et al.*, whereby the authors investigated what effect varying the substituent at the 5- and 7-position and the *para*-position of the phenyl ring of **62** had on selectivity and binding affinity with the TSPO.[69] Focusing on the preparation of compounds where R represents a particular combination of H, Me, OMe, F and Cl substituents, DPA-713 was identified as a potent TSPO ligand. This compound has a high binding affinity (K_i = 4.7 nM) and much greater selectivity for the TSPO over CBR. A further study by the authors aimed at probing the size and linearity of the amide side chain generated a library of compounds with even greater potency for the protein.[70] For example, a binding affinity of 0.8 nM was achieved when the *p*-OMe substituent and diethyl amide of DPA-713 was replaced for H and a di-*n*-propyl amide side chain, respectively.
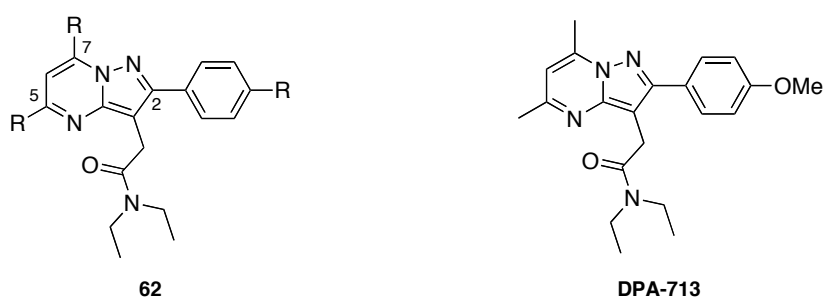
Figure 10. Pyrazolopyrimidine TSPO ligand DPA-713

Kassiou and co-workers have achieved several radiosyntheses of the pyrazolopyrimidine class of compounds, focusing on the preparation of [^{11}C]-labeled analogues through *O*-methylation using [^{11}C]methyl iodide and [^{11}C]methyl triflate independently.[71,72] In addition, a few analogues within this compound class contain a fluorine atom allowing for the genereation of [^{18}F]-labeled PET agents. One particular example is DPA-714, the radiolabelling precursor for which was synthesised as follows (Scheme 12).[71]

Starting from commercially available methyl-4-methoxy benzoate (**63**), reaction with acetonitrile gave aroylacetonitrile **64** which was subsequently reacted with *N,N*-diethylchloroacetamide in the presence of sodium iodide to give 1,4-dione **65**. Pyrazole **66** was then prepared by reaction of the dione with hydrazine hydrate under reflux conditions. A condensation reaction with the electrophilic reagent 2,4-pentadione led to formation of the pyrimidine ring of **67**. It is of interest to note that intermediate **67** is in fact the TSPO ligand DPA-713. Finally, the preparation of a DPA-714 radiolabelling precursor was achieved by demethylation of **68** using 45% hydrobromic acid and tributyl hexadecyl phosphonium bromide (TBHDPB).
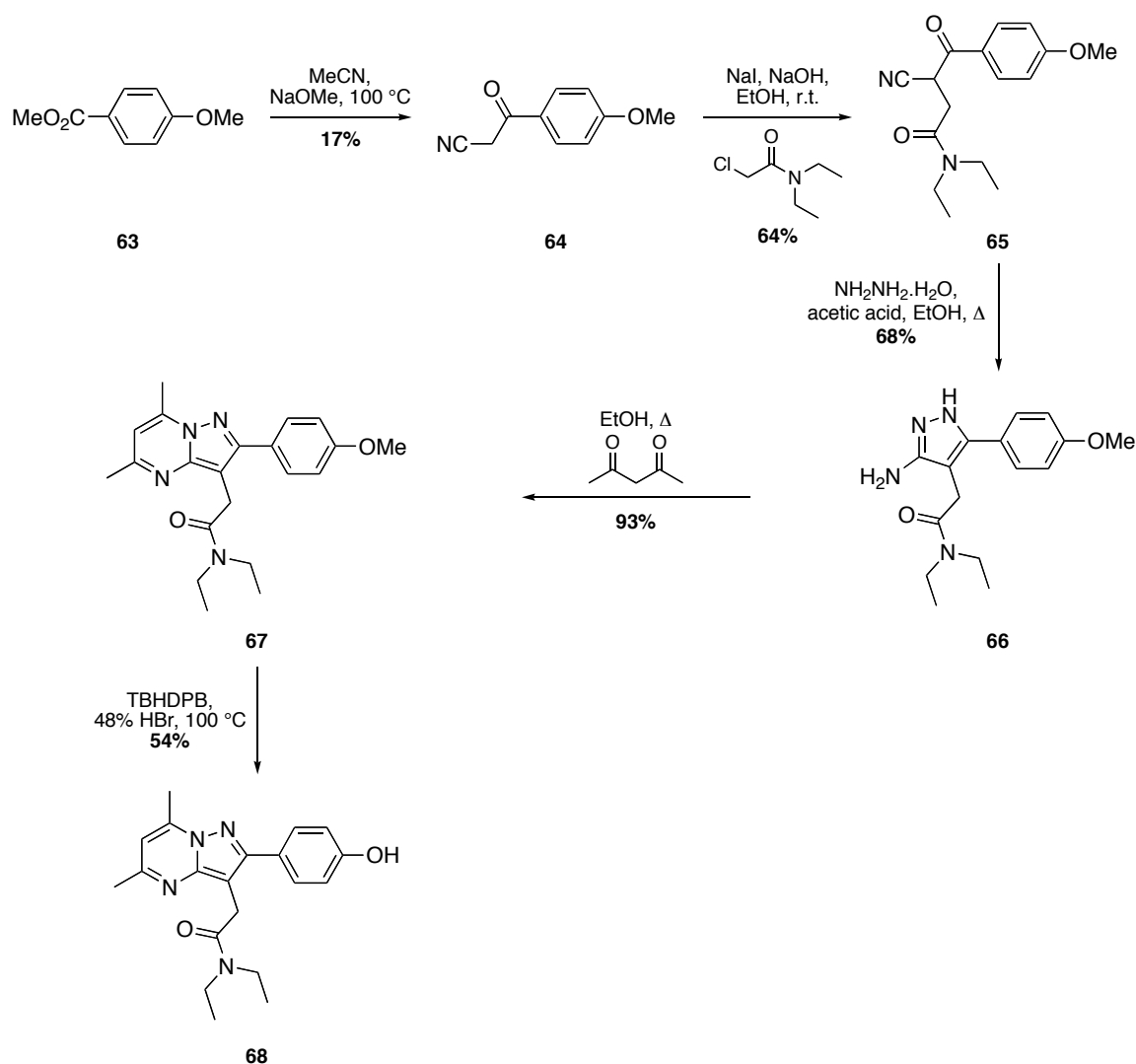
Scheme 12. Synthesis of DPA-714 radiolabelling precursor

Using phenolic pyrazolo[1,5-*a*]pyrimidine compound **68** the synthesis of [^{18}F]DPA-714 could now be achieved (Scheme 13).[73] A Mitsunobu coupling reaction between **68** and toluene-4-sulfonic acid 2-hydroxy-ethyl ester in the presence of DIAD and

triphenylphosphine afforded tosylate precursor **69**. An aliphatic nucleophilic fluorination reaction using [^{18}F]potassium fluoride and Kryptofix® gave [^{18}F]DPA-714 (**70**) in an end of synthesis radiochemical yield of 16%. The ability of this radioligand to image the TSPO was then examined through *in vivo* studies. A dynamic PET scan of baboon brain after administration of [^{18}F]DPA-714 (100 MBq, 270 GBq/μmol) showed uptake during the baseline study and specificity for the TSPO was demonstrated with a blockade study using unlabelled PK11195.
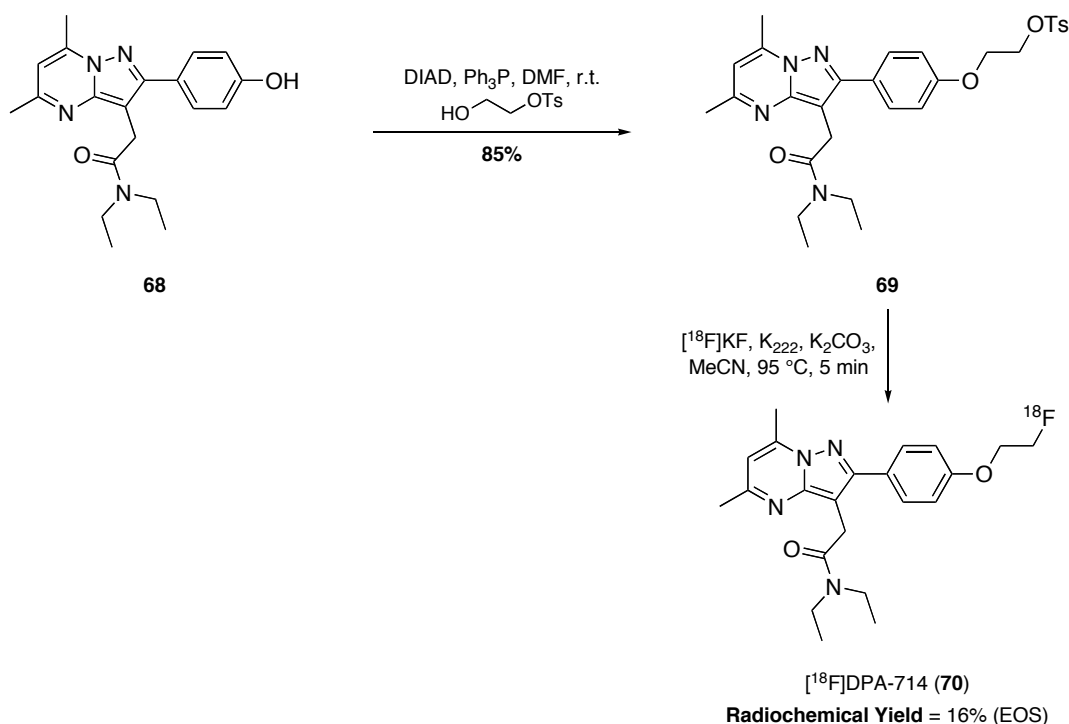
Scheme 13. Radiosynthesis of [^{18}F]DPA-714 (**70**)

In addition to *in vivo* animal studies, [^{18}F]DPA-714 has been applied to the clinic. Two separate studies have shown that this radioligand can be used to image gliomas and,[74] that it can act as a biomarker for neuroinflammation.[75]

1.2.3.7 Phenoxyarylacetamides

In 2004, Nakazato and co-workers developed a new potent class of TSPO ligands.[76] Based on the ring-opening of the diazepine core of Ro 5-4864,[13] the authors synthesised a large library of phenoxyarylacetamides and measured the binding affinity of this class of compounds with the TSPO. From their extensive studies, two compounds in particular were shown to have potent binding with the TSPO, DAA1106 (IC$_{50}$ = 0.28 nM) and

DAA1097 (IC$_{50}$ = 0.92 nM) (Figure 11). Both compounds have demonstrated anxiolytic properties within the laboratory,[77] and DAA1097 has been shown to influence steroidogenesis.[78] These preliminary results implicate a potential therapeutic application for this compound class.
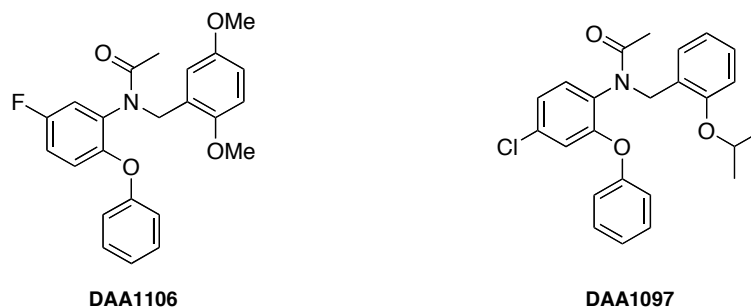
Figure 11. Phenoxyarylacetamide TSPO ligands

Many reported radiosyntheses of phenoxyarylacetamide TSPO ligands can be found in the literature along with their application in PET imaging studies. [^{18}F]PBR06, originally developed by Briard *et al.*, is a potent TSPO radioligand with K_i values ranging from 0.180–0.997 nM in rat, monkey and human brain.[79,80] In 2011, Wang *et al.* developed a new and efficient synthesis of a tosylate labelling precursor and radiosynthesis of [^{18}F]PBR06 (Scheme 14).[81] In their publication the authors reported a facile synthesis starting from commercially available 2,5-dimethoxybenzaldehyde (**72**). Following an initial condensation reaction between the aldehyde and 2-phenoxyaniline (**71**), reduction of the resulting imine using sodium borohydride formed phenoxyaniline intermediate **73**. Intermediate **78** was then prepared in four steps from ethyl glycolate (**74**). Treatment of **74** with *p*-toluenesulfonyl chloride gave tosylate **75**, the ethyl ester group of which was hydrolysed under basic conditions to afford carboxylic acid **76**. Conversion to acyl chloride **77** was then achieved using thionyl chloride. Finally, an amide coupling reaction between these two fragments provided tertiary amide **78**. Radiofluorination of **78** using [^{18}F]potassium fluoride and Kryptofix® in dimethylsulfoxide at 140 °C afforded [^{18}F]PBR06 (**79**) in decay corrected radiochemical yields ranging from 30–60%, within a total synthesis time of 50–60 minutes. Furthermore, the radiotracer was obtained in very high radiochemical purity (>99%) and specific activity (up to 222 GBq/μmol at the end of bombardment).
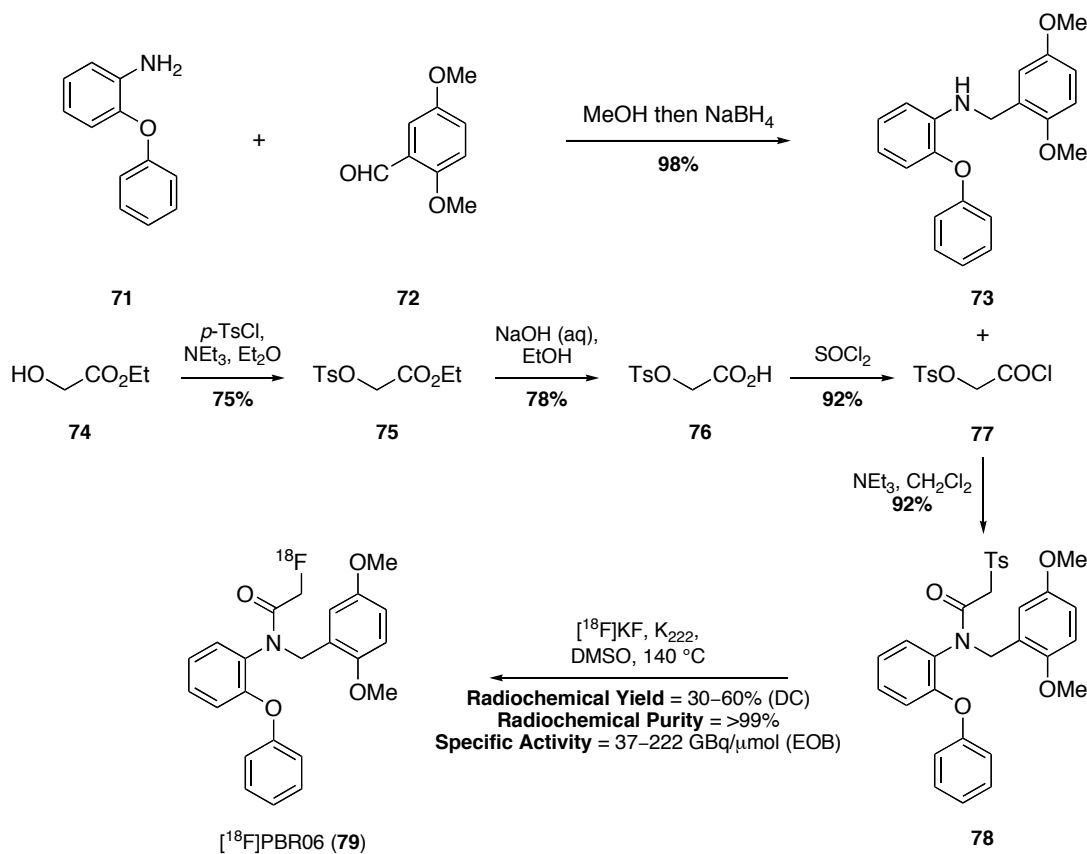
Scheme 14. Radiosynthesis of [^{18}F]PBR06 (**79**)

In terms of clinical applicability, Fujita and co-workers have described a study whereby [^{18}F]PBR06 was compared to [^{11}C]PBR28 as a biomarker for TSPO expression in humans.[82] The preliminary results of this study indicated that [^{18}F]PBR06 has potential to be utilised as a PET imaging agent for TSPO expression and offers the advantage of a longer lived radioisotope ($t_{1/2}$ = 110 minutes for ^{18}F versus 20.3 minutes for ^{11}C).

1.2.3.8 High, Low and Mixed Affinity Binders

In 2010, Owen *et al.* performed an autoradiography study designed to compare the *in vitro* binding characteristics of the TSPO radioligand [^{3}H]PBR28 with [^{3}H]PK11195 within brain tissue.[83] On conclusion of their investigation, the authors reported that approximately 14% of the healthy volunteer cohort enlisted did not display specific binding for [^{3}H]PBR28. Instead, there existed three distinct classes of binders: high affinity binders (HABs, K_i = 3.4 ± 0.5 nM), low affinity binders (LABs, K_i = 188 ± 15.6 nM) and mixed affinity binders (MABs).

A further study by the same group later indicated that this occurrence was more prevalent than originally thought. Through measurement of the binding affinities of TSPO radiotracers for PET currently being investigated for clinical applications, they discovered that all compounds tested recognised HABs, LABs and MABs.[84] The ratios of high to low binding affinity measured for compounds tested are listed in Figure 12. Interestingly, the prototypical ligand for the TSPO, PK11195 was the only compound not to demonstrate large interindividual variations in binding affinity.
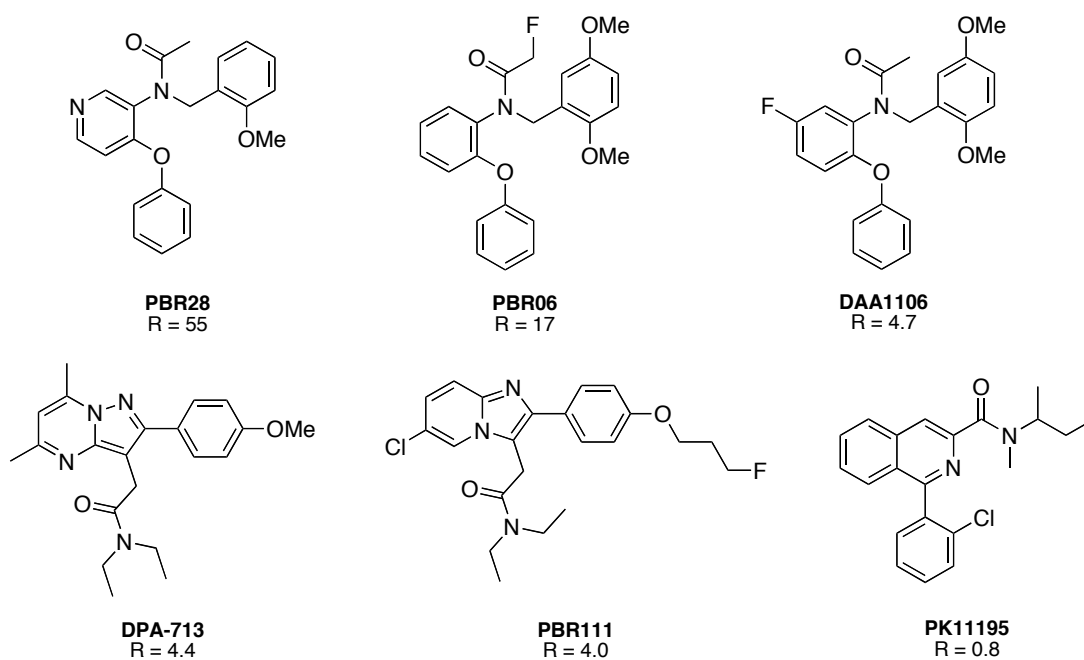
Figure 12. Binding ratios of TSPO ligands

The differences in binding affinities experienced by the population was explained in 2012 by Owen *et al*.[85] A genetic study identified that the TSPO rs6971 polymorphism was responsible. This polymorphism, occurring within exon 4 of the gene encoding the TSPO, results from substitution of alanine for threonine at position 147 of the fifth transmembrane spanning domain. This amino acid substitution therefore presents an additional and unavoidable challenge in TSPO imaging. Conscious efforts to take this polymorphism into account and identify appropriate binders will be required for future studies aimed at developing an imaging agent for the TSPO to be successful. It has been proposed that suitable binders can be selected based on *priori* genetic testing or leukocyte binding assays.[86]

The challenge in development of new radiotracers for the TSPO has been compounded by the discovery of this genetic polymorphism. As the isoquinoline-3-carboxamides are the only structural class of TSPO ligand not to display differences in binding affinity within the population, it was considered logical to attempt to address the problems described in section 1.2.3.2 associated with this compound.

1.3 Proposed Research

The primary aim of this research was to develop a new radiotracer for PET and SPECT imaging of the TSPO. Based on the isoquinoline-3-carboxamide PK11195, a series of quinoline-2-carboxamide analogues would be prepared with two key objectives: to probe structure activity relationships and to reduce compound lipophilicity by variation of the X and R^1–R^4 groups (Figure 13). It was proposed to incorporate groups containing carbon, fluorine or iodine that could be labeled at a later stage using carbon-11 and fluorine-18 for PET imaging, and iodine-123 for SPECT imaging.

PK11195
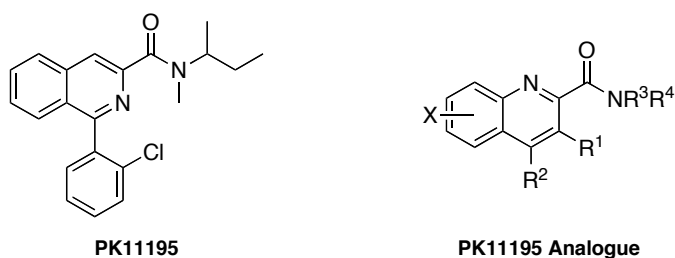
PK11195 Analogue

Figure 13. PK11195 and quinoline-2-carboxamide analogue; potential imaging agent

Upon completion of the synthesis of a small library of quinoline-2-carboxamides it was anticipated that the physicochemical properties of each analogue would be measured, providing an indication of their likelihood to successfully penetrate the blood brain barrier. It was determined that elimination of unsuitable compounds based on lipophilicity and plasma protein binding measurements would ensue, and only those displaying favourable characteristics progressed to the next stage of the study. The *in vitro* binding affinity of selected analogues for the TSPO would then be measured using a competition binding assay. If a lead candidate were identified, a suitable precursor would be radiolabelled and further *in vitro* and *in vivo* studies performed with the aim of developing a novel PET and/or SPECT imaging agent for the TSPO.
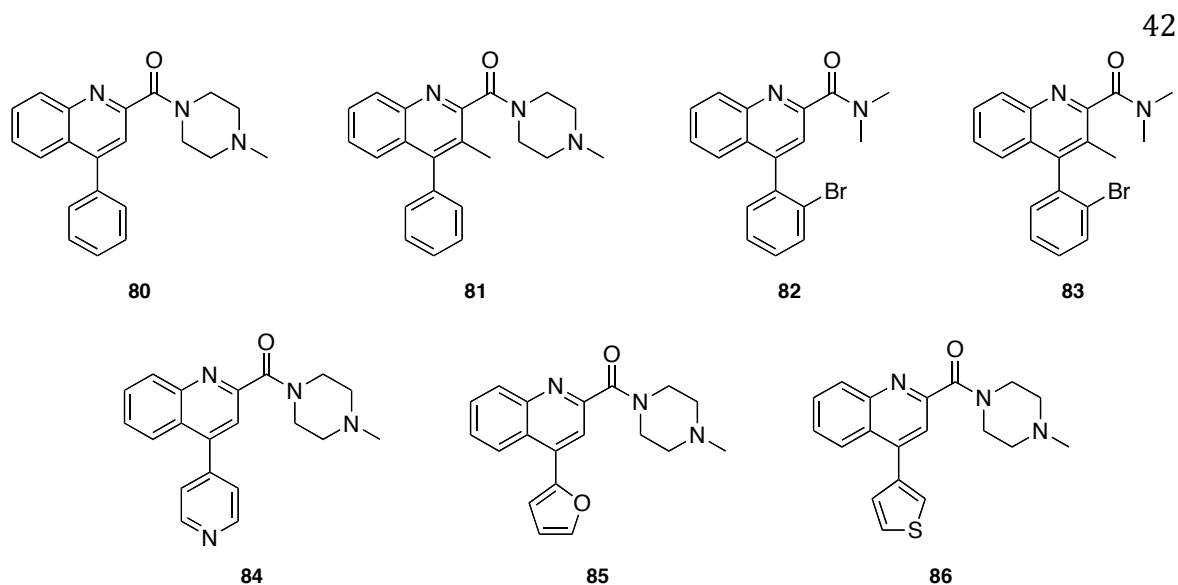
2 Development of Imaging Agents for the TSPO (18 kDa)

2.1 Synthesis of PK11195 Analogues: Potential PET and SPECT Imaging Agents

The first stage of this work required the synthesis of a small library of quinoline-2-carboxamide TSPO ligands analogous with PK11195, the clinically utilised isoquinoline-3-carboxamide PET ligand. It was envisaged that the target compounds could be prepared in a timely and efficient manner, and moreover, that the synthetic routes employed would facilitate structural variation and confirmation of structure activity relationships. Following preparation of the target quinoline-2-carboxamides, assessment of physicochemical properties and measurement of binding affinity with the TSPO would determine potential for successful development into an imaging agent for the TSPO.

2.1.1 Synthesis of Potential PET Imaging Agents

In total, seven quinoline-2-carboxamides were initially identified as interesting targets with possible application as PET imaging agents (Figure 14). Previous studies have shown that the more rigid the ligand, as exerted through restriction of amide bond rotation using strategically positioned substituents, the greater the binding affinity with the protein.[22] It was therefore proposed that compounds **80** and **81** would probe the effect of a methyl group at the 3-position of the quinoline ring on protein binding. Furthermore, compounds **82** and **83** would indicate whether a substituent at this position was necessary, or if the presence of a large *ortho*-bromide substituent was sufficient for potent binding. In addition, the effect of replacing the pendant phenyl ring with a heterocyclic ring system was identified as an area of interest. As such, compounds **84–86**, bearing a pyridin-4-yl, furan-2-yl and thiophen-3-yl substituent were also chosen as targets. In all instances, selection of the amide side chain and heterocyclic system was done in anticipation of reducing compound lipophilicity and increasing bioavailability.
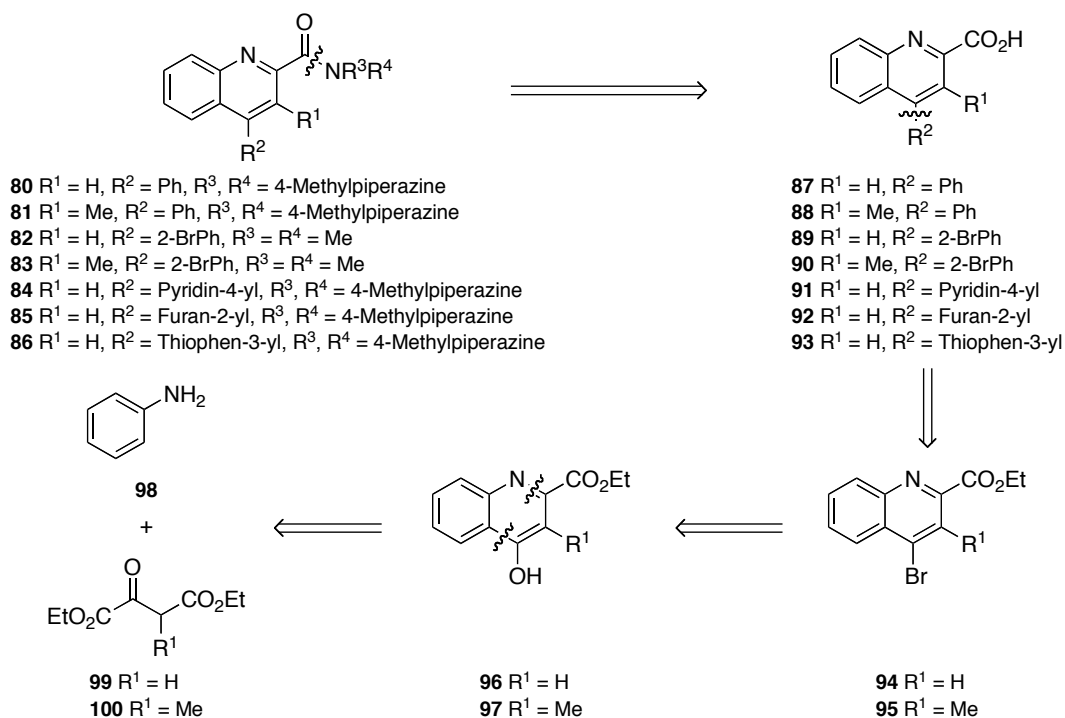
Figure 14. Potential PET imaging agents

If any compound showed promise in terms of binding affinity and physicochemical properties, development of a synthetic route for the preparation of a [^{11}C]-labeling precursor would ensue.

2.1.1.1 Retrosynthetic Analysis of PK11195 Analogues 80–86

A retrosynthetic analysis of the target PET compounds **80–86** is shown in Scheme 15. It was proposed that a disconnection of the amide linkage would afford carboxylic acid intermediates **87–93**, and that further disconnection of the aromatic or heteroaromatic moieties would lead to bromoquinolines **94** and **95**. Functional group interconversion of the halogen would then lead to hydroxyquinolines **96** and **97**. Finally, disconnection of the quinoline core would yield commercially available aniline (**98**) and either diethyl oxalacetate (**99**) or diethyl oxalpropionate (**100**).

80 R^1 = H, R^2 = Ph, R^3, R^4 = 4-Methylpiperazine
81 R^1 = Me, R^2 = Ph, R^3, R^4 = 4-Methylpiperazine
82 R^1 = H, R^2 = 2-BrPh, R^3 = R^4 = Me
83 R^1 = Me, R^2 = 2-BrPh, R^3 = R^4 = Me
84 R^1 = H, R^2 = Pyridin-4-yl, R^3, R^4 = 4-Methylpiperazine
85 R^1 = H, R^2 = Furan-2-yl, R^3, R^4 = 4-Methylpiperazine
86 R^1 = H, R^2 = Thiophen-3-yl, R^3, R^4 = 4-Methylpiperazine

87 R^1 = H, R^2 = Ph
88 R^1 = Me, R^2 = Ph
89 R^1 = H, R^2 = 2-BrPh
90 R^1 = Me, R^2 = 2-BrPh
91 R^1 = H, R^2 = Pyridin-4-yl
92 R^1 = H, R^2 = Furan-2-yl
93 R^1 = H, R^2 = Thiophen-3-yl

98

99 R^1 = H
100 R^1 = Me

96 R^1 = H
**97** R^1 = Me

94 R^1 = H
95 R^1 = Me

Scheme 15. Retrosynthetic analysis of PET compounds **80–86**

The synthetic strategy outlined highlights two molecular handles that will enable structural variation: bromoquinolines **94** and **95** can be subjected to a Suzuki-Miyaura cross-coupling with a range of commercially available boronic acids, and the penultimate carboxylic acids reacted with a variety of amines for final compound preparation.

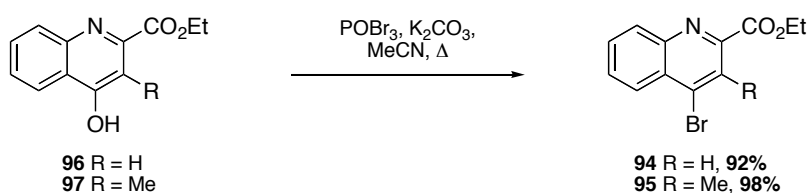## 2.1.1.2 Synthesis of 4-Bromoquinolines 94 and 95

The first step in the synthesis of the target quinoline-2-carboxamides was the preparation of the 2,4-disubstituted quinoline core, which was achieved in two steps using a procedure developed by Bradbury *et al.* (Scheme 16).[87] Condensation of aniline (**98**) with either diethyl oxalacetate (**99**) or diethyl oxalpropionate (**100**) in the presence of *para*-toluenesulfonic acid under Dean-Stark conditions, resulted in the formation of imines **101** and **102**. Due to the instability of these imines on silica, they were applied immediately to the next step without prior purification. Acid-mediated cyclisation of these intermediate imines in the presence of neat polyphosphoric acid at 120 °C afforded the desired 4-hydroxyquinolines **96** and **97** in yields of 37% and 65%, respectively. Construction of a quinoline ring under these conditions is referred to as the Combes quinoline synthesis (*Cf.* Conrad-Limpach synthesis).[88]
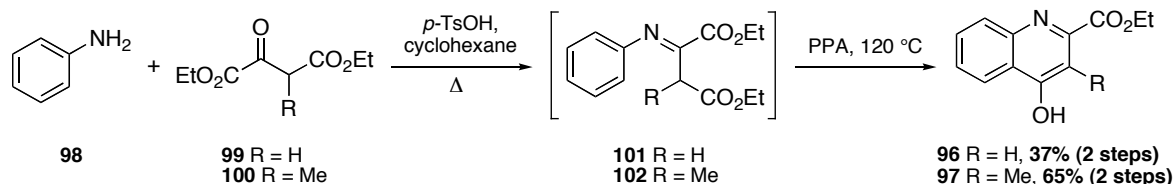
Scheme 16. Synthesis of 4-hydroxyquinolines **96** and **97**

It was expected that a catalytic amount of *para*-toluenesulfonic acid would be sufficient for the preparation of the intermediate imines, and this was true for the preparation of 4-hydroxyquinoline **97**. However, when a catalytic quantity of the acid was used for the preparation of hydroxyquinoline **96**, inspection of the crude reaction mixture by ^{1}H NMR spectroscopy indicated that only a negligible amount of product had formed. In an attempt to increase the yield for this reaction, a stoichiometric amount of acid was employed and the desired 4-hydroxyquinoline was prepared in a low, but acceptable 37% yield.

Having successfully formed the quinoline core structure, the next step required converting the hydroxyl group to the bromide. This transformation was achieved *via* an S_NAr reaction, whereby 4-hydroxyquinolines **96** and **97** were treated with phosphorus oxybromide to give 4-bromoquinolines **94** and **95** in excellent yields of 92% and 98%, respectively (Scheme 17).[46,89] Preparation of the target PET compounds could now be achieved using these key synthetic intermediates.


Scheme 17. Synthesis of 4-bromoquinolines **94** and **95**

2.1.1.3 Synthesis of Potential PET Compounds 80 and 81

In 1979, Suzuki and Miyaura reported the stereoselective synthesis of arylated (*E*)-alkenes by the palladium-catalysed reaction between 1-alkenylboranes and aryl halides.[90] This seminal work paved the way for what is now commonly referred to as the Suzuki cross-coupling reaction, and is defined as the palladium-catalysed cross-coupling reaction of an organoboron with an organic halide or triflate to form a new carbon-carbon bond.[88] It is an

extremely powerful reaction with wide synthetic utility, and allows for the preparation of conjugated olefins, styrenes and biaryls. There are many advantages associated with this reaction; a few of which include mild reaction conditions, tolerance of a wide range of functional groups, stability under aqueous conditions and wide range of commercially available starting materials.[91]

Biaryl compounds **103** and **104** were prepared *via* a palladium(0)-catalysed Suzuki cross-coupling reaction between benzeneboronic acid and either 4-bromoquinoline **94** or **95** (Scheme 18). A wide range of reagents and reaction conditions have been developed for the Suzuki reaction, and in this case tetrakis(triphenylphosphine)palladium(0) and potassium phosphate in DMF were sufficient for the preparation of compounds **103** and **104** in an 81% and 51% yield, respectively.[46]

94 R = H
95 R = Me

103 R = H, **81%**
104 R = Me, **51%**
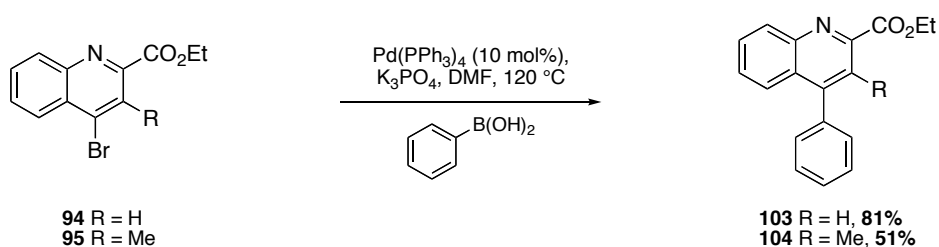
**Scheme 18.** Synthesis of 4-phenylquinolines **103** and **104**

The Suzuki cross-coupling reaction is a palladium(0) to palladium(II)-catalytic cycle (Figure 15).[92] Oxidative addition of the aryl halide bond of **94** to palladium(0) generates a palladium(II) species, and a *cis* complex that rapidly isomerises to *trans* complex **105**.[93] It has been proposed that the role of the base in the reaction is to facilitate the quaternisation of the boron,[94] resulting in the formation of the boronate **106**, which undergoes transmetallation with the palladium(II)-complex. Isomerisation of this newly formed *trans*-palladium(II) intermediate to the corresponding *cis*-palladium(II) complex **107** then allows for the final step of the catalytic cycle to be achieved. Reductive elimination produces the desired biaryl compound **103**, whilst regenerating the palladium(0) species and enabling it to continue the catalytic cycle.
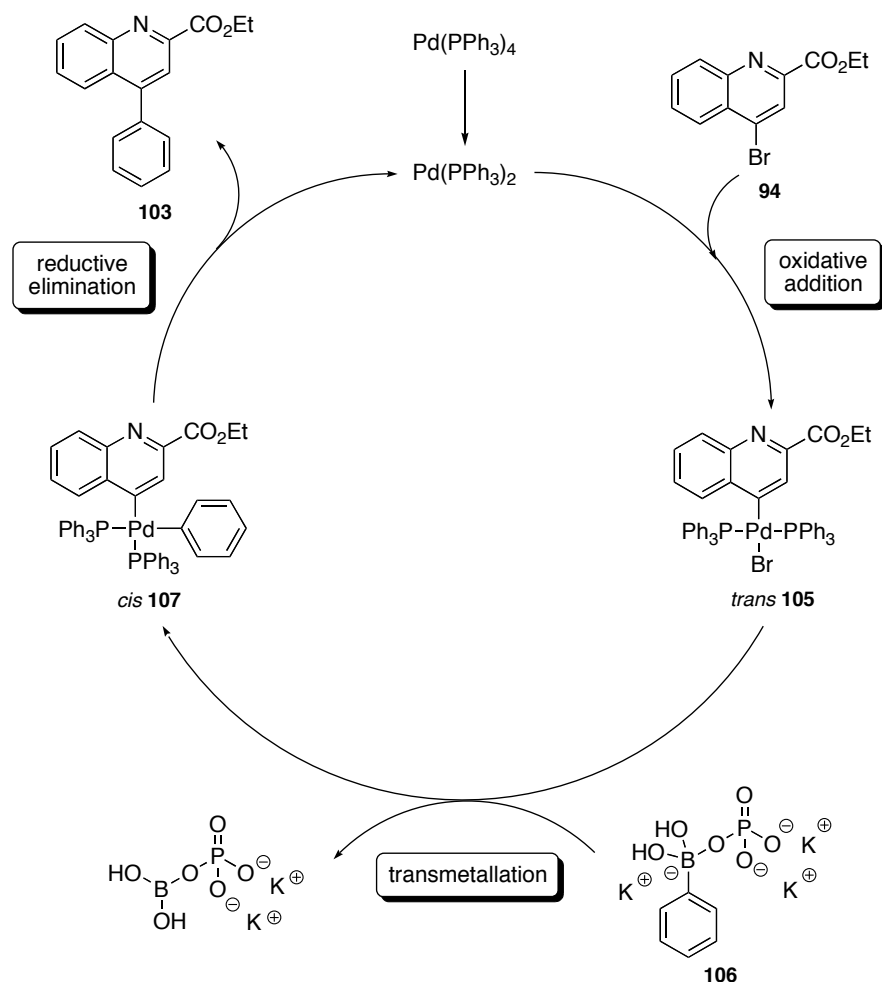
Figure 15. Suzuki-Miyaura cross-coupling reaction mechanism

The synthesis of quinoline-2-carboxamides **80** and **81** could now be completed in just a few short steps (Scheme 19). Hydrolysis of the ethyl ester group of **103** and **104**, under basic conditions, resulted in the formation of quinoline-2-carboxylic acids **87** and **88** in an 89% and 82% yield, respectively. The resulting carboxylic acids were then converted to their corresponding acyl chlorides by reaction with oxalyl chloride and a catalytic quantity of DMF. The acyl chloride intermediates were not isolated, and treated immediately with 1-methylpiperazine *in situ* to form the target compounds **80** and **81** in a moderate yield of 59% and 43%, respectively over 2 steps.
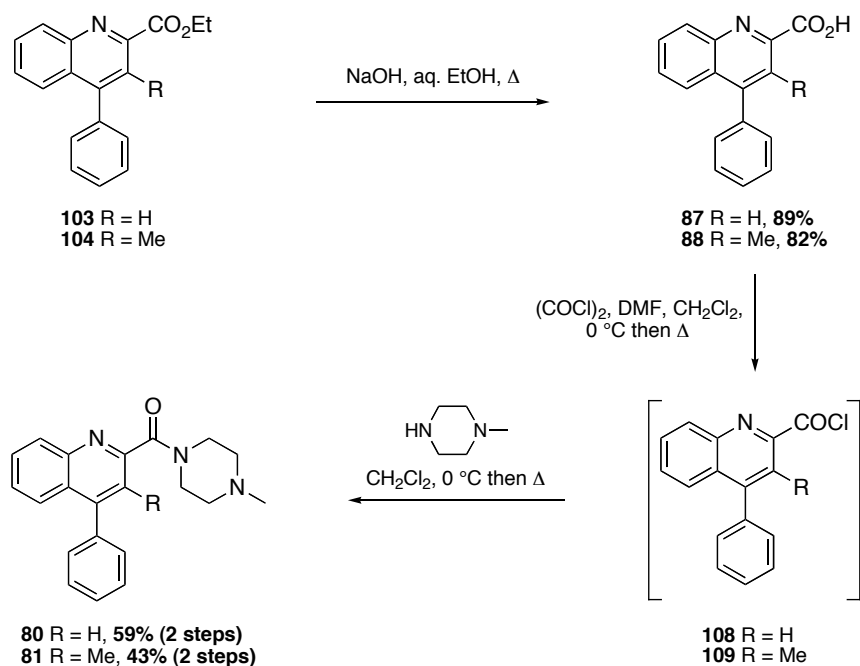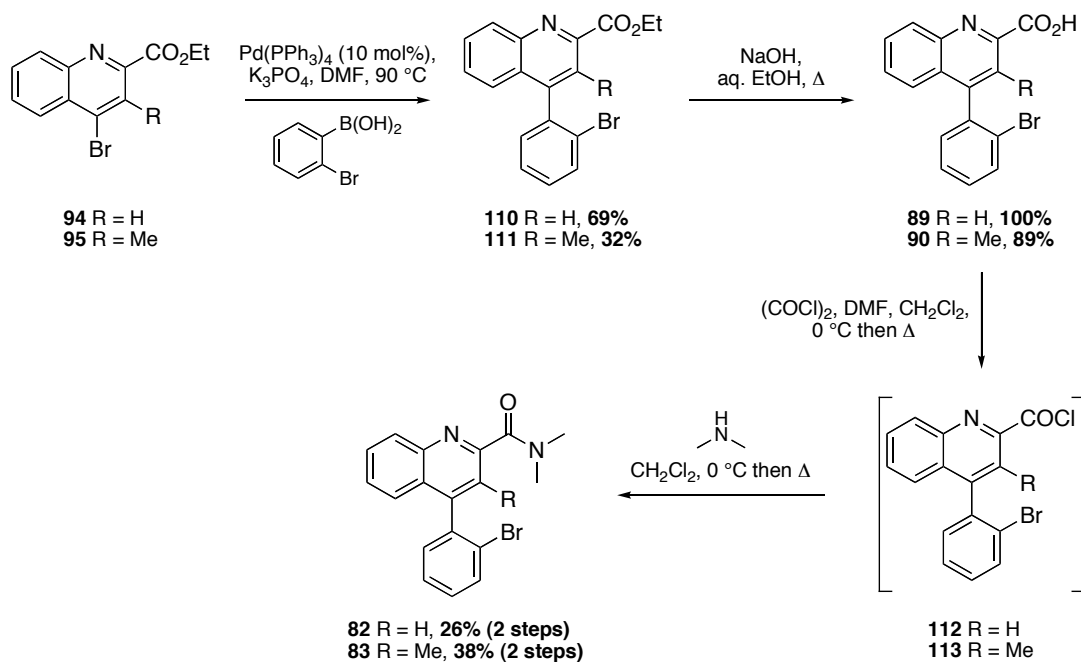
Scheme 19. Synthesis of potential PET compounds **80** and **81**

## 2.1.1.4 Synthesis of Potential PET Compounds 82 and 83

Quinoline-2-carboxamides **82** and **83** were prepared using the same synthetic route described for **80** and **81** (Scheme 20). Briefly, 4-bromoquinolines **94** and **95** were employed in a palladium(0)-catalysed cross-coupling reaction with 2-bromophenylboronic acid to give biaryl compounds **110** and **111** in 69% and 32% yield, respectively. Hydrolysis of the ethyl ester using sodium hydroxide gave carboxylic acids **89** and **90** in an excellent quantitative yield for **89**, and 89% yield for **90**. *In situ* formation of acyl chlorides **112** and **113**, and subsequent treatment with dimethylamine afforded quinoline-2-carboxamides **82** and **83** in low yields of 26% and 38%, respectively. In terms of biological testing, milligram quantities of a compound are required for performing the assay in triplicate, and so despite the low isolated product yields, a sufficient mass was obtained for ensuing biological investigations.

Scheme 20. Synthesis of potential PET compounds **82** and **83**

Despite variations in temperature and reagent equivalents employed, the reaction of compound **95** tended to produce either trace amounts, or very low isolated product yields of **111** (24–32%). Inspection of the crude reaction mixture by ^{1}H NMR spectroscopy indicated that at most, a 2:1 mixture of 4-bromoquinoline starting material to desired product was forming. As such, alternative reagents and reaction conditions were investigated in an attempt to improve the yield of this reaction (Scheme 21, Table 3).

Janin and Guillou reported that by replacing tetrakis(triphenylphosphine)palladium(0) with [1,1'-bis(diphenylphosphino)ferrocene]dichloropalladium(II) as the catalyst employed for Suzuki cross-coupling reactions, they could achieve the synthesis of their target 1-arylisoquinoline-3-carboxylates in much greater yields.[95] As such, these optimised reaction conditions were applied to substrate **95** (Entry 1). However, inspection of the crude reaction mixture using ^{1}H NMR spectroscopy highlighted the presence of starting material and an aromatic by-product only, and the decision to return to tetrakis(triphenylphosphine)palladium(0) was taken. In this instance, an alternative base and reaction conditions were employed, but again only unreacted starting material and aromatic by-products resulted from this reaction (Entry 2). Isolation and identification of the aromatic impurities was not undertaken due to the small-scale nature of the reactions.
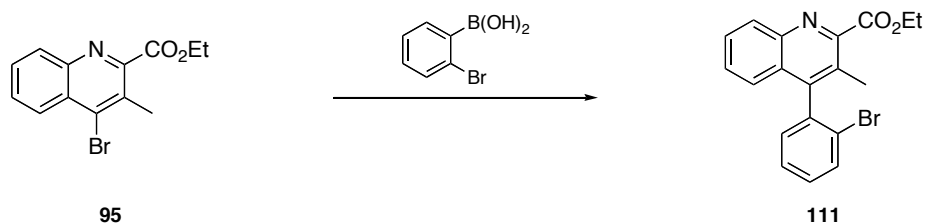
Scheme 21. Suzuki coupling reaction

| Entry	Reagents	Conditions	Outcome
1	PdCl$_2$(dppf) (0.05 mol%), CsCO$_3$ (2.1 eq)	1,4-dioxane/H$_2$O, 85 °C	SM (+ aromatic by-product)
2	Pd(PPh$_3$)$_4$ (10 mol%), Na$_2$CO$_3$ (3.0 eq)	Toluene/H$_2$O/EtOH, 90 °C	SM (+ aromatic by-products)

Table 3. Alternative Suzuki-Miyaura cross-coupling conditions

On the whole, the product yield for the Suzuki coupling reaction between 4-bromoquinoline **95** and 2-bromophenylboronic acid was not improved beyond 32%. The reasons for the low yield of this transformation may be due to interference resulting from a combination of steric and electronic factors. In terms of steric obstruction, the presence of the methyl substituent in the 3-position of the quinoline ring, coupled with the presence of the *ortho*-bromide substituent of the boronic acid, could be hindering the already slow transmetallation step. As well as potentially imparting a steric barrier to the reaction, the inductive effect of the methyl group may also be slowing down the initial oxidative addition step of the aromatic halide bond to the palladium(0) species. Furthermore, it has been reported that under aqueous conditions, reduction of the C-Br bond can occur,[96] and phenylboronic acids with an electron withdrawing substitutent at the *ortho*-position can increase the rate of hydrolytic deboronation.[91]

2.1.1.5 Synthesis of Potential PET Compounds 84, 85 and 86

TSPO ligands **84**, **85** and **86**, bearing a heterocycle in place of the pendant phenyl ring, were prepared in four overall steps (Scheme 22). Again, 4-bromoquinoline **94** was employed in a Suzuki cross-coupling reaction with pyridin-4-ylboronic acid, furan-2-ylboronic acid and thiophen-3-ylboronic acid, under standard coupling conditions, to give biaryl compounds **114**, **115**, and **116** in good yields of 94%, 85% and 76%, respectively.

Subsequent base hydrolysis of the ethyl ester afforded carboxylic acids **91**, **92** and **93** in yields ranging from 79–93%. Finally, conversion of the carboxylic acids to the corresponding acyl chlorides **117**, **118** and **119**, and subsequent reaction with 1-methylpiperazine resulted in the successful completion of the synthesis of target quinoline-2-carboxamides **84**, **85** and **86**. Compounds **84**, **85** and **86** were obtained in a low to moderate yield of 53%, 56% and 32% over two steps, respectively.
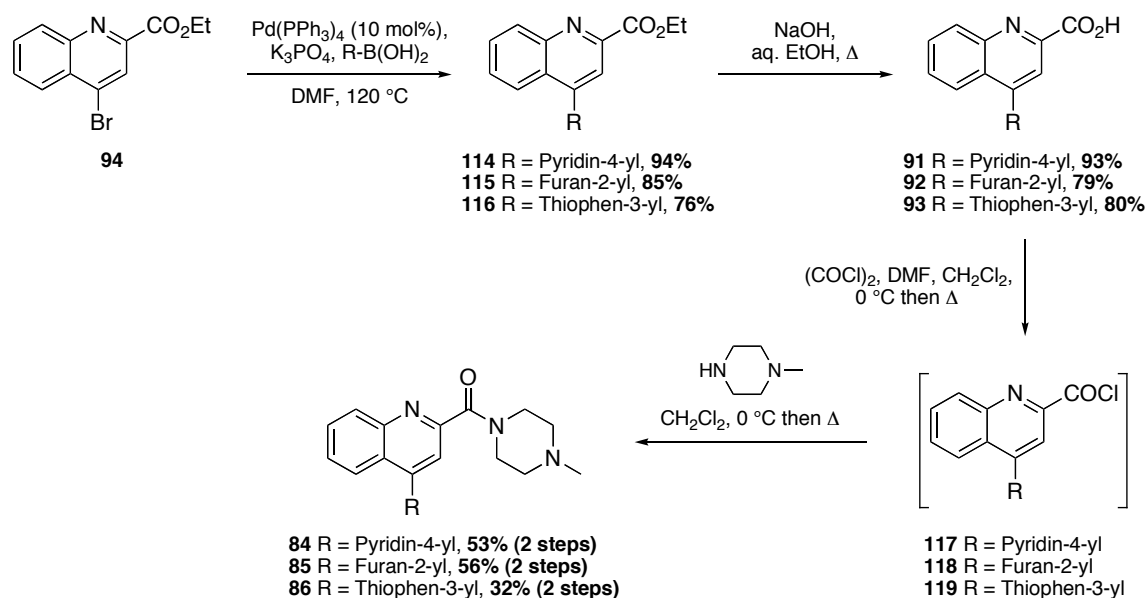

Scheme 22. Synthesis of potential PET compounds **84**, **85** and **86**

Having completed the synthesis of quinoline-2-carboxamides **84–86**, attention now turned to preparation of TSPO ligands with potential application in SPECT imaging.

2.1.2 Synthesis of Potential SPECT Imaging Agents

As mentioned previously, increased binding affinity of a ligand with the TSPO can be achieved by restricting rotation of the amide bond. In doing so, the molecule increases in rigidity and consequently finds favourable interactions within the binding pocket of the protein. It was therefore proposed, that quinoline-2-carboxamides **120** and **121** (Figure 16) were suitable targets, and anticipated that the large *ortho*-iodide substituent would obstruct rotation of the diethyl and morpholine amides.
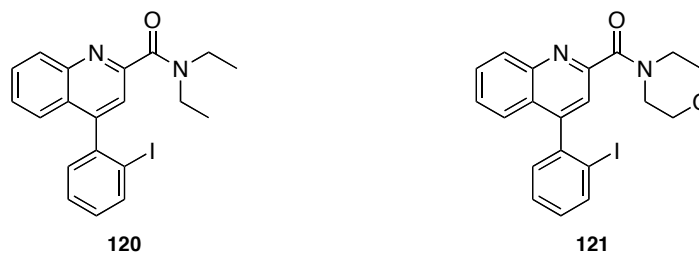
Figure 16. Potential SPECT imaging agents

Following this, synthesis of a labeling precursor for [^{123}I]-incorporation and development as a potential SPECT imaging agent for the TSPO would commence if preliminary *in vitro* investigations yielded promising results.

2.1.2.1 Proposed Synthetic Route for SPECT Compounds 120 and 121

It was originally proposed that compounds **120** and **121** could be prepared using the same synthetic route as that for PET compounds **80–86**, with the addition of a key synthetic step (Scheme 23). Carboxylic acid **89**, the preparation for which was described previously, could be converted to amides **122** and **123** *via* the acid chloride. Finally, a halogen exchange reaction could then be employed for inclusion of the iodide, providing quinoline-2-carboxamides **120** and **121**.
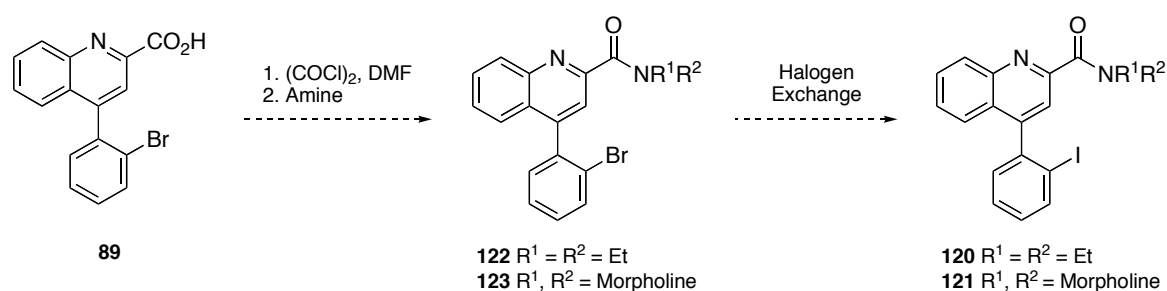
Scheme 23. Proposed synthetic route for quinoline-2-carboxamides **120** and **121**

2.1.2.2 Synthesis of SPECT Compounds 120 and 121

Oxalyl chloride and a catalytic amount of DMF was used to convert carboxylic acid **89** to the corresponding acid chloride intermediate **124**, which was in turn treated immediately with diethylamine to give bromide precursor **122**. This sequence of transformations proceeded with a 46% yield over two steps (Scheme 24).

Scheme 24. Synthesis of bromide precursor **122**

In order to complete the synthesis of the first target SPECT compound, conversion of the aryl bromide to an aryl iodide was required (Scheme 25). It was envisaged that this transformation could be achieved directly by means of a metal-mediated halogen exchange reaction. Several methods have been developed for the preparation of aryl iodides from aryl bromides, which involve nickel- and copper-mediated reactions.[97] However, the disadvantages associated with such procedures, *e.g.* requiring stoichiometric amounts of nickel(0) powder, limits their synthetic and economic utility.[98]

At this point in time, a research project within the group, was aimed at developing a new nickel-mediated halogen exchange reaction for the generation of aryl iodides from aryl bromides.[99] This methodology was therefore used as a starting point. An initial attempt to prepare the iodinated compound employed 10 mol% of nickel(II) bromide, an excess of sodium iodide and 10 mol% of tri-*n*-butylphosphine as the ligand (Table 4, Entry 1). After stirring in NMP for 18 hours at 180 °C, analysis of the ^{1}H MMR spectrum of the crude reaction mixture indicated that complete consumption of the bromide starting material **122** had occurred, however, evidence of the desired iodide product **120** was absent. Instead, it appeared that reduction of the C-Br bond leading to dehalogenated product **125** had occurred. This is a known side reaction of metal mediated halogen exchange reactions.[100] In an attempt to overcome reduction of the starting material, the reaction was carried out using the same reagents, but in the presence of 4Å molecular sieves and at a lower temperature of 150 °C (Table 4, Entry 2). Unfortunately, these reaction conditions also resulted in the formation of the reduced by-product **125**.

The unsuccessful attempts to prepare the target quinoline-2-carboxamide using a nickel-mediated halogen exchange reaction led to the investigation of a different catalytic system. Klapars and Buchwald have reported a highly efficient method for the preparation of a range of aromatic and heteroaromatic iodides from the analogous bromides *via* a copper-catalysed aromatic Finkelstein reaction.[101] Under the reported optimised reaction

conditions, which utilised copper(I) iodide in the presence of a diamine ligand, it was anticipated that the desired iodide could be prepared without formation of the dehalogenated by-product. A first attempt at using this methodology employed 5 mol% copper(I) iodide, an excess of sodium iodide and 10 mol% of *N,N*-dimethylethylenediamine (DMEN) as the diamine ligand (Table 4, Entry 3). The starting material and reagents were dissolved in *n*-butanol and stirred for 18 hours at 180 °C. Analysis of the crude reaction mixture by ^{1}H MNR spectroscopy indicated that a 2:1 mixture of dehalogenated by-product and starting material was present.

A final attempt to exchange the bromide for the iodide using 5 mol% copper(I) iodide, an excess of sodium iodide and 10 mol% of DMEN, and executing the reaction in a microwave was performed (Table 4, Entry 4). After stirring for 1 hour at 200 °C, the reaction mixture was again inspected. From the ^{1}H NMR spectrum, it appeared that a 2:1 mixture of dehalogenated by-product **125** and iodinated product **120** was present. However, despite several attempts to isolate the final compound using flash column chromatography, it could not be achieved due to close running impurities on the silica column. Despite the inability to isolate compound **120**, formation of the small amount of product offered encouragement to pursue an alternative synthetic strategy.
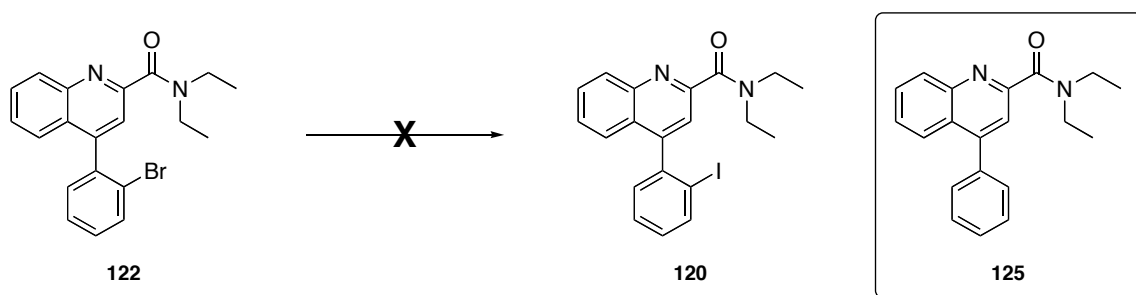
Scheme 25. Attempted halogen exchange reaction of bromide **122**

Entry	Reagents	Conditions	Outcome
1	NiBr$_2$ (10 mol%), NaI (6.0 eq), P(n-Bu)$_3$ (10 mol%)	NMP, 180 °C, 18 h	Dehalogenation
2	NiBr$_2$ (10 mol%), NaI (6.0 eq), P(n-Bu)$_3$ (25 mol%)	NMP, 4Å MS, 150 °C, 18 h	Dehalogenation
3	CuI (5 mol%), NaI (2.0 eq), DMEN (10 mol%)	n-BuOH, 180 °C, 18 h	Dehalogenation/SM 2:1[*]
4	CuI (5 mol%), NaI (2.0 eq), DMEN (10 mol%)	n-BuOH, μW (200 °C), 1 h	Dehalogenation/Product 2:1[*]

[*]Determined by measurement of integrals in ^{1}H NMR spectrum of crude reaction mixture.

Table 4. Conditions trialed for direct halogen exchange reaction

Previous work in the group has shown that the copper(I)-catalysed aromatic Finkelstein reaction can be successfully applied to isoquinolines bearing an ester group in place of the amide side chain. As such, quinoline-2-carboxylate **110** was identified as a potential precursor for the halogen exchange reaction (Scheme 26). The conditions trialed for this reaction are listed in Table 5. Briefly, a nickel-catalysed halogen exchange reaction was initially employed for the synthesis of **126**, but resulted in formation of a complex mixture of dehalogenated and unidentified by-products only (Entry 1). Application of the Klapars and Buchwald conditions was then attempted, but again afforded complex mixtures from which compound identification was difficult (Entries 2 and 3). It should be noted that under the reaction conditions employed, a transesterification reaction occurs forming **127**. In addition to the use of a metal-catalysed halogen exchange reaction, a lithium-halogen exchange reaction was considered for the preparation of **126**,[102,103] however treatment of **110** with n-butyllithium followed by molecular iodine yielded another complex mixture (Entry 4).
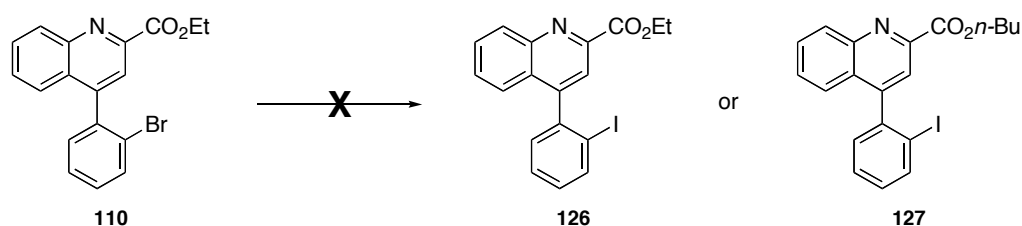
Scheme 26. Attempted halogen exchange reaction of quinoline-2-carboxylate **110**

Entry	Reagents	Conditions	Outcome
1	NiBr$_2$ (5 mol%), NaI (6.0 eq), P(n-Bu)$_3$ (10 mol%)	DMF, 140 ° C, 24 h	Complex Mixture
2	CuI (5 mol%), NaI (2.0 eq), DMEN (10 mol%)	n-BuOH, 150 °C, 10 days	Complex Mixture
3	CuI (5 mol%), NaI (2.0 eq), DMEN (10 mol%)	n-BuOH, 130 °C, 4 days	Complex Mixture
4	n-BuLi (1.1 eq) then I$_2$ (1.4 eq)	THF, −78 °C then r.t.	Complex Mixture

Table 5. Conditions trialed for halogen exchange reaction on quinoline-2-carboxylate

In order to show that the reagents employed for the copper(I)-catalysed aromatic Finkelstein reaction were of sufficient enough quality, and that there were no practical issues surrounding the handling and setting up of this experiment, a model substrate was investigated. 5-Bromoindole was chosen to replicate the experiment carried out by Klapars and Buchwald who had also selected this compound as a substrate. Treatment of 5-bromoindole (**128**) with 5 mol% copper(I) iodide, an excess of sodium iodide and DMEN as the ligand in 1,4-dioxane at 110 °C proceeded to give 5-iodoindole (**129**) in a 63% yield (Scheme 27). This reaction was replicated to ensure reproducibility. These results, therefore, indicate that the attempts to convert the aryl bromide **122** into aryl iodide **120** using the copper(I)-mediated approach, most likely failed due to steric hinderance resulting from the *ortho*-substitution pattern.
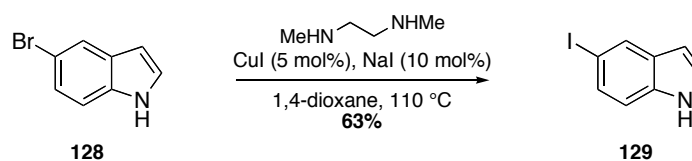
Scheme 27. Synthesis of 5-iodoindole (**129**) *via* a halogen exchange reaction

Unsuccessful attempts to directly convert the aryl bromide to the aryl iodide required an alternative synthetic route to be devised. One such approach involves electrophilic iodo-demetallation.[104] Various metals have been effectively employed for the iodo-demetallation transformation including, but not limited to, silicon, boron and tin.[105] At present, the most commonly used metal is tin, and the reaction proceeds *via* a two-step

process involving an initial palladium(0)-catalysed stannylation of the halogenated arene followed by iodo-destannylation under oxidative conditions.[106] Unfortunately, the reaction of bromide **122** with 10 mol% tetrakis(triphenylphosphine)palladium(0) and hexamethylditin affording organostannane **130** was unsuccessful (Scheme 28). As such, iodo-destannylation in the presence of sodium iodide and chloramine-T to **120** could not be attempted.
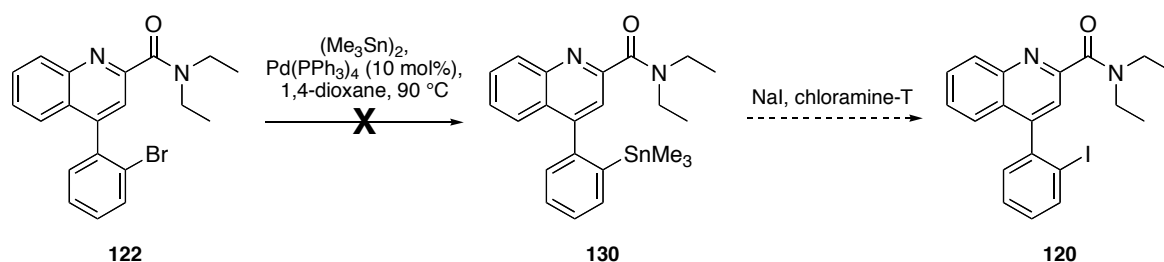
Scheme 28. Attempted synthesis of **120** *via* a stannylation iodo-destannylation sequence

A procedure reported by Lunazzi *et al*. indicated that the more sterically encumbered *ortho*-bromide substituent of a biaryl system could be converted to the trimethylstannane using *tert*-butyllithium and trimethyltin chloride.[107] However, the use of these more forcing reaction conditions would not be compatible with the functionalities of this molecule, as has been previously indicated.

2.1.2.3 New Synthetic Route for the Preparation of SPECT Compounds 120 and 121

Despite several attempts using different approaches, incorporation of the iodide substituent into the quinoline core could not be achieved. An alternate synthetic route, circumventing this troublesome step was therefore necessary. The synthetic utility of aromatic iodides as building blocks for organic chemists in combination with their biological activity,[108] has resulted in an increasing interest in methodology enabling efficient generation of this motif. In 1884, T. Sandmeyer discovered that while attempting to prepare phenylacetylene from benzenediazonium chloride and copper(I) acetylide, he had in fact, synthesised chlorobenzene in good isolated yield with no evidence of the desired product.[88,109] This serendipitous discovery of the ability to substitute an aryldiazonium salt with a halide or pseudo-halide is now refered to as the Sandmeyer reaction, and is a powerful tool for the regioselective preparation of aromatic iodides, bromides and chlorides for example.

It was, therefore, anticipated that the preparation of an aryldiazonium salt followed by a Sandmeyer reaction with an iodine source could be exploited to synthesise the target SPECT compounds. Utilisation of this synthetic transformation would first require generation of the primary aromatic amine starting material, which could be formed from the corresponding nitro functional group.

An initial Suzuki cross-coupling reaction of 4-bromoquinoline **94** and 2-nitrobenzeneboronic acid under standard conditions afforded biaryl compound **131** in an excellent 91% yield (Scheme 29). The success of this coupling reaction provided a chemical handle in the form of the nitro group, allowing for insertion of the iodine atom. Reduction of the nitro group was achieved using conditions reported by Bellamy and Ou,[110] whereby the aromatic nitro group of **131** was converted to the corresponding amine **132** in an excellent 99% yield using tin(II) chloride. Formation of the aromatic amine enabled the key transformation to be investigated. Krasnokutskaya *et al*., reported the preparation of aromatic and heterocyclic iodides *via* a one-pot diazotisation/iodination sequence using a mixture of *para*-toluenesulfonic acid, sodium nitrite and potassium iodide.[111] Initial treatment of aromatic amine **132** with *para*-toluenesulfonic acid in acetonitrile at ambient temperature, followed by the dropwise addition of an aqueous sodium nitrite and potassium iodide solution at 0 °C, resulted in the formation of the intermediate aryldiazonium which reacts immediately to form the desired iodoarene **126**. This key transformation proceeded in very good yield of 83%. Having successfully incorporated the iodine substituent into the molecule over three steps, completion of the target compounds **120** and **121** could now be achieved. Firstly, hydrolysis of ethyl ester **126** under basic conditions resulted in the formation of carboxylic acid **133** in quantitative yield, which was subsequently converted to acid chloride **134**. Treatment with the appropriate amine completed the target compound synthesis. Reaction with diethylamine and morpholine afforded target SPECT compounds **120** and **121** in a moderate 51% and 60% yield over two steps, respectively.
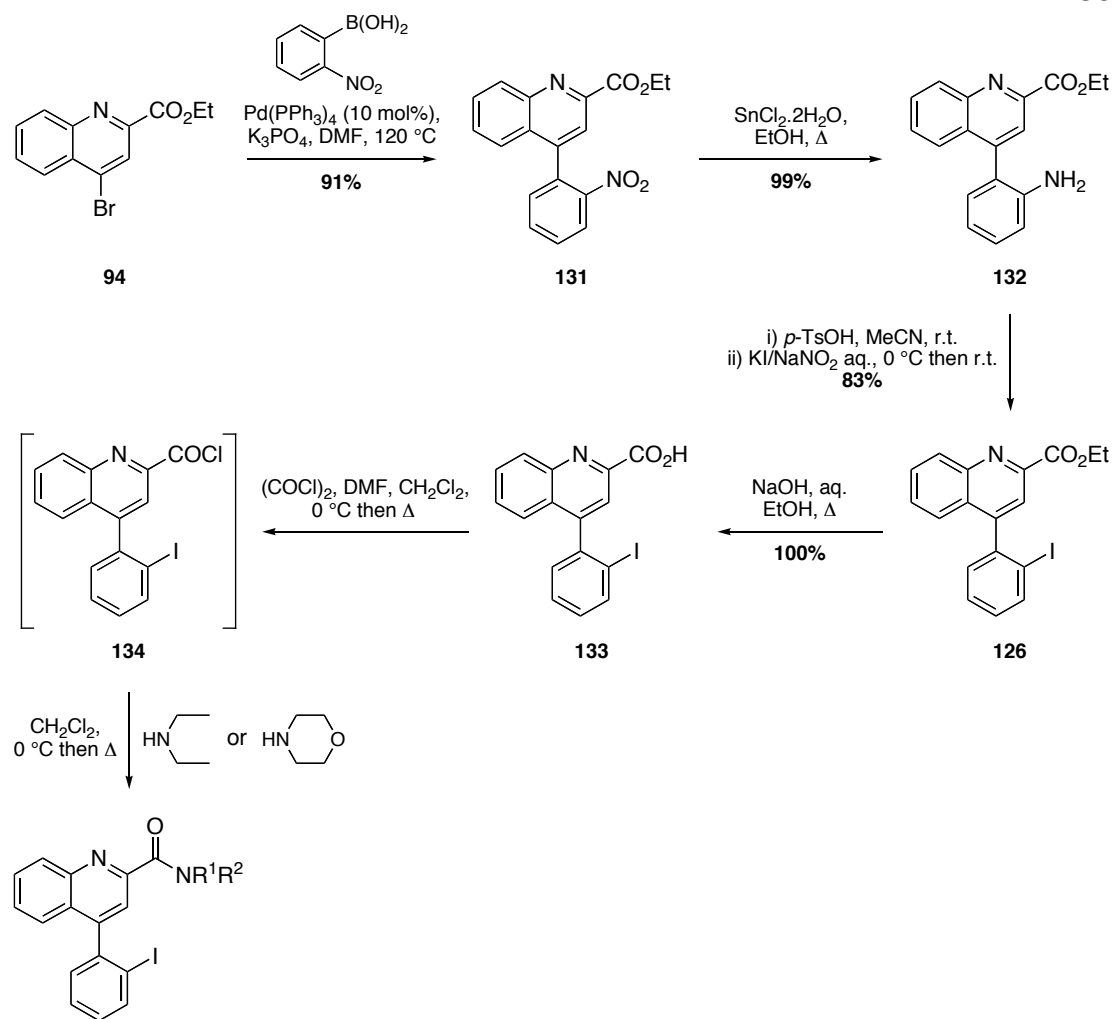
Scheme 29. Synthesis of potential SPECT compounds **120** and **121**

In addition to conferring high binding affinity to its biological target and displaying the appropriate physicochemical properties, the development of a compound as a potential imaging agent relies heavily on the ability to radiolabel a suitable precursor. Regrettably, attempts to incorporate the iodine atom into the quinoline core *via* the more traditional methods of direct halogen exchange and sequential stannylation/iodo-destannylation, both of which have been adapted for radiolabelling procedures, had failed.[112,52] Nevertheless, Pasternak and co-workers have reported conditions for the radioiodination of fully deprotected peptides, which proceed *via* a diazotisation/Sandmeyer sequence.[113] Therefore, if either target compound shows potential as a SPECT imaging agent for the TSPO, the conditions described in the literature could be trialed as a means of incorporating radioactive iodine into the appropriate molecule.

2.1.2.4 Attempted Synthesis of an Additional SPECT Compound

In addition to analogues **120** and **121**, quinoline-2-carboxamide **135** (Figure 17) was also identified as a compound of interest. Prior investigations within the Sutherland group had shown that the presence of a substituent *para*-to the quinoline ring had a detrimental effect on the compounds ability to successfully bind to the TSPO. It was therefore of interest to investigate the effect a large substituent such as iodine at the *meta-* position would have on TSPO binding.
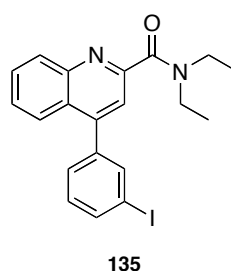
Figure 17. Potential SPECT imaging agent

Synthesis of the bromide precursor of **135** was achieved in four steps (Scheme 30), utilising the synthetic chemistry described for previous analogs. 4-Bromoquinoline **94** was coupled to 3-bromophenylboronic acid under standard Suzuki cross-coupling conditions to give biaryl compound **136** in a good 78% yield. Hydrolysis of the ethyl ester group afforded carboxylic acid **137** in an excellent 94% yield. Finally, conversion of the carboxylic acid to diethyl amide **139**, by reaction of acid chloride **138** with diethylamine, was achieved in a moderate yield of 57% over two steps.
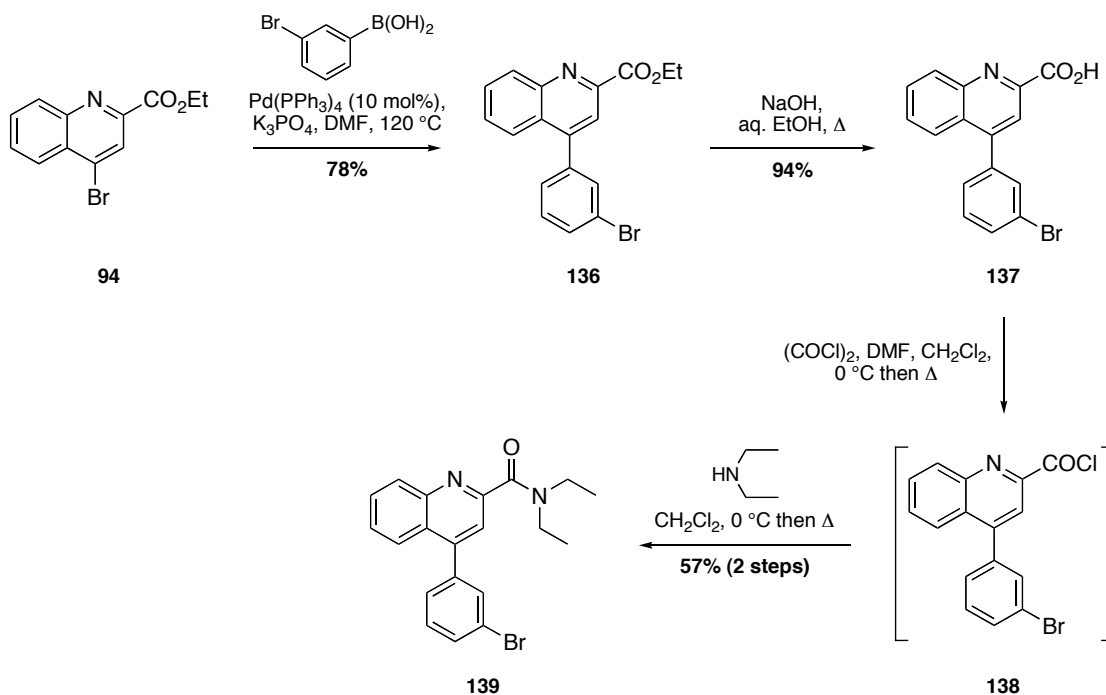
Scheme 30. Synthesis of bromide precursor **139**

In order to complete the synthesis of potential SPECT compound **135**, replacement of the bromine atom for iodine was imperative. Previous attempts at performing a copper(I)-catalysed direct halogen exchange reaction on bromide **122** had shown limited success when applied to a microwave reaction (Scheme 25, Table 4; Entry 4). However, when these conditions were applied to bromide **139**, analysis of the crude reaction mixture by ^{1}H NMR spectroscopy indicated the presence of starting material **139** only (Scheme 31).
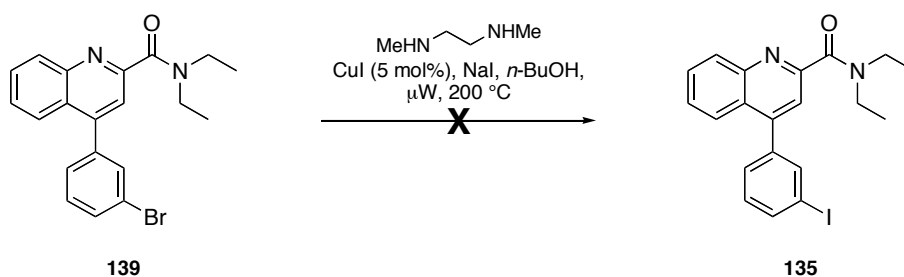
Scheme 31. Attempted halogen exchange on bromide precursor **139**

As the direct halogen exchange approach had once again failed to provide the target compound, the two-step process of stannane formation followed by iodo-destannylation was revisited (Scheme 32). Inspection of the crude reaction mixture by ^{1}H NMR spectroscopy and mass spectrometry indicated the presence of the target iodinated

compound **135**. However, a large proportion of the crude reaction mixture consisted of unreacted bromide starting material **139**. Unfortunately, stringent attempts to isolate the iodinated product from the bromide starting material by flash column chromatography were unsuccessful due to their close running proximity on the silica column.
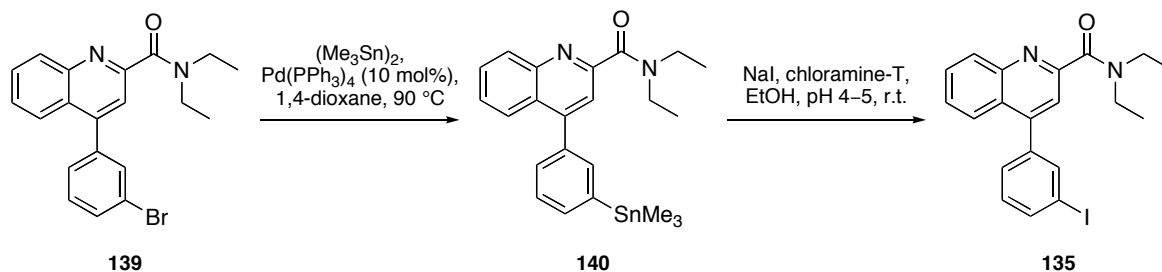
Scheme 32. Attempted synthesis of compound **135** *via* stannane **140**

In the interest of time, the synthesis of this additional target compound was not pursued further. Should it be revisited as part of a future research initiative, focus should center on ensuring the complete conversion of the bromide starting material **139** to the stannane **140**.

The synthesis of potential PET and SPECT imaging agents **80–86** and **120–121** was achieved through application of a well developed route utilising two key steps for diversification: the Suzuki-Miyaura cross-coupling reaction and amide formation using different secondary amines. Attention now turned to a new shorter synthetic route for the preparation of iodinated and fluorinated quinoline-2-carboxamides that could have potential as molecular imaging agents.

2.1.3 Multicomponent Reactions: Synthesis of Potential SPECT and PET Compounds

Despite a great deal of research centred on development of a novel TSPO imaging agent, incorporation of a radioisotope on the phenyl ring of the quinoline core has never been considered. To account for this, we aimed to prepare a series of ligands bearing a fluoride or iodide atom in the 6-position of the quinoline ring (Figure 18). In essence, incorporation of the halogens would allow us to probe the effect a substituent at this position has on binding affinity with the protein, and provide an easily accessible radiolabelling position for [123I]- or [18F]-incorporation if development into a PET and/or SPECT imaging agent for TSPO is deemed appropriate.
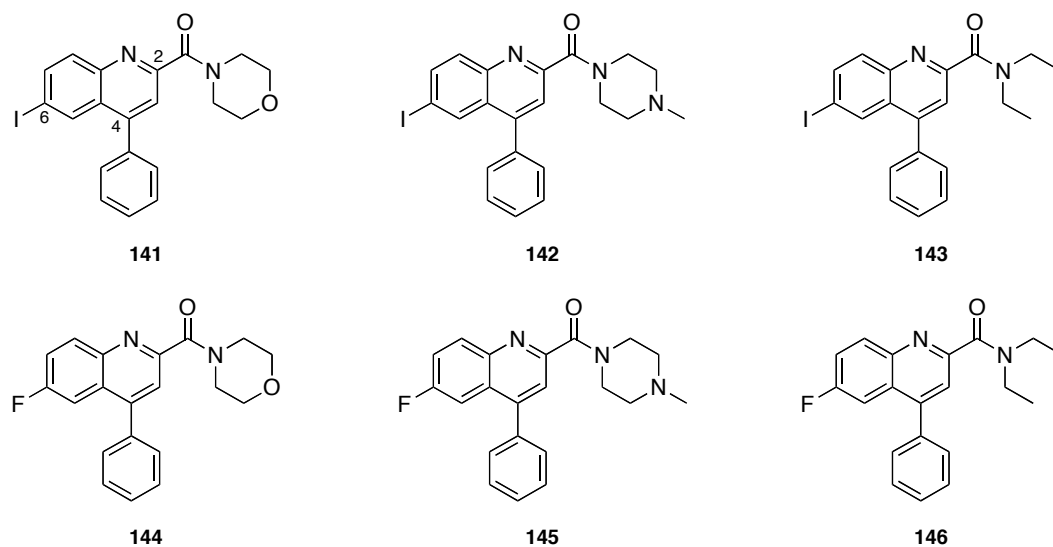
Figure 18. Potential SPECT and PET imaging agents

2.1.3.1 Retrosynthetic Analysis of PK11195 Analogues 141–146

The retrosynthetic analysis of the target SPECT and PET compounds **141–146** is shown (Scheme 33). Disconnection of the amide bond gives carboxylic acid intermediates **147** and **148**, which can in turn be prepared *via* a functional group interconversion from the ethyl esters **149** and **150**. A further disconnection of the quinoline ring gives commercially available phenylacetylene (**151**) and imines **152** and **153**, which are prepared *in situ* from commercially available ethyl glyoxalate solution, 4-iodoaniline (**155**) and 4-fluoroaniline (**156**), respectively.
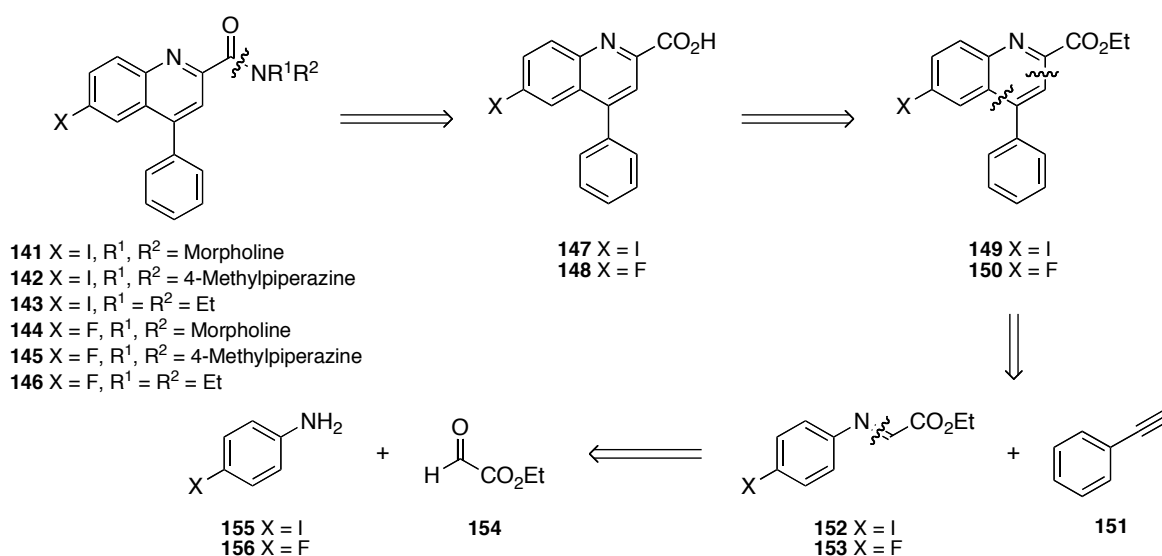
Scheme 33. Retrosynthetic analysis of PET and SPECT compounds **140–146**

The proposed synthetic route will utilise a key molecular iodine-catalysed three-component, one-pot process for the synthesis of the desired quinoline-2-carboxylate intermediates **149** and **150**. The advantages of utilising this chemistry are that it enables the efficient preparation of the substituted quinoline core structure in one step, and also allows for the incorporation of an iodide and fluoride in the 6-position of the quinoline ring. Furthermore, this route could be used for synthesis of a radiolabelling precursor by utilising bromo- or nitroaniline starting materials for [^{123}I]- and [^{18}F]-incorporation, respectively.

2.1.3.2 Synthesis of Potential SPECT and PET Compounds 141–146

In 2011, Li *et al.*, reported the synthesis of substituted quinoline-2-carboxylates using a molecular iodine-catalysed multicomponent reaction.[114] These conditions were utilised to rapidly assemble quinoline-2-carboxylates **149** and **150** in yields of 50% and 57%, from reaction of 4-iodoaniline (**155**) or 4-fluoroaniline (**156**) with ethyl glyoxalate (**154**) and phenylacetylene (**151**), respectively (Scheme 34).
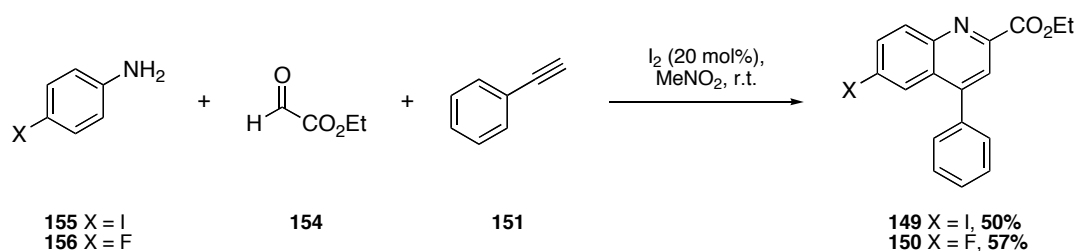
Scheme 34. Three-component synthesis of quinoline-2-carboxylates **149** and **150**

A proposed reaction sequence for this one-pot, three component process is illustrated in Scheme 35.[114] Initially, a condensation reaction between 4-iodoaniline and ethyl glyoxalate gives imine **157**, which undergoes an iodine-catalysed imino-Diels-Alder reaction with phenylacetylene (**151**). Isomerisation of intermediate **158**, and subsequent oxidation of the resulting dihydroquinoline **159**, affords substituted 6-iodoquinoline **149**.
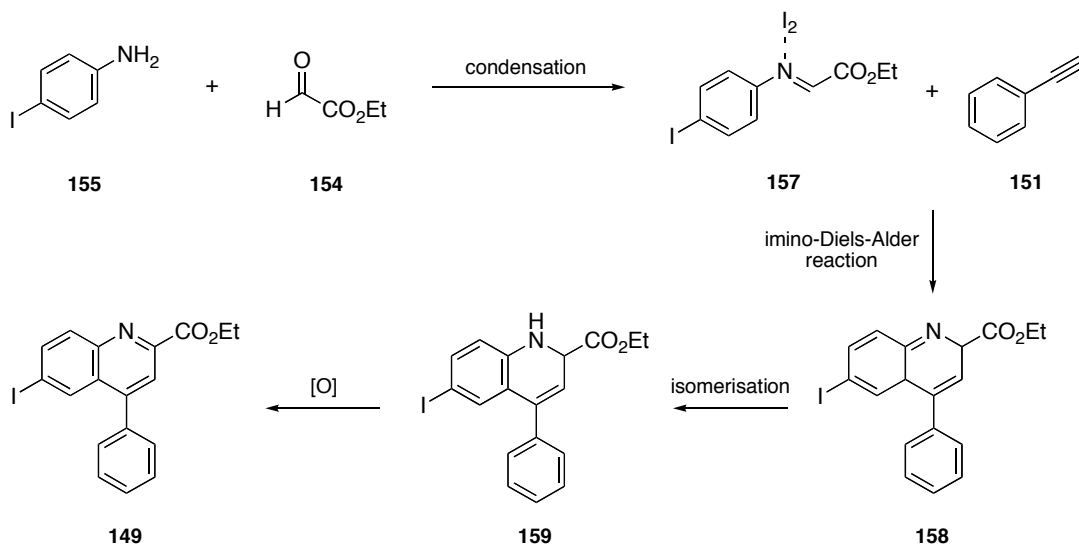
Scheme 35. Proposed reaction sequence for synthesis of 6-iodoquinoline **149**

Preparation of the target compounds was then achieved using the standard synthetic route (Scheme 36). Hydrolysis of the ethyl ester under basic conditions gave carboxylic acids **147** and **148** in yields of 70% and 82%, respectively. 6-Iodoquinolines **141**, **142** and **143** were then prepared in yields of 92%, 46% and 31% by reaction of acid chloride **160** with morpholine, 1-methylpiperazine and diethylamine, respectively. Similarly, 6-fluoroquinolines **144**, **145** and **146** were prepared in yields of 61%, 56% and 28% from the reaction of acid chloride **161** with morpholine, 1-methylpiperazine and diethylamine, respectively.
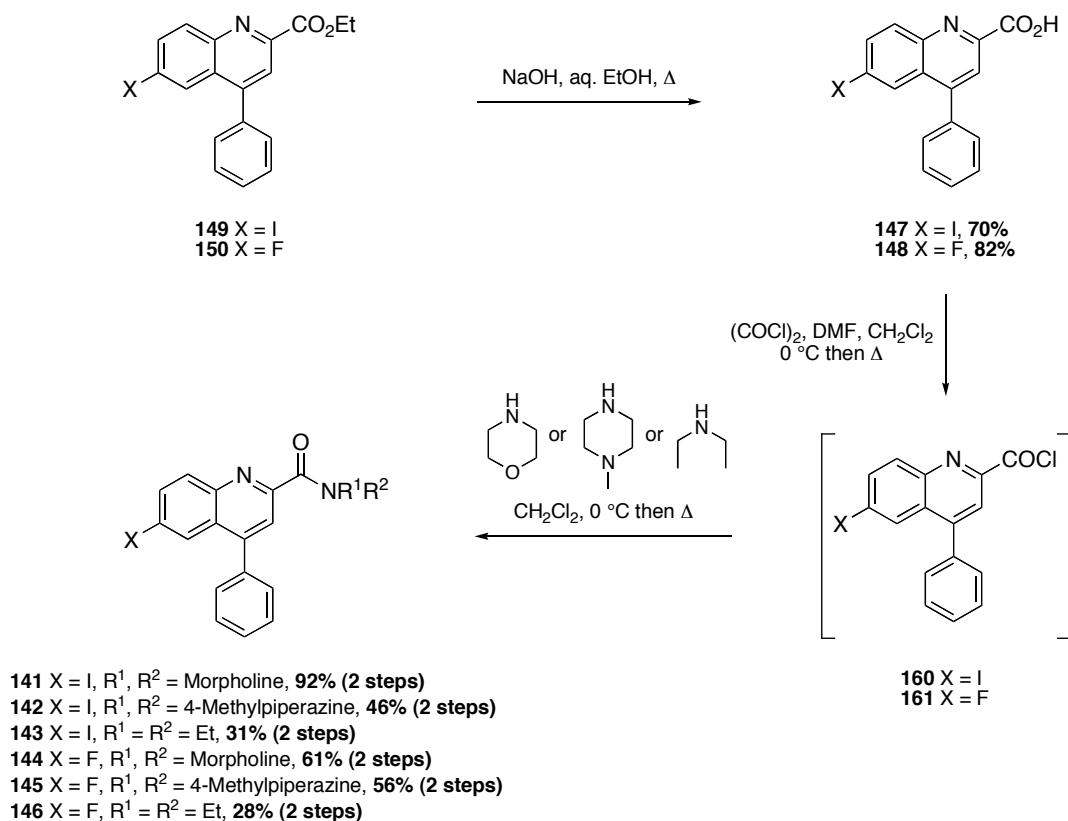
Scheme 36. Synthesis of potential SPECT and PET compounds **141–146**

2.1.3.3 Synthesis of an Additional SPECT Compound

8-Iodoquinoline **162** (Figure 19) was also identified as a potential TSPO imaging agent, and it was anticipated that the same synthetic approach used for compounds **141–146** could be employed for the synthesis of this unlabelled analogue.

162
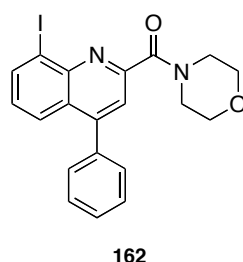
Figure 19. Potential SPECT imaging agent

Initial attempts to prepare quinoline-2-carboxylate **164** utilising the molecular iodine-catalysed method were unsuccessful, with complex mixtures containing starting material forming (Scheme 37). A subsequent search of the literature provided an alternative

procedure by Huang *et al.*, employing a catalytic quantity of copper(II) triflate, for the one-pot tandem synthesis of **164**.[115] This method however also proved ineffective for the preparation of the 8-iodoquinoline core. Monitoring the progress of the reaction using TLC indicated slow consumption of the 2-iodoaniline starting material, and again formation of an unidentified compound mixture.
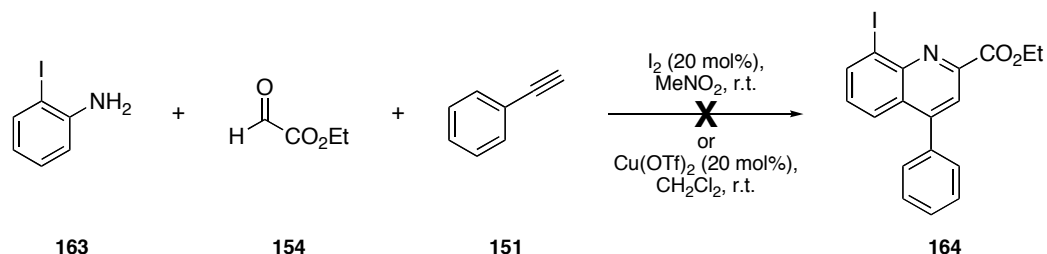
Scheme 37. Attempted one-pot multicomponent synthesis of quinoline-2-carboxylate **164**

A slight modification to the synthetic route proved successful for the preparation of the target compound (Scheme 38). Condensation of 2-iodoaniline (**163**) and ethyl glyoxalate (**154**) separately at ambient temperature, using magnesium sulfate as the dehydrating agent, afforded imine **165**. This intermediate was then reacted with phenylacetylene (**151**) in the presence of catalytic copper(II) triflate to give 2-iodoquinoline **164** in a 22% yield, which was sufficient for completion of the synthetic route. Hydrolysis of the ester group, followed by conversion to the acid chloride and treatment with morpholine gave the 8-iodoquinoline-2-carboxamide **162** in yields of 84% and 57%, respectively.
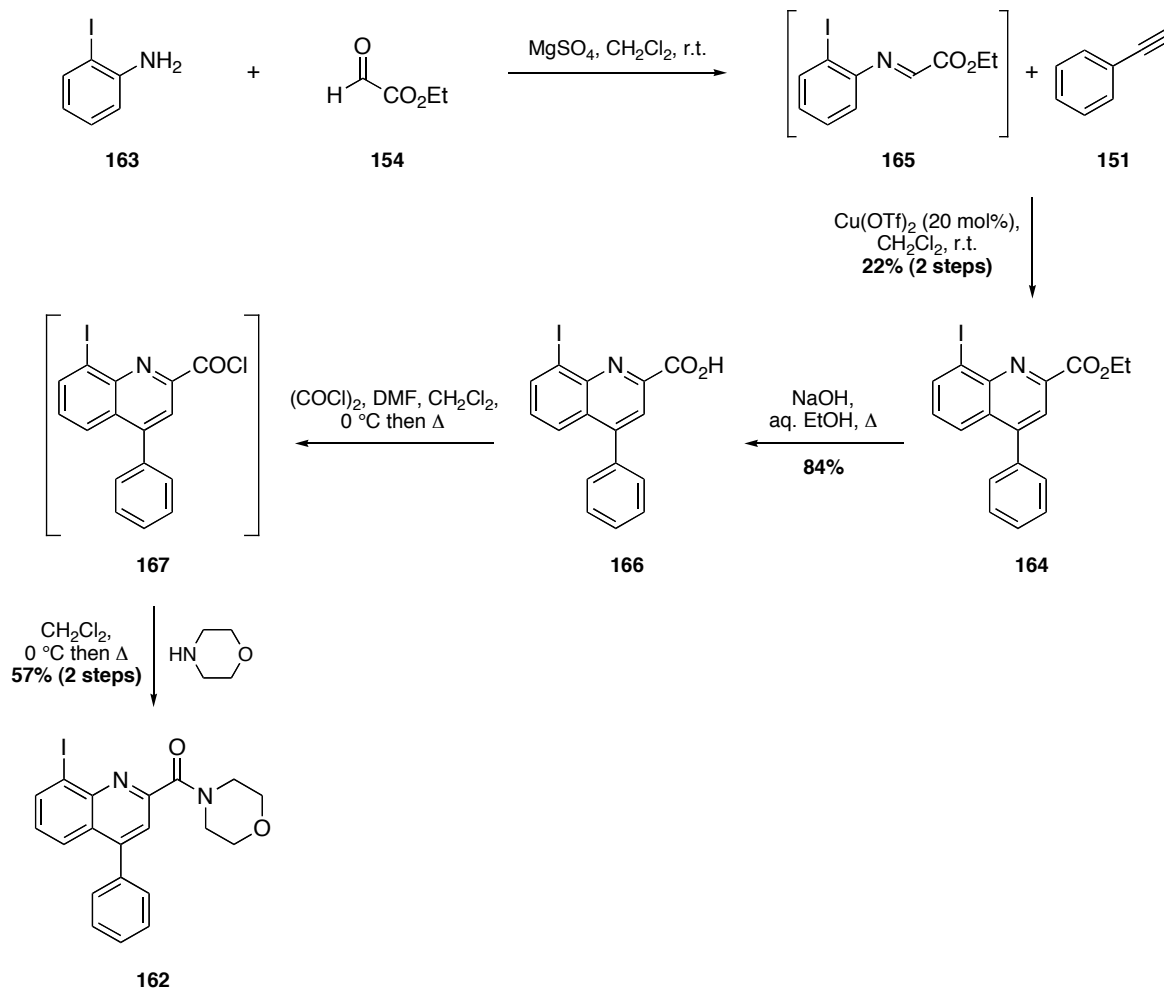
Scheme 38. Synthesis of potential SPECT compound **162**

The low yields obtained for the two-step synthesis of the 2-iodoquinoline core resulted from difficulties separating the desired compound from an unidentified side-product. Chan and co-workers have reported that the copper-catalysed Grignard-type addition of an acetylene to imine forms a propargylic amine.[116] It is proposed that this intermediate then undergoes Friedel-Crafts alkenylation affording the target quinoline core.[115] However, oxidation of the propargylic amine to the corresponding imine prevents this final step occurring. Inspection of the ^{1}H NMR spectrum of the crude reaction mixture indicates that this may be the unidentified side-product, however, isolation and full characterisation is necessary to confirm this.

With a library of sixteen potential TSPO imaging agents in hand, attention now turned to measurement of their physicochemical properties.

2.1.4 Investigation of Physicochemical Properties

A defining feature of higher organisms is the existence of a central nervous system (CNS), which comprises the brain and spinal chord. Despite the substantial blood flow serving the brain, seminal work by Ehrlich and Goldmann proved that the brain and its blood supply were in fact separate.[117] Numerous studies performed since then have shown that the separation of the blood from the CNS is achieved by the presence of two key physiological barriers: the blood brain barrier (BBB) and the blood-cerebrospinal fluid barrier (BCSFB).[118]

2.1.4.1 Blood Brain Barrier

The BBB is formed by a monolayer of cerebrovascular endothelial cells connected by complex tight junctions, with enhanced structural and functional support contributed from pericytes and astrocyte end-feet (Figure 20).[117]
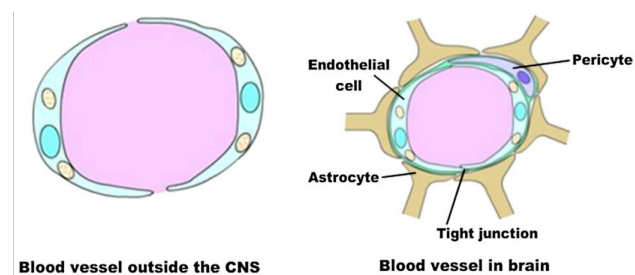
Figure 20. Structure of BBB[117]

(Reprinted from A. M. Palmer, *Neurobiol. Dis.*, 2010, **37**, 3. Copyright 2010, with permission from Elsevier)

Separation of the brain from its blood supply, and the extremely constrained movement of molecules across the BBB result almost entirely from the junctions between adjacent endothelial cells: tight junctions and adherens junctions (Figure 21).[119] Adherens junctions are responsible for maintaining the structural integrity of the BBB by ensuring that adjacent cells are held together and accomplish this role by the interaction of cadherin and catenin proteins through the intercellular cleft.[119] Adherens junctions are crucial for tight junction formation. Tight junctions are composed of three integral proteins: occludin, the claudins and junctional adhesion molecules. These proteins form complexes, which are linked to the cytoskeleton of adjacent cells by interaction with additional cyctoplasmic

proteins such as the zonula occludens.[119,120] The presence of these tight junctions force the majority of molecules to traverse the BBB in a transcellular rather than paracellular fashion, which restricts the entry and exit of molecules from the brain.[121]
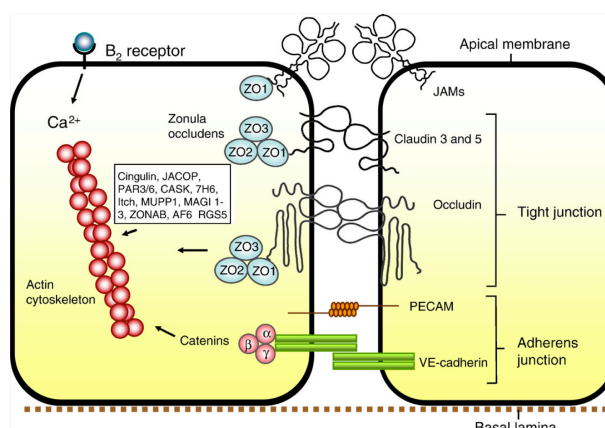
Figure 21. BBB tight junctions[119]

(Reprinted from N. J. Abbot, A. A. K. Patabendige, D. E. M. Dolman, S. R. Yusof and D. J. Begley, *Neurobiol. Dis.*, 2010, **37**, 13. Copyright 2010, with permission from Elsevier)

Several functions are associated with the BBB including being concerned with the supply of essential nutrients to the brain, removal of metabolites through efflux mechanisms, separation of CNS neurotransmitters from the peripheral system and *vice versa*, and the prevention of toxic and infective agents entering the brain.[120,122]

2.1.4.2 Partition Coefficient

The lipophilicity of a compound is determined experimentally as the partition coefficient, and defined as the ratio of concentrations of a compound in a mixture of two immiscible layers at equilibrium.[123] It is usually displayed as the logarithmic form of the octanol-water partition coefficient, Log$P$ (Figure 22), and plays a crucial role in the absorption, distribution, metabolism and elimination characteristics of a compound.[124] Measurement of a compound's Log$P$ is therefore the most widely used indicator for predicting its ability to cross biological membranes.

$$\mathrm{Log}P \;=\; \mathrm{Log}\;\left(\dfrac{[\mathrm{Compound}]_{octanol}}{[\mathrm{Compound}]_{water}}\right)$$

Figure 22. Equation for calculating Log*P* of a compound

The partition coefficient of a molecule is traditionally measured using the flask method, however, there are some disadvantages associated with this technique; it is time consuming, not suitable for all compounds, and influenced by the presence of impurities. Other, more modern methods, circumventing these problems include *in silico* and HPLC methods.[125,126] In particular, HPLC confers the ability to screen large numbers of compounds, and as a technique, it is fast, reliable and reproducible. It does however, have its own limitations, and the most poignant being that it is only able to model hydrophobic compound-membrane interactions.[127]

2.1.4.3 Membrane Partition Coefficient and Permeability

Development of a compound intended for the CNS must take into consideration its ability to cross brain capillary endothelial cells. Penetration of the BBB can therefore be greatly affected by solute-membrane interactions. A characteristic equilibrium constant for partitioning into a compound-lipid membrane mixture can be derived for every compound and, is defined as the membrane partition coefficient (K_m). This physicochemical measurement can be estimated using immobilised artificial membrane (IAM) chromatography as it can model hydrophobic and electrostatic interactions. IAM columns are designed to mimic the lipid surface of fluid cell membranes, and are prepared by covalently imobilising phospholipid analogues onto the chromatographic support (Figure 23).[128,127]
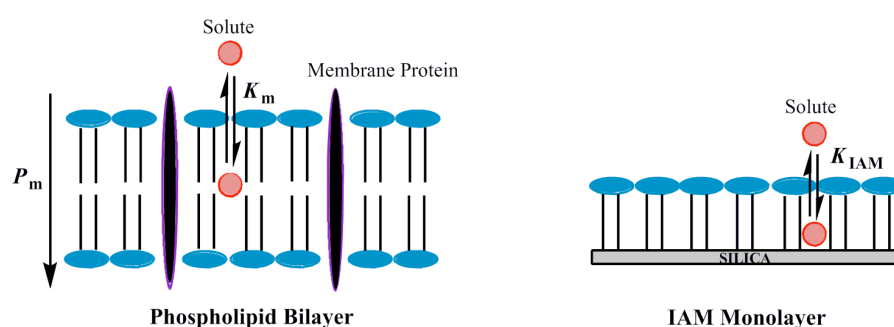
Figure 23. Solute binding to fluid membranes

However, it is important to bear in mind that K_m cannot be used to directly predict membrane transport, as cellular membranes consist of a lipid bilayer. When a compound enters the cytosol it does so by passing through the first lipid membrane. In order to exit, it must then penetrate a second lipid membrane meaning that equilibrium partitioning occurs four times overall. To account for this, an additional measurement is required: permeability (P_m). Permeation of a molecule is directly proportional to K_m (Figure 24a), where D_m is the membrane diffusion coefficient and L is the membrane thickness. Furthermore, D_m is inversely proportional to molecular size, and assuming that molecular weight (MW) is proportional to molecular size and membrane thickness remains constant, P_m can be calculated from K_m (Figure 24b).[128,129]

$$\text{a)} \quad P_m = \frac{D_m K_m}{L} \qquad\qquad \text{b)} \quad P_m = \frac{K_m}{MW}$$

Figure 24. Equations relating K_m and P_m

Limitations to this methodology do exist, including the assumption of passive diffusion across the BBB. It is well known that other forms of active transport mechanisms and efflux pumps are utilised by the BBB,[118] and that this should be considered when applying IAM chromatography for compound selection.

2.1.4.4 Plasma Protein Binding

When a compound intended for the CNS enters the blood stream, in addition to the challenge of crossing the BBB, it also faces potential binding to proteins present in blood serum. Many plasma proteins exist with human serum albumin (HSA) and α_1-acid glycoprotein (AGP) being the two most abundant.[130] If a compound exerts high plasma protein binding, this can have several implications for drug and radiotracer development, including low brain penetration and low blood clearance.[131] A low level of brain penetration results from a reduction in the fraction of unbound compound available to cross the BBB, and is attributed to high lipophilicity. Consequently, deposition of the radiotracer within peripheral organs is often observed.[132] Overall, these notable problems can have a considerable effect on the quality and accuracy of image and data acquisition.

Valko *et al*., have developed a fast and simple HPLC method, utilising a HSA modified chromatographic material to determine plasma protein binding associated with a particular compound.[131]

2.1.4.5 HPLC Measurement of Physicochemical Properties

Tavares *et al*., have indicated that a compounds physicochemical properties can be used to predict its ability to penetrate the BBB.[133] Correlations between HPLC derived measurements and *in vivo* data were established and parameters set to aid lead compound selection (Table 6). However, it should be emphasised that these parameters are for compound ranking and guidance purposes only. The overriding advantages of this method are that it is quick, reproducible and enables the rapid elimination of unsuitable analogues. Percentage injected dose (% ID) and binding potential (BP$_{ND}$) are commonly used indicators of radiotracer performance,[134] and will facilitate compound selection for radiotracer development.

Parameter	HPLC Measurement	Predicted *in vivo* Measurement
P_m	< 0.5	ID > 4.0%
K_m	< 250	BP$_{ND}$ > 2.0*
%PPB	< 95%	ID > 2.0%

* BP$_{ND}$ defined at equilibrium as the ratio of specifically bound to non-displaceable radiotracer
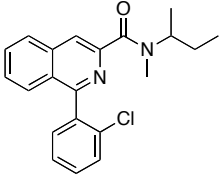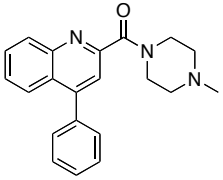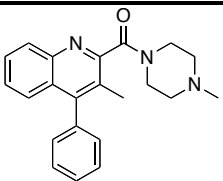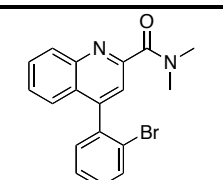
Table 6. Proposed selection criteria for aiding lead compound identification

The library of quinoline-2-carboxamides was subject to the HPLC methods described, and the physicochemical properties of each compound measured (Table 7). PK11195 was included as the standard enabling direct comparison.

An initial observation highlights that the HPLC measured *c*Log*P* values are generally greater than the recommended 1–3.5 for CNS compounds,[132] with the exception of analogues **84** and **86**. The *c*Log*P* values obtained from ChemDraw Ultra 9.0.1 are also included, and a striking lack of consistency amongst the two methods is evident. For some analogues, there is very little difference between the two measurements. However, an obvious discrepancy for others exists, *e.g.* a difference of 2.89 versus 4.37 for *in silico* and
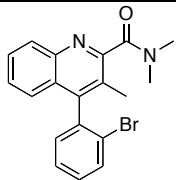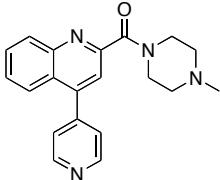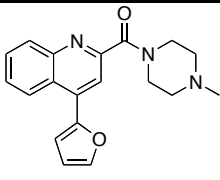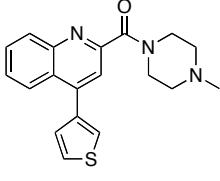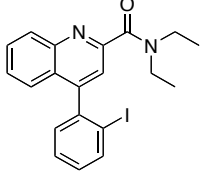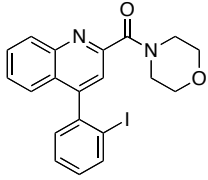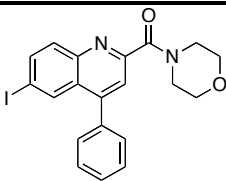
HPLC values, respectively are observed for **85**. This lack of method uniformity has been observed by others,[133] and is why additional physicochemical measurements for P_m, K_m and %PPB are obtained.

Based on these additional HPLC measurements, ten compounds in total were selected as displaying physicochemical properties within (blue), or only marginally outside of (red), defined parameters. Inclusion of an iodine atom has a noticeable effect on a compound's lipophilicity, with the majority eliminated from future studies. Ideally, all compounds would be subject to biological investigation, but due to limited resources only those with the correct physicochemical profile or ability to contribute to the SAR were selected. This reasoning forms the basis for selection of iodoquinoline **120** and exclusion of **81**.

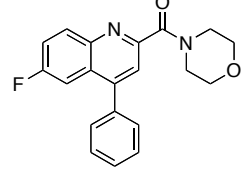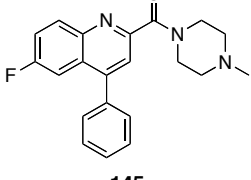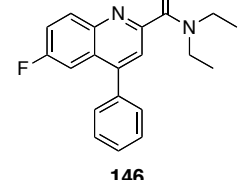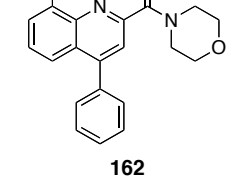| Structure	cLogP^a	LogP^b	$P_m{}^c$	$K_m{}^c$	%PPB^d
PK11195	4.62	3.85*	0.65	229.36	91.51
80	3.50	3.77	0.56	185.59	81.67
81	3.70	3.89	0.46	158.90	85.66
82	3.35	4.11	0.29	103.02	91.87
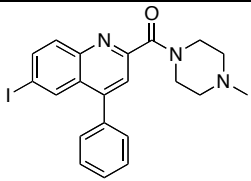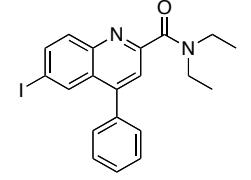
* Taken from literature.[133] Physicochemical properties determined using ^{a} ChemDraw Ultra 9.0.1, ^{b} C$_{18}$ column (mean ± SD, n = 3), ^{c} IAM column, and ^{d} HSA column (mean ± SD, n=3)

Table 7. *In silico* and HPLC determined physicochemical properties

Structure	$cLogP^a$	$LogP^b$	P_m^c	K_m^c	%PPB^d
83	3.55	4.46	**0.20**	**73.85**	**92.81**
84	2.10	2.39	**0.12**	**39.89**	**39.45**
85	2.89	4.37	**0.47**	**158.60**	**78.90**
86	3.19	3.29	**0.35**	**112.48**	**79.02**
120	4.47	5.53	0.67	287.03	94.09
121	3.57	4.58	**0.26**	**115.34**	**91.24**
141	4.09	5.19	**0.55**	**244.35**	**95.38**

Physicochemical properties determined using [a] ChemDraw Ultra 9.0.1, [b] C_{18} column (mean ± SD, $n = 3$), [c] IAM column, and [d] HSA column (mean ± SD, $n = 3$)

**Table 7 (cont.).** *In silico* and HPLC determined physicochemical properties

Structure	$c\text{Log}P^a$	$\text{Log}P^b$	$P_m{}^c$	$K_m{}^c$	$\%\text{PPB}^d$
142	4.66	4.77	0.99	452.74	93.88
143	4.99	6.30	1.42	611.00	96.69
144	3.11	4.37	**0.25**	**84.09**	**87.75**
145	3.68	4.02	0.73	255.06	82.11
146	4.01	5.42	0.62	199.81	92.01
162	4.09	5.69	**0.41**	**182.15**	**98.19**

Physicochemical properties determined using [a] ChemDraw Ultra 9.0.1, [b] C_{18} column (mean ± SD, $n = 3$), [c] IAM column, and [d] HSA column (mean ± SD, $n = 3$)

Table 7 (cont.). *In silico* and HPLC determined physicochemical properties

In addition to BBB penetration, a high binding affinity with the molecular target is essential for an imaging agent targeting the brain. Having selected eleven analogues for progression, the next stage of the project involved biological investigation.

2.1.5 Biological Evaluation

Quantification of the *in vitro* binding interactions of each compound for the TSPO was determined using a competitive binding assay with whole rat brain homogenate. The inhibition constant (K_i) of a ligand denotes affinity of a ligand for a receptor and is defined as the concentration of unlabelled competing ligand that occupies 50% of binding sites in the presence of radioligand at equilibrium.[135] Generation of a sigmoidal dose response curve by plotting radioligand binding (disintegrations per minute) versus log[unlabelled ligand], provides a means from which the K_i value of a compound can be calculated. A representative competition binding curve for PK11195 is illustrated (Figure 25a).

Two important features of a competition binding experiment must be taken into consideration: total binding and non-specific binding. Total binding refers to the binding of a radiolabelled ligand in the absence of a competitor and is represented by the top plateau of the binding curve. In addition, ligands have a tendency to bind to components other than the sites of interest, *e.g.* membranes and other protein receptors, and are referred to as non-specific binding. This characteristic can be measured by exploiting the saturability of the protein target, and is achieved experimentally by addition of a large excess of the unlabelled ligand in the presence of a much lower concentration of isotopically labelled ligand. The bottom plateau of the curve represents non-specific binding. The specific binding of a ligand is therefore calculated by subtracting non-specific binding from total binding.

The K_i of a compound is the equilibrium point in the curve, and is calculated from the IC_{50} value using the Cheng-Prusoff equation (Figure 25b),[136] where IC_{50} is the half maximal inhibitory concentration, $[L]$ is the concentration of free radioligand, and K_d is the equilibrium dissociation constant for radioligand binding to the receptor. This calculation was performed by non-linear regression analysis using GraphPad Prism 4.0 (GraphPad Software Inc).

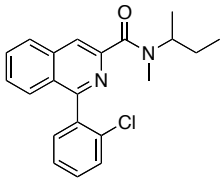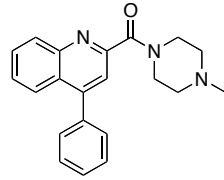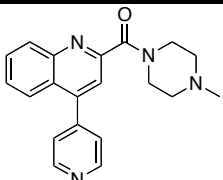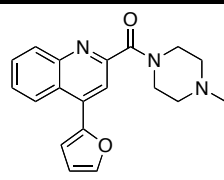a)

b)

$$K_i = \frac{IC_{50}}{1 + \dfrac{[L]}{K_d}}$$
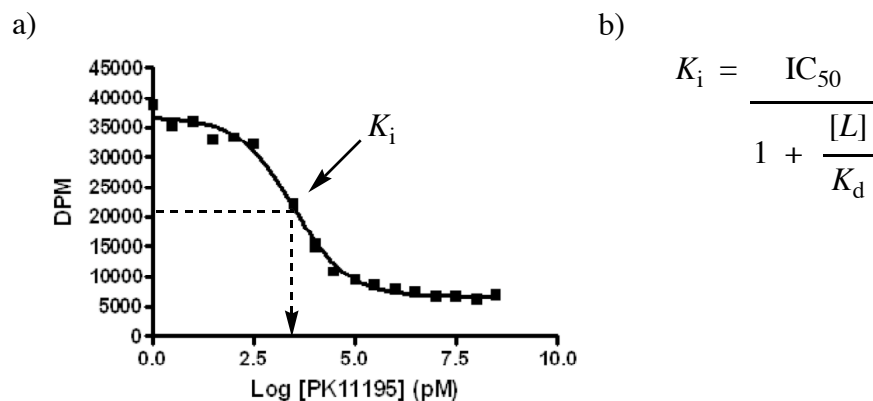
Figure 25. a) Representative PK11195 sigmoidal dose response curve, and b) Cheng-Prusoff equation

The binding affinities of the quinoline-2-carboxamides selected are listed (Table 8). From the results obtained it is evident that replacement of the pendant phenyl ring of the ligand has a negative impact on binding affinity with the TSPO. Compared to **80**, with a low K_i value of 1524 nM, substitution of the phenyl for a heterocyclic moiety further reduces binding affinity, as illustrated by quinoline-carboxamides **84–86**. The K_i values obtained for these analogues ranged from approximately 5000–100000 nM. It has been proposed that the pendant phenyl provides a dispersive, space filling role enabling binding within the hydrophobic binding pocket of the TSPO.[137] A reasonable conclusion may therefore be that despite imparting more favourable physicochemical properties on the molecule, replacement of the phenyl ring with an alternative heterocycle greatly diminishes binding affinity with the TSPO.

It was anticipated that the presence of the *ortho*-bromide substituent on the phenyl ring of **82** would generate a more rigid molecule, resulting in an increase binding affinity with the protein, but the K_i value of this compound was found to be in the low micromolar range (3600 nM). It is probable that the dimethyl amide side chain is too small for effective restricted rotation of the amide bond, resulting in low binding affinity with the TSPO. Incorporation of a 3-methyl group in the quinoline ring of **83**, however, results in a substantial increase in potency by affording a K_i value of 103 nM. The proximity of the methyl group at the C-3 position to the dimethyl amide may provide enough steric interference to restrict rotation of this bond, encouraging a greater H-bonding interaction with a carboxylic acid side chain within the lipophilic binding pocket of the protein.[138]

Morpholine amide **121** was shown to have a relatively low binding affinity for the protein with a K_i value of 929 nM. This was a somewhat surprising outcome, and may be due to the inability of the ligand to adopt the optimum binding conformation, resulting from the presence of the large *ortho*-iodine atom and the relatively large amide side chain. However, a more favourable binding affinity for TSPO was found with diethyl amide compound **120**. The K_i value of this compound was measured at 5.01 nM, which when compared to the PK11195 standard, shown to be twice as potent. This result shows that the large *ortho*-iodine atom provides enough steric bulk to restrict rotation of the diethyl amide effectively, advantageously allowing greater electrostatic interactions with the protein.
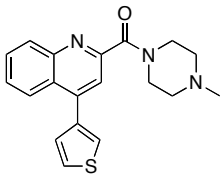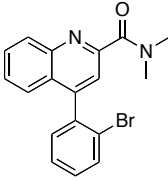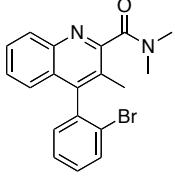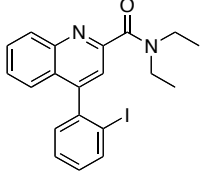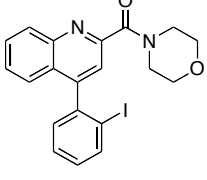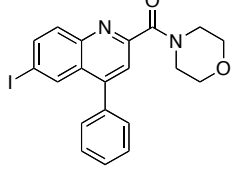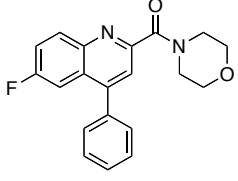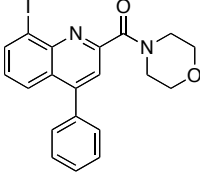
Compounds **141** and **162** were found to have a particularly low binding affinity for the TSPO, with K_i values of 29890 and 76100 nM, respectively. It is evident from these results that the inclusion of an iodine atom at both the 6- and 8-position of the benzene ring of the quinoline moiety has a very negative effect on binding to the target protein. Furthermore, compound **144** bearing a fluorine atom at the 6-position of the quinoline was deemed to have greater than 5-fold increase in binding affinity with the TSPO compared to the analogous iodide compound. Overall, these results demonstrate that the presence of a much larger substituent on the phenyl ring of the quinoline impedes binding to the protein. An unsubstituted phenyl ring appears to be required for molecular recognition of the quinoline pharamcophore.

Structure	K_i (nM)[a]	Structure	K_i (nM)[a]
PK11195	10.0 ± 0.3	80	1524 ± 309
84	99132 ± 14648[*]	85	18722 ± 228

[a] K_i values determined from independent experiments (mean ± SD, $n = 3$), except for those marked [*] (mean ± SD, $n = 2$)

Table 8. Binding affinity of quinoline-2-carboxamides with the TSPO

Structure	K_i (nM)^a	Structure	K_i (nM)^a
86	5276 ± 872	**82**	3600 ± 354
83	103 ± 7[*]	**120**	5.01 ± 1.13
121	929 ± 243	**141**	29890 ± 12090[*]
144	5738 ± 1057	**162**	76100 ± 6550[*]

^{a} K_i values determined from independent experiments (mean ± SD, $n = 3$), except for those marked [*] (mean ± SD, $n = 2$)

Table 8 (cont.). Binding affinity of quinoline-2-carboxamides with the TSPO

2.1.6 Summary

In total, sixteen PK11195 analogues with the potential for molecular imaging applications have been prepared. A combination of routine synthetic transformations in conjunction with relatively novel one-pot multicomponent reactions has enabled preparation of a small library of structurally diverse compounds. Despite repeated attempts to effect a key halogen exchange reaction for the generation of potential SPECT imaging agent for the TSPO, the *ortho*-position of the pendant phenyl ring was deemed too inaccessible. Nevertheless, an alternative diazotisation-Sandmeyer sequence was successfully employed for the preparation of these targets.

An effort to eliminate unsuitable compounds from the study, based on their lipophilicity, was achieved utilising HPLC methodologies. The behavior of each compound *in vivo* was predicted using a series of physicochemical parameters (Log$P$, K_m, P_m and %PPB) with defined limits. This enabled ranking of the compounds relative to PK11195, and those with improved properties were selected for progression to the next stage of the project. As these limits are used for guidance purposes only, certain compounds were progressed despite displaying high lipophilicity in some respects.

Having selected eleven analogues based on their physicochemical properties or interesting structure, the binding affinity of each compound with the TSPO was measured by means of a competitive binding assay. The majority of the compounds were shown to have low binding affinities with the protein with K_i values in the micromolar range. However, two novel TSPO ligands displayed nanomolar affinity with the most potent having a K_i value of 5.01 nM.

Overall, an attempt to lower compound lipophilicity with the ultimate aim of reducing non-specific binding and improving biodistribution was achieved. However, this was not achieved in conjunction with maintaining high binding affinity for the protein target.

## 2.2 Development of [^{18}F]AB5186; A Potential PET Imaging Agent for the TSPO

Results obtained from the previous study, in conjunction with information available in the literature, highlighted that a pendant phenyl ring and restricted rotation of the amide bond of the TSPO ligand was imperative for potent binding affinities. A study published by Stevenson *et al*., focusing on the development of quinoline-2-carboxamides as potential SPECT imaging agents for the TSPO reported the synthesis of compounds **168** and **169** (Figure 26) both of which displayed nanomolar affinity with the protein.[89] However, the lipophilic nature of the iodine atom creates unfavourable physicochemical properties, and renders such compounds unsuitable for targeting the brain. In an effort to overcome these problems, it was anticipated that retention of key structural features in combination with the presence of the less lipophilic fluorine atom of **170** would generate a potential PET imaging agent for the TSPO (Figure 26). Additionally, quinoline-2-carboxamide **171** has been utilised previously as a [^{11}C]-labeled TSPO ligand, and was identified as a potential target for [^{18}F]-labeling, affording it a longer half-life and utility.

168 K_i = 12.0 ± 1.3 nM   **169** K_i = 26.1 ± 4.7 nM   **170**   **171**
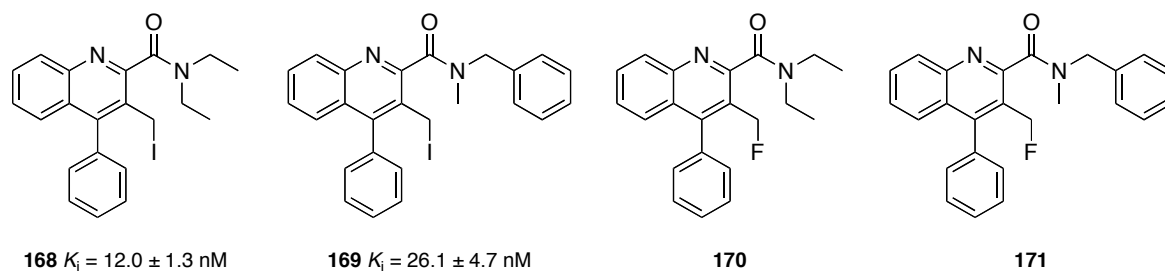
Figure 26. Potential PET Imaging agents **170** and **171**

2.2.1 Retrosynthetic Analysis of PK11195 Analogues 170 and 171

The retrosynthetic analysis of the target PET compounds **170** and **171** is shown in Scheme 39. The proposed synthetic route requires an initial functional group interconversion of the aliphatic fluoride **170** and **171** to the primary alcohol **172** and **173**. A subsequent disconnection of the amide bond results in lactone **174**, which is further disconnected at the C-O bond resulting in intermediate diol **175**. This diol can be prepared from lactone **176**, which is generated *via* intramolecular cyclisation of quinoline **177**. Finally, disconnection of the quinoline moiety of **177** affords commercially available 2-aminobenzophenone (**178**) and ethyl 4-chloroacetoacetate (**179**).
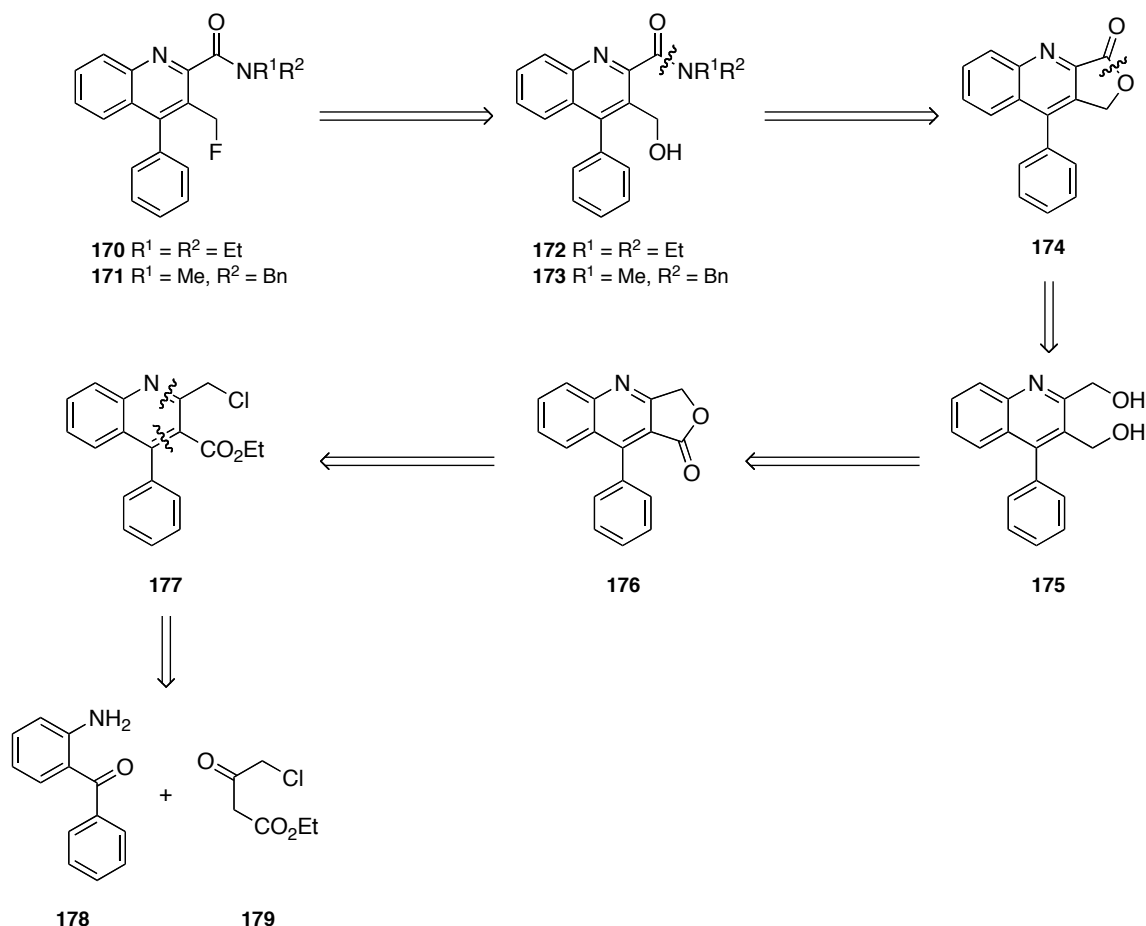
Scheme 39. Retrosynthetic analysis of PET compounds **170** and **171**

The key step in the preparation of compounds **170** and **171** is the ability to convert the primary alcohol **172** and **173** to the target 3-fluoromethyl analogues **170** and **171**. Additionally, these hydroxyl-containing compounds will also act as the radiolabelling precursors for *in vitro* and *in vivo* imaging studies.

2.2.2. Synthesis of Potential PET Compounds 170 and 171

The acid- or base-catalysed condensation reaction between an aromatic 2-amino substituted carbonyl compound and a ketone bearing a reactive α-methylene group, followed by a cyclodehydration reaction is known as the Friedländer synthesis.[139] This transformation is employed for the synthesis of substituted quinoline rings, and was used as the starting point for the synthesis of target compounds **170** and **171**. As such, quinoline **177** was prepared in an excellent 98% yield *via* a trimethylsilyl chloride-mediated Friedländer condensation between 2-aminobenzophenone (**178**) and ethyl 4-chloroacetoacetate (**179**) (Scheme 40).[140]

Scheme 40. Synthesis of quinoline **177**

The second step of the synthesis required formation of lactone **176** (Scheme 41). Initially, this reaction was performed under acidic conditions using a 6 M aqueous hydrochloric acid solution, and the desired product **176** was obtained in a 73% yield (Table 9, Entry 1). However, the drawback of this reaction was that it required stirring under reflux conditions for 4 days, to obtain acceptable quantities of product. This was deemed too inefficient for an early step in the synthesis, and so alternative reagents for the transformation were investigated (Table 9). Briefly, when trifluoroacetic acid and caesium carbonate were employed, no desired product was formed (Entries 2 and 3). A subsequent attempt using silver nitrate proved more successful,[141] with a 58% yield of lactone **176** being obtained (Entry 4). Still, a greater isolated yield was sought and a procedure by Goto and co-workers utilising dimethylsulfoxide was employed.[142] In this instance, the cyclised product **176** was obtained in a 63% yield (Entry 5), with only a 5% improvement in yield over the use of silver nitrate. Granted that the latter two reaction conditions afforded the desired product, the use of silver nitrate and dimethylsulfoxide offered lower product yields compared to hydrochloric acid, and are not highly desirable from a practical point of view.
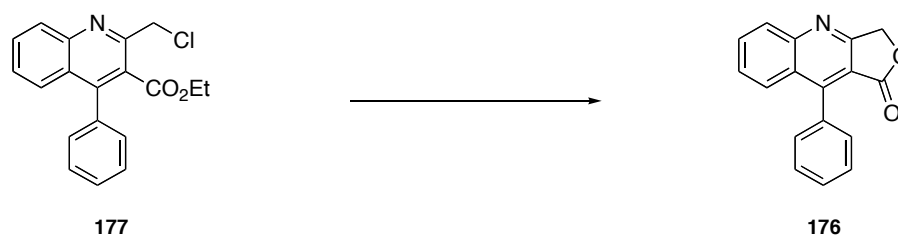

Scheme 41. Lactonisation of quinoline **177**

Entry	Reagents	Conditions	Yield 176 (%)
1	**6 M HCl**	**EtOH, Δ, 4 days**	**73**
2	TFA	r.t, 24 h	-
3	Cs_2CO_3	H_2O/MeOH, Δ, 24 h	-
4	$AgNO_3$	H_2O/1,4-dioxane, 90 °C, 72 h	58
5	DMSO	120 °C, 18 h	63

**Table 9.** Conditions trialed for lactonisation

The wish to avoid the use of these reagents and improve the overall synthesis of the target carboxamides meant that an alternative synthetic route was sought. One such route involved preparation of quinoline dicarboxylate **181** (Scheme 42). Addition of diethyl acetylenedicarboxylate (**180**) to 2-aminobenzophenone (**178**) and subsequent quinoline synthesis was initially attempted using triphenylphosphine to effect an intramolecular Wittig reaction.[143] However, only trace amounts of product were formed while trialing these conditions. On the other hand, when indium(III) chloride was employed for this reaction under solvent free conditions (Scheme 42), quinoline **181** was obtained in quantitative yield and a very short reaction time.[144] This reaction presumably proceeds *via* initial hydroamination followed by a cyclodehydration step to form the quinoline moiety.
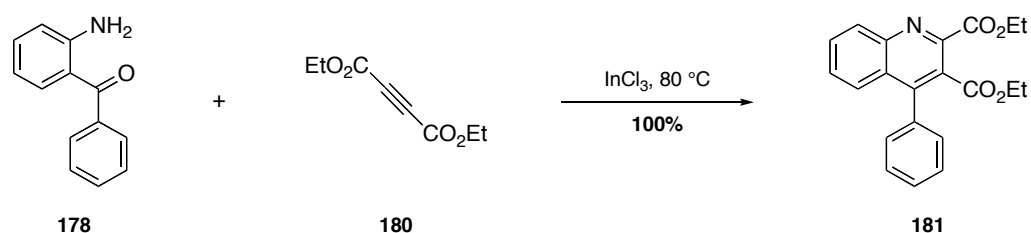
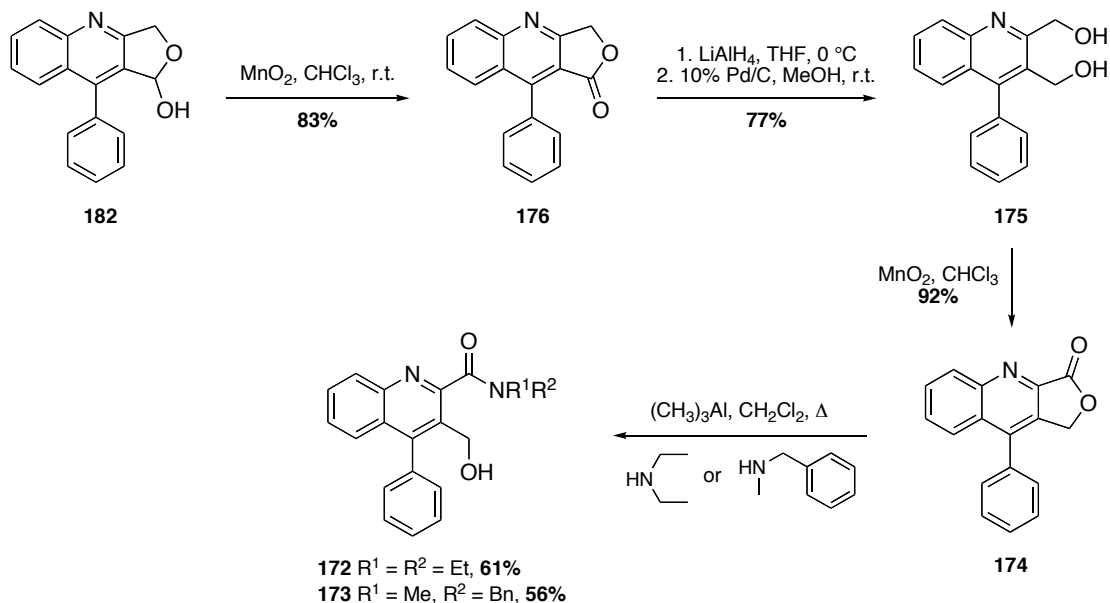**Scheme 42.** Synthesis of quinoline dicarboxylate **181**

Reduction of the ethyl ester groups of **181** to diol **175** was then necessary for continuation of the synthetic route (Scheme 43). A number of reducing agents were investigated for this transformation including diisobutylaluminium hydride, lithium aluminium hydride, lithium borohydride and sodium borohydride. Surprisingly, the majority of the reaction conditions employed did not yield the intended product, nor did the reactions progress cleanly. The main product identified from reduction of **181** with sodium borohydride was

lactol **182** (Scheme 43), and so the reaction was optimised to afford this unexpected intermediate in 93% yield.
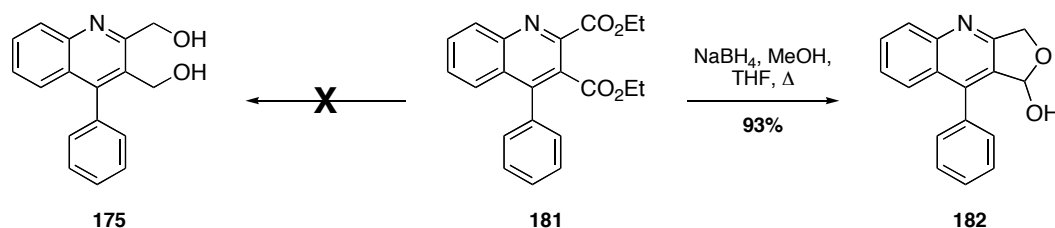

Scheme 43. Synthesis of lactol intermediate **182**

Next, oxidation of lactol **182** to lactone **176** was achieved in 83% yield using manganese(IV) oxide, and from this point, the original synthetic route could be pursued (Scheme 44). Introduction of the appropriate amide side chain within the molecule required switching the lactone from the C-3 to C-2 position, and was achieved in two steps. Firstly, reduction of the lactone to diol **175** was achieved in 77% yield using lithium aluminium hydride.[145] Small quantities of dihydroquinoline are formed during this reaction, and 10% Pd/C is added to reform the quinoline core. Subsequent regioselective oxidation, in the presence of manganese(IV) oxide converted diol **175** to the desired lactone **174** in a high 92% yield. Repositioning of the lactone functionality lends the molecule to inclusion of the appropriate amide side chains under aminolysis conditions.[138] As such, lactone **174** was reacted with diethylamine and *N*-benzylmethylamine in the presence of a trimethylaluminium solution, affording quinoline-2-carboxamides **172** and **173** in a 61% and 56% yield, respectively.

Scheme 44. Synthesis of quinoline-2-carboxamides **172** and **173**

Efforts to convert the hydroxyl group of compound **172** to an effective leaving group failed under standard conditions. Generally, a tosylate or mesylate is the leaving group of choice for substitution reactions in mainstream organic synthesis, and this is also true of radiochemistry.[146,147] As such, incorporation of these leaving groups into the benzylic position of **172** was attempted, but unfortunately both transformations were unsuccessful (Scheme 45). Analysis of the crude reaction mixtures by ^{1}H NMR spectroscopy indicated that in both cases, only starting material remained. It can therefore be reasonably assumed that the failure of these reactions is the result of inaccessibility of the di-*ortho* substituted benzylic position of compound **172**.
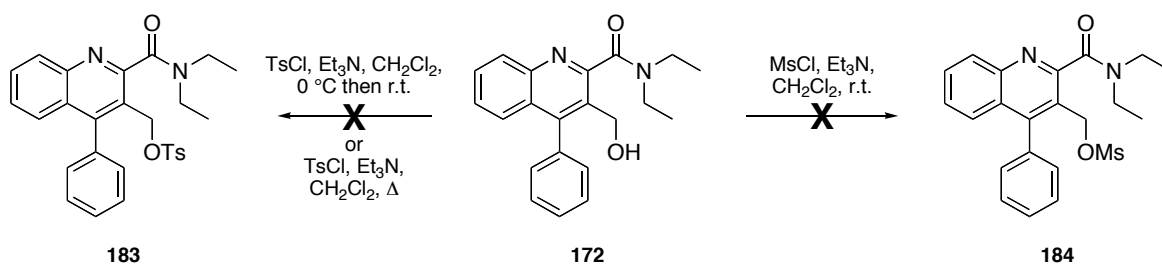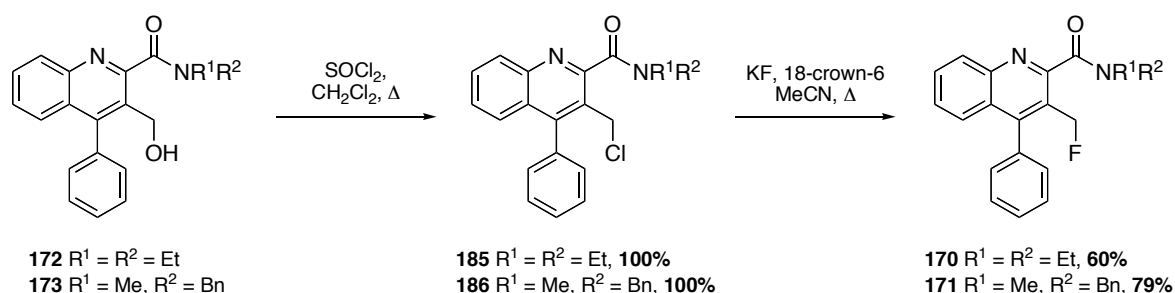

Scheme 45. Attempted tosylation and mesylation of quinoline-2-carboxamide **172**

An alternative and smaller leaving group was therefore required for this transformation and halogenation of the benzylic position of **172** and **173** was considered (Scheme 46). Chlorination of hydroxyl compounds **172** and **173** using thionyl chloride gave chloro-

precursors **185** and **186** in quantitative yields (Scheme 46). Finally, substitution of the chloride for fluoride utilising potassium fluoride in the presence of 18-crown-6,[148] afforded target fluorinated compounds **170** and **171** in good yields of 60% and 79%, respectively.

172 $R^1 = R^2 = Et$
173 $R^1 = Me, R^2 = Bn$

185 $R^1 = R^2 = Et$, **100%**
186 $R^1 = Me, R^2 = Bn$, **100%**

170 $R^1 = R^2 = Et$, **60%**
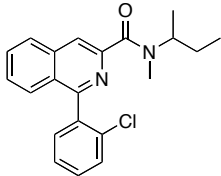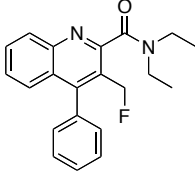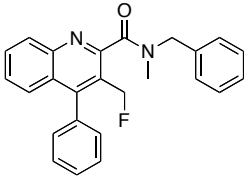**171** $R^1 = Me, R^2 = Bn$, **79%**

Scheme 46. Synthesis of potential PET compounds **170** and **171**

Investigation of the physicochemical properties and biological binding affinity of quinoline-2-carboxamides **170** and **171** with the TSPO was required for the next stage of this project.

2.2.3 Measurement of Physicochemical Properties and Biological Evaluation

The partition coefficient (cLog$P$), and other key physicochemical properties including permeability (P_m), membrane partition coefficient (K_m) and plasma protein binding (PPB), associated with compounds **170** and **171** were measured by HPLC methods (Table 10). Again, using established limits of these parameters ($P_m<0.5$, $K_m<250$, %PPB<95), this would allow the prediction of *in vivo* performance. From Table 10, it is evident that both compounds display very high cLog$P$ values compared to PK11195, but the necessity of additional lipophilicity measurements has been discussed previously. Compared to PK11195, both compounds display better permeability and lower membrane partition coefficient, implying that they will exhibit better BBB penetration and reduced non-specific binding characteristics *in vivo*. In addition, compound **170** shows reduced binding to plasma protein compared to PK11195. Next, the binding affinities of ligands **170** and **171** with the TSPO were evaluated using a competition binding assay. Both were shown to have nanomolar affinity for the protein, with compound **170** displaying the greatest potency. Similar to PK11195, the diethyl amide has a K_i value of 2.79 nM, and is likely

due to the 3-fluoromethyl group restricting rotation of the amide bond within the H-bonding pocket of the TSPO.

Structure	$\text{Log}P^a$	$P_m{}^b$	$K_m{}^b$	%PPB^c	K_i (nM)^d
PK11195	3.85*	0.65	229.36	91.51	3.10 ± 1.51
170	5.19	**0.46**	**154.29**	**89.72**	2.79 ± 0.77
171	5.95	**0.28**	**108.90**	**95.67**	11.96 ± 3.33

* Taken from literature.[133] Physicochemical properties determined using ^{a} C$_{18}$ column (mean ± SD, n = 3), ^{b} IAM column, ^{c} HSA column (mean ± SD, n = 3), and ^{d} K_i values determined from independent experiments (mean ± SD, n = 3)

Table 10. HPLC measured physicochemical properties and biological evaluation of quinoline-2-carboxamides **170** and **171**

From the results obtained, compound **170** was selected for having improved physicochemical properties over PK11195, and similar binding potency with the TSPO. It was therefore determined that this compound should be progressed to the next stages of radiotracer development. Quinoline-2-carboxamide **170** is referred to as AB5186 from this point onwards.
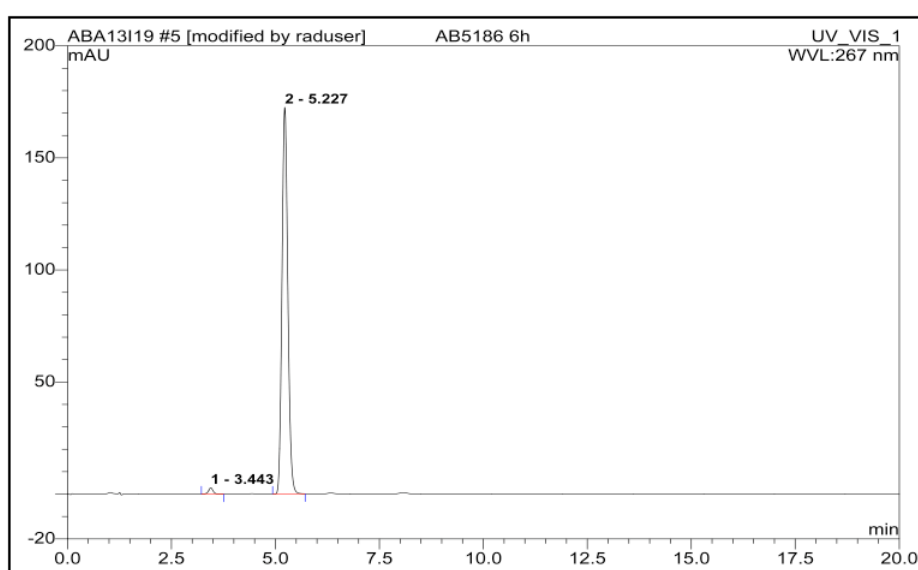
2.2.4 Stability Testing

As AB5186 **170** bears a fluoroalkyl substituent, a potential alkylating agent, *in vitro* stability of the compound under physiological conditions was investigated. A solution of the unlabelled compound in a 1:1 mixture of acetonitrile/phosphate buffered saline was

maintained at 37 °C for 24 hours, and sampled at the times specified (Table 11). From the results obtained it is evident that after an incubation period of 6 hours, only minimal decomposition (0.03%) of the compound has occurred (Table 11, Entry 5 and Figure 27). The presence of the bulky di-*ortho*-substituents in combination with the relatively strong C-F bond (approx. BDE 413 kJ/mol) imparts stability on the compound.[149,150]

This study indicated that AB5186 **170** could be progressed, as toxicity issues arising from alkylation were not apparent at this stage. Furthermore, a patient is normally scanned 2–4 hours after administration of a radiotracer, and it doesn't appear that rapid defluorination at the aliphatic position will be problematic. However, a more robust and detailed *in vivo* investigation will be required at a later date to confirm these preliminary findings.

| Entry	Time (h)	Compound Purity (%)
1	0	98.81
2	1	98.75
3	2	98.76
4	4	98.80
5	6	98.78
6	24	91.94

Table 11. Analytic HPLC measurement of compound purity (t_r = 5.227 min)

**Figure 27.** Representative analytical HPLC trace of unlabelled AB5186 **170** stability test

2.2.5 Synthesis of [^{18}F]AB5186

Previous attempts to generate a tosylate or mesylate precursor for the cold fluorination reactions failed, and so a halogen exchange reaction was revisited for the preparation of an [^{18}F]-labelled version of AB5186. A key factor in the development of any radiolabelling procedure is the ability to isolate with ease, precursor from unlabelled standard and/or radiotracer. In this instance, a semi-preparative HPLC system was employed for separation of the chloride precursor (t_r = 11.841 minutes) and AB5186 standard (t_r = 7.803 minutes), using a 70:30 acetonitrile/water mobile phase (Figure 28).
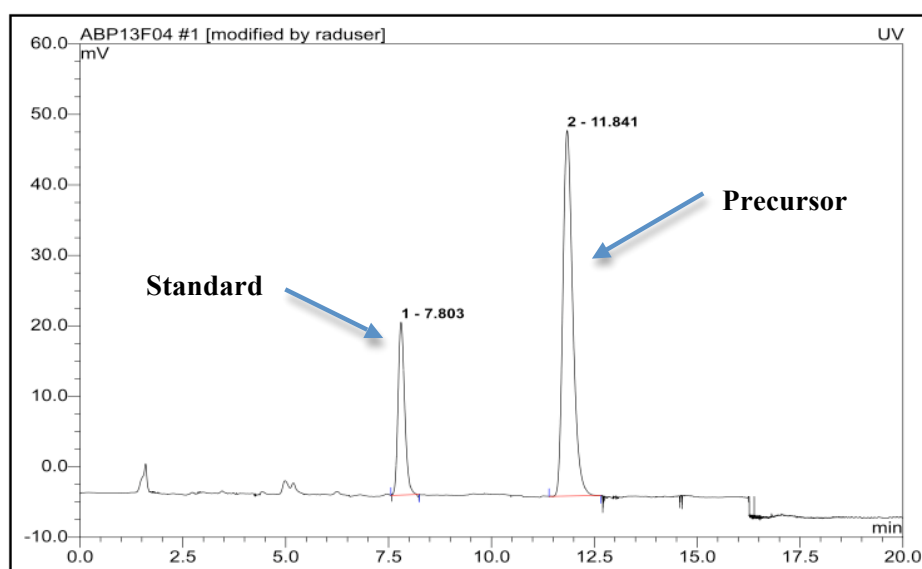

Figure 28. UV chromatogram showing chloride precursor **185** and cold AB5186 standard **170** co-injection on semi-preparative HPLC system

Having found a suitable mobile phase enabling efficient separation of precursor and standard on both semi-preparative and analytical HPLC systems, the synthesis of [^{18}F]AB5186 was investigated. Chloride **185**, the penultimate compound in the synthesis of cold AB5186, was subject to standard aliphatic radiofluorination conditions, utilising [^{18}F]potassium fluoride, Kryptofix® and potassium carbonate at 100 °C for 12 minutes (Scheme 47). Application of these conditions afforded [^{18}F]AB5186 **170** with a percentage incorporation of 66.1 ± 10.7% (n = 3), and radiochemical yield of 35 ± 9% (DC) in 118 ± 24 minutes (n = 3). The specific activity of [^{18}F]AB5186 was determined using a concentration response curve and measured at 0.6 ± 0.2 Ci/μmol (n = 2). A typical radiotrace acquired during the synthesis of [^{18}F]AB5186 is illustrated (Figure 29).
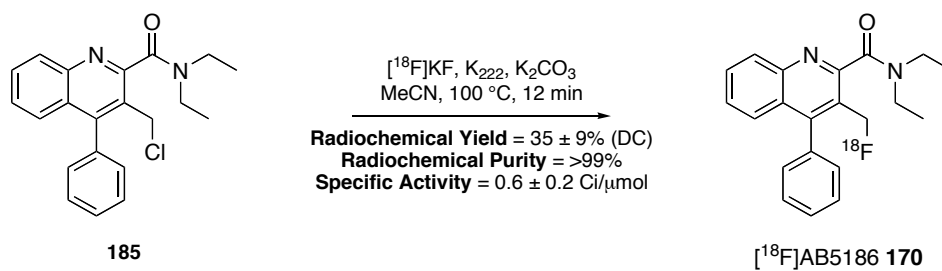
Scheme 47. Radiosynthesis of [^{18}F]AB5186 **170** from chloride **185**
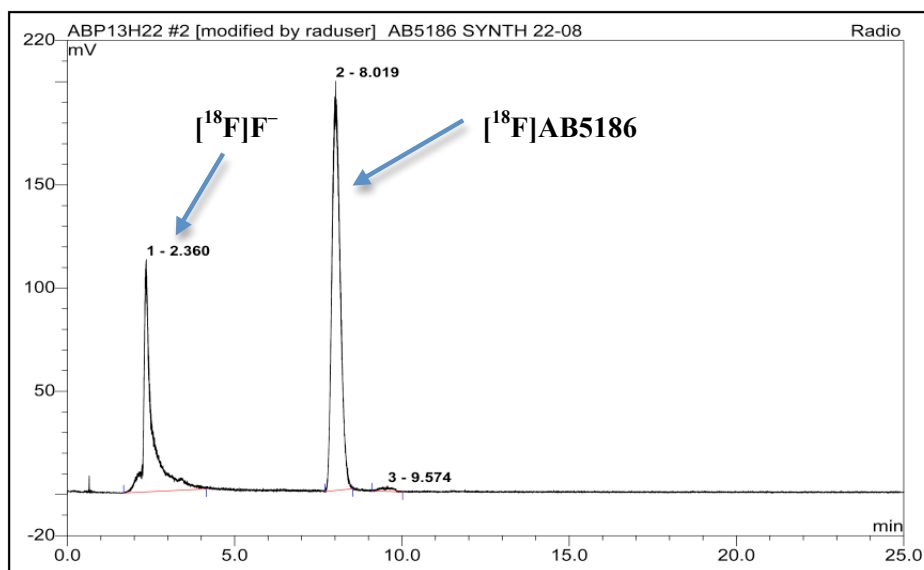
Figure 29. Representative radio-HPLC trace for [^{18}F]AB5186 synthesis

Quality control was performed on a semi-preparative HPLC system to ensure that the radiochemical purity after formulation was of a high enough standard. The radiochemical purity of the final radiofluorinated compound (t_r = 5.591 minutes) was determined by integration of the peaks present in the radiotrace (Figure 30) and found to be >99% (*n* = 3). The identity of the radiolabelled compound was confirmed by co-injection of the QC sample spiked with unlabelled AB5186.
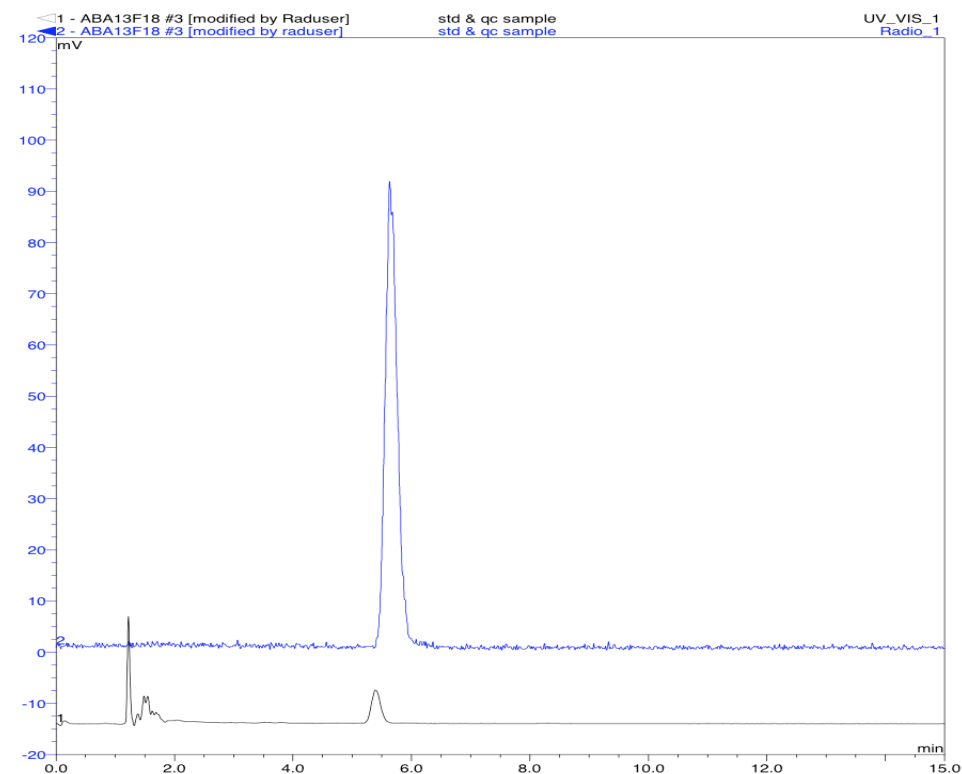
Figure 30. UV chromatogram overlay of AB5186 standard (blue trace) and QC sample (black trace) co-injection

Having successfully radiolabelled the lead candidate, the next stage of this research programme required provision of an initial proof of concept study, whereby, a demonstration that [^{18}F]AB5186 could, in fact, be utilised to image the TSPO.
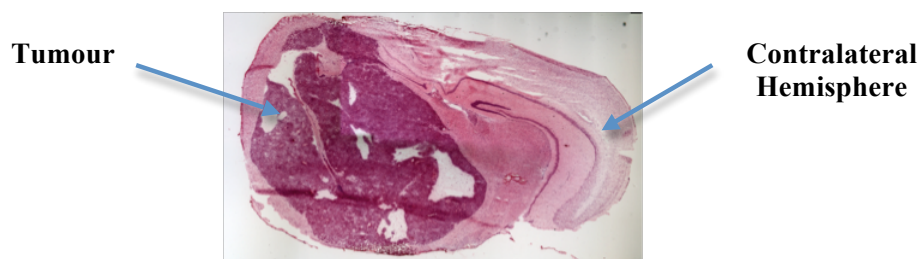
2.2.6 *In vitro* Autoradiography Study of a Human Glioblastoma Mouse Model using [^{3}H]PK11195 and [^{18}F]AB5186

Autoradiography is an imaging technique used to detect and visualise the distribution of a radiolabelled compound bound to a solid biological section, and relies on the use of a radiation-sensitive film.[151] As an imaging technique it offers a few advantages: rapid, simple in practice, and can offer quantitative information. *In vitro* autoradiography is a particularly useful autoradiographic technique that can be employed to investigate the distribution and localisation of receptors within the central nervous system, and do so with sensitivity at a relatively inexpensive cost.[152]

The TSPO has been for some time, a target of interest for studying patients affected by a range of pathological conditions including, but not limited to neurodegenerative disorders,

stroke and brain injury.[21] More recently, the implication of TSPO upregulation in tumours has garnered considerable interest. A number of studies have shown that this protein plays a significant role in the development and maintenance of a plethora of different cancers including cancers of the breast, colon, prostate, mouth and brain.[153,154,155] Furthermore, studies have revealed that there is a remarkable increase in TSPO expression within cancer cells of aggressive tumours,[156] and radioligands targeting this protein can therefore be exploited as a prognostic biomarker for metastasis and cancer imaging.

As such, we sought to determine whether our candidate tracer, [^{18}F]AB5186 could be utilised as a radioligand for TSPO in brain tumours, and more importantly, whether our radioligand provided superior binding characteristics compared to the 'gold standard', PK11195. The potential of [^{18}F]AB5186 binding to TSPO expressed in brain tumours was therefore investigated using an orthotopic mouse model of human glioblastoma prepared and provided by colleagues from The Beatson Institute for Cancer Research. Preparation of the disease model was achieved by injection of 10^5 cultured G7 glioblastoma cells directly into the caudate nucleus of a CD1 nude mouse.[157] Prior to commencement of the autoradiography study, location of the tumour within the mouse brain was determined using a haematoxylin and eosin stain. Haematoxylin and eosin staining is a histological stain that is routinely used in clinical settings,[158] and comprises two different dyes: haematoxylin and eosin. Haematoxylin stains nucleic acids a dark purple colour, and can be used to visualise rapidly replicating cells, whereas eosin stains proteins and other cellular components a pink colour. Consideration of the stained brain section (Figure 31) revealed the presence of a large and locally invasive tumour of unilateral expression. Despite the distorted morphology of the contralateral hemisphere, there was no evidence that tumour infiltration or inflammation had occured.


Figure 31. Haemotoxylin and eosin stained section of a mouse intracranial xenograft model of human glioblastoma

The *in vitro* autoradiography study showed that the total binding of [^{3}H]PK11195 was greater within the tumour tissue compared to that of the contralateral tissue (Figure 32a). Furthermore, a remarkably similar pattern of total radioligand binding was observed for [^{18}F]AB5186, with greater binding evident in the tumour tissue compared to the contralateral hemisphere (Figure 32b).

In addition to poor brain penetration, the utilisation of PK11195 as a TSPO ligand for brain imaging studies confers the further limitation of significant levels of non-specific binding to plasma proteins, resulting in a low signal to noise ratio. The levels of non-specific binding associated with PK11195 and AB5186, in both the tumour and unaffected tissue of the disease model, was determined by incubation of the brain sections with either [^{3}H]PK11195 or [^{18}F]AB5186 in the presence of excess unlabelled PK11195. Non-specific binding of the radioligand was defined as the optical density signal derived from the resulting autoradiogram and measured using MCID basic 7.0 software. The results are shown in Figure 32 and Table 12. In the presence of excess unlabelled PK11195, 55% of [^{3}H]PK11195 was displaced from the tumour tissue, and 25% from the contralateral tissue (Figure 32c, Table 12). It would be expected that 100% displacement of [^{3}]PK11195 would occur in the presence of an excess of unlabelled PK11195, however, this was not the case. This isoquinoline has been described as "sticky", which appears to be an appropriate description in this instance, and serves to highlight the limitations of using PK11195 as an imaging agent for the brain. In addition to total binding and non-specific binding displayed by the radioligands, the level of specific binding of these compounds within the glioblastoma mouse model was also determined, the results of which are listed in Table 12. Specific binding (defined as optical density in the absence of unlabelled ligand minus optical density in the presence of unlabelled ligand) for [^{3}H]PK11195 was measured to be four times greater in the tumour tissue than the contralateral tissue.

In the presence of excess unlabelled PK11195, 76% of [^{18}F]AB5186 was displaced from the tumour tissue, and 23% from the contralateral tissue (Figure 32d, Table 12). Furthermore, the specific binding of [^{18}F]AB5186 was measured to be eleven times greater in the diseased compared to unaffected tissue (Table 12). These preliminary findings indicate that this lead candidate tracer has the potential to act as a PET radioligand for imaging TSPO expression in focal brain pathology.

a)   b)

c)   d)
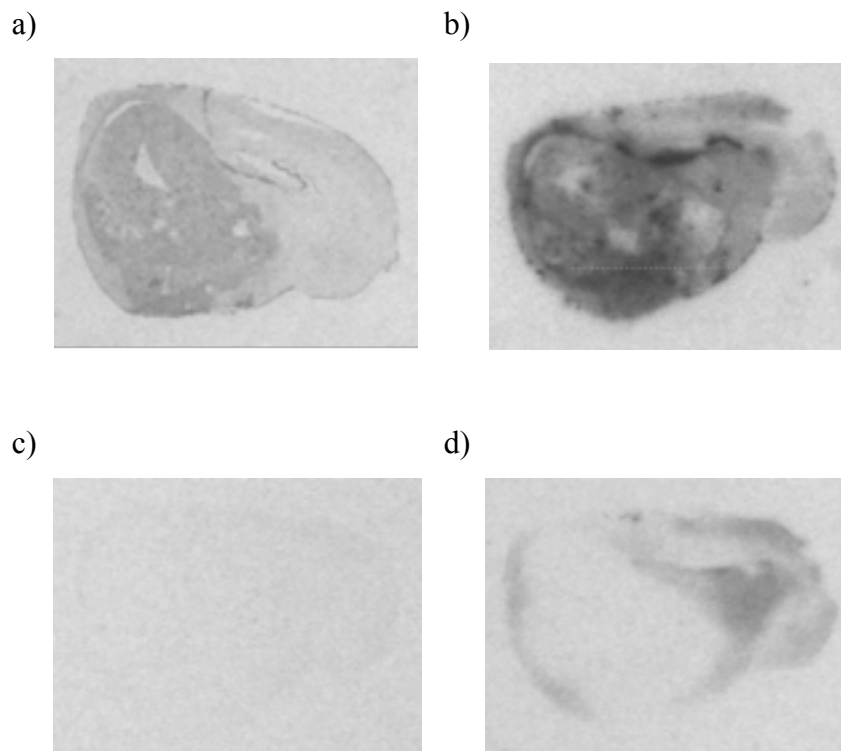
Figure 32. Representative autoradiograms showing total binding: a) [^{3}H]PK11195 and b) [^{18}F]AB5186 and, non-specific binding in the presence of excess cold PK11195: c) [^{3}H]PK11195 and d) [^{18}F]AB5186

Compound	Displacement by PK11195 in tumour tissue	Displacement by PK11195 in contralateral tissue	Ratio of specific binding in tumour:contralateral tissue
[^{3}H]PK11195	55%	25%	4:1
[^{18}F]AB5186	76%	23%	11:1

Table 12. Measurement of radioligand displacement by cold PK11195 and ratio of specific binding (tumour:contralateral tissue)

Information obtained from *in vitro* studies is beneficial as it provides an indication as to whether a compound should be progressed for development. However, this information is limited and only *in vivo* investigations can provide an accurate insight into the behavior of a compound within the body.

2.2.7 Summary

Initial attempts to prepare the quinoline-2-carboxamide targets focused on a Friedlander reaction followed by lactonisation of the resulting product. This latter step, however, proved very time consuming, and several attempts to improve this transformation were trialed but deemed unsatisfactory. As such, an alternative synthetic strategy was sought. Preparation of the PK11195 analogues was subsequently achieved *via* an expeditious eight-step synthesis. This route proved to be quick to execute and efficient, with a key one-pot two component indium(III)-catalysed cyclocondensation reaction utilised for the synthesis of the quinoline core.

Both analogues displayed good physicochemical properties and their binding affinity with the TSPO shown to be in the nanomolar range. In particular, quinoline-2-carboxamide **170**, subsequently named AB5186, was deemed to have lower binding to plasma protein and improved permeability compared to PK11195. Furthermore, the K_i value of this compound (2.79 nM) was comparable to that of PK11195 (3.10 nM).

Synthesis of an [^{18}F]-labelled version of AB5186 was achieved *via* an S_N2 reaction under standard aliphatic radiofluorination conditions, affording the radiotracer in good radiochemical yield and high radiochemical purity. An *in vitro* autoradiography study with a mouse intracranial G7 human glioblastoma xenograft has revealed that [^{18}F]AB5186 has potential application as an imaging agent for neuroinflammation associated with focal neurological disease.

2.2.8 Future Work

Future work centered on the development of [^{18}F]AB5186 as a PET imaging agent for the TSPO is currently underway. An intensive *in vivo* PET study comprising two stages has been initiated; the first is designed to measure the kinetic profile of the radiotracer and the second, to perform a pre-blocking study with unlabelled PK11195. Both studies will utilise a characterised U87 luciferase glioblastoma mouse model. The kinetic profiling study aims to determine the time required for maximal [^{18}F]AB5186 uptake within the target to occur, which can then be applied to the pre-blocking study. This latter study will examine the specificity of radiotracer binding, *i.e.* whether or not AB5186 and PK11195

compete for the same TSPO binding sites. In addition, the metabolic profile of [^{18}F]AB5186 will be examined through blood sampling and subsequent HPLC analysis.

If these preliminary results are encouraging additional *in vivo* studies, *e.g.* measurement of the binding profile within human tissue, will be initiated with the ultimate aim of progressing [^{18}F]AB5186 to the clinic.

# 3 Development of a PET Imaging Agent for PARP-1

3.1 Introduction

Deoxyribonucleic acid (DNA), the molecule from which our genetic material is composed, contains the instructions necessary for creating and maintaining life. As such, the human genome is a vastly complex system that is continuously sustaining high levels of damage originating from both endogenous and exogenous sources. Endogenous sources include biological processes, *e.g.* DNA replication and repair, and exposure to genotoxic agents, such as reactive oxygen species formed during metabolism.[159,160] Damage resulting from exogenous sources, on the other hand, arise from exposure to external radiation and chemical agents.[161] The consequence on the structural integrity of DNA are, therefore, wide and varied, and classified according to the type of changes inflicted. Furthermore, in an effort to rectify these abberations and minimise the probability of a genetic mutation occuring, a range of extensive repair mechanisms has evolved.

DNA lesions in the form of single-strand breaks (SSBs) and double-strand breaks (DSBs) are just two examples of the types of damage routinely caused. DSBs involve both strands of the double helix, and are remedied by non-homologous end joining (NHEJ) and homologous recombination (HR), whereas SSBs affect just one strand of the DNA duplex, and are rectified by base excision repair (BER).[162] SSBs and the BER pathway form the premise for this research program.

3.1.1 PARP-1: Structure and Function

Poly(ADP-ribose) polymerases (PARP) are a family of proteins found in eukaryotic cells responsible for the regulation of a variety of nuclear signal transduction pathways.[163] When activated, they are responsible for catalysing the addition of long linear or branched poly(ADP-ribose) chains to target proteins.[164] At present, this superfamily comprises 18 members, but despite all bearing the strictly conserved catalytic domain,[165] only six (PARP-1 to 4, and tankyrases 1 and 2) exhibit the poly(ADP-ribosylation) activity charactersitic of this family of proteins.[166]

PARP-1 is an abundant, chromatin bound protein that constitutes approximately >90% of total cellular PARP activity, and partners with closely related PARP-2 to function as a DNA damage sensor and ensuing response enzyme.[167,168] This 113 kDa protein consists of three distinct domains that allow it to perform this function: the DNA-binding domain, the automodification domain, and the catalytic domain.[160] As its name suggests, the N-terminal DNA-binding domain is responsible for recognition and binding to SSBs primarily, but includes DSBs, and does so using two highly conserved zinc fingers.[169] A third zinc finger also exists, however, it is not thought to partake in DNA binding.[170] PARP-1 is constitutively expressed in a basally active form, but on binding to transient and localised DNA strand breaks, the C-terminal catalytic domain is activated.[171] When this occurs, the protein rapidly catalyses the cleavage of nicotinamide adenine dinucleotide (NAD$^+$) forming nicotinamide and ADP-ribose moeities, and subsequently transfers the resulting ADP-ribose units to various target proteins (Figure 33).[164] This results in the formation of the long poly(ADP-ribose) (PAR) chains mentioned previously. Finally, the automodification domain, covering the central portion of the protein, displays glutamate and lysine residues required to accept the ADP-ribose moeities, essentially allowing the protein to poly(ADP-ribosyl)ate itself.[172]
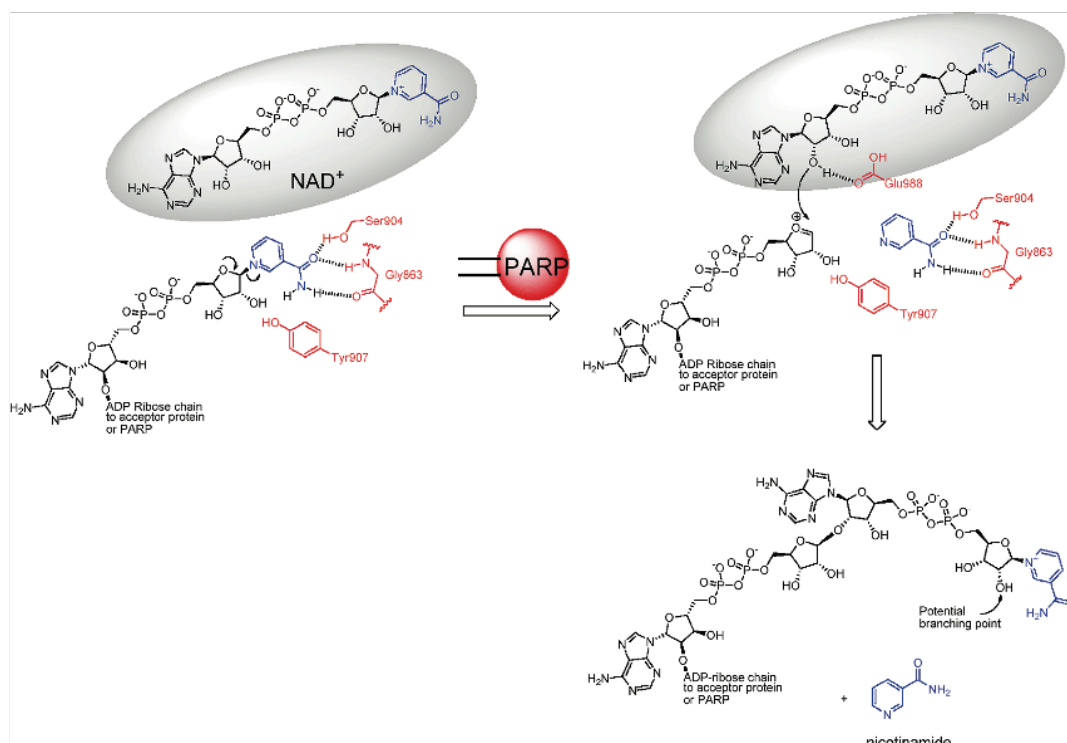
Figure 33. Formation of poly(ADP-ribose) chains[173]
(Reprinted with permission from *J. Med. Chem.*, 2010, **53**, 4561. Copyright 2010 American Chemical Society.)

Implementation of SSB repair by PARP-1 occurs in the following manner: a DNA lesion is recognised and bound to, which signals the relevant repair proteins, and the enzymatic function of PARP-1 is then activated. Histone proteins, and PARP-1 itself, are subsequently poly(ADP-ribosyl)ated, resulting in the generation of large PAR chains bearing a substantial negative charge.[174] The resulting charge repulsion experienced by the DNA and modified proteins, leads to relaxation of the chromosomes, and following poly(ADP-ribose)glycohydrolase (PARG) cleavage of the PAR chains, PARP-1 is subsequently inactivated and disassociates from the DNA.[173] This enables proteins associated with the BER pathway, including XRCC1, DNA Polymerase β and LIG-IIIα, greater access to the damaged DNA.[173,175] Repair of the DNA strand break can now take place. A simplified overview of this process is illustrated in Figure 34.
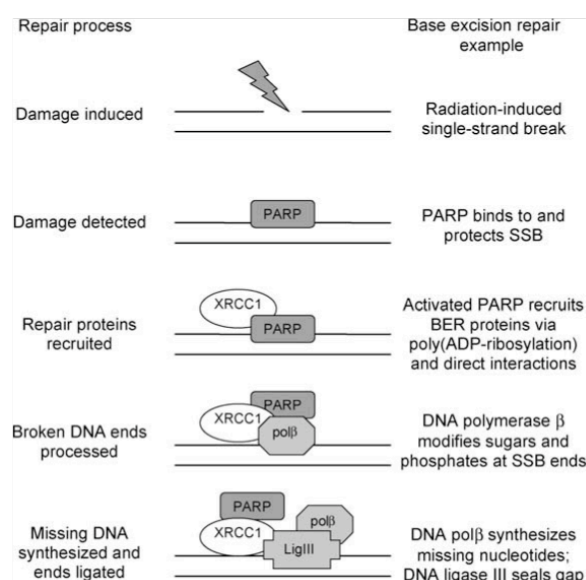

Figure 34. Function of PARP-1 in single-stranded DNA break repair[162]
(Reprinted with permission from *Brit. Med. Bull.*, 2009, **89**, 23. Copyright 2009 Oxford University Press.)

3.1.2 PARP-1 Inhibitors and Application in Cancer Therapy

In 1971, it was shown that nicotinamide could weakly inhibit PARP-1 activity ($K_i = 20$ μM).[176] Since then, PARP-1 inhibitors of varying structural classes have been developed, including benzimides, isoquinolinones, dihydroisoquinolinones, benzimidazoles, indoles, isoindolinones, phenanthridinones, phthalazinones and quinazolinones.[160] A few select examples of potent PARP-1 inhibitors are illustrated in Figure 35.
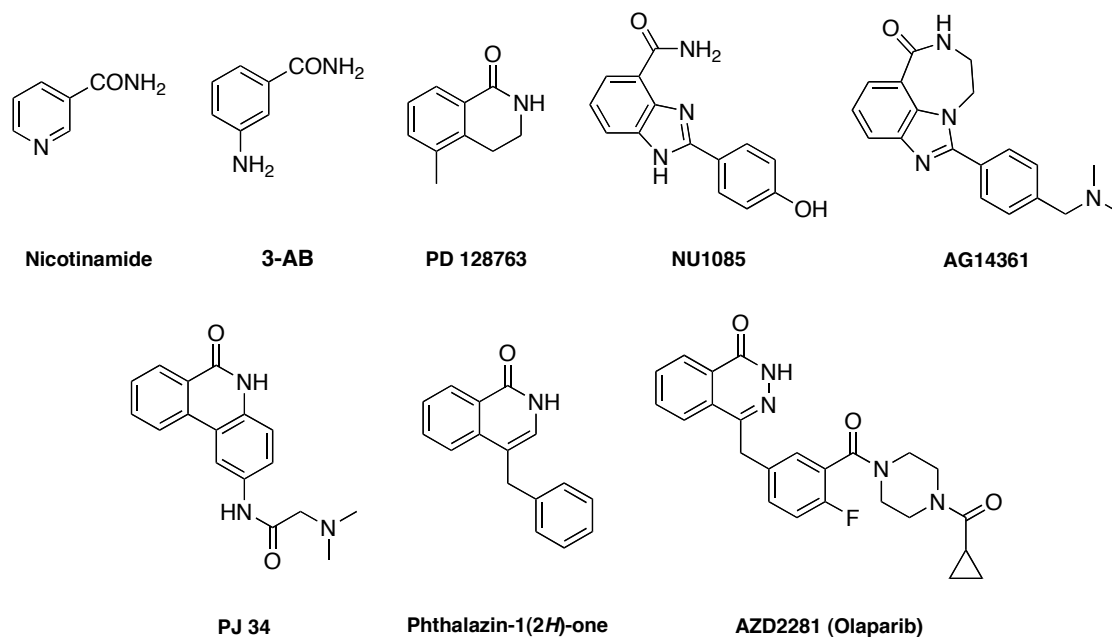
Figure 35. PARP-1 inhibitors

Inhibitors of PARP-1 activity fall into one of two classes: competitive or non-competitive inhibitors. Those that act in a competitive manner, which account for the majority of inhibitors known, are designed to mimic nicotinamide.[165] By imitating the natural substrate, these compounds compete for binding to the catalytic site and, subsequently restrict the enzymatic property of the protein. Rational for compound design is attributed to crystallographic and computational studies that have shown the binding interactions between PD128763, a PARP-1 inhibitor, and the catalytic fragment of chicken PARP-1.[177,178] Generally, inhibitors of PARP-1 tend to be large hydrophilic compounds that bind to a polar site at the entrance to the proteins catalytic binding pocket.[179]

Given that PARP-1 functions to repair DNA, it is unsurprising that it has received a great deal of interest as a potential therapeutic target. In particular, it has been a key focus of those seeking to treat certain cancers.[180] Application of a PARP-1 inhibitor can be effective in one of two ways, either as a chemopotentiator or a single agent. In the first instance, a large number of anticancer drugs aim to bind to DNA and inflict damage on the rapidly dividing tumour cells, ultimately resulting in genome instability and cell death. As such, exploitation of the PARP-1 mediated DNA repair pathway can lead to continued growth of the tumour, and an increase in resistance to chemotherapy.[181] Administration of a PARP-1 inhibitor, however, in combination with chemotherapy or radiation, would impede DNA repair in cancer cells, obstruct continued division and ultimately enhance therapeutic intervention.[182] Even more interestingly, research has shown that tumours lacking breast

cancer susceptibility protein 1 (BRCA1) and 2 (BRCA2) function, which depletes the cells ability to repair damaged DNA *via* the HR pathway, are particularly susceptible to the effects of PARP-1 inhibitors.[183,184] This leads to what is termed 'synthetic lethality', *i.e.* a mutated *BRCA1/2* and *PARP-1* gene leads to cell death, but a mutation in either one does not.[185] It may, therefore, be possible to treat certain tumours with such compounds, negating the need for additional courses of chemo- and/or radiotherapy.

3.1.3 PET Imaging of PARP-1 Activity

Despite the fact that several PARP-1 inhibitors, including olaparib,[186] rucaparib,[187] and veliparib,[188] are currently undergoing clinical evaluation for the treatment of certain cancers, a few key areas still need to be addressed. For instance, the inability to monitor the action of these drugs at the molecular level non-invasively, providing evidence of a specific drug-target site interaction, is proving problematic. Furthermore, as chemopotentiation requires dual administration, detailed studies that aim to determine both optimal PARP inhibitor-chemotherapy drug combination, and establish dosing regimes, are imperative for advancement of this type of therapy.[189] These issues can be addressed using molecular imaging tools that enable quantification, and as such, the potential application of a PET imaging agent for PARP-1 activity is being realised.

In 2005, Tu *et al.* prepared [^{11}C]PJ34, a potential radiotracer for the *in vivo* imaging of PARP-1 activity during cellular necrosis.[190] Starting from phenanthridin-6(5*H*)-one (**187**), the authors prepared the *des*-methyl labeling precursor **188** in three steps. Incorporation of the radiolabel was then achieved using [^{11}C]methyl iodide, giving [^{11}C]PJ34 (**189**) in both a high radiochemical yield and specific activity (Scheme 48). The radiotracer was then administered to a Type 1 diabetes rat model and, following *in vivo* PET imaging biodistribution studies, shown to accumulate in the pancreas and liver, where levels of PARP-1 activity in beta cells would be high due to the focal pathology.
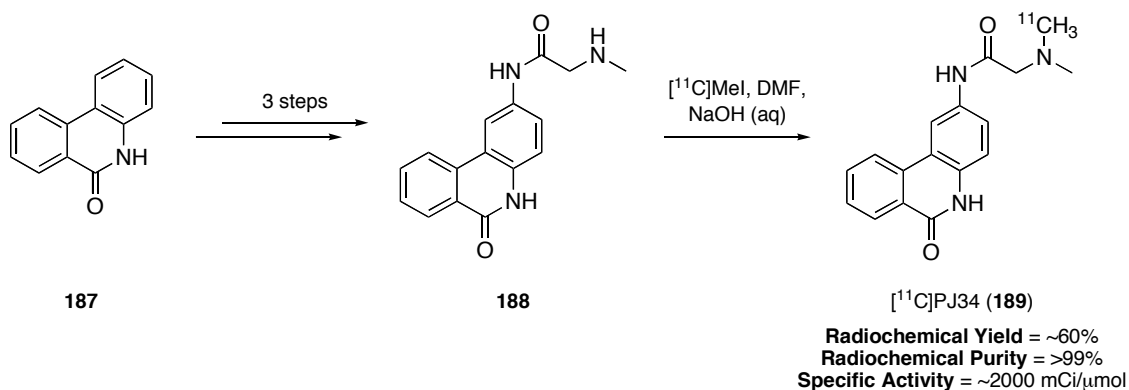
**Scheme 48.** Radiosynthesis of [^{11}C]PJ34 (**189**)

Based on an initial screen of NU1085 and AG14361 analogues (Figure 35), Chen and co-workers identified compound **192** as a potent PARP-1 inhibitor (Scheme 49).[191] As part of their study, the authors investigated the potential for this compound to act as a PET imaging agent for PARP-1 activity, the preparation of which is illustrated in Scheme 49. Mesylate precursor **191**, prepared from amine intermediate **190**, was subject to radiofluorination using [^{18}F]potassium fluoride and Kryptofix® under standard reaction conditions to give [^{18}F]-labeled benzimidazole carboxamide **192** in high radiochemical yield, purity, and specific activity. Total radiosynthesis time was 90 minutes.

Having prepared [^{18}F]**192**, an initial *in vivo* study using an MDA-MB-436 human breast cancer xenograft mouse model to determine radiotracer uptake within the tumour was performed. The preliminary results of the microPET study indicated that there was increased uptake within the tumour and that this uptake was specific, as determined by the use of olaparib and cold **192** in blocking studies.
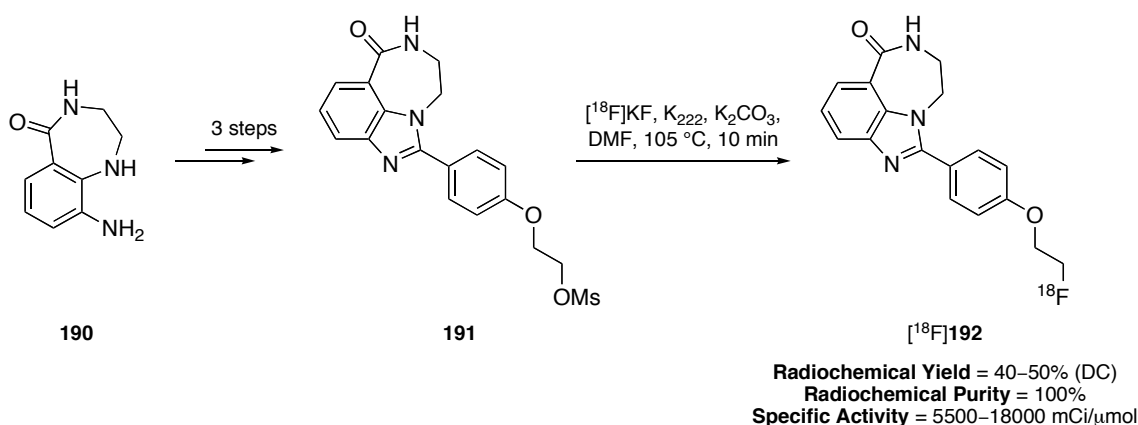
Scheme 49. Radiosynthesis of [^{18}F]benzimidazole carboxamide **192**

In addition to the application of PARP-1 inhibitors as imaging agents, there has also been interest in the development of novel radiolabeling procedures. A highly efficient method for the preparation of an [18F]-labeled PARP-1 inhibitor, based on AZD2281 (olaparib), which utilises a chemically orthogonal scavenger was recently reported by Reiner *et al.*[192] Based on initial studies, whereby the authors used fluorophores to visualise PARP-1 activity at the cellular level and in real-time,[193,194] a technique exploiting the fast reaction time between *trans*-cyclooctene (TCO) and tetrazine was extrapolated for incorporation of an 18F-radiolabel. The reaction sequence of this technique is illustrated in Scheme 50, and proceeds as follows: [18F]-labeled *trans*-cyclooctene **196** is prepared by nucleophilic substitution of the tosylate group of **195**.[195] The resulting intermediate is then reacted with the tetrazine-conjugated analogue of AZD2281 **193** *via* an [4+2] inverse-electron-demand Diels-Alder cycloaddition to give [18F]-labeled compound **194** in very high radiochemical yield. Finally, unreacted tetrazine precursor is removed using a magnetic TCO-decorated scavenger resin. The advantages of this procedure include fast reaction and purification times, the ability to perform the reaction at ambient temperature, and more importantly, reverse-phase HPLC purification of the radiotracer is no longer required.
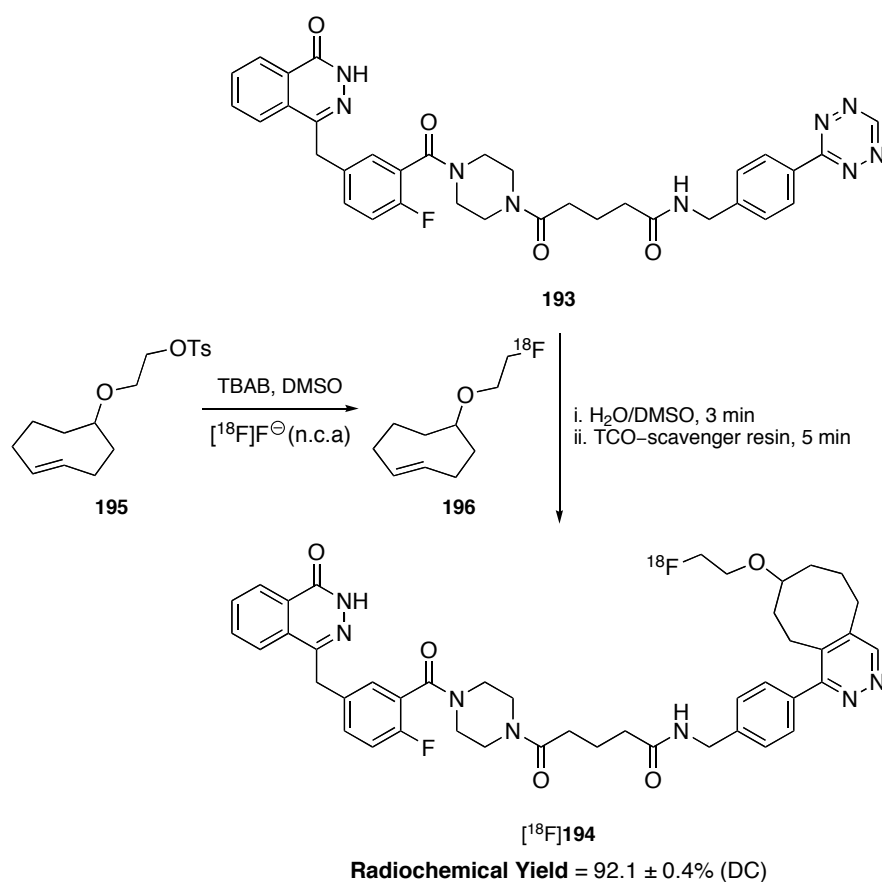

Scheme 50. Radiosynthesis of [18F]**194**, an AZD2281 analogue

The authors also noted successful application of this radiotracer to a PET/CT study using an MDA-MB-436 tumour-bearing mouse, with encouraging results. Accumulation of the radiotracer within the tumour, and specific binding was confirmed. Moreover, uptake of the radiotracer could also be quantified *in vivo*.

This latter study has shown that the development of a PET imaging agent targeting PARP-1 activity has scope and promise.

3.1.4 Proposed Research

The aim of this project was to generate a small library of novel PARP-1 inhibitors based on olaparib (Figure 36), which have the potential to be labeled with either [^{18}F]potassium fluoride or [^{11}C]methyl iodide for PET imaging applications. It was anticipated that analogues of **197** (Figure 36) could be prepared *via* an expeditious route, enabling late structure variation and radiolabelling. Coupling of an appropriate precursor with a range of commercially available carboxylic acids and benzyl halides, bearing either a fluoro- or methoxy-substituent, would accomplish the preparation of the potential PET imaging agents.
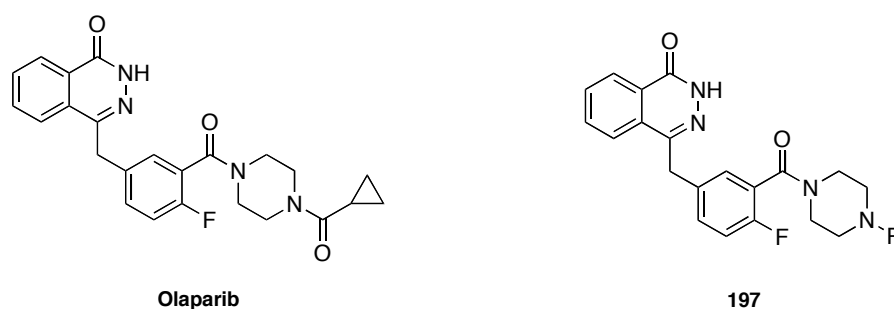
Figure 36. PARP-1 inhibitor Olaparib and structure of potential PET imaging agent

Following optimisation of the synthetic route and completion of the target compound library, the PARP-1 inhibitory potency and pharmacological profile of each compound would be measured and assessed by collaborators. Furthermore, if any of the compounds displayed the appropriate characteristics, development into a potential PET imaging agent that could be used to assess PARP-1 activity in glioblastomas and PARP-1 inhibitor treatments, would be investigated.

In terms of structure-activity relationship, there are particular structural features of olaparib that account for its high binding affinity to PARP-1 protein (Figure 37). The amide functionality of the phthalazinone core provides scope for three key hydrogen-bonding interactions: the carbonyl acts as a H-bond acceptor from Ser-904, and a bidentate interaction is formed with the backbone of Gly-863.[160,165] A hydrophobic π-π stacking interaction between the aromatic rings of the phthalazinone core and Tyr-907 also occurs. In addition, it has been suggested that the *m*-carbonyl group of the benzyl ring accepts a H-bond from Met-890, resulting in the displacement of a conserved water molecule.[196] Extensive studies have shown that the 4-NH-piperazine moiety of olaparib can accommodate a very diverse range of capping groups with no discernable effect on binding affinity,[197,198] and can be rationalised by the discovery of a large hydrophobic pocket that sits adjacent to the nicotinamide binding site.[199] More recently, this has been substantiated by Reiner *et al*., who have studied the inclusion of very large functionalised capping groups and observed no detrimental effect on binding potential.[193] Given that these key binding interfaces remain present and unchanged in the target PET compounds, it is expected that they will retain the inhibitory potency of Olaparib.
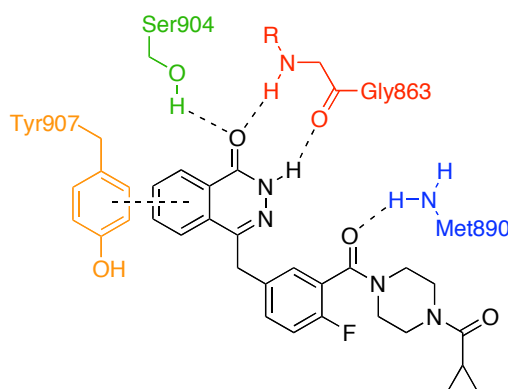

Figure 37. Key Olaparib-PARP-1 binding interactions

3.2 Results and Discussion

3.2.1 Retrosynthetic Analysis of Olaparib Analogues

A proposed retrosynthetic analysis of the target analogues of olaparib is illustrated below in Scheme 51. An initial disconnection of the N-R of **198** bond provides the corresponding commercially available acid or acyl derivative and secondary amine **199**, which can in turn

be prepared by deprotection of Boc-amine **200**. Further disconnection of the amide linkage of **200** affords carboxylic acid **201** and Boc-protected piperazine **205**. Amine fragment **205** can be prepared in a single step from commercially available piperazine. A functional group interconversion of the carboxylic acid yields the corresponding nitrile group, and disconnection of the phthalazinone core of **201** leads to benzofuran-1-one **202**. Disconnection of the double bond then affords commercially available phosphonate ester **203** and 2-fluoro-5-formylbenzaldehyde (**207**). A final functional group interconversion of the phosphonate ester group gives 2-carboxybenzaldehde (**204**) and dimethylphosphite, both of which are commercially available.
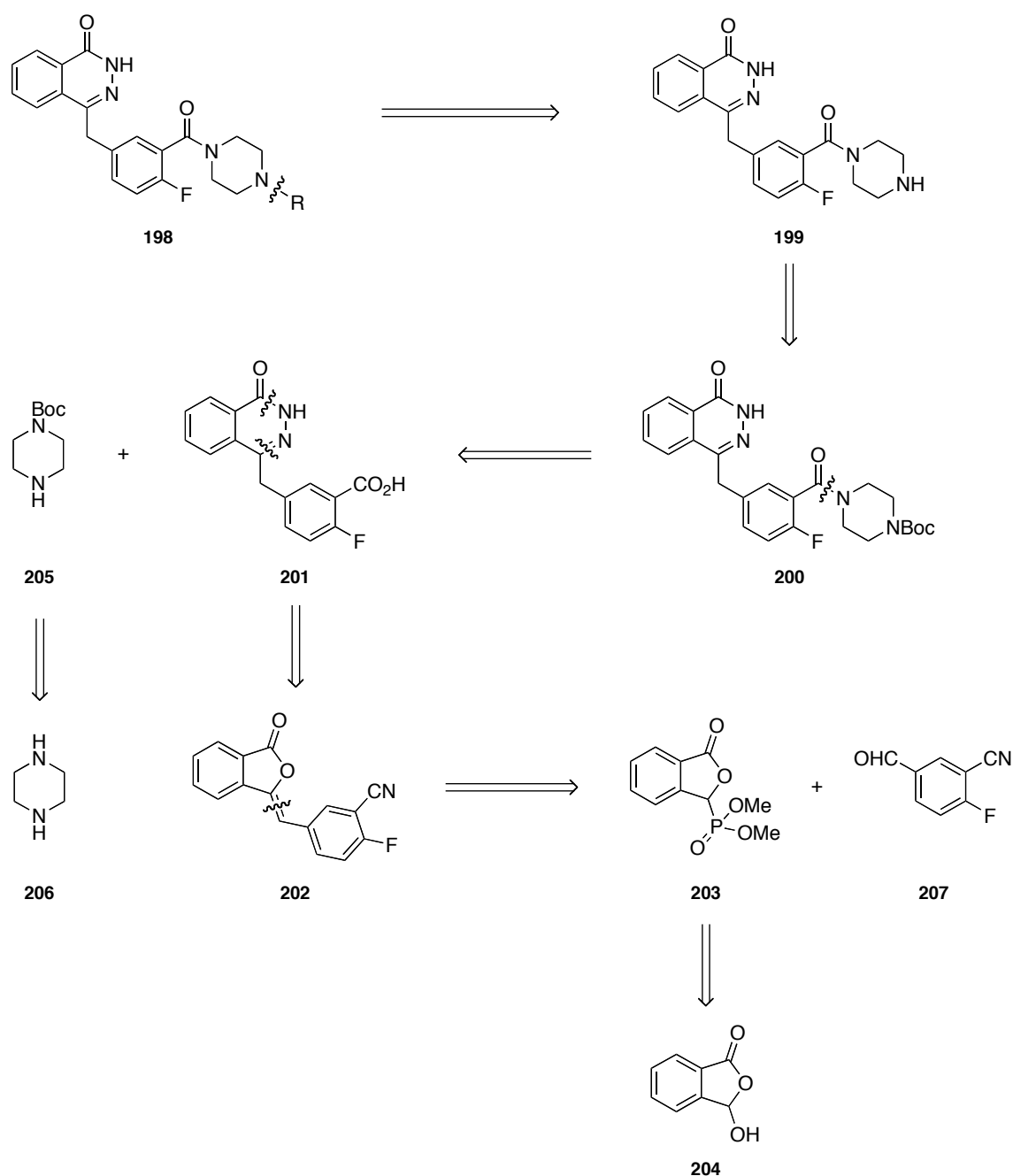

Scheme 51. Retrosynthetic analysis of olaparib analogues

The successful synthesis of a small library of novel PARP-1 inhibitors based on olaparib relies upon the ability to prepare the key phthalazinone core rapidly and with efficiency. Procedures for the preparation of penultimate compound **199** are documented in the literature, and this, coupled with the wide availability of both carboxylic acid and benzyl coupling partners, should enable the rapid synthesis of a range of compounds bearing fluoro- and methoxy-substituents.

3.2.2 Synthesis of Potential PET Imaging Agents for PARP-1

Preparation of olaparib analogues with the potential to be used as PET imaging agents for PARP-1 activity was achieved using synthetic procedures reported by Menear *et al.*[200,201]

The first step towards the preparation of a small library of novel PARP-1 inhibitors required the synthesis of benzofuran-1-one **203**. Starting from commercially available 2-carboxybenzaldehyde (**204**), a coupling reaction with dimethylphosphite in the presence of sodium methoxide gave benzofuran-1-one **203** in an excellent 96% yield (Scheme 52).[200] The phosphonate ester functionality of **203** could then be exploited for the preparation of the phthalazinone precursor by means of the Horner-Wadsworth-Emmons reaction.
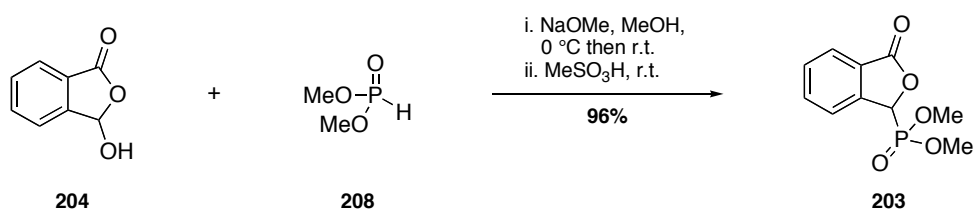

Scheme 52. Benzofuran-1-one **203** synthesis

Originally reported in 1958 by Horner,[202] and subsequently in 1961 by Wadsworth and Emmons,[203] this chemical transformation utilises a phosphoryl-stabilised carbanion for the stereoselective olefination of both aldehydes and ketones. The stereochemical outcome of this olefination reaction is predominantly the (*E*)-alkene, and is probably a consequence of the reversibility of the initial C-C bond forming step and oxaphosphetane formation.[204] However, under certain reaction conditions, formation of the (*Z*)-isomer can be achieved.[205] As such, the modern organic chemist can tailor the reaction conditions to influence formation of one isomer over the other, therefore, enhancing selectivity of the product formed. In this instance, however, the geometry of the resulting double bond is

irrelevant, as conversion to the phthalazinone core structure in the proceeding step will result in removal of the alkene, and so steps to exert control over the selectivity of the reaction are unnecessary.

As such, compound **203** was reacted with commercially available 2-fluoro-5-formylbenzonitrile in the presence of triethylamine, forming alkene **202** in very high yield of 95% (Scheme 53). Inspection of the ^{1}H NMR spectrum of the isolated product indicated a 75:25 mixture of *E*- and *Z*-isomers respectively, which were not separated. Identification and measurement of the isomeric ratio of alkene products was based on data presented in the literature for this compound.[201] It is noteworthy that mixtures are often obtained for trisubstituted alkenes.[206,207]
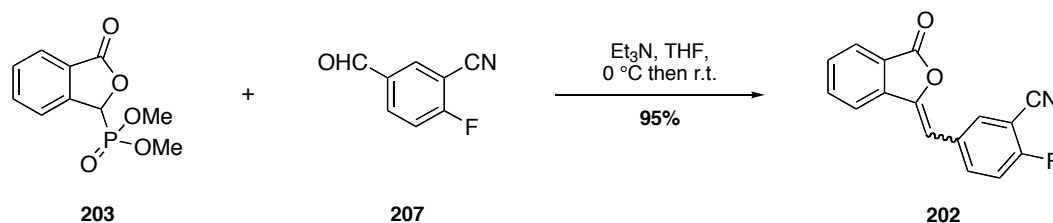

Scheme 53. Synthesis of **202** *via* the Horner-Wadsworth-Emmons reaction

A two-step, one-pot procedure was then employed for the preparation of substituted phthalazinone **201** (Scheme 54). Initial hydrolysis of the pendant nitrile group of benzofuran-1-one **202** to the corresponding carboxylic acid was achieved using a 13 N aqueous sodium hydroxide solution. Following this step, addition of hydrazine monohydrate to the reaction flask at a lower reaction temperature of 70 °C, resulted in the formation of the key phthalazinone core of **201** in quantitative yield over two steps.

**Scheme 54.** Synthesis of the phthalazinone core

Having successfully prepared the key phthalazinone core of the olaparib analogues, progression to the next step of the synthetic route was feasible. This next step involved an amide bond coupling reaction between the carboxylic acid of the phthalazinone core and the piperazine fragment. However, before this transformation could be considered, the mono-protection of commercially available piperazine was necessary to prevent polymerization of the phthalazinone unit. In this instance, the Boc-protecting group was selected for the amine as the conditions needed for its inclusion and subsequent removal will not affect the more sensitive functionalities present within the molecule. As such, *N*-Boc protected piperazine **205** was prepared in a high yield of 88%, by the slow addition of a solution of di-*tert*-butyl dicarbonate (**209**) in dichloromethane to commercially available piperazine (**206**) at 0 °C (Scheme 55).[208]
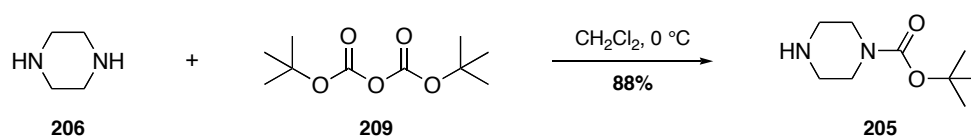
Scheme 55. Mono-*N*-Boc protection

With the mono-*N*-Boc protected piperazine now in hand, attention was turned to the amide coupling reaction with the phthalazinone core (Scheme 56). A few different amide coupling reagents and conditions were trialled for this transformation, and are listed in Table 13. Briefly, the use of EDCI (Entry 1) was inconclusive, as it was not apparent from inspection of the crude reaction mixture by ^{1}H NMR spectroscopy whether any reaction had taken place. Utilisation of HOBt resulted in a 44% yield of the desired amide product (Entry 2). HOBt is known to form diazetidine by-products on reaction with diimides,[209] and due to the potentially explosive nature of this reagent reluctance to increase the reaction temperature in an attempt to improve product yield lead to consideration of another reagent. In keeping with the benzotriazole coupling agents, HBTU was considered, but only starting material remained after an initial attempt (Entry 3). By substituting Hünigs base and DMA for triethylamine and DMF, respectively amide **200** was obtained in a 27% yield (Entry 4). Precipitation of the desired product occurs on addition of water, aiding isolation. Efforts to increase isolated product yield was attempted by raising both reaction and work-up temperature (Entries 5 to 7). In doing so, an optimum product yield of 68% for compound **200** was obtained when the reaction was performed initially at ambient temperature before increasing to 50 °C, and after addition of water, cooled to 0 °C (Entry 6).
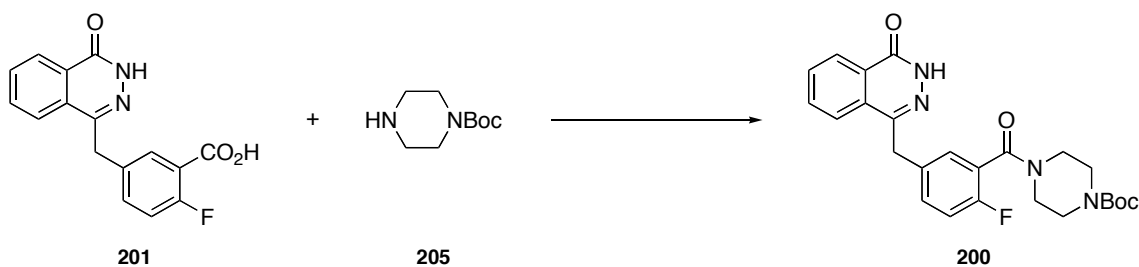
Scheme 56. Amide coupling reaction

Entry	Reagents	Conditions	Work-Up[*]	Yield 200 (%)
1	EDCI, DMAP	DMF, r.t. to 0 °C	-	−
2	HOBt, EDCI	CH_2Cl_2, 0 °C to r.t.	-	44
3	HBTU, DIPEA	DMA, 0 °C to r.t.	-	−
4	HBTU, Et₃N	DMF, r.t.	H_2O, 0 °C	27
5	HBTU, Et₃N	DMF, r.t.	H_2O, 60 °C	42
6	**HBTU, Et₃N**	**DMF, r.t. to 50 °C**	**H_2O, 50 to 0 °C**	**68**
7	HBTU, Et₃N	DMF, 70 °C	-	64

[*] Addition of H_2O to HBTU reactions only

Table 13. Amide coupling conditions trialed

Precipitation of the product was desirable, as it circumvented the need for silica column chromatography as a means of purification. The reason for this was that previous attempts to purify the product using chromatography, proved problematic. In particular, the urea by-product, formed when HBTU is employed as the coupling agent, was difficult to remove.

The proposed mechanism for the HBTU coupling of phthalazinone **201** and *N*-Boc piperazine is illustrated in Scheme 57.[209] Deprotonation of carboxylic acid **201** in the presence of base generates carboxylate anion **210**, which undergoes nucleophilic substitution with the uronium moiety of HBTU **213** to give intermediate **211**. The oxygen anion of benzotriazole **214** then participates in a second S_N2 reaction with **211**, generating the OBt active ester **212** and a urea by-product **215**. The activated ester subsequently reacts with *N*-Boc piperazine (**205**) to afford amide **200** and 1-hydroxybenzotriazole (**214**).
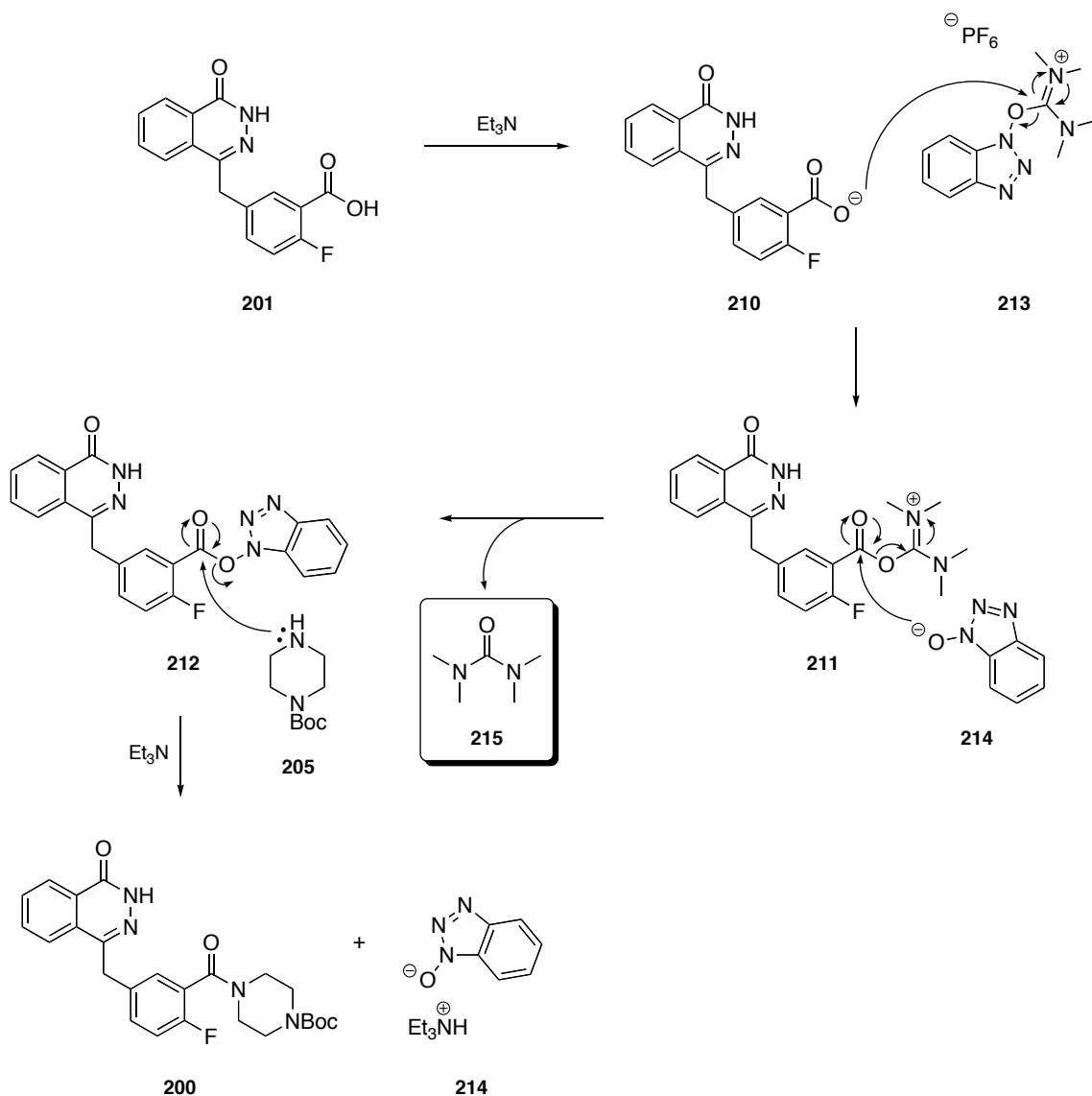
Scheme 57. HBTU amide coupling mechanism

Subsequent removal of the *N*-Boc protecting group under acidic conditions afforded penultimate compound **199** in a 70% yield (Scheme 58). Addition of a linking group to the 4-NH position of the piperazine ring would complete the synthesis of a small library of potential PET imaging agents.
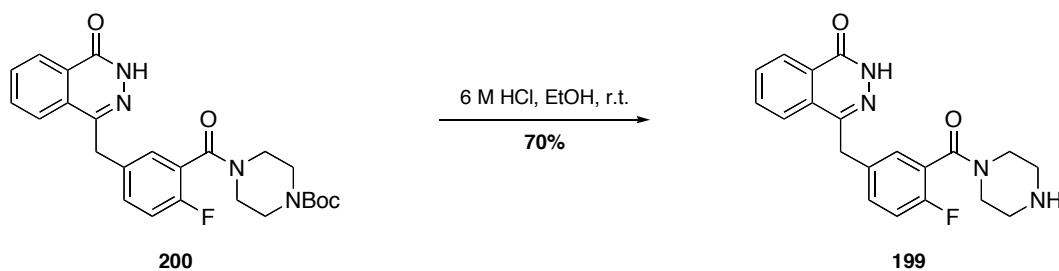
Scheme 58. *N*-Boc protecting group removal

N-Alkylation of the piperazine unit of **199** using either 4-fluoro- or 4-methoxybenzyl chloride in the presence of base (Reaction Conditions A), resulted in the formation of analogues **216** and **222** in a moderate yield of 38% and 42%, respectively (Scheme 59). The remaining final compounds were prepared *via* an amide coupling reaction between phthalazinone **199** and the appropriate carboxylic acid, the conditions for which are listed below in Scheme 59. Target compounds **217**, **218**, **220**, **223** and **224** were prepared using HBTU and Hünigs base (Reaction Conditions B and D) in yields ranging from 40–75%, and EDCI in the presence of catalytic DMAP (Reaction Conditions C) was used to prepare analogues **219** and **221** in yields of 31% and 34%, respectively.

The primary reaction conditions employed for the amide coupling reflected a slightly modified version of that of Menear *et al.*[200] HBTU and Hünigs base was initially trialled in dichloromethane at ambient temperature, but reaction progression proved slow. Stirring the mixture under reflux conditions (Reaction Conditions B) on the other hand, was more constructive and applied to the synthesis of **217** and **218**. Unfortunately, as previously experienced for the synthesis of amide **200**, the high polarity of the amide products lead to purification difficulties, and repetitive rounds of silica column chromatography were required to remove the 1,1,3,3-tetramethylurea (**215**) by-product, which was evident from ^{1}H NMR spectroscopy. In an effort to avoid further use of HBTU, EDCI and DMAP (Reaction Conditions C) was utilised for the preparation of compounds **219** and **221**. However, this coupling agent could not be widely applied, and the synthesis of several of the analogues failed under these conditions. As such, the use of HBTU was once again revisited. In this instance, DMF was employed as the reaction solvent, and after stirring for an initial period of 1 hour at ambient temperature, the reaction temperature was increased to 50 °C and the phthalazinone substrate added. Again, purification of the resulting products proved difficult with losses of yield occurring.
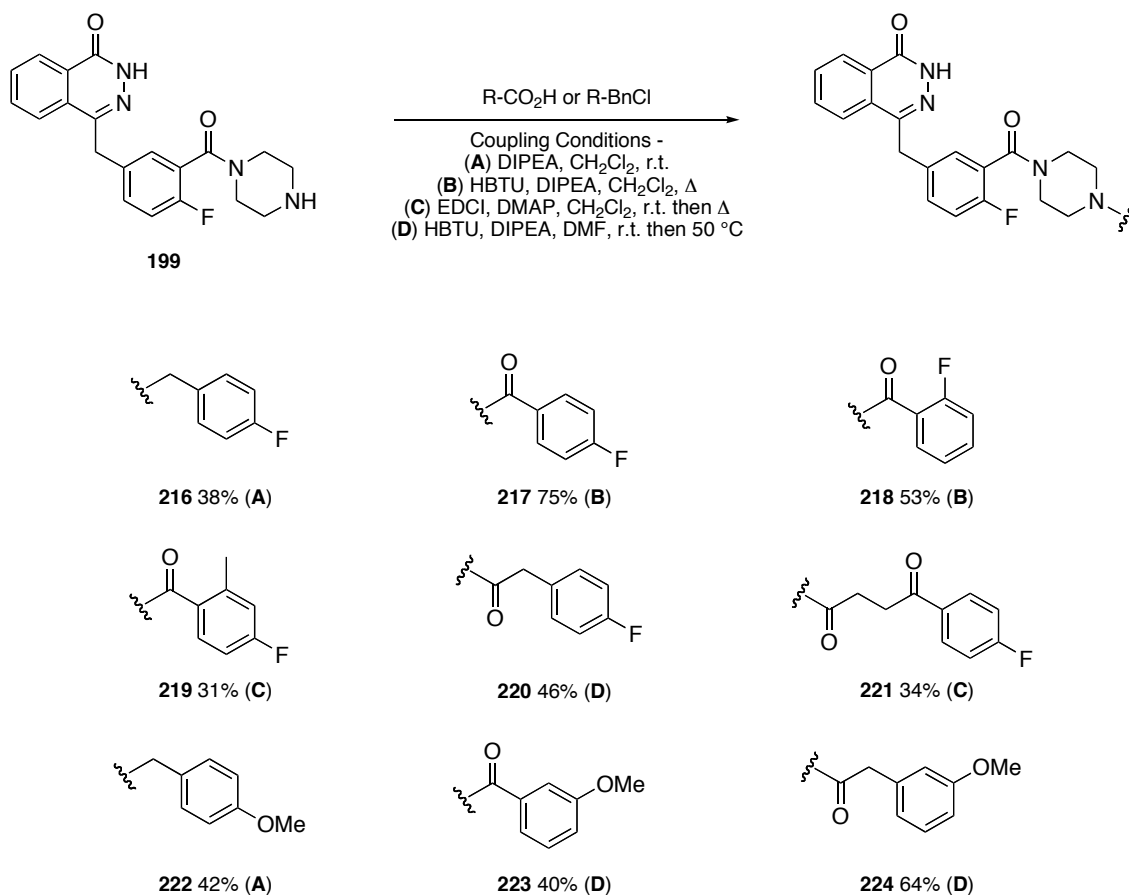
Scheme 59. Synthesis of potential PET imaging agents for PARP-1 activity

Product yields for the final compounds are not optimised, and further work regarding reaction conditions is required to aid purification and develop a more universal method for the amide bond formation.

In an effort to overcome the purification difficulties encountered, a slight modification of the synthetic route was considered. To avoid the use of an amide coupling reagent, formation of an additional target, compound **225**, was achieved *via* the acid chloride (Scheme 60). 4-Methoxyphenylacetic acid (**226**) was treated with thionyl chloride to give acid chloride **227** in a very high 90% yield,[210] which was immediately coupled with phthalazinone **199** in the presence of Hünigs base at ambient temperature. The resulting product **225** was obtained with greater ease of purification in an unoptimised yield of 53%. An advantage of using the coupling reagent is that it reduces the number of overall chemical transformations required to develop the compound library. However, if the use of an acid chloride is advantageous in terms of final product purification, this route may need to be considered for future syntheses.
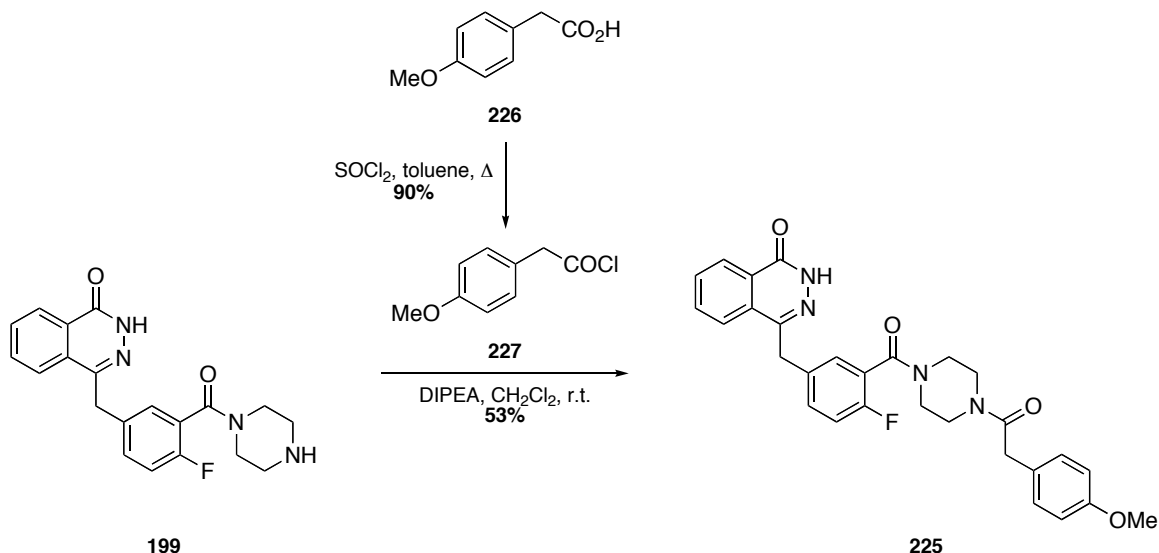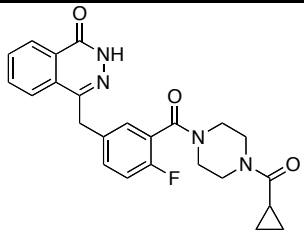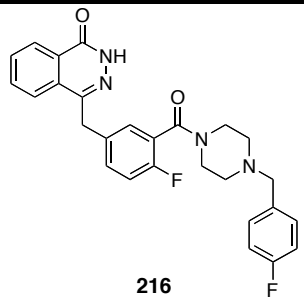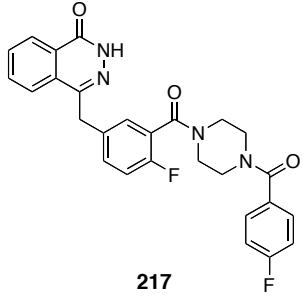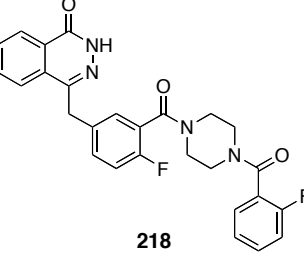
Scheme 60. Synthesis of PARP-1 compound **225** *via* the acyl chloride

3.2.3 Cell-Free PARP-1 Inhibition Study

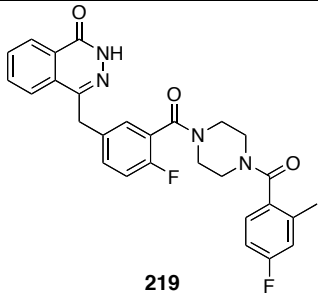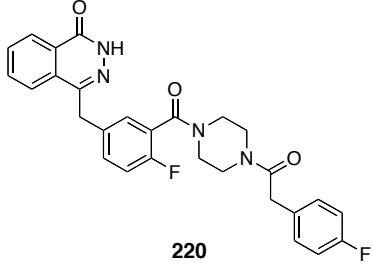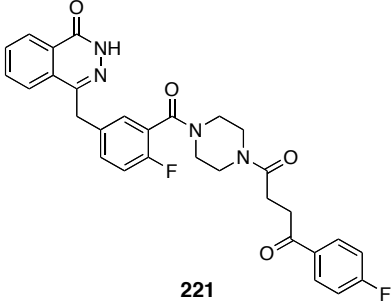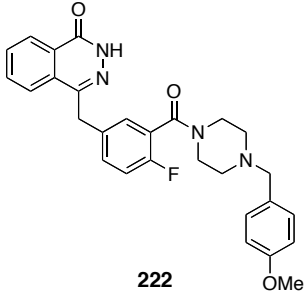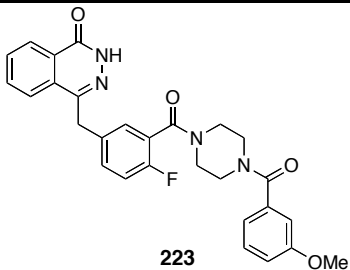Following the synthesis of the novel PARP-1 inhibitors, Filip Zmuda, a PhD student within the Sutherland group, performed an initial biological screen of the compound library. This was achieved using the Trevigen® PARP-1 colourimetric assay, which is an *in vitro* assay designed to measure the PARP-1 IC_{50} value associated with each analogue under cell-free conditions. Performing a rudimentary screen of this sort offers two key advantages: it is a rapid procedure, and allows for the swift elimination of those compounds lacking PARP-1 inhibitory potency.

To ensure that the assay was functioning correctly, and to allow for direct comparison with compounds **216–225**, the IC_{50} value of olaparib was measured as the reference standard. The preliminary IC_{50} values obtained for all compounds are listed below in Tables 14. Consideration of the IC_{50} values obtained indicates that under the assay conditions employed, all analogues confer greater PARP-1 inhibitory potency than that of olaparib, which had an IC_{50} value of 11.9 nM. The most potent compound is methoxy-compound **223** with an IC_{50} of 1.1 nM. A couple of approximate observations can be made at this point. Firstly, as the compounds are all very close in range of IC_{50} values, it would appear that the presence of an electron withdrawing or an electron donating substituent on the aromatic ring has minimal effect on binding potential, and secondly, that the presence of an amide linkage on the terminal benzene moiety provides greater inhibitory potency. The carbonyl group may offer an additional hydrogen bond acceptor site, and thus prevent
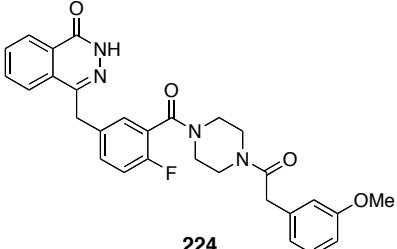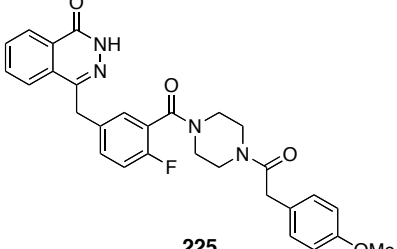
unrestricted rotation around the amide bond leading to an increased binding affinity. However, it should be noted that the differences in inhibitory potency in the presence of an amide bond is not of great magnitude, and that further investigation is required to confirm or reject this rudimentary structure-activity relationship.

Structure	Cell-Free PARP-1 IC$_{50}$ (nM)	95% CI (nM)
Olaparib	11.9	10.5–13.6
216	11.2	7.3–17.3
217	5.9	4.9–7.0
218	3.6	3.4–3.9

Table 14. Cell-Free IC$_{50}$ PARP-1 potency of olaparib and compounds **216–225**

Structure	Cell-Free PARP-1 IC$_{50}$ (nM)	95% CI (nM)
219	2.9	2.3–3.7
220	1.3	0.9–1.7
221	4.1	3.6–4.6
222	9.6	8.0–11.4
223	1.1	0.9–1.4

Table 14 (cont.). Cell-Free IC$_{50}$ PARP-1 potency of olaparib and compounds **216–225**

Structure	Cell-Free PARP-1 IC$_{50}$ (nM)	95% CI (nM)
224	5.1	4.7–5.1
225	4.5	4.0–5.0

Table 14 (cont.). Cell-Free IC$_{50}$ PARP-1 potency of olaparib and compounds **216–225**

Preliminary results from the biological screening of analogues **216–225** are encouraging, and at this point in time no compound should be eliminated from the study. However, a more detailed investigation is required to determine the actions of these compounds within the cellular environment, and gain an appreciation of their physicochemical properties.

3.3 Summary

A research project, which aims to develop a potential PET imaging agent for PARP-1 activity has been initiated. Based on the PARP-1 inhibitor, olaparib, a small library of ten analogues bearing either an aromatic fluoro- or methoxy-substituent has been prepared *via* a rapid seven-step synthesis allowing for late stage structural variation. Furthermore, the route employed allows for the preparation of a suitable radiolabeling precursor, averting the need for an alternative synthetic route. A preliminary biological screen of the compound library has determined cell-free PARP-1 inhibitory potencies ranging from 11.2–1.1 nM, reflecting the potency of the clinical lead, olaparib.

3.4 Future Work

Further work on this project has been initiated and aims to gain further insight into the behavior of these compounds within the cellular environment. This will be achieved by determining the following molecular characteristics: physicochemical properties (lipophilicity and % plasma protein binding), and cellular IC_{50} values. The previously described HPLC methodology will be used to determine physicochemical properties, providing an indication of each compounds ability to penetrate the blood brain barrier. These results, in conjunction with the initial cell-free IC_{50} values, will enable selection of the most appropriate compounds for further studies. A biological screen employing human G7 and T98G glioblastoma cell lines will then be performed, which aims to measure the cellular IC_{50} values of the compounds chosen, and establish whether they target the nucleus. If upon conclusion of this secondary study, any of the analogues are deemed suitable, they will be further developed as potential PET imaging agents for PARP-1 activity.

Additionally, the synthesis and biological evaluation of PARP-1 analogues are ongoing in the Sutherland research group. Variants of olaparib bearing an aliphatic moiety in place of an aromatic fluoride substituent have been identified as interesting targets. Work in this area has already commenced with the attempted synthesis of fluoro-analogue **228** (Scheme 61). Commercially available 3-fluoropropan-1-ol (**229**) was converted to the tosylate **230** in a high yield of 82%,[211] and then subjected to a coupling reaction with phthalazinone **199** to give the *N*-alkylated product **228**. Inspection of the crude reaction mixture by ^{1}H NMR spectroscopy and mass spectrometry indicated the presence of product **228**, but due to time constraints the pure compound was not isolated to a satisfactory standard. Optimisation of reaction conditions and identification of a suitable purification system will enable preparation of additional *N*-alkylated analogues suitable for biological testing.
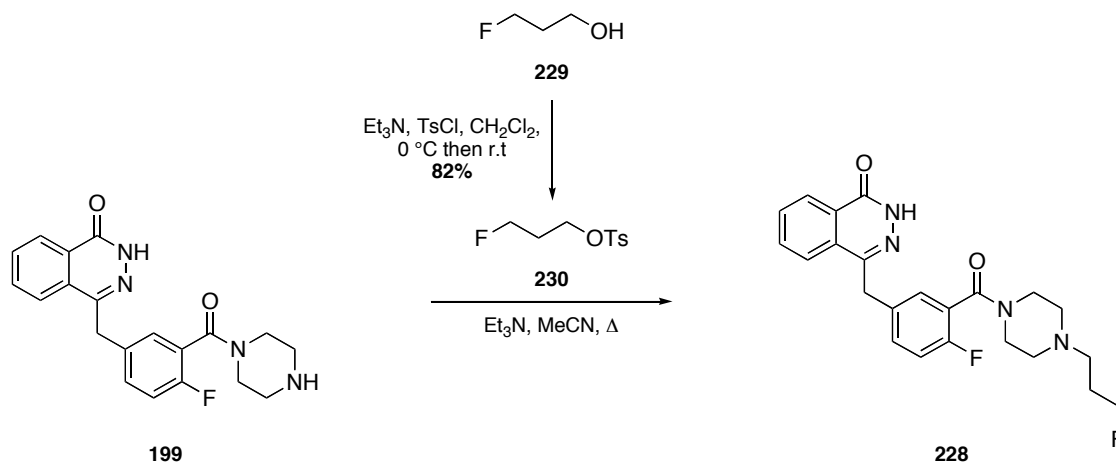
Scheme 61. Attempted synthesis of a potential fluoropropyl PARP-1 inhibitor

# 4 First Total Synthesis of Crispine C

4.1 Introduction

Carduus crispus linn., also known as welted thistle, is a flowering biennial plant that belongs to the asteraceae family (Figure 38).[212] It is native to both Europe and Asia, and has been introduced to North America where it is broadly regarded as an invasive weed. In nature, the principle role of *C. crispus* is sustaining the insect population, *e.g.* it is regarded as the food of choice for the Painted Lady Butterfly and is utilised by bees for the production of honey.[212,213] In addition to its role in wildlife, *C. crispus* is also believed to impart medicinal properties. Extracts of the plant have been utilised in Chinese folk medicine to alleviate the symptoms of common cold, stomachache and rheumatism,[214] and the root has been implicated in the provision of alterative and anodyne properties.[215] Furthermore, *in vitro* screening of the effects of *C. crispus* extracts on cellular growth has shown that the plant confers significant cytotoxic activity against several human cancer cell lines,[214] and has the potential for cancer chemotherapy applications.
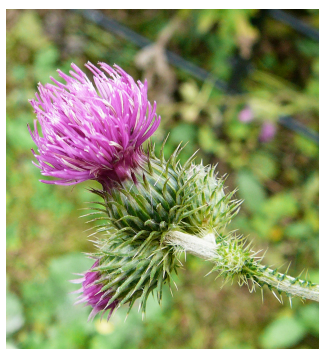
Figure 38. *Carduus crispus* linn.

(Reprinted from www.seasonalwildflowers.com with kind permission of Dr. Keith Jones)[216]

In 2002, Zhang *et al*. reported the isolation and subsequent identification of five natural products from *C. crispuus* (Figure 39).[214] This small library of compounds consisted of two pyrrolo-[2,1-*a*]isoquinoline alkaloids (Crispine A and B) and three bicyclic isoquinoline alkaloids bearing a guanidinyl moiety (Crispine C, D and E).
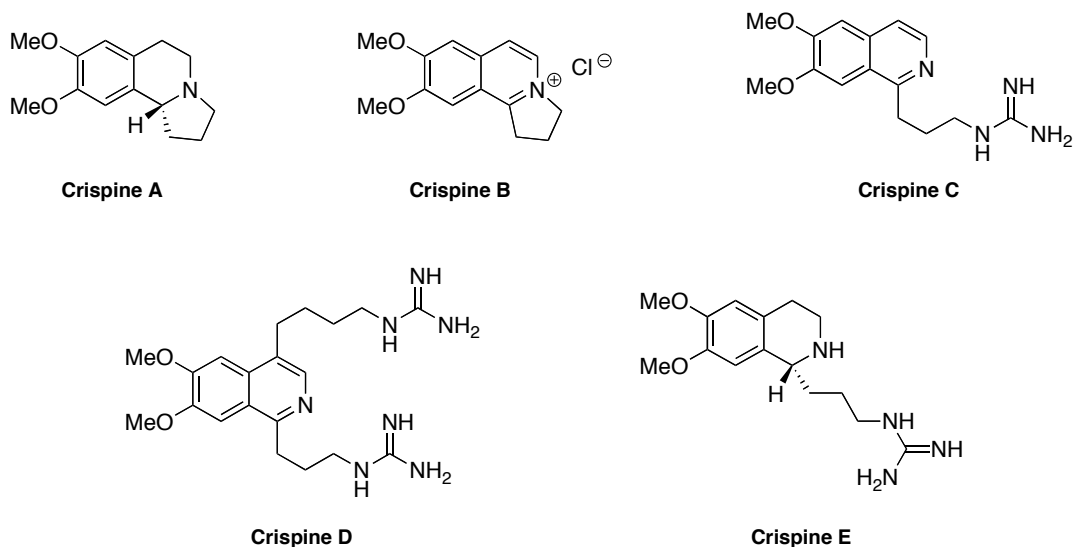
Figure 39. Crispines A–E

Naturally, the interesting chemical structures and pharmacological potential of these five natural alkaloids has led to an increase in the research and development of synthetic routes for the provision of these products. To date, the synthesis of Crispine A, B and E have been reported in the literature, and example syntheses of the pyrrolo-[2,1-*a*]isoquinoline alkaloids (Cripsine A) and bicyclic isoquinoline alkaloids (Crispine E) are described below.

A review of the current literature highlights the diverse range of key chemical transformations that have been successfully employed in the preparation of Crispine A. These reaction sequences have been both racemic and asymmetric,[217,218,219] and have utilised chemistry ranging from a one-pot tandem cyclisation *via* a Bischler-Napieralski reaction followed by cyclopropylimine rearrangement,[220] to a highly diastereoselective *N*-acyliminium cyclisation reaction.[221] More recently, Ruano and co-workers published a very short and highly stereoselective synthesis of (*R*)-(+)-Crispine A (Scheme 62), utilising the *p*-tolylsulfinyl group as a chiral auxiliary.[222] Treatment of 3,4-dimethoxyphenylethylamine (**231**) with strong base, and subsequent reaction with (*S*)-menthyl *p*-toluenesulfinate resulted in the enantioselective preparation of *N*-sulfinyl amine **232** (94.5% *e.e.*). Reaction of this precursor with 4-chlorobutanal in the presence of boron trifluoride as the Lewis acid catalyst gave the desired Pictet-Spengler product **233** in both high diastereo- and enantioselectivities (>98% *d.e.*, 94.8% *e.e.*). Removal of the chiral auxiliary by acidic cleavage of the N-S bond, followed by *in situ* cyclisation of

intermediate **234**, afforded (*R*)-(+)-Crispine A (**235**) in 3 steps with an overall yield of 43%.
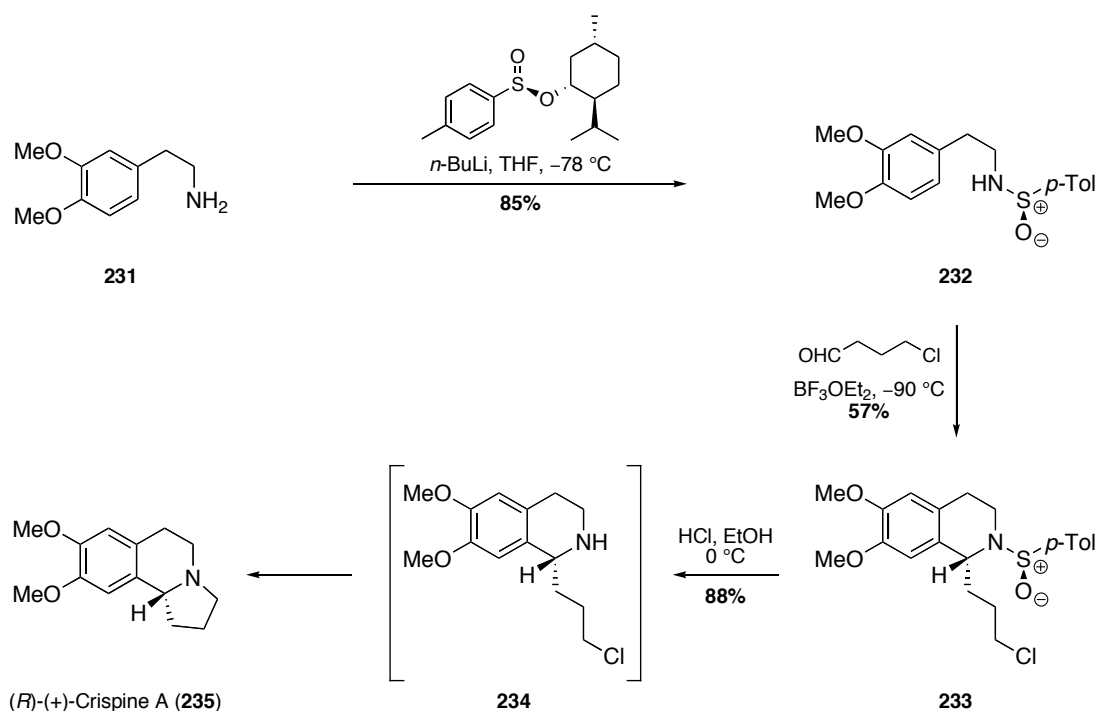
**Scheme 62.** Synthesis of (*R*)-(+)-Crispine A by Ruano and co-workers[222]

In 2008, Czarnocki *et al.* reported the enantioselective synthesis of (*R*)-(+)-Crispine E (Scheme 63).[223] Commercially available γ-phthalimidobutyric acid was initially converted to acid chloride **236**, and coupled to homoveratrylamine (**231**) to form amide **237**. Treatment of this amide with phosphorus(V) oxychloride gave the Bischler-Napieralski product, imine **238**, which was subsequently reduced using (*S,S,*)-**242** to afford intermediate **239** in high enantioselectivity (*e.e.* 89%). Deprotection of the phthalyl group using hydrazine, followed by immediate reaction with *N,N'*-bis(Boc)-*S*-methylisothiourea to introduce the guanidine unit, resulted in the formation of precursor **240**. A final Boc group deprotection of the guanidyl moiety of **240** under acidic conditions afforded the target product (*R*)-(+)-Crispine E (**241**).
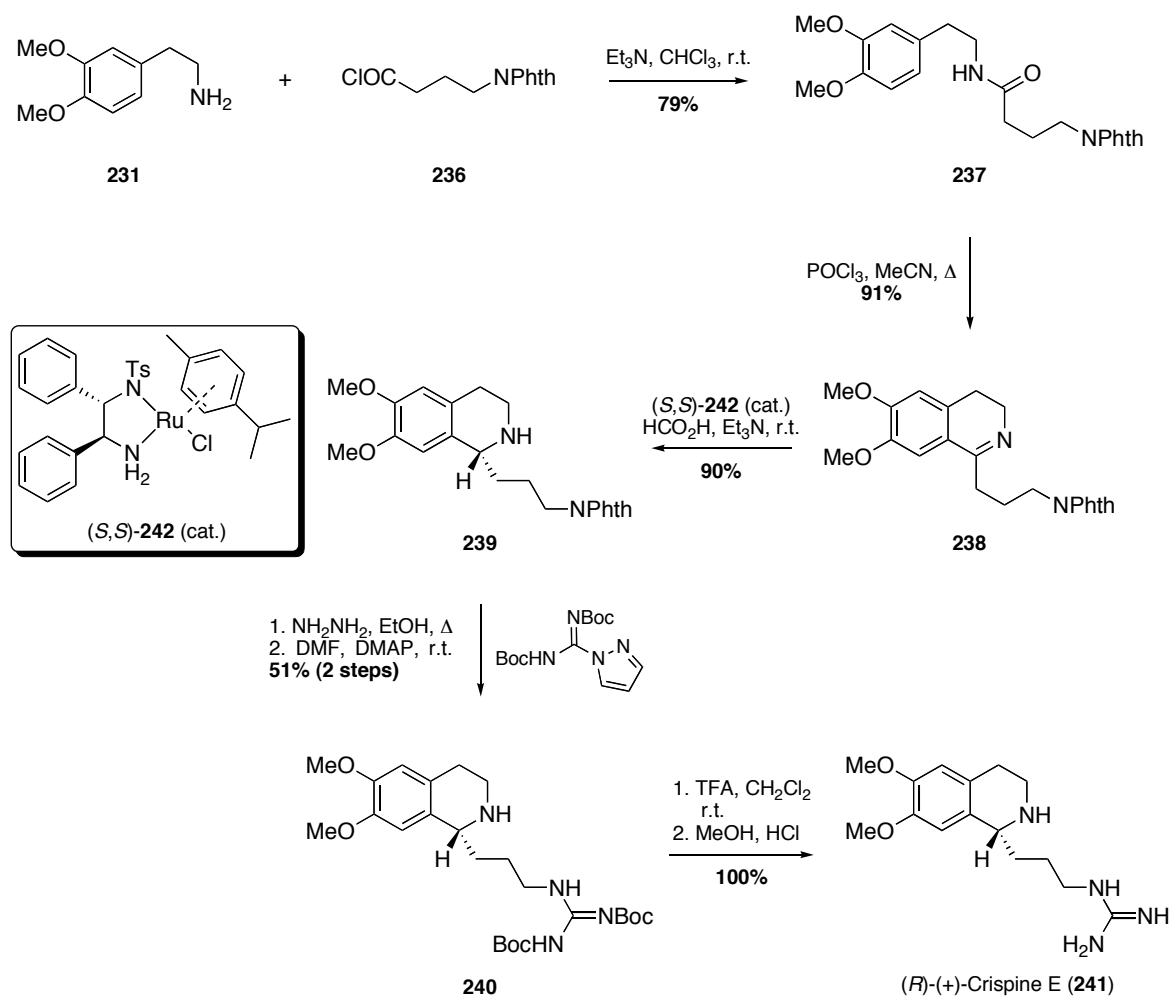
Scheme 63. Synthesis of (*R*)-(+)-Crispine E by Czarnoki *et al.*[223]

4.2 Proposed Research

Owing to the interesting chemical structure of this class of natural products and their potential application in medicine, the synthesis of Crispine A, B and E has thus far been achieved and reported in the literature. To date, there has been no reported synthesis of Crispine C (**243**) (Figure 40), and so the aim of this project was to develop a short and efficient synthetic route enabling the first total synthesis of Crispine C to be achieved.
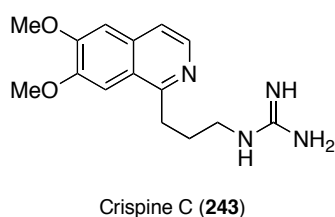
Crispine C (**243**)

Figure 40. Crispine C

4.3 Retrosynthetic Analysis of Crispine C

A proposed retrosynthetic analysis of Crispine C is detailed below in Scheme 64. An initial disconnection of the guanidine unit of **243** gives amine **244**. Further disconnection of the core isoquinoline ring then affords amide **245**, which can in turn be prepared from amine **246** and Cbz protected γ-aminobutyric acid (**250**). γ-aminobutyric acid is a commercially available starting material that can be protected in a single step. Functional group interconversion of amine **246** to the nitro group of compound **247**, followed by disconnection of the methoxy substituent provides, α,β-unsaturated nitro compound **248**. Finally, this nitroalkene can be prepared from commercially available 3,4-dimethoxybenzaldehyde (**249**) *via* a dehydrative Henry reaction.
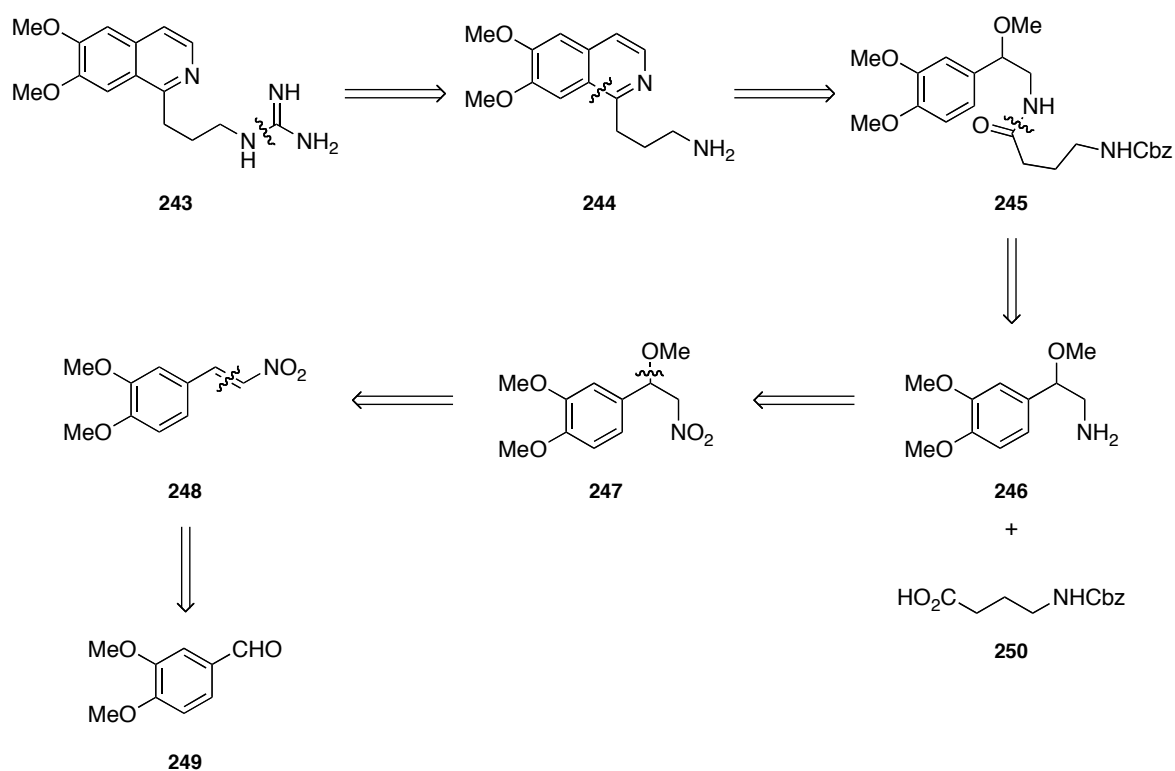
Scheme 64. Retrosynthetic analysis of Crispine C (**249**)

Formation of the isoquinoline core from the corresponding amide **245** *via* the Pictet-Gams modification of the Bischler-Napieralski reaction, will be the key step in this sequence of transformations.

4.4 Steps Towards the First Total Synthesis of Crispine C

4.4.1 Synthesis of Amine 246

The first step towards the total synthesis of Crispine C required the preparation of amine intermediate **246**, which was achieved in three steps starting from commercially available 3,4-dimethoxybenzaldehyde (Scheme 65).   Firstly, reaction of aldehyde **249** with nitromethane in the presence of ammonium acetate under reflux conditions gave (*E*)-nitroalkene **248** exclusively in quantitative yield.[224] Inspection of the ^{1}H NMR spectrum of the crude product indicated that no side products or starting material were present, and the compound was applied to the next synthetic step without prior purification.

Formation of a β-nitro alcohol by reaction of a carbonyl containing compound and nitroalkane under basic conditions is referred to as the Henry or nitro-aldol reaction, and is a completely reversible reaction.[88] In principal, a base is initially used to generate a resonance-stabilised anion of the nitroalkane, which then undergoes an aldol reaction with the carbonyl carbon forming a β-nitro alcohol after protonation.   Under the reaction conditions detailed in step one of Scheme 65, dehydration of the β-nitro alcohol forming nitroalkene **248** occurs. The synthesis of this α,β-unsaturated nitro compound prevents the retro-Henry reaction from occurring, and furthermore, can act as a Michael acceptor in the next step.

Next, conjugate addition of the methoxide ion to nitroalkene **248** using a 25% sodium methoxide in methanol solution, gave β-nitro alkoxide **247** in a moderate 50% yield.[224] In addition to compound **247**, unidentified side-products were an observed consequence of this transformation, making purification troublesome. At times, repetitive cycles of silica column chromatography to remove close running impurities, followed by recrystallisation, was required for purification, and this stringent purification process greatly affected product yield.

Reduction of the nitro group to the corresponding amine was then necessary to complete the synthesis of amine fragment **246**, and this step was initially performed using a lithium aluminium hydride solution in diethyl ether under reflux conditions. Despite several attempts at this reaction, only a low yield of 30% was obtained for compound **246**. Termination of the reaction by addition of water to quench excess reducing agent generates

lithium salts. It is, therefore, possible that the product is becoming trapped in the salts formed during work-up, culminating in an extensively reduced isolated product yield.
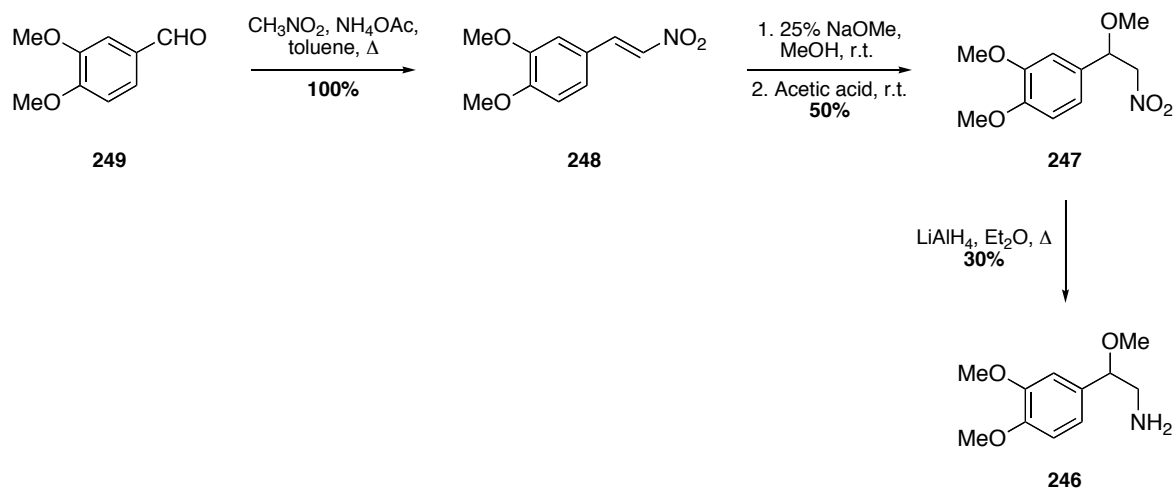
Scheme 65. Synthesis of amine fragment **246**

Aliphatic nitro groups are generally reduced to the corresponding amine using relatively harsh reducing agents and conditions, *e.g.* high-pressure catalytic hydrogenation and lithium aluminium hydride.[225,226] As such, an effort to improve the reduction of compound **247** to amine **246** through application of milder reducing conditions was investigated (Table 15). A procedure developed by Osby and Ganem, utilising an excess of sodium borohydride and a catalytic quantity of nickel(II) chloride to form the active catalyst was trialed for the reduction of compound **247** (Entry 1).[227] Unfortunately, analysis of the crude reaction mixture indicated that these conditions were ineffective, and only starting material remained after 48 hours. Next, a transfer hydrogenation reaction developed by Ram and Ehrenkaufer using 10% palladium on carbon and ammonium formate was then applied to the substrate (Entry 2), but again no reaction had occurred after 24 hours and only the substrate remained.[228] Finally, hydrogenation of the nitro group using 10% palladium on carbon and hydrogen at atmospheric pressure was attempted on a small quantity of crude starting material (Entry 3). Examination of the reaction mixture using ^{1}H NMR spectroscopy indicated that reduction had possibly occurred, but the presence of original impurities prevented effective separation of the compound mixture and the ability to determine the overall success of the reaction. Reduction of the nitro group using milder reaction conditions had, thus far, either failed completely or afforded inconclusive results. At this point in time, only lithium aluminium hydride had been successfully employed for the reduction of compound **247**, albeit in a poor yield. It was, therefore, decided that

progression with the intended synthetic route would ensue. However, application of the palladium-catalysed hydrogenation under atmospheric conditions would be reconsidered for future reductions in this route when necessary.

Entry	Reagents	Conditions	Outcome
1	NaBH$_4$, NiCl$_2$	MeOH, r.t.	No Reaction
2	NH$_4$CO$_2$H, 10% Pd/C	MeOH, Δ	No Reaction
3	10% Pd/C, H$_2$	MeOH, r.t.	Possible Reduction*

* Confirmation and yield not determined due to problems separating reaction mixture

Table 15. Reaction conditions trialed for aliphatic nitro group reduction

The next step of the synthesis required coupling of the amine product of the previous reaction with γ-aminobutyric acid, furnishing the target amide. A wide range of peptide coupling agents and conditions are available, and in an attempt to aid purification and isolation of the product, EDCI and a catalytic quantity of DMAP were chosen as the preferred reagents. Firstly, treatment of butyric acid **251** with benzyl chloroformate under Schotten-Baumann conditions afforded the Cbz-protected carboxylic acid **250** in a 70% yield,[229] which was subsequently coupled with amine **246** to afford amide **245** in a good yield of 79% (Scheme 66).
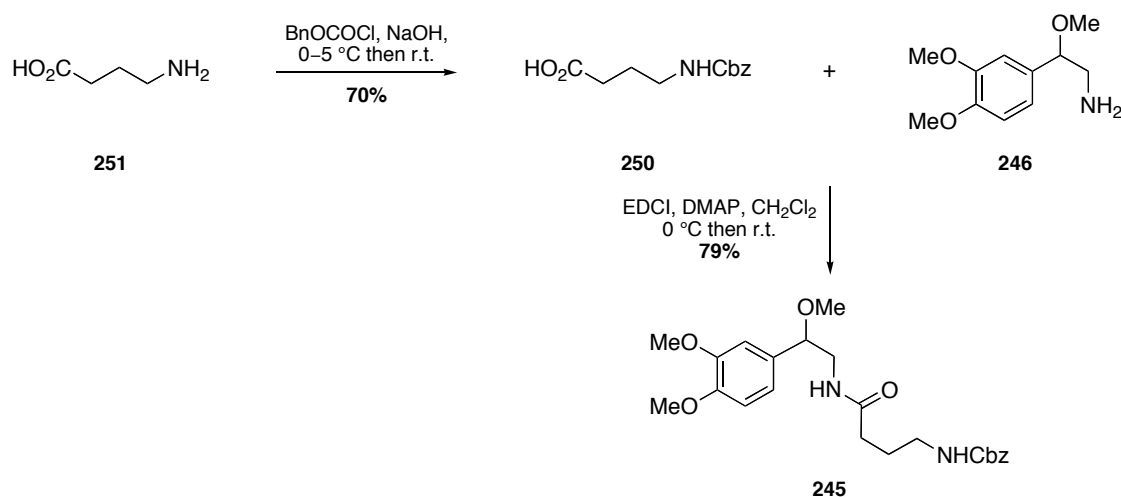
Scheme 66. Amide coupling reaction

With the isoquinoline precursor in hand, the next step involved cyclisation of amide **245** *via* the Pictet-Gams modification of the Bischler-Napieralski reaction. The Pictet-Gams

variation utilises a cyclisation reagent, *e.g.* phosphorus pentaoxide and phosphorus oxychloride, for the cyclodehydration of a β-methoxy- or β-hydroxy-arylethanamine, enabling the direct formation of a fully aromatic isoquinoline.[230] An initial attempt to cyclise amide **245** using modified conditions from Czarnocki *et al.* was unsuccessful (Scheme 67).[223] Analysis of the ^{1}H NMR spectrum of the crude reaction mixture bore no evidence of the desired isoquinoline, and under the acidic conditions employed, the Cbz protecting group had been removed. It should be noted that phosphorus(V) oxybromide was utilised in this reaction due to availability, and that all further chemical manipulations will employ phosphorus(V) oxychloride.
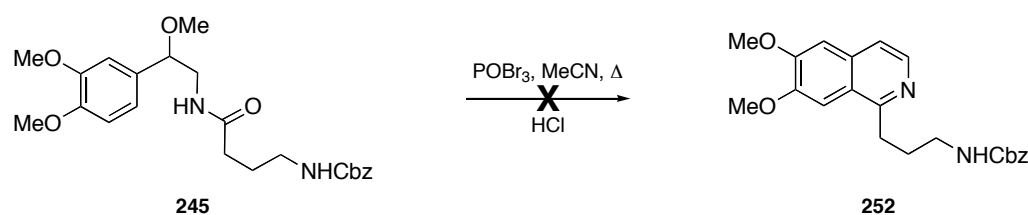
Scheme 67. Attempted cyclisation of amide **245** using Pictet-Gams conditions

The failed attempt to form isoquinoline **252**, coupled with the low to moderate yields obtained for the preparation of β-nitro alkoxide **247** and its ensuing reduction to amine **246**, led to the termination of this approach. It was anticipated that a more efficient and direct preparation of Crispine C could be achieved using a slightly modified version of the original synthetic route.

4.4.2 Synthesis of Amine 254: Cyanohydrin Synthesis

In 1995, Zhao and Wan reported the high yielding preparation of cyanohydrin **253** by reaction of 3,4-dimethoxybenzaldehyde with potassium cyanide in the presence of ammonium chloride at ambient temperature (Scheme 68).[231] Moreover, the authors indicated that the nitrile group could be reduced with ease to amine **254** in very good yield using lithium aluminium hydride. However, despite repeated attempts to replicate the synthesis of cyanohydrin **253**, no product was isolated.

Formation of a cyanohydrin by the nucleophilic addition of cyanide to a carbonyl group is a reversible process.[232] This is a probable explanation as to why attempts to prepare compound **253** were unsuccessful, and efforts to circumvent this problem were attempted.

It was envisaged that the inclusion of methyl iodide and a base to the resulting cyanohydrin would form alkoxide **255**, thereby trapping the oxygen, and preventing reversion of the cyanide addition. However, when aldehyde **249** was treated with potassium cyanide and, following a very quick extraction, reacted with methyl iodide and triethylamine, no desired product was formed and only starting material remained (Scheme 68).[233] A subsequent attempt to synthesise **255** using a procedure adapted from Yadav *et al.*,[234] utilising lithium tetrafluoroborate as the catalyst for coupling the aldehyde, cyanide and methyl iodide in one pot was attempted, but this transformation proved unsuccessful once again.
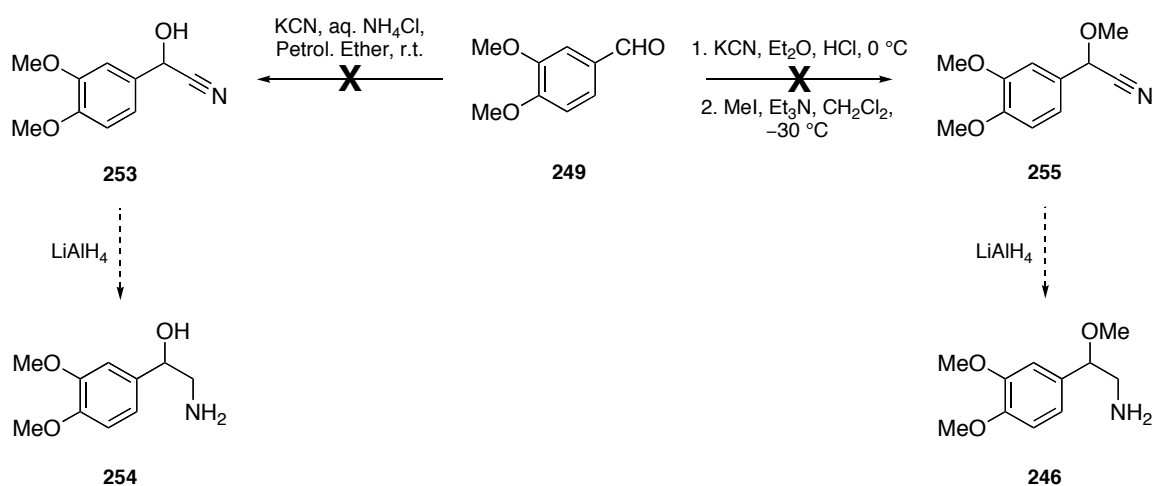

Scheme 68. Attempted synthesis of cyanohydrins **253** and **255**

4.4.3 Synthesis of Amine 254: The Henry Reaction Revisited

The failure to prepare amines **254** and **246** from cyanohydrin intermediates **253** and **255** respectively, led to the decision to revisit the Henry reaction (Scheme 69). However, where dehydration to form the nitroalkene had previously been encouraged, the current strategy aimed to prevent this. The reaction conditions investigated for this transformation are listed below in Table 16. When Hünigs base in tetrahydrofuran was employed for the transformation,[235] no reaction occurred (Entry 1), and a similar result was obtained for triethylamine in toluene (Entry 2). However, when the reaction was performed in neat triethylamine a product yield of 30% was obtained (Entry 3). This yield was unexpected as inspection of the ^{1}H NMR spectrum of crude material indicated a 3:1 mixture of product to aldehyde starting material; highlighting the reversibility of this reaction. Next, the preparation of β-nitro alcohol **256** was attempted using the procedure of Muraoka and co-workers.[236] In the presence of 4 Å molecular sieves, the starting material was treated with

nitromethane in dimethylsulfoxide at ambient temperature, affording compound **256** in a high yield of 85% (Entry 4).
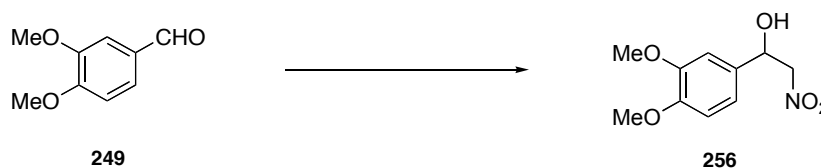
**Scheme 69.** Synthesis of β-nitro alcohol **256** *via* a Henry reaction

Entry	Reagents	Conditions	Yield 256 (%)
1	MeNO$_2$, DIPEA	THF, r.t.	-
2	MeNO$_2$, Et$_3$N	Toluene, r.t.	-
3	MeNO$_2$, Et$_3$N	r.t.	30
4	**MeNO$_2$, DMSO**	**4 Å MS, r.t.**	**85**

Table 16. Reaction conditions trialed for the Henry reaction

Previous, attempts at reduction of the aliphatic nitro group of compound **247** (Scheme 65, Table 15) had proved problematic, with only lithium aluminium hydride providing limited success. Keen to improve this reaction and avoid the loss of product during work-up, the palladium-catalysed reduction of the nitro group with hydrogen at atmospheric pressure was considered (Scheme 70). Application of these conditions to β-nitro alcohol **256** afforded β-amino alcohol **255** in quantitative yield, which was subsequently coupled to the Cbz-protected butyric acid giving amide **257** in a good yield of 79%. Initially, treatment of amide **257** with neat phosphorus(V) oxychloride under reflux resulted in the formation of the desired isoquinoline **252** in 24% yield. Despite this being a low yielding reaction, the formation of compound **252** was a positive step. However, it soon became apparent that this was a capricious reaction, as synthesis of the isoquinoline core could not be repeated. In an effort to replicate the synthesis of **252**, the phosphorus(V) oxychloride was distilled prior to use to remove any phosphoric acid degradation product. Additionally, both reaction temperature and amount of phosphorus(V) oxychloride used was reduced to 50 °C and 2.4 equivalents, respectively and dichloromethane was also trialed as the reaction solvent. However, despite these modifications to the reaction conditions, decomposition of the starting material occurred every time.
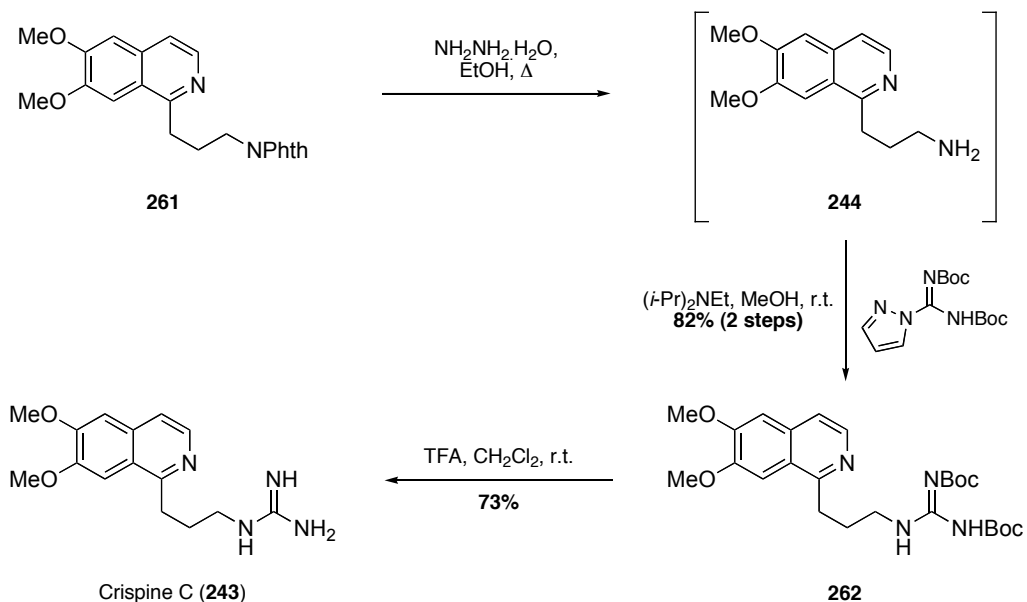
Scheme 70. Synthesis of isoquinoline **252**

4.4.4 Replacement of the Cbz-Protecting Group

In an attempt to overcome the problems encountered during cyclisation of the amide precursor to form the isoquinoline core, the acid-sensitive Cbz protecting group was replaced with the phthalimide group (Scheme 71). Treatment of γ-aminobutyric acid (**251**) with neat phthalic anhydride (**258**) at 170 °C gave carboxylic acid **259** in an excellent yield of 93%.[237]

Scheme 71. Phthalimide protection of γ-aminobutyric acid (**259**)

Amine **255** and the protected butyric acid were then subject to the same peptide coupling conditions employed previously, resulting in the formation of amide **260** in a good yield of 75% (Scheme 72). With the new isoquinoline precursor in hand, the vital cyclodehydration reaction could now be investigated. Using toluene as the reaction solvent, amide **260** was treated with freshly distilled phosphorus(V) oxychloride under reflux conditions to give the target Pictet-Gams product **261**. Variation of the number of reagent equivalents used, enabled an acceptable product yield of 66% for isoquinoline **261**

to be obtained when 3.0 equivalents of phosphorus(V) oxychloride was employed (Table 17, Entry 3).

Scheme 72. Synthesis of isoquinoline **261**
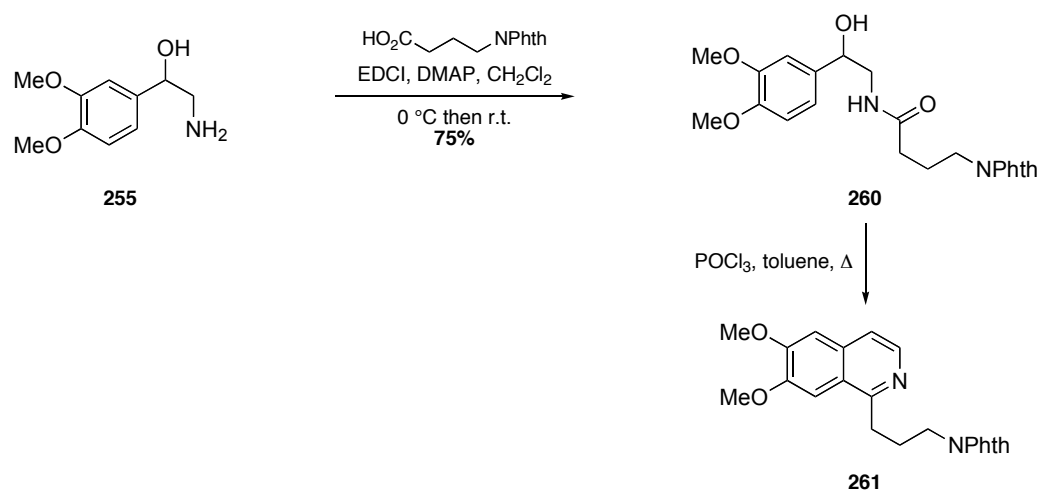
Entry	POCl$_3$ (eq.)	Yield 261 (%)
1	2.4	23
2	2.5	43
3	**3.0**	**66**
4	Excess	Trace

Table 17. Optimisation of Pictet-Gams conditions

Having optimised the synthesis of the isoquinoline core, the remaining steps of the synthetic route could now be undertaken (Scheme 73). Incorporation of the guanidyl moiety was achieved using a two-step process. First, removal of the phthalimide protecting group using hydrazine monohydrate afforded amine **244**. This was then immediately reacted with commercially available *N,N'*-bis(*tert*-butoxycarbonyl)-1*H*-pyrazole-1-carboxamidine in the presence of Hünig's base to give compound **262** in 82% yield over 2 steps.[238,239] Finally, treatment of penultimate compound **262** with trifluoroacetic acid enabled removal of the Boc-protecting groups from the guanidine unit to give Crispine C (**243**) in 73% yield.

Scheme 73. Synthesis of Crispine C (**243**) from isoquinoline **261**

4.5 Summary

In summary, the first total synthesis of Crispine C was achieved in seven steps and with an overall product yield of 25%, from commercially available 3,4-dimethoxybenzaldehde and γ-aminobutyric acid. The key transformation of the synthetic route required formation of the target isoquinoline core, which was achieved using the Pictet-Gams modification of the Bischler-Napieralski reaction. The spectroscopic data obtained for the final isolated compound was in complete agreement with that reported in the literature for Crispine C by Zhang *et al.*[214]

5 Experimental

5.1 General Experimental

All reagents and starting materials were obtained from commercial sources and used as received. All dry solvents were purified using a PureSolv 500 MD solvent purification system. All reactions were performed under an atmosphere of argon unless otherwise stated. Brine is defined as a saturated solution of aqueous sodium chloride. Flash column chromatography was carried out using Fisher Matrix flash 60. Macherey-Nagel aluminium-backed plates pre-coated with silica gel 60 (UV$_{254}$) were used for thin layer chromatography and were visualised using UV light or staining with potassium permanganate. ^{1}H NMR and ^{13}C NMR spectra were recorded on a Bruker DPX 400 or Bruker 500 spectrometer, with chemical shift values reported in ppm relative to tetramethylsilane (δ_H 0.00 and δ_C 0.0), residual chloroform (δ_H 7.26 and δ_C 77.16), dimethylsulfoxide (δ_H 2.50 and δ_C 39.52), or methanol (δ_H 3.31 and δ_C 49.00) as the standard. Proton and carbon assignments are based on two-dimensional COSY and DEPT experiments, respectively. Infrared spectra were recorded using Golden Gate apparatus on a JASCO FTIR 410 spectrometer, and mass spectra were obtained using a JEOL JMS-700 or Bruker Microtof-q spectrometer. Melting points were determined on a Gallenkamp melting point apparatus.

5.2 TSPO Experimental

Ethyl 4-hydroxyquinoline-2-carboxylate (96)[240]
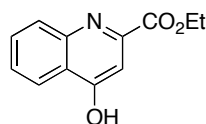
A suspension of aniline (**98**) (2.20 mL, 23.8 mmol), diethyl oxalacetate (**99**) (5.00 g, 23.8 mmol) and *p*-toluenesulfonic acid (4.53 g, 23.8 mmol) in cyclohexane (100 mL) was stirred vigorously under reflux with Dean-Stark conditions for 48 h. After cooling to ambient temperature, the suspension was filtered, washed with cyclohexane and the filtrate concentrated *in vacuo* to yield the desired imine as a yellow oil. Neat polyphosphoric acid (~10 g) was added to the imine and stirred vigorously at 120 °C for 1 h. After cooling to

ambient temperature, excess acid was quenched by the slow addition of a saturated solution of aqueous sodium hydrogen carbonate (100 mL). The aqueous mixture was diluted by the addition of chloroform (100 mL) and separated. The aqueous fraction was washed with chloroform (3 × 100 mL), and the combined organic layers dried (MgSO$_4$), filtered and concentrated *in vacuo* to yield a dark yellow solid. Purification using flash column chromatography (methanol/dichloromethane, 1:9) afforded ethyl 4-hydroxyquinoline-2-carboxylate (**96**) (1.92 g, 37%) as a light tan solid. Mp 215–216 °C (lit.,[240] mp 213 °C); ν_{max}/cm^{-1} (neat) 2882 (CH), 1736 (CO), 1607 (C=C), 1560, 1518, 1312, 1267, 1233, 1009; δ_H (400 MHz, CDCl$_3$) 1.44 (3H, t, *J* 7.2 Hz, OCH$_2$C*H*$_3$), 4.49 (2H, q, *J* 7.2 Hz, OC*H*$_2$CH$_3$), 6.99 (1H, d, *J* 1.6 Hz, ArH), 7.39 (1H, t, *J* 8.0 Hz, ArH), 7.43 (1H, d, *J* 8.4 Hz, ArH), 7.67 (1H, ddd, *J* 8.4, 8.0, 1.6 Hz, ArH), 8.35 (1H, dd, *J* 8.0, 0.4 Hz, ArH), 9.01 (1H, br s, OH); δ_C (101 MHz, CDCl$_3$) 14.1 (CH$_3$), 63.4 (CH$_2$), 111.7 (CH), 118.0 (CH), 124.5 (CH), 126.4 (CH), 126.4 (C), 133.1 (CH), 136.4 (C), 139.0 (C), 163.0 (C), 179.7 (C); *m/z* (EI) 217.0735 (M$^+$. C$_{12}$H$_{11}$NO$_3$ requires 217.0739), 189 (6%), 171 (22), 143 (98), 115 (30), 89 (27), 83 (27), 49 (29).

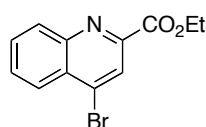**Ethyl 4-hydroxy-3-methylquinoline-2-carboxylate (97)[89]**
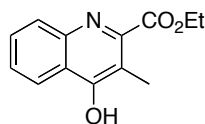
A solution of aniline (**98**) (4.50 mL, 49.4 mmol), diethyl oxalpropionate (**100**) (9.14 mL, 49.4 mmol) and *p*-toluenesulfonic acid (0.070 g, 0.37 mmol) in cyclohexane (125 mL) was stirred vigorously under reflux with Dean-Stark conditions for 48 h. After cooling to ambient temperature, the suspension was filtrered, washed with cyclohexane and the filtrate concentrated *in vacuo* to yield the desired imine as a yellow oil. Neat polyphosphoric acid (~30 g) was added to the imine, and the resultant mixture stirred vigorously at 120 °C for 1 h. On cooling to ambient temperature, excess acid was quenched by the slow addition of a saturated solution of aqueous sodium hydrogen carbonate (100 mL). The resultant precipitate was removed by filtration and reconstituted in chloroform. Insoluble impurities were then removed by hot filtration. The organic layer was dried (MgSO$_4$), filtered and concentrated *in vacuo* to yield an orange solid. Trituration using diethyl ether followed by petroleum ether, gave ethyl 4-hydroxy-3-methylquinoline-2-carboxylate (**97**) (7.35 g, 65%) as a yellow solid. Spectroscopic data in accordance with the literature.[89] Mp 176–177 °C (lit.,[89] mp 176–178

°C); ν_{max}/cm^{-1} (neat) 3372 (OH), 3071 (CH), 1734 (CO), 1603 (C=C), 1547, 1516, 1221, 1117, 1059; δ_H (400 MHz, CDCl$_3$) 1.40 (3H, t, J 7.2 Hz, OCH$_2$CH_3), 2.43 (3H, s, CH$_3$), 4.44 (2H, q, J 7.2 Hz, OCH_2CH$_3$), 7.22–7.29 (1H, m, ArH), 7.41 (1H, d, J 8.4 Hz, ArH), 7.51–7.58 (1H, m, ArH), 8.30 (1H, dd, J 8.4, 1.2 Hz, ArH), 9.50 (1H, br s, OH); δ_C (101 MHz, CDCl$_3$) 11.6 (CH$_3$), 14.2 (CH$_3$), 63.2 (CH$_2$), 117.7 (CH), 122.5 (C), 123.7 (CH), 123.8 (C), 126.4 (CH), 132.6 (CH), 133.2 (C), 138.5 (C), 164.2 (C), 179.6 (C); m/z (EI) 231.0898 (M$^+$. C$_{13}$H$_{13}$NO$_3$ requires 231.0895), 202 (100%), 157 (90), 129 (60), 102 (32), 77 (28).

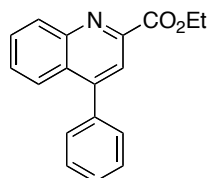**Ethyl 4-bromoquinoline-2-carboxylate (94)[241]**

To a solution of ethyl 4-hydroxyquinoline-2-carboxylate (**96**) (3.36 g, 15.5 mmol) in acetonitrile (150 mL) was added phosphorus oxybromide (13.3 g, 46.4 mmol) followed by potassium carbonate (6.41 g, 46.4 mmol). The resultant suspension was heated under reflux and stirred for 2 h. After cooling to ambient temperature, the solution was concentrated *in vacuo* and water (100 mL) slowly added. The crude product was extracted into ethyl acetate (3 × 100 mL), and the combined organic layers were concentrated *in vacuo* to yield a dark brown oil from which ethyl 4-bromoquinoline-2-carboxylate (**94**) (3.97 g, 92%) crystallized forming a solid. Mp 87–89 °C (lit.,[241] mp 91–92 °C); ν_{max}/cm^{-1} (neat) 2996 (CH), 1709 (CO), 1553 (C=C), 1458, 1366, 1312, 1196, 1146, 1105; δ_H (400 MHz, CDCl$_3$) 1.49 (3H, t, J 7.2 Hz, OCH$_2$CH_3), 4.56 (2H, q, J 7.2 Hz, OCH_2CH$_3$), 7.75 (1H, ddd, J 8.4, 6.8, 1.2 Hz, ArH), 7.84 (1H, ddd, J 8.4, 6.8, 1.2 Hz, ArH), 8.24 (1H, dd, J 8.4, 1.2 Hz, ArH), 8.34 (1H, d, J 8.4 Hz, ArH), 8.47 (1H, s, ArH); δ_C (101 MHz, CDCl$_3$) 14.4 (CH$_3$), 62.7 (CH$_2$), 125.1 (CH), 126.7 (CH), 128.9 (C), 130.0 (CH), 131.1 (CH), 131.2 (CH), 135.4 (C), 147.8 (C), 147.9 (C), 164.2 (C); m/z (CI) 279.9974 (MH$^+$. C$_{12}$H$_{11}^{79}$BrNO$_2$ requires 279.9973), 218 (52%), 202 (47), 157 (3), 85 (9).

Ethyl 4-bromo-3-methylquinoline-2-carboxylate (95)[89]
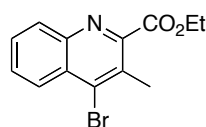
Ethyl 4-bromo-3-methylquinoline-2-carboxylate (**95**) was synthesised as described above for ethyl 4-bromoquinoline-2-carboxylate (**94**) using ethyl 4-hydroxy-3-methylquinoline-2-carboxylate (**97**) (2.21 g, 9.56 mmol), phosphorus oxybromide (8.22 g, 28.7 mmol) and potassium carbonate (3.96 g, 28.7 mmol) in acetonitrile (100 mL). Extraction afforded ethyl 4-bromo-3-methylquinoline-2-carboxylate (**95**) (2.75 g, 98%) as a dark brown oil, which crystallised on standing to form a solid. Spectroscopic data in accordance with the literature.[89] Mp 50–51 °C (lit.,[89] mp 48–50 °C); ν_{max}/cm^{-1} (neat) 3117, 2990 (CH), 1713 (CO), 1622 (C=C), 1478, 1377, 1310, 1206, 1146; δ_H (400 MHz, CDCl$_3$) 1.47 (3H, t, J 7.2 Hz, OCH$_2$CH_3), 2.70 (3H, s, CH$_3$), 4.53 (2H, q, J 7.2 Hz, OCH_2CH$_3$), 7.67 (1H, ddd, J 8.4, 7.2, 1.6 Hz, ArH), 7.73 (1H, ddd, J 8.4, 7.2, 1.6 Hz, ArH), 8.12–8.16 (1H, m, ArH), 8.22 (1H, dd, J 8.4, 0.8 Hz, ArH); δ_C (101 MHz, CDCl$_3$) 14.2 (CH$_3$), 19.8 (CH$_3$), 62.3 (CH$_2$), 126.8 (CH), 128.5 (C), 129.1 (CH), 129.4 (C), 129.9 (CH), 130.2 (CH), 137.2 (C), 146.0 (C), 151.2 (C), 166.4 (C); m/z (EI) 293.0045 (M$^+$. C$_{13}$H$_{12}$^{79}BrNO$_2$ requires 293.0051), 264 (34%), 221 (59), 140 (100), 113 (23), 69 (52), 44 (13).
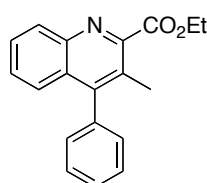
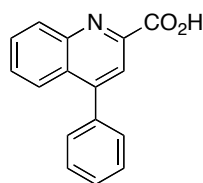**Ethyl 4-phenylquinoline-2-carboxylate (103)[89]**

To a solution of ethyl 4-bromoquinoline-2-carboxylate (**94**) (0.200 g, 0.714 mmol) in *N,N'*-dimethylformamide (10 mL) was added benzeneboronic acid (0.174 g, 1.43 mmol), potassium phosphate (0.227 g, 1.07 mmol) and tetrakis(triphenylphosphine)palladium(0) (0.083 g, 0.072 mmol). The resultant suspension was stirred vigorously at 120 °C for 24 h and then cooled to ambient temperature. An additional aliquot of benzeneboronic acid (0.174 g, 1.43 mmol) and tetrakis(triphenylphosphine)palladium(0) (0.083 g, 0.072 mmol) was added to the reaction mixture and stirred at 120 °C for a further 24 h. On cooling to ambient temperature, the mixture was diluted with dichloromethane (50 mL). The organic layer was then washed with water (3 × 30 mL), dried (MgSO$_4$), filtered and concentrated *in vacuo*. Purification using flash column chromatography (ethyl acetate/petroleum ether, 15:85) afforded ethyl 4-phenylquinoline-2-carboxylate (**103**) (0.160 g, 81%) as a pale yellow solid. Spectroscopic data in accordance with the literature.[89] Mp 114–116 °C (lit.,[89] mp 115–118 °C); ν_{max}/cm^{-1} (neat) 2972 (CH), 1711 (CO), 1587 (C=C), 1375, 1333, 1252,

1134, 1115, 1022; δ_H (400 MHz, CDCl$_3$) 1.49 (3H, t, J 7.2 Hz, OCH$_2$CH_3), 4.57 (2H, q, J 7.2 Hz, OCH_2CH$_3$), 7.48–7.56 (5H, m, 5 × ArH), 7.59 (1H, ddd, J 8.4, 6.8, 1.2 Hz, ArH), 7.78 (1H, ddd, J 8.4, 6.8, 1.2 Hz, ArH), 7.97 (1H, dd, J 8.4, 0.8 Hz, ArH), 8.14 (1H, s, ArH), 8.38 (1H, d, J 8.4 Hz, ArH); δ_C (101 MHz, CDCl$_3$) 14.4 (CH$_3$), 62.3 (CH$_2$), 121.3 (CH), 125.7 (CH), 127.8 (C), 128.6 (CH), 128.7 (2 × CH), 128.7 (CH), 129.6 (2 × CH), 130.0 (CH), 131.2 (CH), 137.6 (C), 147.8 (C), 148.2 (C), 149.8 (C), 165.5 (C); m/z (EI) 277.1103 (M$^+$. C$_{18}$H$_{15}$NO$_2$ requires 277.1103), 233 (9%), 205 (100), 204 (30), 176 (10), 84 (55).
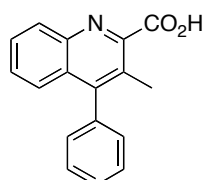
Ethyl 3-methyl-4-phenylquinoline-2-carboxylate (104)[89]

Ethyl 3-methyl-4-phenylquinoline-2-carboxylate (**104**) was synthesised as described above for ethyl 4-phenylquinoline-2-carboxylate (**103**) using ethyl 4-bromoquinoline-2-carboxylate (**95**) (0.200 g, 0.680 mmol), benzeneboronic acid (0.108 g, 0.884 mmol), potassium phosphate (0.188 g, 0.884 mmol) and tetrakis(triphenylphosphine)palladium(0) (0.079 g, 0.068 mmol) in *N,N'*-dimethylformamide (10 mL). An additional aliquot of benzeneboronic acid (0.108 g, 0.884 mmol), potassium phosphate (0.188 g, 0.884 mmol) and tetrakis(triphenylphosphine)palladium(0) (0.079 g, 0.068 mmol) was added and the suspension stirred at 120 °C for a further 72 h. Purification using flash column chromatography (ethyl acetate/petroleum ether, 2:3) afforded ethyl 3-methyl-4-phenylquinoline-2-carboxylate (**104**) (0.100 g, 51%) as a pale yellow solid. Spectroscopic data in accordance with the literature.[89] Mp 105–107 °C (lit.,[89] mp 110–112 °C); ν_{max}/cm^{-1} (neat) 3076, 2981 (CH), 1725 (CO), 1593 (C=C), 1473, 1269, 1199, 1068, 861; δ_H (400 MHz, CDCl$_3$) 1.43 (3H, t, J 7.2 Hz, OCH$_2$CH_3), 2.34 (3H, s, CH$_3$), 4.51 (2H, q, J 7.2 Hz, OCH_2CH$_3$), 6.84–6.92 (1H, m, ArH), 7.10–7.27 (2H, m, 2 × ArH), 7.37–7.47 (2H, m, 2 × ArH), 7.48–7.57 (2H, m, 2 × ArH), 7.66 (1H, ddd, J 8.4, 6.8, 1.6 Hz, ArH), 8.22 (1H, d, J 8.4 Hz, ArH); δ_C (101 MHz, CDCl$_3$) 14.2 (CH$_3$), 16.8 (CH$_3$), 62.2 (CH$_2$), 126.1 (CH), 126.5 (C), 127.9 (CH), 128.2 (CH), 128.3 (C), 128.8 (2 × CH), 129.2 (2 × CH), 129.3 (CH), 129.5 (CH), 136.6 (C), 145.4 (C), 149.1 (C), 151.3 (C), 167.3 (C); m/z (CI) 292.1333 (MH$^+$. C$_{19}$H$_{18}$NO$_2$ requires 292.1338), 220 (4%), 81 (7).

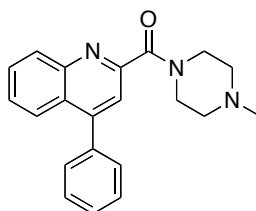## 4-Phenylquinoline-2-carboxylic acid (87)[89]

To a solution of ethyl 4-phenylquinoline-2-carboxylate (**103**) (0.160 g, 0.577 mmol) in a 50% aqueous ethanol mixture (20 ml) was added ground sodium hydroxide (0.923 g, 2.31 mmol), and the reaction mixture stirred vigorously under reflux for 18 h. On cooling to ambient temperature, the ethanol was removed *in vacuo,* and the aqueous layer acidified (pH ~4) using a 1 M hydrochloric acid solution (~10 mL). The crude product was extracted using dichloromethane (3 × 50 mL), dried (MgSO$_4$), filtered and concentrated *in vacuo* to give 4-phenylquinoline-2-carboxylic acid (**87**) (0.128 g, 89%) as a brown solid, which was used without further purification. Spectroscopic data in accordance with the literature.[89] Mp 161–162 °C (lit.,[89] mp 164–167 °C); ν_{max}/cm^{-1} (neat) 2972, 2930 (CH), 1713 (CO), 1589 (C=C), 1462, 1379, 1229, 905, 845; δ_H (400 MHz, CDCl$_3$) 7.51–7.60 (5H, m, 5 × ArH), 7.67 (1H, ddd, *J* 8.4, 6.8, 1.2 Hz, ArH), 7.86 (1H, ddd, *J* 8.4, 6.8, 1.2 Hz, ArH), 8.05 (1H, d, *J* 8.4 Hz, ArH), 8.22–8.26 (2H, m, 2 × ArH); δ_C (101 MHz, CDCl$_3$) 119.4 (CH), 126.2 (CH), 128.5 (C), 128.8 (2 × CH), 129.1 (CH), 129.2 (CH), 129.6 (2 × CH), 129.8 (CH), 130.8 (CH), 137.0 (C), 145.4 (C), 146.4 (C), 151.7 (C), 164.4 (C); *m/z* (CI) 250.0869 (MH$^+$. C$_{16}$H$_{12}$NO$_2$ requires 250.0868), 249 (6%), 206 (7), 174 (2), 85 (4), 69 (5).

3-Methyl-4-phenylquinoline-2-carboxylic acid (88)[89]

3-Methyl-4-phenylquinoline-2-carboxylic acid (**88**) was synthesised as describe above for 4-phenylquinoline-2-carboxylic acid (**87**) using ethyl 3-methyl-4-phenylquinoline-2-carboxylate (**104**) (0.042 g, 0.14 mmol) and ground sodium hydroxide (0.023 g, 0.58 mmol) in a 50% aqueous ethanol mixture (10 mL). Extraction afforded 3-methyl-4-phenylquinoline-2-carboxylic acid (**88**) (0.031 g, 82%) as an off white

solid, which was used without further purification. Spectroscopic data in accordance with the literature.[89] Mp 135–137 °C (lit.,[89] mp 130–132 °C); ν_{max}/cm^{-1} (neat) 3044 (CH), 2932, 1720 (CO), 1590 (C=C), 1473, 1368, 1322, 1232, 1068; δ_H (400 MHz, CDCl$_3$) 2.64 (3H, s, CH$_3$), 6.82–6.94 (1H, m, ArH), 7.20–7.27 (2H, m, 2 × ArH), 7.43 (1H, dd, J 8.4, 0.8 Hz, ArH), 7.50–7.60 (3H, m, 3 × ArH), 7.75 (1H, ddd, J 8.4, 6.8, 1.2 Hz, ArH), 8.17 (1H, d, J 8.4 Hz, AH); δ_C (101 MHz, CDCl$_3$) 17.4 (CH$_3$), 126.5 (CH), 128.4 (CH), 128.8 (2 × CH), 129.0 (CH), 129.2 (2 × CH), 129.6 (CH), 129.7 (C), 130.0 (CH), 130.2 (C), 136.3 (C), 143.3 (C), 144.6 (C), 151.7 (C), 164.5 (C); m/z (CI) 264.1024 (MH$^+$. C$_{17}$H$_{14}$NO$_2$ requires 264.1025), 234 (13%), 220 (58), 188 (3), 124 (7).
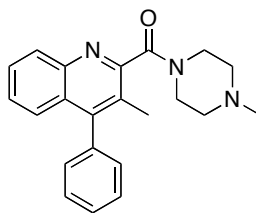
4-Phenylquinoline-2-N-(4'-methylpiperazine)carboxamide (80)

A solution of 4-phenylquinoline-2-carboxylic acid (**87**) (0.128 g, 0.514 mmol) in dichloromethane (10 mL) was cooled to 0 °C, and to this was added a few drops of N,N'-dimethylformamide followed by oxalyl chloride (62.5 µL, 0.770 mmol). The resultant solution was allowed to warm to ambient temperature and then stirred under reflux for 14 h. After cooling to ambient temperature, the reaction mixture was concentrated *in vacuo* and excess oxalyl chloride removed by azeotroping with toluene (3 × 20 mL). The crude residue was then reconstituted in dichloromethane (10 mL) and cooled to 0 °C. 1-Methylpiperazine (0.285 mL, 2.57 mmol) was added to the solution dropwise and the reaction mixture stirred under reflux for a further 18 h. On cooling to ambient temperature, the mixture was diluted with water (10 mL) and the aqueous layer extracted using ethyl acetate (3 × 20 mL). The organic layer was dried (MgSO$_4$), filtered and concentrated *in vacuo*. Purification using flash column chromatography (ethyl acetate/petroleum ether, 1:1) gave 4-phenylquinoline-2-N-(4'-methylpiperazine)carboxamide (**80**) (0.100 g, 59%) as a brown solid. Mp 112–114 °C; ν_{max}/cm^{-1} (neat) 2899, 2801 (CH), 1626 (CO), 1551 (C=C), 1439, 1290, 1258, 1132, 1001; δ_H (400 MHz, CDCl$_3$) 2.35 (3H, s, CH$_3$), 2.47 (2H, br s, NCH$_2$), 2.58 (2H, br s, NCH$_2$), 3.71–3.81 (2H, m, NCH$_2$), 3.86–3.95 (2H, m, NCH$_2$), 7.46–7.57 (6H, m, 6 × ArH), 7.65 (1H, s, ArH), 7.75 (1H, ddd, J 8.0, 6.8, 1.2 Hz, ArH), 7.93–7.97

(1H, m, ArH), 8.16 (1H, d, J 8.0 Hz, ArH); δ_C (101 MHz, CDCl$_3$) 42.3 (CH$_2$), 46.0 (CH$_3$), 47.2 (CH$_2$), 54.7 (CH$_2$), 55.4 (CH$_2$), 120.9 (CH), 125.8 (CH), 126.6 (C), 127.6 (CH), 128.7 (2 × CH), 128.7 (CH), 129.6 (2 × CH), 129.9 (CH), 130.1 (CH), 137.6 (C), 147.2 (C), 149.8 (C), 153.4 (C), 167.6 (C); m/z (EI) 331.1689 (M$^+$. C$_{21}$H$_{21}$N$_3$O requires 331.1685), 261 (9%), 204 (20), 128 (6), 84 (88), 49 (100).

**3-Methyl-4-phenylquinoline-2-N-(4'-methylpiperazine)carboxamide (81)**

3-Methyl-4-phenylquinoline-2-N-(4'-methylpiperazine)carboxamide (**81**) was synthesised as described above for 4-phenylquinoline-2-N-(4'-methylpiperazine)carboxamide (**80**) using 3-methyl-4-phenylquinoline-2-carboxylic acid (**88**) (0.014 g, 0.053 mmol), a few drops of N,N'-dimethylformamide, oxalyl chloride (6.7 μL, 0.079 mmol) and 1-methylpiperazine (29.5 μL, 0.266 mmol) in dichloromethane (5 mL). Purification using flash column chromatography (methanol/dichloromethane, 1:9) afforded 3-methyl-4-phenylquinoline-2-N-(4'-methylpiperazine)carboxamide (**81**) (0.008 g, 43%) as a yellow solid. Mp 162–163 °C; ν_{max}/cm^{-1} (neat) 2936 (CH), 2787, 1626 (CO), 1582 (C=C), 1483, 1445, 1290, 1132, 1017; δ_H (400 MHz, CDCl$_3$) 2.23 (3H, s, CH$_3$), 2.34 (3H, s, CH$_3$), 2.40 (2H, t, J 5.2 Hz, NCH$_2$), 2.57 (2H, t, J 4.8 Hz, NCH$_2$), 3.38 (2H, t, J 5.2 Hz, NCH$_2$), 3.93 (2H, t, J 4.8 Hz, NCH$_2$), 7.26 (1H, d, J 1.6 Hz, ArH), 7.28 (1H, d, J 1.6 Hz, ArH), 7.37–7.45 (2H, m, 2 × ArH), 7.46–7.58 (3H, m, 3 × ArH), 7.66 (1H, ddd, J 8.4, 6.0, 2.4 Hz, ArH), 8.10 (1H, d, J 8.4 Hz, ArH); δ_C (101 MHz, CDCl$_3$) 16.2 (CH$_3$), 41.4 (CH$_2$), 46.1 (CH$_3$), 46.6 (CH$_2$), 54.7 (CH$_2$), 55.2 (CH$_2$), 125.2 (C), 126.0 (CH), 127.0 (CH), 127.5 (C), 128.1 (CH), 128.7 (2 × CH), 128.9 (CH), 129.2 (2 × CH), 129.4 (CH), 136.6 (C), 145.9 (C), 148.2 (C), 155.4 (C), 167.7 (C); m/z (EI) 345.1841 (M$^+$. C$_{22}$H$_{23}$N$_3$O requires 345.1841), 275 (50%), 218 (100), 189 (10), 140 (8), 99 (25).
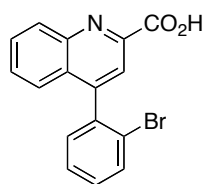
Ethyl 4-(2'-bromophenyl)quinoline-2-carboxylate (110)
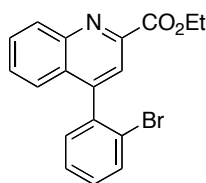
To a solution of ethyl 4-bromoquinoline-2-carboxylate (**94**) (0.100 g, 0.357 mmol) in *N,N'*-dimethylformamide (7 mL) was added 2-bromophenylboronic acid (0.093 g, 0.46 mmol), potassium phosphate (0.099 g, 0.47 mmol) and tetrakis(triphenylphosphine)palladium(0) (0.013 g, 0.011 mmol). The resultant suspension was stirred vigorously at 90 °C for 24 h and then cooled to ambient temperature. An additional aliquot of 2-bromophenylboronic acid (0.046 g, 0.23 mmol), potassium phosphate (0.049 g, 0.23 mmol) and tetrakis(triphenylphosphine)palladium(0) (0.013 g, 0.011 mmol) was added to the reaction mixture and stirred at 90 °C for a further 24 h. On cooling to ambient temperature, the mixture was diluted with dichloromethane (20 mL). The organic layer was then washed with water (3 × 10 mL) and the aqueous layer back extracted with dichloromethane (10 mL). The combined organic layer was dried (MgSO$_4$), filtered and concentrated *in vacuo*. Purification using flash column chromatography (ethyl acetate/petroleum ether, 1:4) afforded ethyl 4-(2'-bromophenyl)quinoline-2-carboxylate (**110**) (0.088 g, 69%) as a pale yellow solid. Mp 76–78 °C; ν_{max}/cm^{-1} (neat) 3059, 2982 (CH), 1713 (CO), 1555 (C=C), 1462, 1370, 1246, 1103, 1022; δ_H (400 MHz, CDCl$_3$) 1.50 (3H, t, *J* 7.2 Hz, OCH$_2$C*H*$_3$), 4.53–4.62 (2H, m, OC*H*$_2$CH$_3$), 7.32–7.42 (2H, m, 2 × ArH), 7.44–7.50 (1H, m, ArH), 7.51–7.62 (2H, m, 2 × ArH), 7.75–7.82 (2H, m, 2 × ArH), 8.09 (1H, s, ArH), 8.39 (1H, d, *J* 8.4 Hz, ArH); δ_C (101 MHz, CDCl$_3$) 14.4 (CH$_3$), 62.3 (CH$_2$), 121.7 (CH), 123.0 (C), 125.7 (CH), 127.5 (CH), 127.8 (C), 128.7 (CH), 130.2 (CH), 130.2 (CH), 131.2 (CH), 131.2 (CH), 133.1 (CH), 138.4 (C), 147.9 (C), 147.9 (C), 148.7 (C), 165.4 (C); *m/z* (CI) 356.0292 (MH$^+$. C$_{18}$H$_{15}$^{79}BrNO$_2$ requires 356.0286), 278 (10%), 276 (20), 202 (9).

Ethyl 4-(2'-bromophenyl)-3-methylquinoline-2-carboxylate (111)
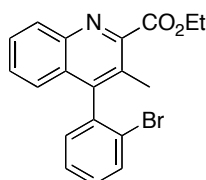
Ethyl 4-(2'-bromophenyl)-3-methylquinoline-2-carboxylate (**111**) was synthesised as described above for ethyl 4-(2'-bromophenyl)quinoline-2-carboxylate (**110**) using ethyl 4-bromo-3-methylquinoline-2-carboxylate (**95**) (0.300 g, 1.02 mmol), 2-bromophenylboronic acid (0.266 g, 1.33 mmol), potassium phosphate (0.282 g, 1.33 mmol) and tetrakis(triphenylphosphine)palladium(0) (0.118 g, 0.102 mmol) in *N,N'*-dimethylformamide (15 mL). After 24 h, an additional aliquot of 2-bromophenylboronic acid (0.133 g, 0.663 mmol) and potassium phosphate (0.141 g, 0.663 mmol) was added and the suspension stirred at 100 °C for a further 18 h. Purification using flash column chromatography (ethyl acetate/petroleum ether, 1:4) gave ethyl 4-(2'-bromophenyl)-3-methylquinoline-2-carboxylate (**111**) (0.121 g, 32%) as a pale yellow oil, which crystallised to form a solid on standing . Mp 86–87 °C; v_{max}/cm^{-1} (neat) 2982 (CH), 1721 (CO), 1562 (C=C), 1470, 1373, 1242, 1200, 1134, 1069; δ_H (500 MHz, CDCl$_3$) 1.47 (3H, t, *J* 7.0 Hz, OCH$_2$C*H*$_3$), 2.28 (3H, s, CH$_3$), 4.54 (2H, q, *J* 7.0 Hz, OC*H*$_2$CH$_3$), 7.15–7.23 (2H, m, 2 × ArH), 7.36 (1H, td, *J* 8.0, 1.5 Hz, ArH), 7.43–7.49 (2H, m, 2 × ArH), 7.67 (1H, ddd, *J* 8.4, 6.9, 1.2 Hz, ArH), 7.76 (1H, dd, *J* 8.0, 1.0 Hz, ArH), 8.21 (1H, d, *J* 8.4 Hz, ArH); δ_C (126 MHz, CDCl$_3$) 14.3 (CH$_3$), 16.4 (CH$_3$), 62.1 (CH$_2$), 123.3 (C), 125.4 (CH), 126.9 (C), 127.5 (C), 127.8 (CH), 128.1 (CH), 129.2 (CH), 130.0 (CH), 130.0 (CH), 130.8 (CH), 133.1 (CH), 137.7 (C), 145.7 (C), 147.4 (C), 151.3 (C), 167.2 (C); *m/z* (EI) 369.0365 (M$^+$. C$_{19}$H$_{16}$^{79}BrNO$_2$ requires 369.0364), 340 (10%), 297 (60), 290 (39), 216 (100), 189 (32), 108 (12).
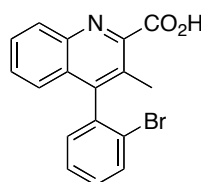
4-(2'-Bromophenyl)quinoline-2-carboxylic acid (89)

To a solution of ethyl 4-(2'-bromophenyl)quinoline-2-carboxylate (**110**) (0.632 g, 1.77 mmol) in a 50% aqueous ethanol mixture (60 mL) was added ground sodium hydroxide (0.284 g, 7.10 mmol) and the reaction mixture stirred vigorously under reflux for 4 h. On cooling to ambient temperature, the ethanol was removed *in vacuo*, and the aqueous layer acidified (pH ~4) using a 1 M hydrochloric acid solution (~10 mL). The crude product was extracted using dichloromethane (3 × 50 mL) and washed with water (3 × 50 mL). The organic layer was dried (MgSO$_4$), filtered and concentrated *in vacuo* to give 4-(2'-bromophenyl)quinoline-2-carboxylic acid (**89**) (0.582 g, 100%) as a light yellow

solid, which was used without further purification. Mp 65–66 °C; ν_{max}/cm^{-1} (neat) 3063, 2924 (CH), 1713 (CO), 1589 (C=C), 1466, 1381, 1227, 903, 763; δ_H (400 MHz, CDCl$_3$) 7.33 (1H, dd, J 7.2, 1.6 Hz, ArH), 7.40 (1H, td, J 8.0, 2.0 Hz, ArH), 7.45–7.67 (3H, m, 3 × ArH), 7.77 (1H, dd, J 8.0, 1.2 Hz, ArH), 7.85 (1H, ddd, 8.4, 6.4, 1.6 Hz, ArH), 8.20 (1H, s, ArH), 8.27 (1H, d, J 8.4 Hz, ArH); δ_C (101 MHz, CDCl$_3$) 120.1 (CH), 122.8 (C), 126.2 (CH), 127.6 (CH), 128.5 (C), 129.4 (CH), 129.7 (CH), 130.6 (CH), 131.1 (CH), 131.1 (CH), 133.2 (CH), 137.8 (C), 145.6 (C), 146.0 (C), 150.6 (C), 164.4 (C); m/z (CI) 327.9983 (MH$^+$. C$_{16}$H$_{11}$^{79}BrNO$_2$ requires 327.9973), 284 (50%), 250 (100), 206 (57), 204 (19), 174 (10).

3-Methyl-4-(2'-bromophenyl)quinoline-2-carboxylic acid (90)
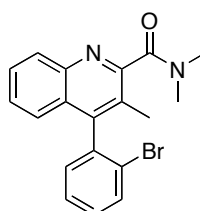

3-Methyl-4-(2'-bromophenyl)quinoline-2-carboxylic acid (**90**) was synthesised as described above for 4-(2'-bromophenyl)quinoline-2-carboxylic acid (**89**) using ethyl 4-(2-bromophenyl)-3-methylquinoline-2-carboxylate (**111**) (0.051 g, 0.14 mmol) and ground sodium hydroxide (0.022 g, 0.55 mmol) in a 50% aqueous ethanol mixture (10 mL). Extraction afforded 3-methyl-4-(2'-bromophenyl)quinoline-2-carboxylic acid (**90**) (0.042 g, 89%) as a pale brown solid, which was used without further purification. Mp 130–132 °C; ν_{max}/cm^{-1} (neat) 3329 (OH), 2976 (CH), 1717 (CO), 1593 (C=C), 1368, 1321, 1234, 1020, 762; δ_H (400 MHz, CDCl$_3$) 2.61 (3H, s, CH$_3$), 7.18–7.30 (1H, m, ArH), 7.39–7.45 (1H, m, ArH), 7.49–7.60 (3H, m, 3 × ArH), 7.73–7.82 (2H, m, 2 × ArH), 8.17 (1H, d, J 8.0 Hz, ArH); δ_C (101 MHz, CDCl$_3$) 16.9 (CH$_3$), 125.8 (CH), 127.9 (CH), 128.4 (C), 128.8 (C), 129.1 (CH), 129.2 (C), 129.4 (CH), 130.1 (CH), 130.2 (CH), 130.7 (CH), 133.2 (CH), 137.3 (C), 143.7 (C), 144.4 (C), 150.1 (C), 164.3 (C); m/z (EI) 341.0056 (M$^+$. C$_{17}$H$_{12}$^{79}BrNO$_2$ requires 341.0051), 297 (32%), 262 (100), 217 (100), 216 (100), 189 (55), 163 (12), 108 (27).

## 4-(2'-Bromophenyl)quinoline-2-*N*-dimethylcarboxamide (82)
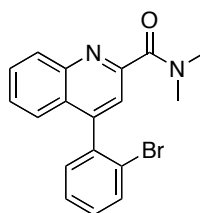
A solution of 4-(2'-bromophenyl)quinoline-2-carboxylic acid (**89**) (0.075 g, 0.23 mmol) in dichloromethane (10 mL) was cooled to 0 °C, and to this was added a few drops of *N,N'*-dimethylformamide followed by oxalyl chloride (23.0 μL, 0.274 mmol). The resultant solution was allowed to warm to ambient temperature and then stirred under reflux for 4 h. After cooling to ambient temperature, the reaction mixture was concentrated *in vacuo* and excess oxalyl chloride removed by azeotroping with toluene (3 × 10 mL). The crude residue was then reconstituted in dichloromethane (10 mL) and cooled to 0 °C. Dimethylamine (2.0 M in tetrahydrofuran) (0.570 mL, 1.14 mmol) was added to the solution dropwise and the reaction mixture stirred under reflux for a further 24 h. On cooling to ambient temperature, the mixture was diluted with water (10 mL) and the aqueous layer extracted using ethyl acetate (3 × 10 mL). The organic layer was dried (MgSO$_4$), filtered and concentrated *in vacuo*. Purification using flash column chromatography (methanol/dichloromethane, 1:99) afforded 4-(2'-bromophenyl)quinoline-2-*N*-dimethylcarboxamide (**82**) (0.021 g, 26%) as a pale yellow oil. ν_{max}/cm^{-1} (neat) 3059 (CH), 1640 (CO), 1553 (C=C), 1462, 1397, 1343, 1142, 1026, 909; δ_H (400 MHz, CDCl$_3$) 3.21 (6H, s, 2 × NCH$_3$), 7.34–7.40 (2H, m, 2 × ArH), 7.44–7.49 (1H, m, ArH), 7.51–7.54 (2H, m, 2 × ArH), 7.60 (1H, s, ArH), 7.74–7.79 (2H, m, 2 × ArH), 8.19 (1H, d, *J* 8.4 Hz, ArH); δ_C (101 MHz, CDCl$_3$) 34.8 (CH$_3$), 38.1 (CH$_3$), 120.1 (CH), 121.9 (C), 124.8 (CH), 125.5 (C), 126.4 (CH), 126.6 (CH), 129.0 (CH), 129.0 (CH), 129.1 (CH), 130.2 (CH), 132.0 (C), 137.3 (C), 145.9 (C), 147.5 (C), 152.7 (C), 167.9 (C); *m/z* (ESI) 377.0251 (MNa$^+$. C$_{18}$H$_{15}$^{79}BrN$_2$NaO requires 377.0260).

3-Methyl-4-(2'-bromophenyl)quinoline-2-*N*-dimethylcarboxamide (83)

3-Methyl-4-(2'-bromophenyl)quinoline-2-*N*-dimethylcarboxamide (**83**) was synthesised as described above for 4-(2'-bromophenyl)quinoline-2-*N*-dimethylcarboxamide (**82**) using 3-methyl-4-(2-bromophenyl)quinoline-2-carboxylic acid (**90**) (0.042 g, 0.12 mmol), a few drops of *N,N'*-dimethylformamide, oxalyl chloride (15.6 μL, 0.184 mmol) and dimethylamine (2.0 M in tetrahydrofuran) (0.307 mL, 0.614 mmol) in dichloromethane (10 mL). Purification using flash column chromatography (ethyl acetate/petroleum ether, 7:3) afforded 3-methyl-4-(2'-bromophenyl)quinoline-2-*N*-dimethylcarboxamide (**83**) (0.017 g, 38%) as a pale yellow oil. ν_{max}/cm^{-1} (neat) 3063 (CH), 2934 (CH), 1641 (CO) 1499, 1393, 1263, 1128, 1061, 909; δ_H (400 MHz, CDCl$_3$) 2.16 (3H, s, CH$_3$), 2.92 (3H, s, CH$_3$), 3.22 (3H, s, CH$_3$), 7.20–7.28 (2H, m, 2 × ArH), 7.34–7.55 (3H, m, 3 × ArH), 7.67 (1H, ddd, *J* 8.4, 6.8, 1.6 Hz, ArH), 7.77 (1H, dd, *J* 8.0, 1.2 Hz, ArH), 8.13 (1H, d, *J* 8.0 Hz, ArH); δ_C (101 MHz, CDCl$_3$) 15.6 (CH$_3$), 34.6 (CH$_3$), 38.0 (CH$_3$), 123.3 (C), 125.3 (CH), 125.6 (C), 126.8 (C), 127.3 (CH), 127.8 (CH), 129.1 (CH), 129.5 (CH), 130.0 (CH), 130.7 (CH), 133.1 (CH), 137.6 (C), 146.0 (C), 146.8 (C), 155.9 (C), 169.1 (C); *m/z* (CI) 369.0606 (MH$^+$. C$_{19}$H$_{18}$^{79}BrN$_2$O requires 369.0602), 306 (5%), 291 (100), 250 (40), 206 (20), 113 (19).
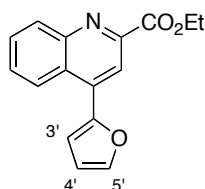
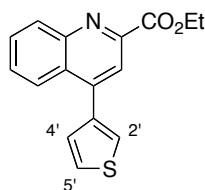**Ethyl 4-(pyridin-4'-yl)quinoline-2-carboxylate (114)**
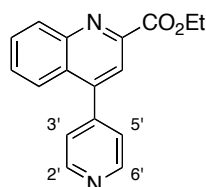
To a solution of ethyl 4-bromoquinoline-2-carboxylate (**94**) (0.100 g, 0.357 mmol) in *N,N'*-dimethylformamide (5 mL) was added pyridin-4-ylboronic acid (0.053 g, 0.43 mmol), potassium phosphate (0.091 g, 0.43 mmol) and tetrakis(triphenylphosphine)palladium(0) (0.042 g, 0.036 mmol). The resultant suspension was stirred vigorously at 120 °C for 24 h, and then cooled to ambient temperature. An additional aliquot of pyridin-4-ylboronic acid (0.053 g, 0.43 mmol) and tetrakis(triphenylphosphine)palladium(0) (0.042 g, 0.036 mmol) was added to the reaction mixture and stirred at 120 °C for a further 18 h. On cooling to ambient temperature, the mixture was concentrated *in vacuo* and then reconstituted in dichloromethane (10 mL). The organic layer was then washed with water (3 × 10 mL), dried (MgSO$_4$), filtered and concentrated *in vacuo*. Purification using flash column chromatrography (ethyl acetate)

afforded ethyl 4-(pyridin-4'-yl)quinoline-2-carboxylate (**114**) (0.093 g, 94%) as a yellow oil. ν_{max}/cm^{-1} (neat) 3055, 2986 (CH), 1721 (CO), 1582 (C=C), 1435, 1373, 1250, 1180, 1111; δ_H (400 MHz, CDCl$_3$) 1.50 (3H, t, *J* 7.2 Hz, CH$_2$C*H*$_3$), 4.59 (2H, q, *J* 7.2 Hz, C*H*$_2$CH$_3$), 7.48 (2H, app dd, *J* 4.4, 1.6 Hz, 3'-H and 5'-H), 7.65 (1H, ddd, *J* 8.4, 7.2, 1.2 Hz, ArH), 7.81–7.90 (2H, m, 2 × ArH), 8.13 (1H, s, ArH), 8.42 (1H, d, *J* 8.4 Hz, ArH), 8.82 (2H, app dd, *J* 4.4, 1.6 Hz, 2'-H and 6'-H); δ_C (101 MHz, CDCl$_3$) 14.4 (CH$_3$), 62.5 (CH$_2$), 120.9 (CH), 124.3 (2 × CH), 124.9 (CH), 126.8 (C), 129.3 (CH), 130.5 (CH), 131.5 (CH), 145.4 (C), 146.8 (C), 147.9 (C), 148.2 (C), 150.3 (2 × CH), 165.2 (C); *m/z* (CI) 279.1135 (MH$^+$. C$_{17}$H$_{15}$N$_2$O$_2$ requires 279.1134), 207 (24%), 165 (6), 149 (9), 113 (13), 71 (31).
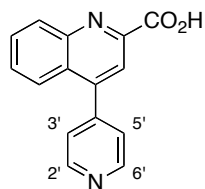
Ethyl 4-(furan-2'-yl)quinoline-2-carboxylate (115)

Ethyl 4-(furan-2'-yl)quinoline-2-carboxylate (**115**) was synthesised as described above for ethyl 4-(pyridin-4'-yl)quinoline-2-carboxylate (**114**) using ethyl 4-bromoquinoline-2-carboxylate (**94**) (0.100 g, 0.357 mmol), furan-2-boronic acid (0.048 g, 0.43 mmol), potassium phosphate (0.090 g, 0.42 mmol) and tetrakis(triphenylphosphine)palladium(0) (0.042 g, 0.036 mmol) in *N,N'*-dimethylformamide (5 mL). Purification using flash column chromatography (ethyl acetate/petroleum ether, 2:3) gave ethyl 4-(furan-2'-yl)quinoline-2-carboxylate (**115**) (0.081 g, 85%) as a yellow oil. ν_{max}/cm^{-1} (neat) 3101, 2987 (CH), 1715 (CO), 1591 (C=C), 1370, 1328, 1255, 1214, 1021; δ_H (400 MHz, CDCl$_3$) 1.51 (3H, t, *J* 7.2 Hz, CH$_2$C*H*$_3$), 4.58 (2H, q, *J* 7.2 Hz, C*H*$_2$CH$_3$), 6.66 (1H, dd, *J* 3.2, 1.6 Hz, 4'-H), 7.08 (1H, d, *J* 3.2 Hz, 3'-H), 7.69 (1H, ddd, *J* 8.4, 6.8, 1.2 Hz, ArH), 7.73 (1H, d, *J* 1.6 Hz, 5'-H), 7.80 (1H, ddd, *J* 8.4, 6.8, 1.2 Hz, ArH), 8.35 (1H, dd, *J* 8.4, 0.4 Hz, ArH), 8.42 (1H, s, ArH), 8.57 (1H, dd, *J* 8.4, 0.4 Hz, ArH); δ_C (101 MHz, CDCl$_3$) 14.4 (CH$_3$), 62.4 (CH$_2$), 112.2 (CH), 112.9 (CH), 118.5 (CH), 125.3 (C), 125.4 (CH), 129.0 (CH), 130.0 (CH), 131.5 (CH), 136.9 (C), 144.4 (CH), 148.0 (C), 148.7 (C), 150.8 (C), 165.4 (C); *m/z* (EI) 267.0898 (M$^+$. C$_{16}$H$_{13}$NO$_3$ requires 267.0895), 195 (100%), 166 (38), 140 (30), 85 (100), 47 (53).

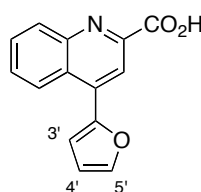**Ethyl 4-(thiophen-3'-yl)quinoline-2-carboxylate (116)**

Ethyl 4-(thiophen-3'-yl)quinoline-2-carboxylate (**116**) was synthesised as described above for ethyl 4-(pyridin-4'-yl)quinoline-2-carboxylate (**114**) using ethyl 4-bromoquinoline-2-carboxylate (**94**) (0.100 g, 0.357 mmol), 3-thienylboronic acid (0.055 g, 0.43 mmol), potassium phosphate (0.091 g, 0.43 mmol) and tetrakis(triphenylphosphine)palladium(0) (0.042 g, 0.036 mmol) in *N,N'*-dimethylformamide (5 mL). Purification using flash column chromatography (ethyl acetate/petroleum ether, 3:7) afforded ethyl 4-(thiophen-3'-yl)quinoline-2-carboxylate (**116**) (0.077 g, 76%) as a pale yellow oil. v_{max}/cm^{-1} (neat) 3069 (CH), 1709 (CO), 1584 (C=C), 1327, 1250, 1150, 1113, 1030, 810; δ_H (400 MHz, CDCl$_3$) 1.50 (3H, t, *J* 7.2 Hz, CH$_2$C*H$_3$*), 4.58 (2H, q, *J* 7.2 Hz, C*H$_2$*CH$_3$), 7.39 (1H, dd, *J* 4.8, 1.2 Hz, 4'-H), 7.55 (1H, dd, *J* 4.8, 2.8 Hz, 5'-H), 7.60 (1H, dd, *J* 2.8, 1.2 Hz, 2'-H), 7.64 (1H, ddd, *J* 8.4, 6.8, 1.6 Hz, ArH), 7.80 (1H, ddd, *J* 8.4, 6.8, 1.6 Hz, ArH), 8.14 (1H, dd, *J* 8.4, 1.2 Hz, ArH), 8.18 (1H, s, ArH), 8.34 (1H, d, *J* 8.4 Hz, ArH); δ_C (101 MHz, CDCl$_3$) 14.4 (CH$_3$), 62.4 (CH$_2$), 121.0 (CH), 121.1 (CH), 125.6 (CH), 126.6 (CH), 127.8 (C), 128.7 (CH), 128.8 (CH), 130.1 (CH), 131.2 (CH), 138.0 (C), 144.6 (C), 147.8 (C), 148.2 (C), 165.5 (C); *m/z* (EI) 283.0665 (M$^+$. C$_{16}$H$_{13}$NO$_2$S requires 283.0667), 239 (18%), 211 (100), 184 (27), 139 (18), 83 (10).

4-(Pyridin-4'-yl)quinoline-2-carboxylic acid (91)

To a solution of ethyl 4-(pyridin-4'-yl)quinoline-2-carboxylate (**114**) (0.093 g, 0.33 mmol) in a 50% aqueous ethanol mixture (10 ml) was added ground sodium hydroxide (0.053 g, 1.3 mmol), and the reaction mixture stirred vigorously under reflux for 18 h. On cooling to ambient temperature, the ethanol was removed *in vacuo*, and the aqueous layer acidified

(pH ~4) using a 1 M hydrochloric acid solution (~10 mL). The crude product was extracted using dichloromethane (3 × 10 mL), dried (MgSO$_4$), filtered and concentrated *in vacuo* to give 4-(pyridin-4'-yl)quinoline-2-carboxylic acid (**91**) (0.078 g, 93%) as an off white solid, which was used without further purification. Mp >201 °C (decomp.); ν_{max}/cm^{-1} (neat) 3067 (CH), 2376 (OH), 1717 (CO), 1612 (C=C), 1498, 1409, 1217, 1032, 895; δ_H (400 MHz, DMSO-d_6) 7.65 (2H, app dd, *J* 4.4, 1.6 Hz, 3'-H and 5'-H), 7.76 (1H, ddd, *J* 8.0, 6.8, 1.2 Hz, ArH), 7.86–7.91 (1H, m, ArH), 7.94 (1H, ddd, *J* 8.0, 6.8, 1.2 Hz, ArH), 8.02 (1H, s, ArH), 8.27 (1H, d, *J* 8.0 Hz, ArH), 8.80 (2H, app dd, *J* 4.4, 1.6 Hz, 2'-H and 6'-H); δ_C (101 MHz, DMSO-d_6) 120.6 (CH), 124.2 (2 × CH), 124.9 (CH), 125.9 (C), 129.3 (CH), 130.5 (CH), 130.6 (CH), 144.6 (C), 146.1 (2 × CH), 147.3 (C), 150.1 (2 × CH), 166.2 (C); *m/z* (ESI) 249.0661 (M–H$^-$. C$_{15}$H$_9$N$_2$O$_2$ requires 249.0670).
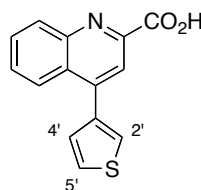
4-(Furan-2'-yl)quinoline-2-carboxylic acid (92)

4-(Furan-2'-yl)quinoline-2-carboxylic acid (**92**) was synthesised as described above for 4-(pyridin-4'-yl)quinoline-2-carboxylic acid (**91**) using ethyl 4-(furan-2'-yl)quinoline-2-carboxylate (**115**) (0.081 g, 0.30 mmol) and ground sodium hydroxide (0.049 g, 1.2 mmol) in a 50% aqueous ethanol mixture (10 mL). Extraction afforded 4-(furan-2'-yl)quinoline-2-carboxylic acid (**92**) (0.058 g, 79%) as a yellow oil, which was used without further purification. ν_{max}/cm^{-1} (neat) 3358 (OH), 2928 (CH), 1674 (CO), 1593 (C=C), 1464, 1398, 1149, 1014, 801; δ_H (400 MHz, CDCl$_3$) 6.69 (1H, dd, *J* 3.6, 1.6 Hz, 4'-H), 7.17 (1H, d, *J* 3.6 Hz, 3'-H), 7.74–7.79 (2H, m, 5'-H and ArH), 7.86 (1H, ddd, *J* 8.4, 6.8, 1.2 Hz, ArH), 8.19–8.23 (1H, m, ArH), 8.52 (1H, s, ArH), 8.67–8.72 (1H, m, ArH); δ_C (101 MHz, CDCl$_3$) 112.5 (CH), 113.8 (CH), 116.5 (CH), 125.9 (C), 126.0 (CH), 129.5 (CH), 129.9 (CH), 130.9 (CH), 138.6 (C), 145.1 (C), 145.5 (CH), 146.8 (C), 150.6 (C), 164.2 (C); *m/z* (EI) 239.0586 (M$^+$. C$_{14}$H$_9$NO$_3$ requires 239.0582), 195 (100%), 166 (30), 139 (24), 77 (11).
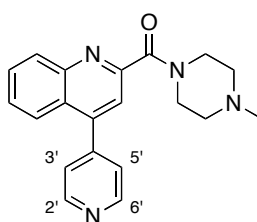
4-(Thiophen-3'-yl)quinoline-2-carboxylic acid (93)

4-(Thiophen-3'-yl)quinoline-2-carboxylic acid (**93**) was synthesised as described above for 4-(pyridin-4'-yl)quinoline-2-carboxylic acid (**91**) using ethyl 4-(thiophen-3'-yl)quinoline-2-carboxylate (**116**) (0.077 g, 0.27 mmol) and ground sodium hydroxide (0.044 g, 1.1 mmol) in a 50% aqueous ethanol mixture (10 mL).   Extraction afforded 4-(thiophen-3'-yl)quinoline-2-carboxylic acid (**93**) (0.055 g, 80%) as a pale yellow oil, which was used without further purification. ν_{max}/cm^{-1} (neat) 3097 (CH), 1681 (CO), 1592 (C=C), 1513, 1360, 1156, 1024, 802, 766; δ_H (400 MHz, CDCl$_3$) 7.39 (1H, dd, J 4.8, 1.2 Hz, 4'-H), 7.57 (1H, dd, J 4.8, 2.8 Hz, 5'-H), 7.63 (1H, dd, J 2.8, 1.2 Hz, 2'-H), 7.70 (1H, ddd, J 8.4, 6.8, 1.2 Hz, ArH), 7.86 (1H, ddd, J 8.4, 6.8, 1.6 Hz, ArH), 8.20–8.24 (2H, m, 2 × ArH), 8.28 (1H, s, ArH); δ_C (101 MHz, CDCl$_3$) 119.1 (CH), 126.0 (CH), 126.1 (CH), 126.9 (CH), 128.4 (C), 128.6 (CH), 129.3 (CH), 129.9 (CH), 130.9 (CH), 137.6 (C), 145.5 (C), 146.4 (C), 146.5 (C), 164.3 (C); m/z (ESI) 278.0238 (MNa$^+$. C$_{14}$H$_9$NNaO$_2$S requires 278.0246).

4-(Pyridin-4'-yl)quinoline-2-*N*-(4''-methylpiperazine)carboxamide (84)

A solution of 4-(pyridin-4'-yl)quinoline-2-carboxylic acid (**117**) (0.020 g, 0.080 mmol) in dichloromethane (5 mL) was cooled to 0 °C, and to this was added a few drops of *N,N'*-dimethylformamide followed by oxalyl chloride (10.1 µL, 0.120 mmol).   The resultant solution was allowed to warm to ambient temperature and then stirred under reflux for 18 h.   After cooling to ambient temperature, the reaction mixture was concentrated *in vacuo* and excess oxalyl chloride removed by azeotroping with toluene (3 × 5 mL). The crude residue was then reconstituted in dichloromethane (5 mL) and cooled

to 0 °C. 1-Methylpiperazine (44.3 μL, 0.400 mmol) was added to the solution dropwise and the reaction mixture stirred under reflux for a further 3 h. On cooling to ambient temperature, the mixture was diluted with water (10 mL) and the aqueous layer extracted using ethyl acetate (3 × 10 mL). The organic layer was dried (MgSO$_4$), filtered and concentrated *in vacuo*. Purification using flash column chromatography (methanol/dichloromethane, 1:9) afforded 4-(pyridin-4'-yl)quinoline-2-*N*-(4''-methylpiperazine)carboxamide (**84**) (0.014 g, 53%) as a yellow oil. ν_{max}/cm^{-1} (neat) 3433, 2926 (CH), 2795, 1667 (CO), 1587 (C=C), 1437, 1290, 1257, 999; δ_H (400 MHz, CDCl$_3$) 2.36 (3H, s, CH$_3$), 2.48 (2H, t, *J* 4.8 Hz, NCH$_2$), 2.58 (2H, t, *J* 5.2 Hz, NCH$_2$), 3.80 (2H, t, *J* 4.8 Hz, NCH$_2$), 3.92 (2H, t, *J* 5.2 Hz, NCH$_2$), 7.47 (2H, d, *J* 5.2 Hz, 3'-H and 5'-H), 7.60 (1H, ddd, *J* 8.4, 7.2, 1.2 Hz, ArH), 7.68 (1H, s, ArH), 7.81 (1H, ddd, *J* 8.4, 7.2, 1.2 Hz, ArH), 7.82–7.86 (1H, m, ArH), 8.20 (1H, d, *J* 8.4 Hz, ArH), 8.81 (2H, br s, 2'-H and 6'-H); δ_C (101 MHz, CDCl$_3$) 42.4 (CH$_2$), 46.1 (CH$_3$), 47.3 (CH$_2$), 54.7 (CH$_2$), 55.4 (CH$_2$), 120.8 (CH), 124.2 (2 × CH), 125.0 (CH), 125.7 (C), 128.3 (CH), 130.3 (CH), 130.5 (CH), 145.4 (C), 146.7 (C), 147.0 (C), 150.2 (2 × CH), 153.3 (C), 167.1 (C); *m/z* (ESI) 355.1520 (MNa$^+$. C$_{20}$H$_{20}$N$_4$NaO requires 355.1529).

4-(Furan-2'-yl)quinoline-2-*N*-(4''-methylpiperazine)carboxamide (85)

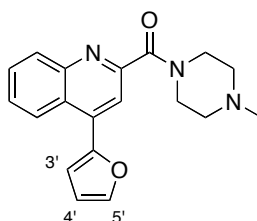4-(Furan-2'-yl)quinoline-2-*N*-(4''-methylpiperazine)carboxamide (**85**) was synthesised as described above for 4-(pyridin-4'-yl)quinoline-2-*N*-(4''-methylpiperazine)carboxamide (**84**) using 4-(furan-2'-yl)quinoline-2-carboxylic acid (**118**) (0.058 g, 0.24 mmol), a few drops of *N*,*N'*-dimethylformamide, oxalyl chloride (30.8 μL, 0.364 mmol) and 1-methylpiperazine (0.134 mL, 1.21 mmol) in dichloromethane (10 mL). Purification using flash column chromatography (methanol/dichloromethane, 1:9) gave 4-(furan-2'-yl)quinoline-2-*N*-(4''-methylpiperazine)carboxamide (**85**) (0.044 g, 56%) as a brown oil. ν_{max}/cm^{-1} (neat) 3482, 2938 (CH), 2795, 1626 (CO), 1551 (C=C), 1472, 1290, 1260, 1132; δ_H (400 MHz, CDCl$_3$) 2.35 (3H, s, CH$_3$), 2.45 (2H, br s, NCH$_2$), 2.58 (2H, br s, NCH$_2$), 3.74 (2H, t, *J* 4.8 Hz, NCH$_2$), 3.92 (2H, t, *J* 4.8 Hz, NCH$_2$), 6.64 (1H, dd, *J* 3.4, 1.8 Hz, 4'-H), 7.04 (1H, d, *J* 3.4 Hz, 3'-H), 7.65 (1H, ddd, *J* 8.4, 6.8, 1.2 Hz, ArH), 7.70

(1H, d, J 1.8 Hz, 5'-H), 7.77 (1H, ddd, J 8.4, 6.8, 1.2 Hz, ArH), 7.94 (1H, s, ArH), 8.15 (1H, dd, J 8.4, 0.8 Hz, ArH), 8.56 (1H, dd, J 8.4, 0.8 Hz, ArH); δ_C (101 MHz, CDCl$_3$) 42.3 (CH$_2$), 46.1 (CH$_3$), 47.2 (CH$_2$), 54.7 (CH$_2$), 55.4 (CH$_2$), 112.2 (CH), 112.6 (CH), 118.2 (CH), 124.2 (C), 125.5 (CH), 128.0 (CH), 129.9 (CH), 130.4 (CH), 136.9 (C), 144.3 (CH), 147.7 (C), 150.9 (C), 153.4 (C), 167.5 (C); m/z (EI) 321.1484 (M$^+$. C$_{19}$H$_{19}$N$_3$O$_2$ requires 321.1477), 251 (100%), 194 (63), 166 (49), 140 (28), 99 (28), 83 (35), 70 (60).

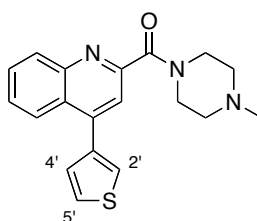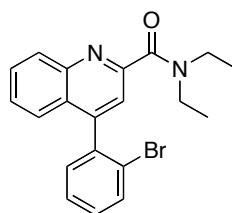**4-(Thiophen-3'-yl)quinoline-2-N-(4''-methylpiperazine)carboxamide (86)**


4-(Thiophen-3'-yl)quinoline-2-N-(4''-methylpiperazine)carboxamide (**86**) was synthesised as described above for 4-(pyridin-4'-yl)quinoline-2-N-(4''-methylpiperazine)carboxamide (**84**) using 4-(thiophen-3'-yl)quinoline-2-carboxylic acid (**119**) (0.055 g, 0.22 mmol), a few drops of N,N'-dimethylformamide, oxalyl chloride (27.3 μL, 0.323 mmol) and 1-methylpiperazine (0.119 mL, 1.08 mmol) in dichloromethane (10 mL). Purification using flash column chromatography (methanol/dichloromethane, 1:9) afforded 4-(thiophen-3'-yl)quinoline-2-N-(4''-methylpiperazine)carboxamide (**86**) (0.023 g, 32%) as a yellow oil. ν_{max}/cm^{-1} (neat) 3065, 2801 (CH), 1626 (CO), 1589 (C=C), 1551, 1439, 1258, 997, 891; δ_H (400 MHz, CDCl$_3$) 2.35 (3H, s, CH$_3$), 2.47 (2H, br s, NCH$_2$), 2.58 (2H, br s, NCH$_2$), 3.76 (2H, t, J 4.8 Hz, NCH$_2$), 3.91 (2H, t, J 4.8 Hz, NCH$_2$), 7.36 (1H, dd, J 4.8, 1.2 Hz, 4'-H), 7.52 (1H, dd, J 4.8, 2.8 Hz, 5'-H), 7.55–7.61 (2H, m, 2'-H and ArH), 7.70 (1H, s, ArH), 7.76 (1H, ddd, J 8.4, 6.8, 1.2 Hz, ArH), 8.12 (1H, dd, J 8.4, 0.8 Hz, ArH), 8.10–8.14 (1H, m, ArH); δ_C (101 MHz, CDCl$_3$) 42.2 (CH$_2$), 46.0 (CH$_3$), 47.1 (CH$_2$), 54.6 (CH$_2$), 55.3 (CH$_2$), 120.6 (CH), 125.4 (CH), 125.7 (CH), 126.5 (CH), 126.6 (CH), 127.7 (CH), 128.8 (C), 130.0 (CH), 130.2 (CH), 138.0 (C), 144.5 (C), 147.3 (C), 153.3 (C), 167.6 (C); m/z (EI) 337.1247 (M$^+$. C$_{19}$H$_{19}$N$_3$O$_5$ requires 337.1249), 267 (95%), 210 (100), 166 (14), 139 (14), 99 (30), 70 (68).

4-(2'-Bromophenyl)quinoline-2-*N*-diethylcarboxamide (122)

4-(2'-Bromophenyl)quinoline-2-*N*-diethylcarboxamide (**122**) was synthesised as described above for 4-(pyridin-4'-yl)quinoline-2-*N*-(4''-methylpiperazine)carboxamide (**84**) using 4-(2'-bromophenyl)quinoline-2-carboxylic acid (**89**) (0.150 g, 0.457 mmol), a few drops of *N,N'*-dimethylformamide, oxalyl chloride (46.0 μL, 0.549 mmol) and diethylamine (0.236 mL, 2.29 mmol) in dichloromethane (20 mL). Purification using flash column chromatography (ethyl acetate/petroleum ether, 3:2) afforded 4-(2'-bromophenyl)quinoline-2-*N*-diethylcarboxamide (**122**) (0.080 g, 46%) as a pale yellow oil. v_{max}/cm^{-1} (neat) 2981 (CH), 1627 (CO), 1551 (C=C), 1497, 1435, 1273, 1095, 1018, 910; δ_H (400 MHz, CDCl$_3$) 1.25 (3H, t, *J* 7.2 Hz, NCH$_2$C*H$_3$*), 1.32 (3H, t, *J* 7.2 Hz, NCH$_2$C*H$_3$*), 3.40–3.58 (2H, m, NC*H$_2$*CH$_3$), 3.63 (2H, qd, *J* 7.2, 1.6 Hz, NC*H$_2$*CH$_3$), 7.33–7.39 (2H, m, 2 × ArH), 7.43–7.48 (1H, m, ArH), 7.49–7.53 (2H, m, 2 × ArH), 7.55 (1H, s, ArH), 7.72–7.78 (2H, m, 2 × ArH), 8.18 (1H, d, *J* 8.4 Hz, ArH); δ_C (101 MHz, CDCl$_3$) 13.0 (CH$_3$), 14.5 (CH$_3$), 40.4 (CH$_2$), 43.5 (CH$_2$), 120.8 (CH), 123.0 (C), 125.7 (CH), 126.5 (C), 127.4 (CH), 127.5 (CH), 129.9 (CH), 130.1 (CH), 130.1 (CH), 131.3 (CH), 133.0 (CH), 138.4 (C), 147.0 (C), 148.3 (C), 154.3 (C), 168.6 (C); *m/z* (CI) 385.0736 (MH$^+$. C$_{20}$H$_{20}$^{81}BrN$_2$O requires 385.0741), 383 (100%), 351 (24), 303 (73).

5-Iodoindole (129)[101]
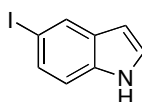
A schlenk tube was charged with copper(I) iodide (0.010 g, 0.052 mmol) and sodium iodide (0.300 g, 2.00 mmol), evacuated and then backfilled with argon. *N,N*-Dimethylethylenediamine (10.8 μL, 0.100 mmol) and 5-bromoindole (**128**) (0.197 g, 1.00 mmol) were dissolved in 1,4-dioxane (1 mL) and added to the Schlenk tube under a stream of argon. The tube was then sealed and the resultant mixture stirred vigorously at 110 °C for 72 h. On cooling to ambient temperature, water (20 mL) was added and the crude

product extracted using dichloromethane (3 × 20 mL). The organic layer was dried (MgSO₄), filtered and concentrated *in vacuo*. Purification using flash column chromatography (ethyl acetate/petroleum ether, 15:85) gave 5-iodoindole (**129**) (0.154 g, 63%) as an off white solid. Spectroscopic data in accordance with the literature.[101] Mp 96–97 °C (lit.,[101] mp 99–100 °C); ν_{max}/cm^{-1} (neat) 3414 (NH), 3103 (CH), 1562 (C=C), 1442, 1409, 1314, 1090, 999, 886; δ_H (400 MHz, CDCl₃) 6.49 (1H, dd, *J* 3.1, 2.0 Hz, 2-H), 7.16–7.21 (2H, m, 3-H and ArH), 7.44 (1H, dd, *J* 8.5, 1.5 Hz, ArH), 7.98–7.99 (1H, m, ArH), 8.17 (1H, br s, NH); δ_C (101 MHz, CDCl₃) 83.3 (C), 102.1 (CH), 112.9 (CH), 124.9 (CH), 129.6 (CH), 130.3 (CH), 130.5 (C), 134.8 (C); *m/z* (ESI) 241.9462 (MH⁻. C₈H₅IN requires 241.9472).

Ethyl 4-(2'-nitrophenyl)quinoline-2-carboxylate (131)
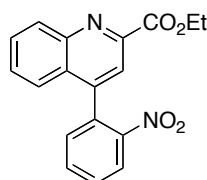
To a solution of ethyl 4-bromoquinoline-2-carboxylate (**94**) (0.196 g, 0.699 mmol) in *N,N'*-dimethylformamide (10 mL) were added 2-nitrophenylboronic acid (0.140 g, 0.839 mmol), potassium phosphate (0.178 g, 0.839 mmol) and tetrakis(triphenylphosphine)palladium(0) (0.081 g, 0.070 mmol). The resultant suspension was stirred at 120 °C for 24 h. An additional aliquot of 2-nitrophenylboronic acid (0.140 g, 0.839 mmol) and tetrakis(triphenylphosphine)palladium(0) (0.081 g, 0.070 mmol) was added and the suspension stirred for a further 24 h. After cooling to ambient temperature, the reaction mixture was concentrated *in vacuo* and reconstituted in dichloromethane (20 mL). The organic layer was washed with water (3 × 20 mL), dried (MgSO₄), filtered and concentrated *in vacuo*. Purification using flash column chromatography (ethyl acetate/petroleum ether, 2:3) afforded ethyl 4-(2'-nitrophenyl)quinoline-2-carboxylate (**131**) (0.205 g, 91%) as a yellow solid. Mp 156–157 °C; ν_{max}/cm^{-1} (neat) 2990 (CH), 1713 (CO), 1512, 1350, 1251, 1136, 1107, 1020; δ_H (500 MHz, CDCl₃) 1.49 (3H, t, *J* 7.1 Hz, CH₂C*H*₃), 4.52–4.62 (2H, m, C*H*₂CH₃), 7.43–7.48 (2H, m, 2 × ArH), 7.55 (1H, ddd, *J* 8.3, 6.9, 1.2 Hz, ArH), 7.70 (1H, ddd, *J* 8.0, 7.5, 1.5 Hz, ArH), 7.75–7.80 (2H, m, 2 × ArH), 8.05 (1H, s, ArH), 8.24 (1H, dd, *J* 8.0, 1.5 Hz, ArH), 8.39 (1H, d, *J* 8.3 Hz, ArH); δ_C (126 MHz, CDCl₃) 14.3 (CH₃), 62.2 (CH₂), 120.4 (CH), 124.4 (CH), 124.8 (CH), 127.5 (C),

129.1 (CH), 129.9 (CH), 130.2 (CH), 131.4 (CH), 132.3 (CH), 132.7 (C), 133.3 (CH), 146.2 (C), 147.7 (C), 148.0 (C), 148.7 (C), 165.2 (C); *m/z* (EI) 322.0951 (M$^+$. $C_{18}H_{14}N_2O_4$ requires 322.0954), 278 (7%), 250 (100), 205 (10), 165 (9), 131 (11), 103 (9), 77 (7), 43 (15).

Ethyl 4-(2'-aminophenyl)quinoline-2-carboxylate (132)
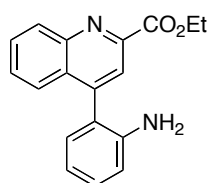
Tin(II) chloride dihydrate (0.700 g, 3.10 mmol) was added in one portion to a stirred solution of ethyl 4-(2'-nitrophenyl)quinoline-2-carboxylate (**131**) (0.200 g, 0.621 mmol) in ethanol (10 mL) and the reaction mixture stirred under reflux for 15 h. After cooling to ambient temperature, a saturated solution of sodium hydrogen carbonate (20 mL) was added, and the crude product extracted with ethyl acetate (3 × 30 mL). The organic layer was washed with water (30 mL), dried (MgSO$_4$), filtered and concentrated *in vacuo* to afford ethyl 4-(2'-aminophenyl)quinoline-2-carboxylate (**132**) (0.180 g, 99%) as a yellow solid, which was used without further purification. Mp 138–139 °C; v_{max}/cm^{-1} (neat) 3356 (NH), 2926 (CH), 1716 (CO), 1494, 1452, 1375, 1247, 1230, 1108; δ$_H$ (400 MHz, CDCl$_3$) 1.48 (3H, t, *J* 7.1 Hz, CH$_2$C*H*$_3$), 4.56 (2H, q, *J* 7.1 Hz, C*H*$_2$CH$_3$), 6.86 (1H, d, *J* 8.0 Hz, ArH), 6.92 (1H, td, *J* 7.5, 1.2 Hz, ArH), 7.15 (1H, dd, *J* 7.5, 1.2 Hz, ArH), 7.32 (1H, td, *J* 8.0, 1.5 Hz, ArH), 7.59 (1H, ddd, *J* 8.0, 6.8, 1.2 Hz, ArH), 7.74–7.82 (2H, m, 2 × ArH), 8.17 (1H, s, ArH), 8.38 (1H, d, *J* 8.0, 0.7 Hz, ArH); δ$_C$ (101 MHz, CDCl$_3$) 14.4 (CH$_3$), 62.3 (CH$_2$), 115.8 (CH), 118.6 (CH), 122.2 (CH), 122.6 (C), 125.9 (CH), 128.0 (C), 128.8 (CH), 130.0 (CH), 130.3 (CH), 130.6 (CH), 131.3 (CH), 143.7 (C), 147.5 (C), 148.2 (C), 148.4 (C), 165.4 (C); *m/z* (EI) 292.1208 (M$^+$. $C_{18}H_{16}N_2O_4$ requires 292.1212), 219 (18), 190 (3), 165 (2), 83 (3), 47 (18).
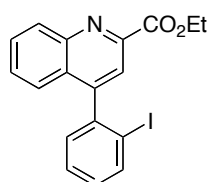
Ethyl 4-(2'-iodophenyl)quinoline-2-carboxylate (126)

To a solution of ethyl 4-(2'-aminophenyl)quinoline-2-carboxylate (**132**) (0.030 g, 0.10 mmol) in acetonitrile (1 mL) was added *p*-toluenesulfonic acid monohydrate (0.059 g, 0.31 mmol) at ambient temperature. The resulting solution was then cooled to 0 °C and a solution of potassium iodide (0.043 g, 0.26 mmol) and sodium nitrite (0.014 g, 0.20 mmol) in water (0.10 mL) was added dropwise over a period of 0.25 h. The reaction mixture was stirred at 0 °C for 1 h, and then allowed to gradually warm to ambient temperature and stirred overnight. The reaction mixture was made alkaline (pH ~9) by the addition of a saturated solution of sodium hydrogen carbonate, and excess iodine quenched by the addition of a 0.5 M sodium thiosulfate solution (~2 mL). The crude mixture was extracted with dichloromethane (2 × 10 mL), dried (MgSO$_4$), filtered and concentrated *in vacuo*. Purification using flash column chromatography (ethyl acetate/petroleum ether, 3:2) gave ethyl 4-(2'-iodophenyl)quinoline-2-carboxylate (**126**) (0.034 g, 83%) as a pale yellow solid. Mp 107–109 °C; ν_{max}/cm^{-1} (neat) 2928 (CH), 1717 (CO), 1555 (C=C), 1458, 1370, 1250, 1231, 1105, 1015; δ_H (500 MHz, CDCl$_3$) 1.50 (3H, t, *J* 7.1 Hz, CH$_2$C*H*$_3$), 4.54–4.61 (2H, m, C*H*$_2$CH$_3$), 7.20 (1H, td, *J* 8.0, 1.5 Hz, ArH), 7.32 (1H, dd, *J* 7.5, 1.5 Hz, ArH), 7.49–7.50 (2H, m, 2 × ArH), 7.57 (1H, ddd, *J* 8.5, 6.5, 1.5 Hz, ArH), 7.79 (1H, ddd, *J* 8.5, 6.5, 1.5 Hz, ArH), 8.04 (1H, s, ArH), 8.05 (1H, d, *J* 1.5 Hz, ArH), 8.40 (1H, d, *J* 8.5 Hz, ArH); δ_C (126 MHz, CDCl$_3$) 14.3 (CH$_3$), 62.2 (CH$_2$), 98.2 (C), 121.5 (CH), 125.7 (CH), 127.6 (C), 128.2 (CH), 128.6 (CH), 130.0 (CH), 130.1 (CH), 130.2 (CH), 131.2 (CH), 139.5 (CH), 142.5 (C), 148.0 (C), 148.1 (C), 151.5 (C), 165.3 (C); *m/z* (EI) 403.0065 (M$^+$. C$_{18}$H$_{14}$INO$_2$ requires 403.0069), 388 (12%), 358 (6), 330 (70), 205 (18), 136 (24), 84 (100).

4-(2'-Iodophenyl)quinoline-2-carboxylic acid (133)
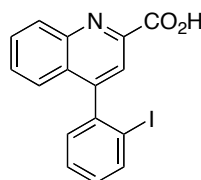
To a solution of ethyl 4-(2'-iodophenyl)quinoline-2-carboxylate (**126**) (0.133 g, 0.330 mmol) in a 50% aqueous ethanol mixture (5 ml) was added ground sodium hydroxide (0.053 g, 1.3 mmol), and the reaction mixture stirred vigorously under reflux for 24 h. On cooling to ambient temperature, the ethanol was removed *in vacuo*, and the aqueous layer acidified (pH ~4) using a 1 M hydrochloric acid solution (~10 mL). The crude product was extracted using dichloromethane (3 × 10 mL), dried (MgSO$_4$), filtered and

concentrated *in vacuo* to yield 4-(2'-iodophenyl)quinoline-2-carboxylic acid (**133**) (0.124 g, 100%) as a yellow solid, which was used without further purification. Mp 166–168 °C; ν_{max}/cm^{-1} (neat) 2922 (CH), 2340 (OH), 1707 (CO), 1593 (C=C), 1462, 1377, 1227, 1015; δ_H (500 MHz, CDCl$_3$) 7.22 (1H, td, *J* 8.0, 1.0 Hz, Ar*H*), 7.31 (1H, dd, *J* 7.6, 1.5 Hz, Ar*H*), 7.52 (1H, td, *J* 7.6, 1.0 Hz, Ar*H*), 7.57 (1H, d, *J* 8.3 Hz, Ar*H*), 7.64 (1H, t, *J* 7.6 Hz, Ar*H*), 7.85 (1H, t, *J* 7.6 Hz, Ar*H*), 8.05 (1H, d, *J* 8.0 Hz, Ar*H*), 8.16 (1H, s, Ar*H*), 8.25 (1H, d, *J* 8.3 Hz, Ar*H*); δ_C (126 MHz, CDCl$_3$) 97.8 (C), 119.8 (CH), 126.3 (CH), 128.3 (CH), 128.4 (C), 129.2 (CH), 129.8 (CH), 130.1 (CH), 130.3 (CH), 130.9 (CH), 139.6 (CH), 142.0 (C), 145.7 (C), 146.3 (C), 153.3 (C), 164.0 (C); *m/z* (EI) 374.9755 (M$^+$. C$_{16}$H$_{10}$INO$_2$ requires 374.9756), 331 (87%), 277 (100), 204 (45), 176 (22), 152 (10), 77 (14).

4-(2'-Iodophenyl)quinoline-2-*N*-diethylcarboxamide (120)
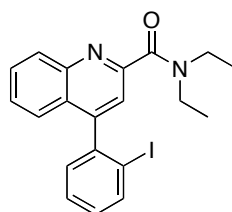
A solution of 4-(2'-iodophenyl)quinoline-2-carboxylic acid (**133**) (0.045 g, 0.12 mmol) in dichloromethane (5 mL) was cooled to 0 °C, and to this was added a few drops of *N,N'*-dimethylformamide followed by oxalyl chloride (15.1 μL, 0.178 mmol). The resultant solution was allowed to warm to ambient temperature and then stirred under reflux for 18 h. After cooling to ambient temperature, the reaction mixture was concentrated *in vacuo* and excess oxalyl chloride removed by azeotroping with toluene (3 × 10 mL). The crude residue was then reconstituted in dichloromethane (5 mL) and cooled to 0 °C. Diethylamine (61.4 μL, 0.593 mmol) was added to the solution dropwise and the reaction mixture stirred under reflux for a further 24 h. On cooling to ambient temperature, the mixture was diluted with water (5 mL) and the aqueous layer extracted using ethyl acetate (3 × 5 mL). The organic layer was dried (MgSO$_4$), filtered and concentrated *in vacuo*. Purification using flash column chromatography (ethyl acetate/petroleum ether, 9:1) afforded 4-(2'-iodophenyl)quinoline-2-*N*-diethylcarboxamide (**120**) (0.021 g, 51%) as a pale yellow oil, which crystallised to form a solid on standing. Mp 64–66 °C; ν_{max}/cm^{-1} (neat) 2969 (CH), 1626 (CO), 1464, 1404, 1275, 1096, 1015; δ_H (400 MHz, CDCl$_3$) 1.25 (3H, t, *J* 7.1 Hz, CH$_2$C*H*$_3$), 1.33 (3H, t, *J* 7.1 Hz, CH$_2$C*H*$_3$), 3.39–3.60 (2H, m, C*H*$_2$CH$_3$), 3.64 (2H, q, *J* 7.1 Hz, C*H*$_2$CH$_3$), 7.19 (1H, td, *J* 7.8, 1.4, Hz, Ar*H*),

7.33 (1H, dd, *J* 7.8, 1.7 Hz, ArH), 7.45–7.54 (4H, m, 4 × ArH), 7.76 (1H, ddd, *J* 8.3, 6.6, 1.6 Hz, ArH), 8.02 (1H, dd, *J* 7.8, 1.4 Hz, ArH), 8.19 (1H, d, *J* 8.3 Hz, ArH); δ_C (101 MHz, CDCl$_3$) 13.0 (CH$_3$), 14.6 (CH$_3$), 40.4 (CH$_2$), 43.5 (CH$_2$), 98.4 (C), 120.6 (CH), 125.8 (CH), 126.3 (C), 127.5 (CH), 128.2 (CH), 130.0 (2 × CH), 130.1 (CH), 130.2 (CH), 139.3 (CH), 142.4 (C), 147.1 (C), 151.2 (C), 154.4 (C), 168.6 (C); *m/z* (EI) 430.0544 (M$^+$. C$_{20}$H$_{19}$IN$_2$O requires 430.0542), 359 (23%), 331 (28), 203 (35), 176 (9), 84 (100).

## 4-(2'-Iodophenyl)quinoline-2-*N*-morpholinecarboxamide (121)
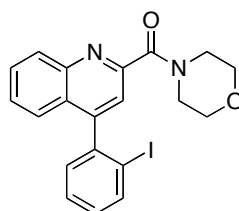
4-(2'-Iodophenyl)quinoline-2-*N*-morpholinecarboxamide (**121**) was synthesised as described above for 4-(2'-iodophenyl)quinoline-2-*N*-diethylcarboxamide (**120**) using 4-(2'-iodophenyl)quinoline-2-carboxylic acid (**133**) (0.045 g, 0.12 mmol), a few drops of *N,N'*-dimethylformamide, oxalyl chloride (15.1 μL, 0.178 mmol) and morpholine (51.9 μL, 0.593 mmol) in dichloromethane (5 mL). Purification using flash column chromatography (ethyl acetate) afforded 4-(2'-iodophenyl)quinoline-2-*N*-morpholinecarboxamide (**121**) (0.032 g, 60%) as a yellow solid. Mp 118–120 °C; ν_{max}/cm^{-1} (neat) 2853 (CH), 1628 (CO), 1551, 1466, 1404, 1273, 1244, 1111; δ_H (400 MHz, CDCl$_3$) 3.68–3.96 (8H, m, 4 × CH$_2$), 7.20 (1H, td, *J* 7.8, 1.6 Hz, ArH), 7.33 (1H, dd, *J* 7.8, 1.6 Hz, ArH), 7.47–7.57 (3H, m, 3 × ArH), 7.58 (1H, s, ArH), 7.77 (1H, ddd, *J* 8.4, 6.6, 1.7 Hz, ArH), 8.03 (1H, dd, *J* 7.8, 1.2 Hz, ArH), 8.18 (1H, d, *J* 8.4 Hz, ArH); δ_C (101 MHz, CDCl$_3$) 42.9 (CH$_2$), 47.9 (CH$_2$), 66.9 (CH$_2$), 67.1 (CH$_2$), 98.3 (C), 121.3 (CH), 125.9 (CH), 126.5 (C), 127.9 (CH), 128.2 (CH), 130.1 (CH), 130.1 (CH), 130.2 (CH), 130.3 (CH), 139.5 (CH), 142.3 (C), 147.0 (C), 151.5 (C), 152.9 (C), 167.5 (C); *m/z* (EI) 444.0332 (M$^+$. C$_{20}$H$_{17}$IN$_2$O$_2$ requires 444.0335), 359 (8%), 331 (100), 203 (75), 176 (15), 83 (66).

Ethyl 4-(3'-bromophenyl)quinoline-2-carboxylate (136)
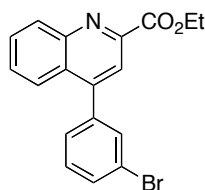
To a solution of ethyl 4-bromoquinoline-2-carboxylate (**94**) (0.200 g, 0.714 mmol) in *N,N'*-dimethylformamide (15 mL) was added 3-bromophenylboronic acid (0.172 g, 0.857 mmol), potassium phosphate (0.182 g, 0.857 mmol) and tetrakis(triphenylphosphine)palladium(0) (0.082 g, 0.071 mmol). The resultant suspension was stirred vigorously at 120 °C for 24 h and then cooled to ambient temperature. An additional aliquot of 3-bromophenylboronic acid (0.172 g, 0.857 mmol), potassium phosphate (0.182 g, 0.857 mmol) and tetrakis(triphenylphosphine)palladium(0) (0.082 g, 0.071 mmol) was added to the reaction mixture and stirred at 120 °C for a further 24 h. On cooling to ambient temperature, the mixture was concentrated *in vacuo* and then reconstituted in dichloromethane (20 mL). The organic layer was then washed with water (3 × 20 mL), dried (MgSO$_4$), filtered and concentrated *in vacuo*. Purification using flash column chromatrography (ethyl acetate/petroleum ether, 1:1) afforded ethyl 4-(3'-bromophenyl)quinoline-2-carboxylate (**136**) (0.197 g, 78%) as a pale yellow solid. Mp 102–104 °C; ν_{max}/cm^{-1} (neat) 2980 (CH), 1715 (CO), 1584 (C=C), 1373, 1333, 1246, 1132, 1107, 1018; δ_H (400 MHz, CDCl$_3$) 1.50 (3H, t, *J* 7.2 Hz, CH$_2$C*H$_3$*), 4.58 (2H, q, *J* 7.2 Hz, C*H$_2$*CH$_3$), 7.40–7.50 (2H, m, 2 × ArH), 7.60–7.71 (3H, m, 3 × ArH), 7.81 (1H, ddd, *J* 8.4, 6.8, 1.2 Hz, ArH), 7.91 (1H, dd, *J* 8.4, 0.8 Hz, ArH), 8.11 (1H, s, ArH), 8.39 (1H, dd, *J* 8.4. 0.4 Hz, ArH); δ_C (101 MHz, CDCl$_3$) 14.4 (CH$_3$), 62.4 (CH$_2$), 121.2 (CH), 122.8 (C), 125.3 (CH), 127.4 (C), 128.2 (CH), 129.0 (CH), 130.2 (2 × CH), 131.3 (CH), 131.8 (CH), 132.4 (CH), 139.5 (C), 147.8 (C), 148.1 (C), 148.2 (C), 165.3 (C); *m/z* (EI) 355.0202 (M$^+$. C$_{18}$H$_{14}$^{79}BrNO$_2$ requires 355.0208), 203 (63%), 176 (12), 101 (4).

4-(3'-Bromophenyl)quinoline-2-carboxylic acid (137)
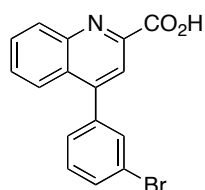
To a solution of ethyl 4-(3'-bromophenyl)quinoline-2-carboxylate (**136**) (0.157 g, 0.441 mmol) in a 50% aqueous ethanol mixture (20 mL) was added ground sodium hydroxide (0.071 g, 1.8 mmol), and the reaction mixture stirred vigorously under reflux for 18 h. On cooling to ambient temperature, the ethanol was removed *in vacuo*, and the aqueous layer acidified (pH ~4) using a 1 M hydrochloric acid solution (~10 mL). The crude product was extracted using dichloromethane (3 × 20 mL) and washed with water (3 × 20 mL). The organic fraction was dried (MgSO$_4$), filtered and concentrated *in vacuo* to give 4-(3'-bromophenyl)quinoline-2-carboxylic acid (**137**) (0.136 g, 94%) as an orange solid, which was used without further purification. Mp 91–92 °C; ν_{max}/cm^{-1} (neat) 3067 (CH), 1710 (CO), 1586 (C=C), 1462, 1375, 1229, 1072, 901, 765; δ_H (400 MHz, CDCl$_3$) 7.51–7.60 (3H, m, 3 × ArH), 7.63–7.72 (2H, m, 2 × ArH), 7.85 (1H, ddd, *J* 8.4, 6.8, 1.2 Hz, ArH), 8.05 (1H, d, *J* 8.0 Hz, ArH), 8.22–8.26 (2H, s, 2 × ArH); δ_C (101 MHz, CDCl$_3$) 119.4 (CH), 126.2 (CH), 128.5 (C), 128.6 (CH), 128.8 (CH), 129.1 (CH), 129.2 (CH), 129.6 (CH), 129.8 (CH), 130.8 (CH), 132.1 (C), 137.0 (C), 145.4 (C), 146.5 (C), 151.7 (C), 164.4 (C); *m/z* (ESI) 325.9812 (MH$^-$. C$_{16}$H$_9$^{79}BrNO$_2$ requires 325.9822).

4-(3'-Bromophenyl)quinoline-2-*N*-diethylcarboxamide (139)
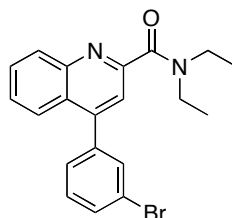
A solution of 4-(3'-bromophenyl)quinoline-2-carboxylic acid (**137**) (0.136 g, 0.414 mmol) in dichloromethane (10 mL) was cooled to 0 °C, and to this was added a few drops of *N,N'*-dimethylformamide followed by oxalyl chloride (52.6 μL, 0.622 mmol). The resultant solution was allowed to warm to ambient temperature and then stirred under reflux for 18 h. After cooling to ambient temperature, the reaction mixture was concentrated *in vacuo* and excess oxalyl chloride removed by azeotroping with toluene (3 × 10 mL). The crude residue was then reconstituted in dichloromethane (10 mL) and cooled to 0 °C. Diethylamine (0.214 mL, 2.07 mmol) was added to the solution dropwise and the reaction mixture stirred under reflux for a further 18 h. On cooling to ambient temperature, the mixture was diluted with water (10 mL) and the aqueous layer extracted using dichloromethane (3 × 10 mL). The organic layer was dried (MgSO$_4$), filtered and concentrated *in vacuo*. Purification using flash column chromatography (ethyl

acetate/petroleum ether, 1:1) afforded 4-(3'-bromophenyl)quinoline-2-*N*-diethylcarboxamide (**139**) (0.090 g, 57%) as a colourless oil. ν_{max}/cm^{-1} (neat) 2977 (CH), 2933, 1627 (CO), 1553 (C=C), 1480, 1406, 1271, 1097, 908; δ_H (400 MHz, CDCl$_3$) 1.27 (3H, t, *J* 7.2 Hz, CH$_2$C*H$_3$*), 1.32 (3H, t, *J* 7.2 Hz, CH$_2$C*H$_3$*), 3.49 (2H, q, *J* 7.2 Hz, C*H$_2$*CH$_3$), 3.63 (2H, q, *J* 7.2 Hz, C*H$_2$*CH$_3$), 7.46–7.56 (5H, m, 5 × ArH), 7.61 (1H, s, ArH), 7.71–7.78 (1H, m, ArH), 7.95 (1H, d, *J* 8.0 Hz, ArH), 8.17 (1H, d, *J* 8.4 Hz, ArH); δ_C (101 MHz, CDCl$_3$) 13.0 (CH$_3$), 14.5 (CH$_3$), 40.3 (CH$_2$), 43.5 (CH$_2$), 120.4 (CH), 125.8 (CH), 126.5 (C), 127.3 (CH), 128.6 (2 × CH), 128.9 (C), 129.6 (2 × CH), 129.7 (CH), 130.2 (CH), 137.7 (C), 147.3 (C), 149.5 (C), 154.4 (C), 168.8 (C); *m/z* (CI) 385.0738 (MH$^+$. C$_{20}$H$_{20}$^{81}BrN$_2$O requires 385.0741), 381 (18%), 345 (14), 305 (100), 233 (9), 206 (7).

Ethyl 6-Iodo-4-phenylquinoline-2-carboxylate (149)
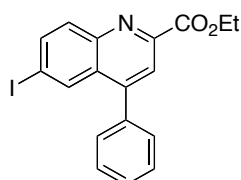
To a solution of 4-iodoaniline (**155**) (0.657 g, 3.00 mmol) in nitromethane (5 mL) was added phenylacetylene (**151**) (0.494 mL, 4.50 mmol), ethyl glyoxalate solution (50% in toluene) (**154**) (0.595 mL, 3.00 mmol) and iodine (0.152 g, 0.600 mmol). The resultant solution was stirred vigorously at ambient temperature for 72 h and then diluted with ethyl acetate (20 mL). The organic layer was washed with 0.1 M sodium thiosulfate solution (20 mL) and water (20 mL), dried (MgSO$_4$), filtered and concentrated *in vacuo*. Purification by trituration with diethyl ether gave ethyl 6-iodo-4-phenylquinoline-2-carboxylate (**149**) (0.608 g, 50%) as a pale yellow solid. Mp 200–201 °C; ν_{max}/cm^{-1} (neat) 3048 (CH), 1721 (CO), 1481, 1366, 1250, 1111, 1018, 826, 702; δ_H (400 MHz, CDCl$_3$) 1.49 (3H, t, *J* 7.2 Hz, CH$_2$C*H$_3$*), 4.56 (2H, q, *J* 7.2 Hz, C*H$_2$*CH$_3$), 7.49–7.61 (5H, m, 5 × ArH), 8.03 (1H, dd, *J* 8.8, 1.6 Hz, ArH), 8.09 (1H, d, *J* 8.8 Hz, ArH), 8.13 (1H, s, ArH), 8.33 (1H, d, *J* 1.6 Hz, ArH); δ_C (101 MHz, CDCl$_3$) 14.4 (CH$_3$), 62.4 (CH$_2$), 95.4 (C), 122.0 (CH), 128.9 (2 × CH), 129.0 (CH), 129.3 (C), 129.5 (2 × CH), 132.7 (CH), 134.6 (CH), 136.9 (C), 138.9 (CH), 147.1 (C), 148.2 (C), 148.8 (C), 165.2 (C); *m/z* (EI) 403.0067 (M$^+$. C$_{18}$H$_{14}$INO$_2$ requires 403.0069), 358 (10%), 330 (100), 203 (45), 176 (17), 150 (4), 83 (38).

Ethyl 6-fluoro-4-phenylquinoline-2-carboxylate (150)
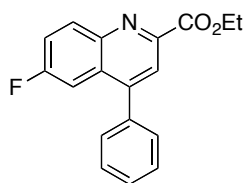
Ethyl 6-fluoro-4-phenylquinoline-2-carboxylate (**150**) was synthesised as described above for 6-iodo-4-phenylquinoline-2-carboxylate (**149**) using 4-fluoroaniline (**156**) (94.6 µL, 1.00 mmol), phenylacetylene (**151**) (0.165 mL, 1.50 mmol), ethyl glyoxalate solution (50% in toluene) (**154**) (0.198 mL, 1.00 mmol) and iodine (0.051 g, 0.20 mmol) in nitromethane (2 mL). Purification by trituration with diethyl ether afforded ethyl 6-fluoro-4-phenylquinoline-2-carboxylate (**150**) (0.169 g, 57%) as a pale yellow solid. Mp 154–155 °C; ν_{max}/cm^{-1} (neat) 2986 (CH), 1713 (CO), 1512, 1466, 1373, 1227, 1196, 1026, 833, 702; δ_H (400 MHz, CDCl$_3$) 1.49 (3H, t, *J* 7.1 Hz, CH$_2$C*H*$_3$), 4.57 (2H, q, *J* 7.1 Hz, C*H*$_2$CH$_3$), 7.49–7.60 (7H, m, 7 × ArH), 8.15 (1H, s, ArH), 8.35–8.41 (1H, m, ArH); δ_C (100 MHz, CDCl$_3$) 14.4 (CH$_3$), 62.3 (CH$_2$), 109.2 (CH, d, J_{C-C-F} 23.4 Hz), 120.5 (CH, d, J_{C-C-F} 26.2 Hz), 121.8 (CH), 128.9 (C, d, $J_{C-C-C-F}$ 10.0 Hz), 128.9 (2 × CH), 129.0 (CH), 129.4 (2 × CH), 133.8 (CH, d, $J_{C-C-C-F}$ 9.4 Hz), 137.1 (C), 145.4 (C), 147.3 (C, d, *J* 2.9 Hz), 149.3 (C, d, $J_{C-C-C-F}$ 5.9 Hz), 161.9 (C, d, J_{C-F} 251.0 Hz), 165.3 (C); *m/z* (CI) 296.1088 (MH$^+$. C$_{18}$H$_{15}$FNO$_2$ requires 296.1087), 224 (6%), 198 (5), 113 (22), 85 (45), 73 (100).

6-Iodo-4-phenylquinoline-2-carboxylic acid (147)
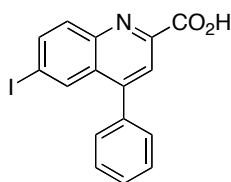
To a solution of ethyl 6-iodo-4-phenylquinoline-2-carboxylate (**149**) (0.078 g, 0.19 mmol) in a 50% aqueous ethanol mixture (10 ml) was added ground sodium hydroxide (0.031 g, 0.77 mmol), and the reaction mixture stirred under reflux for 18 h. On cooling to ambient temperature, the ethanol was removed *in vacuo*, and the aqueous layer acidified (pH ~4) using a 1 M hydrochloric acid solution (~10 mL). The crude product was extracted using dichloromethane (3 × 20 mL), washed with water (2 × 20 mL), dried (MgSO$_4$), filtered and concentrated *in vacuo*. Purification by trituration with diethyl ether afforded

6-iodo-4-phenylquinoline-2-carboxylic acid (**147**) (0.051 g, 70%) as a yellow solid. Mp 198–200 °C; ν_{max}/cm^{-1} (neat) 2901 (CH), 1705 (CO), 1582 (C=C), 1458, 1366, 1250, 1134, 972, 787; δ_H (400 MHz, CDCl$_3$) 7.48–7.63 (5H, m, 5 × ArH), 7.94 (1H, d, J 9.0 Hz, ArH), 8.09 (1H, dd, J 9.0, 1.8 Hz, ArH), 8.24 (1H, s, ArH), 8.40 (1H, d, J 1.8 Hz, ArH); δ_C (101 MHz, CDCl$_3$) 96.0 (C), 120.2 (CH), 129.1 (2 × CH), 129.4 (CH), 129.5 (2 × CH), 129.9 (C), 131.2 (CH), 135.1 (CH), 136.4 (C), 139.8 (CH), 145.5 (C), 145.8 (C), 150.6 (C), 164.0 (C); m/z (CI) 375.9832 (MH$^+$. C$_{16}$H$_{11}$INO$_2$ requires 375.9835), 332 (8%), 250 (41), 206 (4), 113 (3), 69 (7).

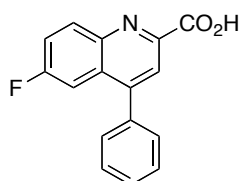## 6-Fluoro-4-phenylquinoline-2-carboxylic acid (148)

6-Fluoro-4-phenylquinoline-2-carboxylic acid (**148**) was synthesised as described above for 6-iodo-4-phenylquinoline-2-carboxylic acid (**147**) using ethyl 6-fluoro-4-phenylquinoline-2-carboxylate (**150**) (0.160 g, 0.542 mmol) and ground sodium hydroxide (0.087 g, 2.2 mmol) in a 50% aqueous ethanol solution (10 mL). Purification by trituration with diethyl ether yielded 6-fluoro-4-phenylquinoline-2-carboxylic acid (**148**) (0.119 g, 82%) as a colourless solid. Mp 129–131 °C; ν_{max}/cm^{-1} (neat) 3228 (OH), 3053 (CH), 1704 (CO), 1588 (C=C), 1485, 1451, 1373, 1315, 1061, 810; δ_H (500 MHz, CDCl$_3$) 7.49–7.68 (7H, m, 7 × ArH), 8.23–8.27 (2H, m, 2 × ArH); δ_C (126 MHz, CDCl$_3$) 109.8 (CH, d, J_{C-C-F} 23.6 Hz), 120.0 (CH), 121.4 (CH, d, J_{C-C-F} 26.3 Hz), 129.0 (2 × CH), 129.3 (2 × CH), 129.4 (CH), 129.7 (C, d, $J_{C-C-C-F}$ 9.7 Hz), 132.6 (CH, d, $J_{C-C-C-F}$ 9.4 Hz), 136.6 (C), 143.7 (C), 145.0 (C), 151.1 (C, d, $J_{C-C-C-C-F}$ 5.7 Hz), 162.2 (C, d, J_{C-F} 252.5 Hz), 164.2 (C); m/z (EI) 267.0694 (M$^+$. C$_{16}$H$_{10}$FNO$_2$ requires 267.0696), 223 (16%), 135 (5), 82 (100), 46 (18).

6-Iodo-4-phenylquinoline-2-*N*-morpholinecarboxamide (141)
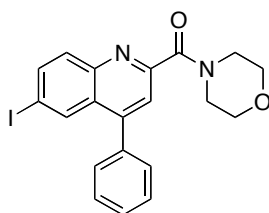
A solution of 6-iodo-4-phenylquinoline-2-carboxylic acid (**147**) (0.051 g, 0.14 mmol) in dichloromethane (10 mL) was cooled to 0 °C, and to this was added a few drops of *N,N'*-dimethylformamide followed by oxalyl chloride (17.3 μL, 0.204 mmol). The resultant solution was allowed to warm to ambient temperature and then stirred under reflux for 18 h. After cooling to ambient temperature, the reaction mixture was concentrated *in vacuo* and excess oxalyl chloride removed by azeotroping with toluene (3 × 20 mL). The crude residue was then reconstituted in dichloromethane (10 mL) and cooled to 0 °C. Morpholine (59.5 μL, 0.680 mmol) was added to the solution dropwise and the reaction mixture stirred under reflux for a further 5 h. On cooling to ambient temperature, the mixture was diluted with water (10 mL) and the aqueous layer extracted using dichloromethane (3 × 10 mL). The organic layer was dried (MgSO$_4$), filtered and concentrated *in vacuo*. Purification using flash column chromatography (methanol/dichloromethane, 1:9) afforded 6-iodo-4-phenylquinoline-2-*N*-morpholinecarboxamide (**141**) (0.055 g, 92%) as a pale yellow solid. Mp 116–118 °C; v_{max}/cm^{-1} (neat) 2853 (CH), 1628 (CO), 1468, 1439, 1271, 1244, 1111, 1028; δ_H (400 MHz, CDCl$_3$) 3.72–3.91 (8H, m, 4 × CH$_2$), 7.48–7.59 (5H, m, 5 × ArH), 7.69 (1H, s, ArH), 7.86 (1H, d, *J* 8.8 Hz, ArH), 8.00 (1H, dd, *J* 8.8, 2.0 Hz, ArH), 8.30 (1H, d, *J* 2.0 Hz, ArH); δ_C (101 MHz, CDCl$_3$) 42.9 (CH$_2$), 47.9 (CH$_2$), 66.9 (CH$_2$), 67.1 (CH$_2$), 94.1 (C), 121.8 (CH), 128.3 (C), 128.9 (2 × CH), 129.0 (CH), 129.4 (2 × CH), 131.7 (CH), 134.7 (CH), 136.8 (C), 138.8 (CH), 146.1 (C), 148.8 (C), 153.3 (C), 167.2 (C); *m/z* (CI) 445.0415 (MH$^+$. C$_{20}$H$_{18}$IN$_2$O$_2$ requires 445.0413), 319 (100%), 206 (4), 116 (5), 69 (10).

6-Iodo-4-phenylquinoline-2-*N*-(4'-methylpiperazine)carboxamide (141)
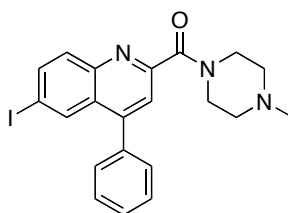
6-Iodo-4-phenylquinoline-2-*N*-(4'-methylpiperazine)carboxamide (**142**) was synthesised as described above for 6-iodo-4-phenylquinoline-2-*N*-morpholinecarboxamide (**141**) using 6-iodo-4-phenylquinoline-2-carboxylic acid (**147**) (0.065 g, 0.17 mmol), a few drops of *N,N'*-dimethylformamide, oxalyl chloride (22.0 μL, 0.260 mmol) and 1-methylpiperazine (96.1 μL, 0.866 mmol) in dichloromethane (5 mL). Purification using flash column chromatography (methanol/dichloromethane, 1:9) gave 6-iodo-4-phenylquinoline-2-*N*-(4'-methylpiperazine)carboxamide (**142**) (0.036 g, 46%) as a pale brown solid. Mp 132–133 °C; ν_{max}/cm^{-1} (neat) 2916 (CH), 2790, 1631 (CO), 1547 (C=C), 1446, 1289, 1131, 1024; δ_H (500 MHz, CDCl$_3$) 2.37 (3H, s, CH$_3$), 2.51 (2H, br s, NCH$_2$), 2.60 (2H, br s, NCH$_2$), 3.73–3.81 (2H, m, NCH$_2$), 3.92 (2H, br s, NCH$_2$), 7.48–7.58 (5H, m, 5 × ArH), 7.65 (1H, s, ArH), 7.87 (1H, d, *J* 8.9 Hz, ArH), 8.00 (1H, dd, *J* 8.9, 1.9 Hz, ArH), 8.30 (1H, d, *J* 1.9 Hz, ArH); δ_C (126 MHz, CDCl$_3$) 42.2 (CH$_2$), 45.9 (CH$_3$), 47.0 (CH$_2$), 54.6 (CH$_2$), 55.3 (CH$_2$), 93.9 (C), 121.6 (CH), 128.3 (C), 128.9 (2 × CH), 129.0 (CH), 129.4 (2 × CH), 131.7 (CH), 134.6 (CH), 136.8 (C), 138.8 (CH), 146.1 (C), 148.7 (C), 153.7 (C), 167.2 (C); *m/z* (CI) 458.0730 (MH$^+$. C$_{21}$H$_{21}$IN$_3$O requires 458.0729), 391 (35%), 327 (18), 248 (69), 205 (41), 171 (100).

6-Iodo-4-phenylquinoline-2-*N*-diethylcarboxamide (143)
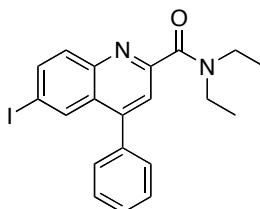
6-Iodo-4-phenylquinoline-2-*N*-diethylcarboxamide (**143**) was synthesised as described above for 6-iodo-4-phenylquinoline-2-*N*-morpholinecarboxamide (**141**) using 6-iodo-4-phenylquinoline-2-carboxylic acid (**147**) (0.175 g, 0.466 mmol), a few drops of *N,N'*-dimethylformamide, oxalyl chloride (59.2 μL, 0.700 mmol) and diethylamine (0.241

mL, 2.33 mmol) in dichloromethane (10 mL). Purification using flash column chromatography (ethyl acetate/petroleum ether, 4:1) afforded 6-iodo-4-phenylquinoline-2-*N*-diethylcarboxamide (**143**) (0.062 g, 31%) as yellow oil. v_{max}/cm^{-1} (neat) 2972 (CH), 1624 (CO), 1589 (C=C), 1547, 1476, 1460, 1377, 1269, 1098; δ_H (400 MHz, CDCl$_3$) 1.27 (3H, t, *J* 6.8 Hz, CH$_3$), 1.31 (3H, t, *J* 7.2 Hz, CH$_3$), 3.47 (2H, q, *J* 6.8 Hz, CH$_2$), 3.62 (2H, q, *J* 7.2 Hz, CH$_2$), 7.49–7.58 (5H, m, 5 × ArH), 7.61 (1H, s, ArH), 7.88 (1H, d, *J* 8.8 Hz, ArH), 7.99 (1H, dd, *J* 8.8, 1.6 Hz, ArH), 8.29 (1H, d, *J* 1.6 Hz, ArH); δ_C (101 MHz, CDCl$_3$) 12.9 (CH$_3$), 14.5 (CH$_3$), 40.4 (CH$_2$), 43.5 (CH$_2$), 93.5 (C), 121.2 (CH), 128.2 (C), 128.9 (2 × CH), 128.9 (CH), 129.5 (2 × CH), 131.8 (CH), 134.6 (CH), 137.0 (C), 138.6 (CH), 146.2 (C), 148.5 (C), 154.8 (C), 168.4 (C); *m/z* (CI) 431.0626 (MH$^+$. C$_{20}$H$_{20}$IN$_2$O requires 431.0620), 347 (10%), 305 (100), 221 (12), 178 (47), 113 (40).

6-Fluoro-4-phenylquinoline-2-*N*-morpholinecarboxamide (144)

6-Fluoro-4-phenylquinoline-2-*N*-morpholinecarboxamide (**144**) was synthesised as described above for 6-iodo-4-phenylquinoline-2-*N*-morpholinecarboxamide (**141**) using 6-fluoro-4-phenylquinoline-2-carboxylic acid (**148**) (0.048 g, 0.18 mmol), a few drops of *N,N'*-dimethylformamide, oxalyl chloride (22.8 μL, 0.269 mmol) and morpholine (78.6 μL, 0.898 mmol) in dichloromethane (10 mL). Purification using flash column chromatography (diethyl ether/petroleum ether, 9:1) afforded 6-fluoro-4-phenylquinoline-2-*N*-morpholinecarboxamide (**144**) (0.037 g, 61%) as a pale yellow oil. v_{max}/cm^{-1} (neat) 2855 (CH), 1622 (CO), 1474, 1435, 1229, 1196, 1111, 1028; δ_H (400 MHz, CDCl$_3$) 3.71–3.93 (8H, m, 4 × CH$_2$), 7.48–7.59 (7H, m, 7 × ArH), 7.73 (1H, s, ArH), 8.16 (1H, dd, *J* 9.2, 5.6 Hz, ArH); δ_C (101 MHz, CDCl$_3$) 42.9 (CH$_2$), 47.9 (CH$_2$), 66.9 (CH$_2$), 67.1 (CH$_2$), 109.3 (CH, d, J_{C-C-F} 23.4 Hz), 120.3 (CH, d, J_{C-C-F} 25.9 Hz), 121.7 (CH), 127.7 (C, d, $J_{C-C-C-F}$ 9.5 Hz), 128.9 (2 × CH), 129.0 (CH), 129.3 (2 × CH), 132.7 (CH, d, $J_{C-C-C-F}$ 9.3 Hz), 137.1 (C), 144.2 (C), 149.4 (C, d, $J_{C-C-C-F}$ 5.3 Hz), 152.3 (C), 161.4 (C, d, J_{C-F} 250.6 Hz), 167.3 (C); *m/z* (CI) 337.1348 (MH$^+$. C$_{20}$H$_{18}$FN$_2$O$_2$ requires 337.1352), 220 (5), 188 (4), 69 (7).

6-Fluoro-4-phenylquinoline-2-*N*-(4'-methylpiperazine)carboxamide (145)

6-Fluoro-4-phenylquinoline-2-*N*-(4'-methylpiperazine)carboxamide (**145**) was synthesised as described above for 6-iodo-4-phenylquinoline-2-*N*-morpholinecarboxamide (**141**) using 6-fluoro-4-phenylquinoline-2-carboxylic acid (**148**) (0.065 g, 0.24 mmol), a few drops of *N,N'*-dimethylformamide, oxalyl chloride (30.9 μL, 0.365 mmol) and 1-methylpiperazine (0.135 mL, 1.22 mmol) in dichloromethane (10 mL). Purification using flash column chromatography (methanol/dichloromethane, 1:9) afforded 6-fluoro-4-phenylquinoline-2-*N*-(4'-methylpiperazine)carboxamide (**145**) (0.048 g, 56%) as a yellow oil. ν_{max}/cm^{-1} (neat) 2938 (CH), 2793, 1622 (CO), 1437, 1290, 1229, 1198, 1138, 1001; δ_H (400 MHz, CDCl$_3$) 2.35 (3H, s, CH$_3$), 2.47 (2H, br s, NCH$_2$), 2.57 (2H, br s, NCH$_2$), 3.76 (2H, t, *J* 4.8 Hz, NCH$_2$), 3.91 (2H, t, *J* 4.8 Hz, NCH$_2$), 7.39–7.59 (7H, m, 7 × ArH), 7.68 (1H, s, ArH), 8.16 (1H, dd, *J* 8.8, 5.2 Hz, ArH); δ_C (101 MHz, CDCl$_3$) 42.3 (CH$_2$), 46.0 (CH$_3$), 47.2 (CH$_2$), 54.7 (CH$_2$), 55.4 (CH$_2$), 109.3 (CH, d, J_{C-C-F} 23.5 Hz), 120.2 (CH, d, J_{C-C-F} 26.0 Hz), 121.5 (CH, d, $J_{C-C-C-F}$ 3.5 Hz), 127.6 (C, d, $J_{C-C-C-F}$ 9.8 Hz), 128.8 (2 × CH), 128.9 (CH), 129.3 (2 × CH), 132.7 (CH, d, $J_{C-C-C-F}$ 9.2 Hz), 137.1 (C), 144.3 (C), 149.3 (C, d, $J_{C-C-C-C-F}$ 5.6 Hz), 152.7 (C, d, $J_{C-C-C-F}$ 2.9 Hz), 161.3 (C, d, J_{C-F} 249.0 Hz), 167.4 (C); *m/z* (CI) 350.1665 (MH$^+$. C$_{21}$H$_{21}$FN$_3$O requires 350.1669), 184 (81%), 170 (22), 129 (6), 113 (28), 81 (62), 69 (100).
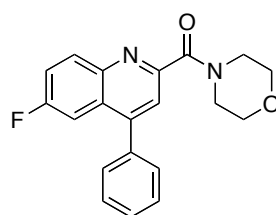
6-Fluoro-4-phenylquinoline-2-*N*-diethylcarboxamide (146)

6-Fluoro-4-phenylquinoline-2-*N*-diethylcarboxamide (**146**) was synthesised as described above for 6-iodo-4-phenylquinoline-2-*N*-morpholinecarboxamide (**141**) using 6-fluoro-4-phenylquinoline-2-carboxylic acid (**148**) (0.119 g, 0.445 mmol), a few drops of

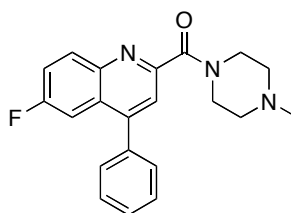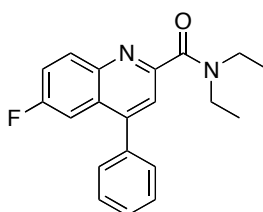*N,N'*-dimethylformamide, oxalyl chloride (56.5 μL, 0.668 mmol) and diethylamine (0.230 mL, 2.23 mmol) in dichloromethane (15 mL). Purification using flash column chromatography (diethyl ether/petroleum ether, 4:1) afforded 6-fluoro-4-phenylquinoline-2-*N*-diethylcarboxamide (**146**) (0.040 g, 28%) as a brown oil. ν_{max}/cm^{-1} (neat) 2974 (CH), 2934, 1622 (CO), 1593 (C=C), 1481, 1269, 1229, 1200, 1096; δ_H (400 MHz, CDCl$_3$) 1.28 (3H, t, *J* 7.2 Hz, CH$_3$), 1.32 (3H, t, *J* 7.2 Hz, CH$_3$), 3.49 (2H, q, *J* 7.2 Hz, CH$_2$), 3.63 (2H, q, *J* 7.2 Hz, CH$_2$), 7.48–7.58 (7H, m, 7 × ArH), 7.64 (1H, s, ArH), 8.16 (1H, dd, *J* 9.2, 5.6 Hz, ArH); δ_C (101 MHz, CDCl$_3$) 12.9 (CH$_3$), 14.5 (CH$_3$), 40.4 (CH$_2$), 43.5 (CH$_2$), 109.2 (CH, d, J_{C-C-F} 23.2 Hz), 120.0 (CH, d, J_{C-C-F} 25.7 Hz), 121.1 (CH), 127.4 (C, d, $J_{C-C-C-F}$ 9.5 Hz), 128.8 (2 × CH), 128.8 (CH), 129.3 (2 × CH), 132.7 (CH, d, $J_{C-C-C-F}$ 9.2 Hz), 137.2 (C), 144.3 (C), 149.0 (C, d, $J_{C-C-C-F}$ 6.0 Hz), 153.8 (C, d, $J_{C-C-C-F}$ 2.7 Hz), 161.2 (C, d, J_{C-F} 248.7 Hz), 168.5 (C); *m/z* (CI) 323.1562 (MH$^+$. C$_{20}$H$_{20}$FN$_2$O requires 323.1560), 322 (13%), 251 (4), 223 (3), 178 (3).

8-Iodo-4-phenylquinoline-2-carboxylate (164)
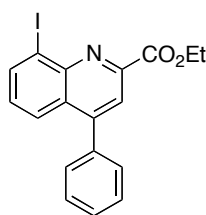
To a suspension of magnesium sulfate (1.0 g) in dichloromethane (20 mL) was added 2-iodoaniline (**163**) (0.300 g, 1.37 mmol) followed by ethyl glyoxalate solution (50% in toluene) (**154**) (0.27 mL, 1.37 mmol). The resultant suspension was stirred at ambient temperature for 24 h and then filtered. Phenylacetylene (**151**) (0.150 mL, 1.37 mmol) and copper(II) triflate (0.099 g, 0.27 mmol) was added to the filtrate and the reaction mixture stirred at ambient temperature for a further 48 h. The mixture was washed with water (2 × 20 mL). The organic layer was dried (MgSO$_4$), filtered and concentrated *in vacuo*. Purification using flash column chromatography (diethyl ether/petroleum ether, 1:9) followed by crystallisation in hexane afforded ethyl 8-iodo-4-phenylquinoline-2-carboxylate (**164**) (0.121 g, 22%) as a colourless solid. Mp 102–104 °C; ν_{max}/cm^{-1} (neat) 2987 (CH), 1722 (CO), 1601 (C=C), 1488, 1373, 1244, 1120, 1026; δ_H (500 MHz, CDCl$_3$) 1.52 (3H, t, *J* 7.0 Hz, C*H*$_3$CH$_2$), 4.55 (2H, q, *J* 7.0 Hz, CH$_3$C*H*$_2$), 7.28 (1H, dd, *J* 8.5, 7.5 Hz, ArH), 7.49–7.58 (5H, m, 5 × ArH), 7.95 (1H, dd, *J* 8.5, 1.0 Hz, ArH), 8.15 (1H, s, ArH), 8.42 (1H, dd, *J* 7.5, 1.0 Hz, ArH); δ_C (126 MHz,

CDCl$_3$) 14.3 (CH$_3$), 62.2 (CH$_2$), 105.5 (C), 122.1 (CH), 126.7 (CH), 128.5 (C), 128.7 (2 × CH), 128.9 (CH), 129.4 (CH), 129.6 (2 × CH), 137.1 (C), 140.8 (CH), 147.0 (C), 148.6 (C), 150.8 (C), 165.0 (C); *m/z* (ESI) 425.9947 (MNa$^+$. C$_{18}$H$_{14}$INNaO$_2$ requires 425.9961).

8-Iodo-4-phenylquinoline-2-carboxylic acid (166)
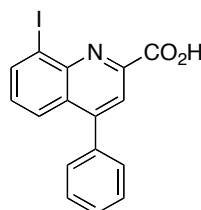
To a solution of ethyl 8-iodo-4-phenylquinoline-2-carboxylate (**164**) (0.050 g, 0.12 mmol) in a 50% aqueous ethanol mixture (5 ml) was added ground sodium hydroxide (0.020 g, 0.50 mmol) and the reaction mixture stirred under reflux for 18 h. On cooling to ambient temperature, the ethanol was removed *in vacuo,* and the aqueous layer acidified (pH ~4) using a 1 M hydrochloric acid solution (~3 mL). The crude product was extracted using dichloromethane (3 × 5 mL), washed with water (2 × 5 mL), dried (MgSO$_4$), filtered and concentrated *in vacuo*.   Purification by trituration with hexane afforded 8-iodo-4-phenylquinoline-2-carboxylic acid (**166**) (0.039 g, 84%) as a colourless solid. Mp 128–130 °C; ν_{max}/cm^{-1} (neat) 3310 (OH), 3061 (CH), 1763 (CO), 1599 (C=C), 1489, 1443, 1408, 1383, 1319; δ$_H$ (500 MHz, CDCl$_3$) 7.37 (1H, dd, *J* 8.0, 7.5 Hz, ArH), 7.47–7.60 (5H, m, 5 × ArH), 8.03 (1H, dd, *J* 8.0, 0.5 Hz, ArH), 8.28 (1H, s, ArH), 8.45 (1H, dd, *J* 7.5, 0.5 Hz, ArH); δ$_C$ (126 MHz, CDCl$_3$) 103.6 (C), 120.3 (CH), 127.1 (CH), 128.9 (2 × CH), 129.3 (C), 129.4 (CH), 129.6 (2 × CH), 130.1 (CH), 136.5 (C), 141.4 (CH), 145.3 (C), 145.8 (C), 152.9 (C), 163.7 (C); *m/z* (EI) 374.9752 (M$^+$. C$_{16}$H$_{10}$INO$_2$ requires 374.9756), 330 (83%), 282 (22), 199 (68), 176 (21), 115 (100), 105 (80), 83 (60).

8-Iodo-4-phenylquinoline-2-*N*-morpholinecarboxamide (162)
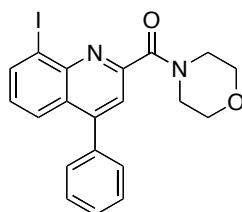
A solution of 8-iodo-4-phenylquinoline-2-carboxylic acid (**166**) (0.039 g, 0.10 mmol) in dichloromethane (3 mL) was cooled to 0 °C, and to this was added a few drops of *N,N'*-dimethylformamide followed by oxalyl chloride (13.2 μL, 0.156 mmol). The resultant solution was allowed to warm to ambient temperature and then stirred under reflux for 18 h. After cooling to ambient temperature, the reaction mixture was concentrated *in vacuo* and excess oxalyl chloride removed by azeotroping with toluene (3 × 5 mL). The crude residue was then reconstituted in dichloromethane (3 mL) and cooled to 0 °C. Morpholine (45.5 μL, 0.520 mmol) was added to the solution dropwise and the reaction mixture stirred under reflux for a further 5 h. On cooling to ambient temperature, the mixture was diluted with water (5 mL) and the aqueous layer extracted using dichloromethane (3 × 5 mL). The organic layer was dried (MgSO$_4$), filtered and concentrated *in vacuo*. Purification using flash column chromatography (methanol/dichloromethane, 1:99) gave 8-iodo-4-phenylquinoline-2-*N*-morpholinecarboxamide (**162**) (0.026 g, 57%) as a colourless solid. Mp 119–120 °C; ν_{max}/cm^{-1} (neat) 2855 (CH), 1626 (CO), 1460, 1437, 1267, 1246, 1109, 1026; δ_H (400 MHz, CDCl$_3$) 3.88–3.93 (4H, m, 2 × NCH$_2$), 3.96 (2H, t, *J* 4.6 Hz, OCH$_2$), 4.20 (2H, t, *J* 4.6 Hz, OCH$_2$), 7.27 (1H, m, ArH), 7.47–7.56 (5H, m, 5 × ArH), 7.91 (1H, s, ArH), 7.93 (1H, dd, *J* 8.4, 1.2 Hz, ArH), 8.37 (1H, dd, *J* 7.3, 1.2 Hz, ArH); δ_C (101 MHz, CDCl$_3$) 43.5 (CH$_2$), 48.4 (CH$_2$), 67.1 (CH$_2$), 67.9 (CH$_2$), 104.5 (C), 123.0 (CH), 126.8 (CH), 127.6 (C), 128.7 (2 × CH), 128.9 (2 × CH), 129.6 (2 × CH), 137.1 (C), 140.6 (CH), 145.5 (C), 150.7 (C), 153.0 (C), 166.1 (C); *m/z* (EI) 444.0334 (M$^+$. C$_{20}$H$_{17}$IN$_2$O$_2$ requires 444.0335), 358 (25%), 331 (100), 203 (91), 176 (30), 86 (31), 83 (42).

Ethyl 2-(chloromethyl)-4-phenylquinoline-3-carboxylate (177)[140]
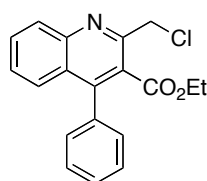
Ethyl 4-chloroacetoacetate (**179**) (1.04 mL, 7.61 mmol) was added to a solution of 2-aminobenzophenone (**178**) (1.50 g, 7.61 mmol) in *N,N'*-dimethylformamide (10 mL) in a Schlenk tube. Chlorotrimethylsilane (3.86 mL, 30.4 mmol) was then added dropwise and the tube was sealed. The resultant reaction mixture was stirred at 100 °C for 24 h. After

cooling to ambient temperature the solution was diluted with dichloromethane (50 mL) and washed with water (3 × 50 mL). The organic layer was dried (MgSO$_4$), filtered and concentrated *in vacuo*. Purification using flash column chromatography (ethyl acetate/petroleum ether, 1:4) gave ethyl 2-(chloromethyl)-4-phenylquinoline-3-carboxylate (**177**) (2.43 g, 98%) as a yellow solid. Mp 108–109 °C (lit.,[140] mp 111–112 °C); ν_{max}/cm^{-1} (neat) 2982 (CH), 2959 (CH), 1709 (CO), 1562 (C=C), 1404, 1300, 1234, 1065, 883; δ_H (500 MHz, CDCl$_3$) 0.95 (3H, t, *J* 7.5 Hz, OCH$_2$C*H*$_3$), 4.06 (2H, q, *J* 7.5 Hz, OC*H*$_2$CH$_3$), 5.03 (2H, s, CH$_2$Cl), 7.35–7.39 (2H, m, 2 × ArH), 7.46–7.52 (4H, m, 4 × ArH), 7.62 (1H, dd, *J* 8.5, 0.5 Hz, ArH), 7.77 (1H, ddd, *J* 8.5, 7.0, 1.5 Hz, ArH), 8.16 (1H, d, *J* 8.5 Hz, ArH); δ_C (126 MHz, CDCl$_3$) 13.4 (CH$_3$), 45.9 (CH$_2$), 61.5 (CH$_2$), 126.3 (C), 126.3 (C), 126.6 (CH), 127.7 (CH), 128.2 (2 × CH), 128.5 (CH), 129.3 (2 × CH), 129.7 (CH), 130.6 (CH), 135.8 (C), 147.5 (C), 148.1 (C), 153.1 (C), 167.5 (C); *m/z* (EI) 325.0876 (M^{+}. C$_{19}$H$_{16}$^{35}ClNO$_2$ requires 325.0870), 280 (52%), 262 (53), 232 (18), 217 (49), 204 (24), 176 (25).

9-Phenylfuro[3,4-*b*]quinolin-1(3*H*)-one (176)[145]
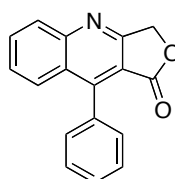
Method A: A solution of ethyl 2-(chloromethyl)-4-phenylquinoline-3-carboxylate (**177**) (0.100 g, 0.307 mmol) in a 1:1 mixture of ethanol and 6 M hydrochloric acid solution (20 mL total) was stirred under reflux for 4 days. On cooling to ambient temperature, the ethanol was removed *in vacuo* and the aqueous layer made alkaline (pH ~10) by the slow addition of solid sodium carbonate. The crude product was extracted using chloroform (3 × 20 mL), and the organic layer dried (MgSO$_4$), filtered and concentrated *in vacuo*. Purificaiton by flash column chromatography (ethyl acetate/petroleum ether, 2:3) gave 9-phenylfuro[3,4-*b*]quinolin-1(3*H*)-one (**176**) (0.058 g, 73%) as a yellow solid. Mp 201–203 °C (lit.,[145] mp 203–204 °C); ν_{max}/cm^{-1} (neat) 2957 (CH), 2843, 1771 (CO), 1603 (C=C), 1449, 1219, 1119, 1049, 1028, 889; δ_H (500 MHz, CDCl$_3$) 5.45 (2H, s, OCH$_2$), 7.43–7.49 (2H, m, 2 × ArH), 7.57–7.61 (4H, m, 4 × ArH), 7.89–7.93 (2H, m, 2 × ArH), 8.19–8.22 (1H, m, ArH); δ_C (126 MHz, CDCl$_3$) 69.6 (CH$_2$), 113.5 (C), 127.1 (C), 127.4 (CH), 128.1 (CH), 128.3 (2 × CH), 129.4 (CH), 129.5 (CH), 129.8 (2 × CH), 131.7 (C),

132.6 (CH), 151.3 (C), 151.5 (C), 163.6 (C), 167.9 (C); *m/z* (EI) 261.0794 (M$^+$. C$_{17}$H$_{11}$NO$_2$ requires 261.0790), 232 (56%), 204 (42), 203 (32), 176 (21), 151 (9), 131 (8), 91 (10).

Method B: A solution of ethyl 2-(chloromethyl)-4-phenylquinoline-3-carboxylate (**177**) (0.200 g, 0.614 mmol) in dimethylsulfoxide (3 mL) was stirred at 120 °C for 18 h and then cooled to ambient temperature. Water (10 mL) was added to the mixture and the resultant precipitate collected by filtration. The crude product was then reconstituted in ethyl acetate (20 mL) and washed with water (3 × 20 mL), dried (MgSO$_4$), filtered and concentrated *in vacuo*. Purification using flash column chromatography (ethyl acetate/petroleum ether, 2:3) afforded 9-phenylfuro[3,4-*b*]quinolin-1(3*H*)-one (**176**) (0.101 g, 63%) as a yellow solid. Spectroscopic data as reported above.

Method C: A solution of silver nitrate (1.06 g, 6.22 mmol) in a 2:1 aqueous dioxane mixture (30 mL) was heated to 90 °C. To this was added a solution of ethyl 2-(chloromethyl)-4-phenylquinoline-3-carboxylate (**177**) (0.810 g, 2.49 mmol) in 1,4-dioxane (10 mL) dropwise, and the resultant mixture stirred at 90 °C for 48 h. On cooling to ambient temperature, an additional aliquot of silver nitrate (1.06 g, 6.22 mmol) in a 50% aqueous 1,4-dioxane mixture (20 mL) was added to the reaction mixture, which was heated to and stirred at 90 °C for a further 24 h. The mixture was then cooled to ambient temperature and the 1,4-dioxane removed *in vacuo*. The remaining aqueous layer was extracted using ethyl acetate (2 × 50 mL), and the organic layer dried (MgSO$_4$), filtered and concentrated *in vacuo*. Purification using flash column chromatography (ethyl acetate/petroleum ether, 2:3) afforded 9-phenylfuro[3,4-*b*]quinolin-1(3*H*)-one (**176**) (0.377 g, 58%) as a pale yellow solid. Spectroscopic data as reported above.

Method D: To a solution of 9-phenyl-1*H*,3*H*-furo[3,4-*b*]quinolin-1-ol (**182**) (3.29 g, 12.5 mmol) in chloroform (150 mL) was added activated manganese(IV) oxide (32.6 g, 374 mmol) in one portion. The resultant suspension was stirred vigorously at ambient temperature for 4 h and then filtered through Celite®. After washing with chloroform (200 mL), the solvent was removed *in vacuo* to afford 9-phenylfuro[3,4-*b*]quinolin-1(3*H*)-one (**176**) (2.72 g, 83%) as a white solid, which was used without further purification. Spectroscopic data as reported above.

Ethyl 4-phenylquinoline-2,3-dicarboxylate (181)[144]
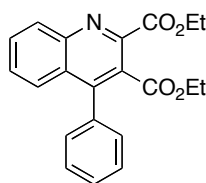
Indium(III) chloride (0.679 g, 3.07 mmol) was added to 2-aminobenzophenone (**178**) (5.00 g, 15.3 mmol) and diethyl acetylenedicarboxylate (**180**) (2.95 mL, 18.4 mmol), and the neat mixture stirred at 80 °C for 3 h. On cooling to ambient temperature, water (50 mL) was added and the mixture extracted using ethyl acetate (150 mL). The organic layer was then washed with water (100 mL) and brine (100 mL), dried (MgSO$_4$), filtered and concentrated *in vacuo*. Purification using flash column chromatography (ethyl acetate/hexane, 15:85) afforded ethyl 4-phenylquinoline-2,3-dicarboxylate (**181**) (5.36 g, 100%) as a yellow solid. Spectroscopic data in accordance with the literature.[144] Mp 89–91 °C (lit.,[144] mp 95–96 °C); ν_{max}/cm^{-1} (neat) 2984 (CH), 1741 (CO), 1722 (CO), 1560 (C=C), 1441, 1376, 1247, 1202, 1048, 768; δ_H (400 MHz, CDCl$_3$) 0.99 (3H, t, *J* 7.2 Hz, OCH$_2$C*H*$_3$), 1.46 (3H, t, *J* 7.2 Hz, OCH$_2$C*H*$_3$), 4.09 (2H, q, *J* 7.2 Hz, OC*H*$_2$CH$_3$), 4.54 (2H, q, *J* 7.2 Hz, OC*H*$_2$CH$_3$), 7.34–7.40 (2H, m, 2 × ArH), 7.47–7.53 (3H, m, 3 × ArH), 7.57 (1H, ddd, *J* 8.4, 6.4, 1.6 Hz, ArH), 7.63 (1H, d, *J* 8.4, 1.6, 0.6 Hz, ArH), 7.81 (1H, ddd, *J* 8.4, 6.4, 1.6 Hz, ArH), 8.38 (1H, ddd, *J* 8.4, 1.6, 0.6 Hz, ArH); δ_C (101 MHz, CDCl$_3$) 13.6 (CH$_3$), 14.2 (CH$_3$), 61.6 (CH$_2$), 62.6 (CH$_2$), 126.6 (CH), 127.1 (C), 127.5 (C), 128.2 (2 × CH), 128.7 (CH), 129.0 (CH), 129.4 (2 × CH), 130.7 (CH), 130.9 (CH), 134.8 (C), 145.9 (C), 147.1 (C), 148.0 (C), 165.3 (C), 167.2 (C); *m/z* (EI) 349.1311 (M$^+$. C$_{21}$H$_{19}$NO$_4$ requires 349.1314), 305 (20%), 276 (55), 205 (100), 204 (82), 165 (12), 84 (5).

9-Phenyl-1*H*,3*H*-furo[3,4-*b*]quinolin-1-ol (182)
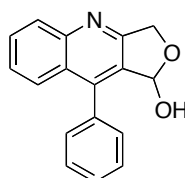
A solution of ethyl 4-phenylquinoline-2,3-dicarboxylate (**181**) (4.72 g, 13.5 mmol) in tetrahydrofuran (50 mL) was heated under reflux with vigorous stirring. To this was added dropwise, a solution of sodium borohydride (5.11 g, 135 mmol) in methanol (50 mL), and

the resultant reaction mixture stirred under reflux for 15 h. After cooling to ambient temperature, excess sodium borohydride was quenched by the dropwise addition of a saturated solution of ammonium chloride (~50 mL). The crude reaction mixture was extracted using dichloromethane (3 × 50 mL) and washed with water (2 × 50 mL), dried (MgSO$_4$), filtered and concentrated *in vacuo*. Trituration with diethyl ether afforded 9-phenyl-1*H*,3*H*-furo[3,4-*b*]quinolin-1-ol (**182**) (3.29 g, 93%) as a pale yellow solid. Mp 208–210 °C; ν_{max}/cm^{-1} (neat) 3327 (OH), 2927 (CH), 1727, 1538, 1486, 1443, 1213, 1026, 749; δ_H (400 MHz, DMSO-d_6) 4.87 (1H, dd, *J* 15.7, 0.8 Hz, CH*H*O), 4.98 (1H, d, *J* 15.7 Hz, C*H*HO), 5.02 (1H, br s, C*H*OH), 6.87–6.94 (2H, m, 2 × ArH), 7.04 (1H, d, *J* 6.8 Hz, ArH), 7.10–7.17 (2H, m, 2 × ArH), 7.18–7.28 (4H, m, 4 × ArH), 10.0 (1H, br s, CHO*H*); δ_C (101 MHz, DMSO-d_6) 65.0 (CH$_2$), 95.2 (C), 116.2 (CH), 123.1 (CH), 124.3 (C), 126.2 (CH), 127.5 (CH), 127.6 (2 × CH), 128.3 (2 × CH), 130.8 (CH), 136.1 (C), 146.8 (C), 158.5 (C), 172.0 (C); *m/z* (ESI) 286.0830 (MNa$^+$. C$_{17}$H$_{13}$NNaO$_2$ requires 286.0838).

2,3-Bis(hydroxymethyl)-4-phenylquinoline (175)[145]
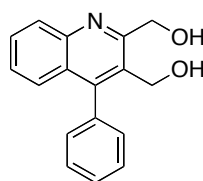
A suspension of lithium aluminium hydride (0.581 g, 15.3 mmol) in tetrahydrofuran (25 mL) was cooled to 0 °C, and to this was added dropwise, a solution of 9-phenylfuro[3,4-*b*]quinolin-1(3*H*)-one (**176**) (1.00 g, 3.83 mmol) in tetrahydrofuran (25 mL). The temperature of the reaction mixture was maintained at 0 °C and stirred vigorously for 3 h. After gradually warming to ambient temperature, the mixture was quenched by the dropwise addition of a 1 M hydrochloric acid solution, and then extracted using ethyl acetate (3 × 25 mL). The organic layer was dried (MgSO$_4$), filtered and concentrated *in vacuo* to afford a colourless residue which was dissolved in methanol (50 mL). 10% Palladium on carbon (1.00 g) was added to the reaction flask and the resultant suspension stirred at ambient temperature for 15 h. The suspension was then filtered through a pad of Celite®, washed with methanol and concentrated *in vacuo*. Trituration with diethyl ether afforded 2,3-bis(hydroxymethyl)-4-phenylquinoline (**175**) (0.777 g, 77%) as a white solid. Mp 171–173 °C (lit.,[145] mp 175–177 °C); ν_{max}/cm^{-1} (neat) 3422 (OH), 3074, 2991 (CH), 1571 (C=C), 1490, 1442, 1231, 1022, 1006; δ_H (400 MHz, CD$_3$OD) 4.59 (2H, s, C*H$_2$*OH),

5.11 (2H, s, CH_2OH), 7.34–7.38 (2H, m, 2 × ArH), 7.41 (1H, dd, J 8.4, 1.2 Hz, ArH)), 7.44–7.50 (1H, m, ArH), 7.51–7.60 (3H, m, 3 × ArH), 7.73 (1H, ddd, J 8.4, 6.4, 1.2 Hz, ArH), 8.11 (1H, d, J, 8.4 Hz, ArH); δ_C (101 MHz, CD$_3$OD) 59.1 (CH$_2$), 64.7 (CH$_2$), 127.8 (CH), 127.9 (CH), 128.6 (C), 129.4 (CH), 129.5 (CH), 129.5 (2 × CH), 130.0 (C), 130.8 (CH), 130.8 (2 × CH), 137.3 (C), 147.4 (C), 150.4 (C), 160.9 (C); m/z (CI) 266.1186 (MH$^+$. C$_{17}$H$_{16}$NO$_2$ requires 266.1181), 264 (50%), 248 (42), 218 (21), 206 (4), 151 (3).

9-Phenylfuro[3,4-*b*]quinolin-3(1*H*)-one (174)[145]
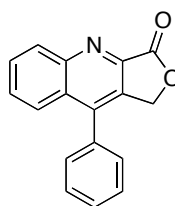
To a solution of 2,3-bis(hydroxymethyl)-4-phenylquinoline (**175**) (0.777 g, 2.93 mmol) in chloroform (50 mL) was added activated manganese(IV) oxide (7.64 g, 87.9 mmol) in one portion. The resultant suspension stirred vigorously at ambient temperature for 4 h and then filtered through Celite®. After washing with chloroform (100 mL), the solvent was removed *in vacuo* to afford 9-phenylfuro[3,4-*b*]quinolin-3(1*H*)-one (**174**) (0.700 g, 92%) as a white solid, which was used without further purification. Spectroscopic data in accordance with the literature.[145] Mp 188–190 °C (lit.,[145] mp 190–192 °C); ν_{max}/cm^{-1} (neat) 3005 (CH), 1775 (CO), 1582 (C=C), 1414, 1371, 1152, 1121, 1055, 1007; δ_H (400 MHz, CDCl$_3$) 5.41 (2H, s, OCH$_2$), 7.45 (2H, dd, J 8.0, 2.0 Hz, 2 × ArH), 7.57–7.70 (4H, m, 4 × ArH), 7.84–7.90 (1H, m, ArH), 7.92 (1H, d, J 8.4 Hz, ArH), 8.46 (1H, d, J 8.4 Hz, ArH); δ_C (101 MHz, CDCl$_3$) 67.8 (CH$_2$), 125.7 (CH), 127.9 (C), 128.9 (2 × CH), 129.3 (2 × CH), 129.4 (CH), 129.6 (CH), 130.7 (CH), 131.5 (CH), 132.3 (C), 133.6 (C), 143.9 (C), 144.4 (C), 150.7 (C), 168.7 (C); m/z (ESI) 284.0677 (MNa$^+$. C$_{17}$H$_{11}$NNaO$_2$ requires 284.0682).

3-(Hydroxymethyl)-4-phenylquinoline-2-*N*-diethylcarboxamide (172)[138]
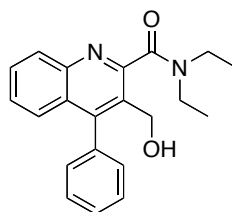
To a solution of diethylamine (0.238 mL, 2.30 mmol) in dichloromethane (20 mL) was added trimethylaluminium solution (2.0 M in toluene) (1.15 mL, 2.30 mmol) dropwise, and the mixture stirred at ambient temperature for 0.3 h. A solution of 9-phenylfuro[3,4-*b*]quinolin-3(1*H*)-one (**174**) (0.300 g, 1.15 mmol) in dichloromethane (20 mL) was then added dropwise and the resultant reaction mixture stirred under reflux for 15 h. On cooling to ambient temperature, the reaction was quenched by the careful addition of a 1 M hydrochloric acid solution (25 mL), and the crude mixture extracted using dichloromethane (2 × 20 mL). The organic layer was dried (MgSO$_4$), filtered and concentrated *in vacuo*. Purification using flash column chromatography (ethyl acetate/petroleum ether, 1:3) gave 3-(hydroxymethyl)-4-phenylquinoline-2-*N*-diethylcarboxamide (**172**) (0.235 g, 61%) as a pale yellow solid. Spectroscopic data in accordance with the literature.[138] Mp 117–119 °C; v_{max}/cm^{-1} (neat) 3408 (OH), 2972, 2932 (CH), 1613 (CO), 1483, 1443, 1267, 1216, 1069; δ_H (400 MHz, CDCl$_3$) 1.27 (3H, t, *J* 7.2 Hz, NCH$_2$C*H*$_3$), 1.36 (3H, t, *J* 7.2 Hz, NCH$_2$C*H*$_3$), 3.42 (2H, q, *J* 7.2 Hz, NC*H*$_2$CH$_3$), 3.68 (2H, q, *J* 7.2 Hz, NC*H*$_2$CH$_3$), 4.12 (1H, t, *J* 6.4 Hz, CH$_2$O*H*), 4.39 (2H, d, *J* 6.4 Hz, C*H*$_2$OH), 7.41–7.58 (7H, m, 7 × ArH), 7.72 (1H, ddd, *J* 8.4, 6.8, 1.6 Hz, ArH), 8.12 (1H, ddd, *J* 8.4, 1.2, 0.8 Hz, ArH); δ_C (101 MHz, CDCl$_3$) 12.9 (CH$_3$), 14.2 (CH$_3$), 40.3 (CH$_2$), 43.7 (CH$_2$), 59.7 (CH$_2$), 127.0 (CH), 127.4 (CH), 127.6 (C), 128.4 (3 × CH), 129.4 (C), 129.6 (CH), 129.8 (CH), 129.9 (2 × CH), 135.2 (C), 146.1 (C), 149.3 (C), 155.1 (C), 169.8 (C); *m/z* (ESI) 357.1576 (MNa$^+$. C$_{21}$H$_{22}$N$_2$NaO$_2$ requires 357.1573); Anal. Calcd for C$_{21}$H$_{22}$N$_2$O$_2$: C, 75.42; H, 6.63; N, 8.38. Found: C, 75.03; H, 6.57; N, 8.23.

3-(Hydroxymethyl)-4-phenylquinoline-2-*N*-methyl-*N*-benzylcarboxamide (173)[44]
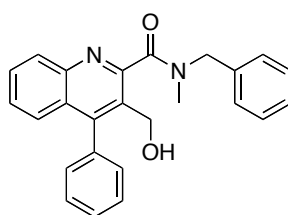
3-(Hydroxymethyl)-4-phenylquinoline-2-*N*-methyl-*N*-benzylcarboxamide (**173**) was synthesised as describe above for 3-(hydroxymethyl)-4-phenylquinoline-2-*N*-diethylcarboxamide (**172**) using *N*-benzylmethylamine (0.295 mL, 2.30 mmol), trimethylaluminium solution (2.0 M in toluene) (1.15 mL, 2.30 mmol) and 9-phenylfuro[3,4-*b*]quinolin-3(1*H*)-one (**174**) (0.300 g, 1.15 mmol) in dichloromethane (40 mL). Purification using flash column chromatography (ethyl acetate/petroleum ether, 1:4)

followed by trituration with diethyl ether afforded 3-(hydroxymethyl)-4-phenylquinoline-2-*N*-methyl-*N*-benzylcarboxamide (**173**) (0.245 g, 56%) as a white solid. Spectroscopic data in accordance with literature.[44] NMR spectra showed a 1:1 mixture of rotamers, of which only the signals for one rotamer are recorded. Mp 143–145 °C; ν_{max}/cm^{-1} (neat) 3428 (OH), 2960 (CH), 1623 (CO), 1486, 1395, 1263, 1062, 980, 703; δ_H (500 MHz, CDCl$_3$) 3.19 (3H, s, NCH$_3$), 4.08 (1H, t, *J* 7.0 Hz, CH$_2$O*H*), 4.45 (2H, d, *J* 7.0 Hz, C*H*$_2$OH), 4.72 (2H, s, C*H*$_2$Ph), 7.27–7.35 (3H, m, 3 × ArH), 7.37–7.57 (9H, m, 9 × ArH), 7.69–7.76 (1H, m, ArH), 8.10 (1H, d, *J* 8.5 Hz, ArH); δ_C (126 MHz, CDCl$_3$) 33.5 (CH$_3$), 55.1 (CH$_2$), 59.7 (CH$_2$), 126.9 (CH), 127.6 (CH), 127.6 (C), 127.8 (CH), 127.8 (CH), 127.9 (CH), 128.3 (CH), 128.4 (2 × CH), 128.6 (CH), 128.9 (CH), 129.5 (CH), 129.8 (CH), 129.8 (2 × CH), 135.2 (2 × C), 136.4 (C), 146.1 (C), 149.5 (C), 154.4 (C), 170.5 (C); *m/z* (ESI) 405.1559 (MNa$^+$. C$_{25}$H$_{22}$N$_2$NaO$_2$ requires 405.1573).

3-(Chloromethyl)-4-phenylquinoline-2-*N*-diethylcarboxamide (185)[138]

To a solution of 3-(hydroxymethyl)-4-phenylquinoline-2-*N*-diethylcarboxamide (**172**) (0.100 g, 0.299 mmol) in dichloromethane (10 mL) was added thionyl chloride (0.654 mL, 8.97 mmol) and the reaction mixture stirred under reflux for 24 h. On cooling to ambient temperature, the mixture was concentrated *in vacuo* and azeotroped with toluene (3 × 10 mL) to remove excess thionyl chloride. Purification using flash column chromatography (diethyl ether/petroleum ether, 1:1) gave 3-(chloromethyl)-4-phenylquinoline-2-*N*-diethylcarboxamide (**185**) (0.105 g, 100%) as a colourless oil. ν_{max}/cm^{-1} (neat) 2981 (CH), 2936, 1630 (CO), 1560 (C=C), 1482, 1443, 1270, 1218, 1127, 1067, 728; δ_H (500 MHz, CDCl$_3$) 1.30 (3H, t, *J* 7.0 Hz, NCH$_2$C*H*$_3$), 1.35 (3H, t, *J* 7.5 Hz, NCH$_2$C*H*$_3$), 3.28 (2H, q, *J* 7.0 Hz, NC*H*$_2$CH$_3$), 3.68 (2H, q, *J* 7.5 Hz, NC*H*$_2$CH$_3$), 4.70 (2H, s, CH$_2$Cl), 7.36–7.40 (2H, m, 2 × ArH), 7.41–7.49 (2H, m, 2 × ArH), 7.51–7.59 (3H, m, 3 × ArH), 7.73 (1H, ddd, *J* 8.5, 6.5, 1.5 Hz, ArH), 8.13 (1H, d, *J* 8.5 Hz, ArH); δ_C (126 MHz, CDCl$_3$) 12.3 (CH$_3$), 13.5 (CH$_3$), 39.2 (CH$_2$), 40.3 (CH$_2$), 43.6 (CH$_2$), 125.9 (C), 126.9 (CH), 127.3 (C), 127.4 (CH), 128.6 (2 × CH), 128.7 (CH), 129.4 (2 × CH), 129.6 (CH), 130.2 (CH), 134.9 (C), 146.4

(C), 149.4 (C), 155.6 (C), 168.1 (C); *m/z* (ESI) 375.1218 (MNa$^+$. C$_{21}$H$_{21}$^{35}ClN$_2$NaO requires 375.1235).
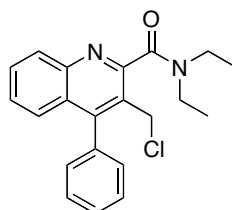
3-(Chloromethyl)-4-phenylquinoline-2-*N*-methyl-*N*-benzylcarboxamide (186)[44]
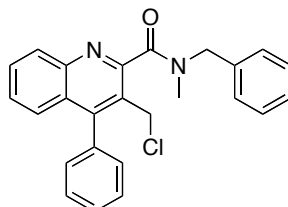
3-(Chloromethyl)-4-phenylquinoline-2-*N*-methyl-*N*-benzylcarboxamide **(186)** was synthesised as described above for 3-(chloromethyl)-4-phenylquinoline-2-*N*-diethylcarboxamide **(185)** using 3-(hydroxymethyl)-4-phenylquinoline-2-*N*-methyl-*N*-benzylcarboxamide **(173)** (0.031 g, 0.081 mmol) and thionyl chloride (0.177 mL, 2.43 mmol) in dichloromethane (5 mL). Purification using flash column chromatography (diethyl ether/hexane, 1:1) afforded 3-(chloromethyl)-4-phenylquinoline-2-*N*-methyl-*N*-benzylcarboxamide **(186)** (0.032 g, 100%) as a pale yellow solid. Spectroscopic data in accordance with the literature.[44] NMR spectra showed a 1.5:1 mixture of rotamers, of which only the signals for the major rotamer are recorded. Mp 124–125 °C (lit.,[44] mp 130–132 °C); ν_{max}/cm^{-1} (neat) 3064 (CH), 1637 (CO), 1485, 1443, 1396, 1262, 1115, 1055; δ_H (500 MHz, CDCl$_3$) 2.94 (3H, s, NCH$_3$), 4.75 (2H, s, CH$_2$Cl), 4.91 (2H, s, C*H*$_2$Ph), 7.29–7.35 (1H, m, ArH), 7.36–7.63 (11H, m, ArH), 7.68–7.78 (1H, m, ArH), 8.14 (1H, d, *J* 8.4 Hz, ArH) ; δ_C (126 MHz, CDCl$_3$) 36.3 (CH$_3$), 40.2 (CH$_2$), 50.6 (CH$_2$), 126.2 (C), 126.9 (CH), 127.3 (C), 127.5 (CH), 127.6 (CH), 127.8 (CH), 128.4 (CH), 128.5 (CH), 128.6 (2 × CH), 128.7 (CH), 129.3 (2 × CH), 129.5 (CH), 129.6 (CH), 130.3 (CH), 134.8 (C), 136.4 (C), 146.5 (C), 149.6 (C), 155.2 (C), 168.9 (C); *m/z* (ESI) 423.1219 (MNa$^+$. C$_{25}$H$_{21}$^{35}ClN$_2$NaO requires 423.1235).

3-(Fluoromethyl)-4-phenylquinoline-2-*N*-diethylcarboxamide (170)
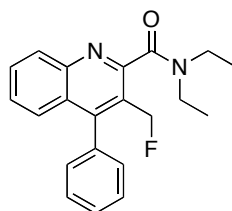
To a solution of 18-crown-6 (0.038 g, 0.14 mmol) in acetonitrile (2.5 mL) was added potassium fluoride (0.041 g, 0.71 mmol) and the resultant suspension stirred at ambient temperature for 0.5 h. A solution of 3-(chloromethyl)-4-phenylquinoline-2-*N*-diethylcarboxamide (**185**) (0.050 g, 0.14 mmol) in acetonitrile (2.5 mL) was then added dropwise to the reaction mixture and stirred under reflux for 24 h. On cooling to ambient temperature, water (10 mL) was added to the mixture and then extracted using dichloromethane (3 × 15 mL). The organic layer was dried (MgSO$_4$), filtered and concentrated *in vacuo*. Purification using flash column chromatography (diethyl ether/petroleum ether, 1:1), followed by washing with acetonitrile gave 3-(fluoromethyl)-4-phenylquinoline-2-*N*-diethylcarboxamide (**170**) (0.028 g, 60%) as a white solid. ν_{max}/cm^{-1} (neat) 2976, 2936 (CH), 1634 (CO), 1560 (C=C), 1481, 1269, 1213, 1069, 970; δ_H (400 MHz, CDCl$_3$) 1.22 (3H, t, *J* 7.2 Hz, NCH$_2$C*H*$_3$), 1.34 (3H, t, *J* 7.2 Hz, NCH$_2$C*H*$_3$), 3.28 (2H, q, *J* 7.2 Hz, NC*H*$_2$CH$_3$), 3.67 (2H, q, *J* 7.2 Hz, NC*H*$_2$CH$_3$), 5.38 (2H, d, *J* 47.8 Hz, C*H*$_2$F), 7.32–7.38 (2H, m, 2 × ArH), 7.46–7.57 (5H, m, 5 × ArH), 7.73–7.78 (1H, m, ArH), 8.16 (1H, d, *J* 8.4 Hz, ArH); δ_C (101 MHz, CDCl$_3$) 12.6 (CH$_3$), 13.7 (CH$_3$), 39.4 (CH$_2$), 43.2 (CH$_2$), 79.2 (CH$_2$F, d, *J*$_{C-F}$ 162.2), 123.4 (C, d, *J*$_{C-C-F}$ 15.1 Hz), 127.0 (CH), 127.1 (C, d, *J*$_{C-C-C-C-F}$ 1.8 Hz), 127.4 (CH), 128.5 (2 × CH), 128.7 (CH), 129.6 (CH), 129.7 (2 × CH), 130.5 (CH, d, *J*$_{C-C-C-C-F}$ 1.5 Hz), 134.8 (C), 147.1 (C, d, *J*$_{C-C-C-F}$ 2.9 Hz), 150.7 (C, d, *J*$_{C-C-C-F}$ 4.9 Hz), 155.9 (C, d, *J*$_{C-C-C-F}$ 1.7 Hz), 168.2 (C); *m/z* (ESI) 359.1520 (MNa$^+$. C$_{21}$H$_{21}$FN$_2$NaO requires 359.1530).

3-(Fluoromethyl)-4-phenylquinoline-2-*N*-methyl-*N*-benzylcarboxamide (171)[148]
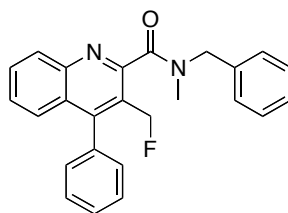
3-(Fluoromethyl)-4-phenylquinoline-2-*N*-methyl-*N*-benzylcarboxamide (**171**) was synthesised as described above for 3-(fluoromethyl)-4-phenylquinoline-2-*N*-diethylcarboxamide (**170**) using 18-crown-6 (0.020 g, 0.076 mmol), potassium fluoride (0.023 g, 0.40 mmol) and 3-(chloromethyl)-4-phenylquinoline-2-*N*-methyl-*N*-benzylcarboxamide (**186**) (0.031 g, 0.077 mmol) in acetonitrile (5 mL). Purification using flash column chromatography (diethyl ether/petroleum ether, 2:3), followed by washing with acetonitrile afforded 3-(fluoromethyl)-4-phenylquinoline-2-*N*-methyl-*N*-

benzylcarboxamide (**171**) (0.023 g, 79%) as a colourless oil. NMR spectra showed a 1:1 mixture of rotamers, of which only the signals for one rotamer is recorded. ν_{max}/cm^{-1} (neat) 2926 (CH), 1636 (CO), 1560 (C=C), 1485, 1397, 1119, 1055, 968; δ_H (500 MHz, CDCl$_3$) 2.89 (3H, s, NCH_3), 4.90 (2H, s, CH_2Ph), 5.40 (2H, d, J 47.7 Hz, CH$_2$F), 7.28–7.41 (5H, m, 5 × ArH), 7.42–7.58 (7H, m, 7 × ArH), 7.72–7.80 (1H, m, ArH), 8.18 (1H, d, J 8.5 Hz, ArH); m/z (ESI) 407.1511 (MNa$^+$. C$_{25}$H$_{21}$FN$_2$NaO requires 407.1530).

5.3 HPLC Methods for Physicochemical Analysis[133]

All physicochemical analyses were performed using a Dionex Ultimate 3000 series, and data acquisition and processing performed using Chromeleon 6.8 Chromatography software. Standard and test compounds were dissolved in 1:1 organic/aqueous phases, and prepared to a concentration of 0.5 mg/mL. The HPLC system was set to 25 °C, and UV detection achieved using a diode array detector (190 – 800 nm). Analysis was performed using 5 µL sample injections.

C$_{18}$ chromatography for determination of lipophilicity (Log$P$)

Log$P$ values were determined using a Phenomenex Luna 5 micron C$_{18}$ 100 A (50 × 3 mm) column. The retention time for each compound of interest was measured using filtered acetonitrile and 0.01 mM phosphate buffered saline as the mobile phase at pH 7.4, pH 2.5 and pH 10.0, and pH was adjusted by the addition of concentrated hydrochloric acid and 0.05 M sodium hydroxide solution respectively. The mobile phase flow rate was set at 1.0 mL/min. The CHI value for all compounds of interest was determined by measuring the retention time of each compound under the following mobile phase conditions: 0–10.5 min, 0–100% acetonitrile; 10.5–11.5 min, 100% acetonitrile; 11.5–12.0 min, 100–0% acetonitrile; 12.0–15.0 min, 0% acetonitrile. System calibration was achieved using the following compounds and plotting their mean CHI values against the measured retention time under all three pH conditions: theophylline (CHI = 15.76), phenyltetrazole (CHI = 20.18), benzimidazole (CHI = 30.71), colchicine (CHI = 41.37), acetophenone (CHI = 64.90), indole (CHI = 69.15), propiophenone (CHI = 78.41), butyrophenone (CHI = 88.49) and valerophenone (CHI = 97.67). Using the calibration curves obtained and the following equations from a validated study, the Log$P$ of the compounds were calculated using Excel 2008 Software.

CHI Log D = 0.054 CHI − 1.467

where CHI Log D is the CHI value projected to the logarithmic scale

Log P = 0.054 CHIN + 1.32 A − 1.88

where CHIN = CHI values the compound in a neutral form, and A = Abraham H-bond acidity parameter, which was determined using ADME Suite 5.0 software.

Immobilised Artificial Membrane (IAM) chromatography for determination of membrane permeability (P_m) and membrane partition coefficient (K_m)

P_m and K_m values were determined using previously developed methodology on a Registech IAM.PC.DD2 (15 cm × 4.6 mm) column. Acetonitrile and 0.01 mM phosphate buffered saline at pH 7.4 was used as the mobile phase, with a flow rate of 1.0 mL/min. The retention time of each compound was measured under an isocratic mobile phase with the percentage acetonitrile ranging from 30–40%. The retention time of citric acid, as an unretained compound, under an isocratic mobile phase of 100% phosphate buffered saline was used for system corrections. The following equations were used to calculate P_m and K_m of the compounds of interest using Excel 2008 Software.

$$k_{IAM} = \frac{(t_r - t_0)}{t_0}$$

where k_{IAM} = solute capacity factor on the column, t_r = compound retention time and t_0 = unretained compound retention time

$$k_{IAM} = \left(\frac{V_s}{V_m}\right) \times K_m$$

where V_s = volume of the IAM interphase created by the immobilized phospholipids, V_m = total volume of the solvent within the IAM column and K_m = membrane partition coefficient

$$V_m = \frac{W_{PhC}}{\delta_{PhC}} + \frac{W_{C10}}{\delta_{C10}} + \frac{W_{C3}}{\delta_{C3}}$$

where the specific weight of PhC (δ_{PhC}) = 1.01779 g/mL and C_{10}/C_3 ($\delta_{C10/C3}$) = 0.86 g/mL; W_{PhC} = 133 mg, W_{C10} = 12.73 mg and W_{C3} = 2.28 mg

$$V_m = f_r \times t_0$$

where f_r = flow rate

$$P_m = \frac{K_m}{MW}$$

where P_m = permeability and MW = molecular weight

Human Serum Albumin (HSA) chromatography for determination of percentage of plasma protein binding (%PPB)

%PPB values were determined using previously developed methodology on a ChromTech HSA 5 μm (3.0 × 50 mm) column. Isopropanol and 0.01 mM phosphate buffered saline at pH 7.4 was used as the mobile phase, with a flow rate of 1.8 mL/min. The retention time of each compound was measured under the following mobile phase conditions: 0–3 min, 0–30% IPA; 3–10 min, 30% IPA; 10.5–11.0 min, 30–0% IPA; 11.0–15.0 min, 0% IPA. System calibration was achieved using the following compounds and plotting %PPB values against their mean retention times: warfarin (%PPB = 98.0), nizatidine (%PPB = 35.0), bromazepam (%PPB = 60.0), carbamazepine (%PPB = 75.0), budesonide (%PPB = 88.0), nicardipine (%PPB = 95.0), ketoprofen (%PPB = 98.7), indomethacin (%PPB = 99.0) and diclofenac (%PPB = 99.8). For each standard compound, the literature %PPB value was converted to its corresponding Log k value, which when plotted against t_r on the HSA column, afforded a line equation from which the Log k value of the unknown compounds could be extracted. The Log k values of the unknown compounds could then be converted to %PPB. Log k and subsequent %PPB calculation for the compounds of interest were performed using Excel 2008 Software.

$$Log k = Log \left[\frac{\%PPB}{(101 - \%PPB)} \right]$$

$$\%PPB = \left[\frac{(101 - 10^{\log k})}{(1 + 10^{\log k})} \right]$$

5.4 Radioligand Binding Methodology[242]

Preparation of Rat Brain Membranes

Whole brains from male Sprague-Dawley rats (200–300 g) were obtained and immediately added to 25 mL of ice-cold Tris-Base buffer (50 nM, pH 7.4) and thoroughly homogenised using a Polytron. The resultant homogenates were centrifuged at 39100 g for 10 min (4 °C) using a Beckman J2-21M/E centrifuge. After discarding the supernatant, the pellet was resuspended in 25 mL of ice-cold buffer and the centrifugation process repeated. The resultant pellet was then resuspended in 10 mL of ice-cold buffer and the homogenate stored at –50 °C until further use. Total protein content of the brain homogenate was measured using the Bicinchoninic acid (BCA) based protein assay. A Bio-Rad solution (solution A/solution B, 50:1) was prepared and 1 mL added to centrifuge tubes. To each tube was added 50 μL of pre-prepared bovine serum albumin (BSA) standards in 50 mM tris-base buffer (pH 7.4) in the following pre-defined concentrations: 2000, 1500, 1000, 750, 500, 250, 125, 25, and 0 μg/mL. 5μL of the freshly prepared brain homogenate was added to three centrifuge tubes. The tubes were thoroughly vortexed and incubated at 37 °C for 0.5 h. After incubation, the tubes were left at ambient temperature for 5 min and the absorbance measured at 562 nm using a spectrophotometer. A calibration curve was generated by plotting absorbance against protein content, which was subsequently used to determine the protein content of the rat brain homogenate.

Competition Binding Assays

Brain homogenate stock was diluted to give a final assay concentration of approximately 0.6 mg of protein. Total binding was determined using a final concentration of 1 nM [³H]PK11195, and non-specific binding was measured using a final concentration of 8 μM unlabelled PK11195 in the presence of [³H]PK11195. The K_i value of the compound was determined using a range of competitor concentrations (3 pM–300 μM). Assays were carried out in triplicate, and a typical assay consisted of 100 μL labelled competitor, 100 μL test compound and 200 μL of brain homogenate to give a final assay volume of 400 μL (with <1% ethanol present). The assay components were thoroughly mixed and then

incubated at 5 °C for 1.5 h. The binding assay was terminated by the rapid filtration through Whatman GF/B glass fiber filters, which were pre-soaked in 0.3% w/v polyethylenimine, using a 24-well Brandel cell harvester. Filters received 3 rapid washes with ice-cold tris-base buffer and were added to prepared scintillation vials containing 10 mL of Eco-scint. After a minimum of 48 h at ambient temperature, tritium counts were measured using a liquid scintillation counter. The resultant radioactive counts were used to determine the K_i value of the compound of interest by performing non-linear regression analysis using GraphPad Prism 4.0 (GraphPad Softare Inc). Mean and standard deviation ($n = 3$) was calculated using Excel 2008 software.

5.5 Stability Testing

3-(Fluoromethyl)-4-phenylquinoline-2-*N*-diethylcarboxamide (**170**) (2 mg, 0.005 mmol) was dissolved in a 1:1 mixture of 0.01 mM phosphate buffered saline and acetonitrile (2 mL) and incubated at 37 ° C. 5 μL of the solution was injected onto the HPLC system (conditions described below in section 5.6) at various time points (0, 1, 2, 4, 6 and 24 h). The purity of the compound at these time points was detemined by measuring the area under the peaks of the resultant UV chromatograms.

5.6 Radiochemistry

Manual Synthesis of [^{18}F]AB5186

A v-vial containing 0.3 μL of non-carrier added [^{18}F]fluoride (455 MBq) was decapped; to this was added 250 μL of a solution containing 0.106 M Kryptofix® K222 and 0.0347 M potassium carbonate, and then immediately recapped. The fluoride was dried by passing a constant stream of argon over the solution at 100 °C. Additional aliquots of anhydrous acetonitrile (3 × 0.5 mL) was added to facilitate azeotropic drying (approximately 30 min). A solution of the chloride precursor **185** (2.4 mg) in acetonitrile (0.5 mL) was then added to the v-vial and the reaction allowed to proceeded for 12 mins at 100 °C. After removal from the heating block, the reaction mixture was allowed to cool for a few minutes before being diluted by the addition of 0.21 mL of distilled water.

Semi-Preparative HPLC Purification of [^{18}F]AB5186

The crude [^{18}F]AB5186 reaction mixture was loaded onto a Phenomenex Synergi 4 μm Hydro-RP 80A (150 × 10.00 mm) column. Acetonitrile and water was used as the mobile phase, with a flow rate of 3 mL/min. Purification was achieved using the following isocratic mobile phase: 0 min, 70% acetonitrile; 15 min, 70% acetonitrile; 15.1 min, 95% acetonitrile; 25 min, 95% acetonitrile. The radiolabelled product was detected using a radiodetector, and collected at approximately 8 min. The fraction containing [^{18}F]AB5186 was concentrated *in vacuo* and then reconstituted in 2 mL of a 10% ethanol/0.9% saline solution. Passing the sample through a pre-treated 13 mm 0.2 μm filter then completed formulation of the radiotracer. The identity of the radiolabelled product was confirmed by co-injection with a cold sample of AB5186. Quality control was performed by analytical HPLC, using a Phenomenex Synergi 4μm Hydro-RP 80A (150 × 4.60 mm) column and the mobile phase described above for the semi-prep HPLC purification step. Radiochemical purity was determined by measuring the area under the peaks on the chromatogram.

Measurement of Specific Activity of [^{18}F]AB5186

A concentration response curve was generated on the semi-preparative HPLC system used for purification of [^{18}F]AB5186, by injection of 10 μL samples of unlabelled AB5186 in the following concentrations: 1 mg/mL, 0.5 mg/mL, 0.1 mg/mL, 0.05 mg/mL, 0.01 mg/mL and 0.005 mg/mL in a 7:3 acetonitrile/water mixture. The UV response (mV/min) of each concentration was then plotted against the corresponding moles of unlabelled AB5186. For calculation of the specific activity, the entire crude radiolabelling reaction mixture was injected onto the semi-preparative HPLC system, and the resulting UV response (mV/min) of the relevant peak measured. The UV response was then used to calculate the number of moles of [^{18}F]AB5186 present. Recording the amount of radioactivity present immediately before injection onto the column, in conjunction with integration of the relevant peak of the radiotrace, enabled calculation of specific activity after decay correction.

5.7 Autoradiography[243]

***In vitro* Autoradiography with [³H]PK11195 and [¹⁸F]AB5186**

The brain from an orthotopic mouse model of human glioblastoma generated by injecting 10^5 cultured G7 glioblastoma cells into the caudate nucleus of a CD1 nude mouse was used. Coronal sections (20 μm thick) were cut in a cryostat at –20 °C from the frozen brain, mounted onto poly-L-lysine coated slides and stored at –50 °C until further use. All incubations and washing steps of the autoradiographic protocol were performed in a freshly prepared 50 mM Tris-base buffer (pH 7.4). Slide mounted brain sections were thawed and pre-washed three times in buffer for 5 min. The slides were then incubated with either 1 nM [³H]PK11195 (85.7 Ci/mmol, Perkin-Elmer) or 3 nM [¹⁸F]AB5186 **170** (7.67 MBq/nmol) for 1 h at ambient temperature. Non-specific binding was determined in adjacent sections by incubating then with either 1 nM [³H]PK11195 or [¹⁸F]AB5186 **170** in the presence of 10 μM PK11195 (Tocris, UK). At the end of the incubation, sections were washed twice in ice-cold buffer for 5 min, and then dipped into ice-cold distilled water for 10 sec. The slides were subsequently dried at ambient temperature either overnight ([³H]PK11195) or for approximately 10 min ([¹⁸F]AB5186) by passing a gentle stream of cool air over them. Slides were exposed to [³H]-hyperfilm (Amersham, UK) for 21 days ([³H]PK11195) or 1 h ([¹⁸F]AB5186) and then developed. Optical density measurements were made from the resulting autoradiograms using MCID basic 7.0 software (MCID, UK).

5.8 PARP Experimental

(±)-3-Dimethoxyphosphoryl-3*H*-2-benzofuran-1-one (203)[200]
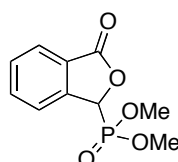
A solution of sodium methoxide (0.685 g, 12.7 mmol) in methanol (20 mL) was cooled to 0 °C, and to this was added dimethyl phosphite (**208**) (1.08 mL, 11.8 mmol) dropwise. 2-Carboxybenzaldehyde (**204**) (1.50 g, 9.99 mmol) was then added in portions to the

reaction mixture, which was gradually warmed to ambient temperature and stirred for 2 h. Methanesulfonic acid (0.908 mL, 14.0 mmol) was added dropwise to the reaction mixture and a white suspension formed. The mixture was concentrated *in vacuo* and resuspended in water (20 mL). The crude product was extracted using dichloromethane (3 × 20 mL) and washed with water (2 × 20 mL). The organic layer was dried (MgSO₄), filtered and concentrated *in vacuo*. Purification by trituration with diethyl ether afforded (±)-3-dimethoxyphosphoryl-3*H*-2-benzofuran-1-one (**203**) (2.33 g, 96%) as a white solid. Spectroscopic data in accordance with the literature. Mp 90–93 °C; ν_{max}/cm^{-1} (neat) 2963 (CH), 1763 (CO), 1466, 1285 (P=O), 1258, 1194, 1024, 895, 849; δ_H (400 MHz, CD₃OD) 3.72 (3H, d, *J* 10.8 Hz, OCH₃), 3.91 (3H, d, *J* 11.2 Hz, OCH₃), 6.10 (1H, d, *J* 10.8 Hz, 3-H), 7.64–7.70 (1H, m, ArH), 7.73–7.77 (1H, m, ArH), 7.83 (1H, t, *J* 7.6 Hz, ArH), 7.94 (1H, dd, *J* 7.6, 0.8 Hz, ArH); δ_C (126 MHz, CD₃OD) 53.7 (CH₃, d, J_{C-O-P} 7.1 Hz), 54.1 (CH₃, d, J_{C-O-P} 6.7 Hz), 75.3 (CH, d, J_{C-P} 166.1 Hz), 123.5 (CH), 125.1 (C, d, J_{C-C-P} 4.2 Hz), 125.6 (CH), 130.0 (CH), 134.7 (CH), 144.0 (C, d, $J_{C-C-C-P}$ 4.3 Hz), 170.1 (C); *m/z* (CI) 243.0423 (MH⁺. C₁₀H₁₂O₅P requires 243.0422), 242 (33%), 213 (8), 133 (87), 105 (6).

2-Fluoro-5-[(*Z/E*)-(3''-oxo-2''-benzofuran-1''-ylidene)methyl]benzonitrile (202)[200]
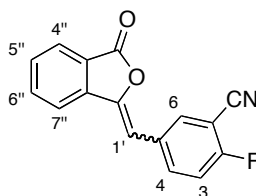
A solution of 3-dimethoxyphosphoryl-3*H*-2-benzofuran-1-one (**203**) (2.00 g, 8.26 mmol) and 2-fluoro-5-formylbenzonitrile (**207**) (1.17 g, 7.85 mmol) in tetrahydrofuran (40 mL) was cooled to 0 °C, and to this was added triethylamine (1.51 mL, 8.26 mmol) dropwise. The resultant solution was allowed to warm to ambient temperature and vigorously stirred for 24 h. The resultant suspension was concentrated *in vacuo* and water (40 mL) added to the residue. After stirring at ambient temperature for 0.5 h, the product was collected by vacuum filtration and stringently washed with water (2 × 50 mL), hexane (2 × 50 mL) and diethyl ether (2 × 50 mL) before drying under high vacuum to give 2-fluoro-5-[(*Z/E*)-(3''-oxo-2''-benzofuran-1''-ylidene)methyl]benzonitrile (**202**) (1.97 g, 95%) as a white solid. NMR spectra showed a 75:25 mixture of *E* and *Z* isomers, of which only the signals for the major isomer are recorded. The product was carried forward without prior separation of the isomers. Mp 203–205 °C; ν_{max}/cm^{-1} (neat) 2990 (CH), 2332 (CN), 1713 (CO), 1514,

1352, 1252, 1233, 1136, 1022; δ_H (500 MHz, DMSO-d_6) 6.96 (1H, s, 1'-H), 7.63 (1H, t, J 9.1 Hz, ArH), 7.70–7.74 (1H, m, ArH), 7.90–7.94 (1H, m, ArH), 7.99 (1H, dt, J 8.0, 1.0 Hz, ArH), 8.08 (1H, dt, J 8.0, 1.0 Hz, ArH), 8.15–8.21 (2H, m, 2 × ArH); δ_C (126 MHz, DMSO-d_6) 100.9 (C, d, $J_{C\text{-}C\text{-}F}$ 16.2 Hz), 103.4 (CH), 113.7 (C), 117.3 (CH, d, $J_{C\text{-}C\text{-}F}$ 20.1 Hz), 120.9 (CH), 122.6 (C), 125.3 (CH), 130.9 (CH), 131.0 (C, d, $J_{C\text{-}C\text{-}C\text{-}F}$ 3.8 Hz), 134.2 (CH), 135.3 (CH), 136.7 (CH, d, $J_{C\text{-}C\text{-}C\text{-}F}$ 9.0 Hz), 139.6 (C), 145.4 (C), 161.5 (C, d, $J_{C\text{-}F}$ 258.3 Hz), 165.9 (C); m/z (EI) 265.0543 (M$^+$. $C_{16}H_8FNO_2$ requires 265.0539), 237 (15%), 208 (93), 182 (12), 133 (24), 104 (28), 84 (41).

2-Fluoro-5-[(4''-oxo-3''H-phthalazin-1''-yl)methyl]benzoic acid (201)[200]
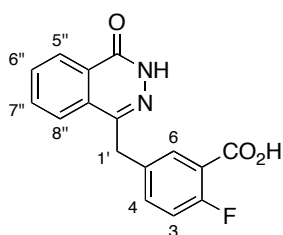
To a suspension of 2-fluoro-5-[(Z/E)-(3''-oxo-2''-benzofuran-1''-ylidene)methyl]benzonitrile (**202**) (3.84 g, 14.5 mmol) in water (100 mL) was added a 13 N sodium hydroxide solution (15 mL), and the resultant mixture stirred vigorously at 90 °C for 24 h. After cooling to 70 °C, hydrazine monohydrate (10.0 mL, 0.207 mol) was added to the reaction mixture dropwise and stirred for a further 72 h. On cooling to ambient temperature, the mixture was acidified (pH ~4) by the addition of a 6 M hydrochloric acid solution. The resultant precipitate was collected by vacuum filtration and washed with water (3 × 100 mL) and diethyl ether (3 × 100 mL) before drying under high vacuum to afford 2-fluoro-5-[(4''-oxo-3''H-phthalazin-1''-yl)methyl]benzoic acid (**201**) (4.31 g, 100%) as a pale pink solid. Mp 251–252 °C; ν_{max}/cm^{-1} (neat) 3142 (NH), 2927 (CH), 1695 (CO), 1631 (C=C), 1500, 1316, 1268, 1236, 1084; δ_H (500 MHz, DMSO-d_6) 4.34 (2H, s, 1'-H$_2$), 7.21 (1H, dd, J 8.5, 2.0 Hz, ArH), 7.53–7.58 (1H, m, ArH), 7.78–7.84 (2H, m, 2 × ArH), 7.89 (1H, td, J 8.0, 1.5 Hz, ArH), 7.96 (1H, d, J 8.0 Hz, ArH), 8.26 (1H, dd, J 8.0, 1.0 Hz, ArH), 12.5 (1H, s, NH); δ_C (126 MHz, DMSO-d_6) 36.3 (CH$_2$), 116.9 (CH, d, $J_{C\text{-}C\text{-}F}$ 22.6 Hz), 119.3 (C, d, $J_{C\text{-}C\text{-}F}$ 10.9 Hz), 125.4 (CH), 126.0 (CH), 127.9 (C), 129.1 (C), 131.5 (CH), 131.7 (CH), 133.5 (CH), 134.2 (C, d, $J_{C\text{-}C\text{-}C\text{-}F}$ 3.7 Hz), 134.7 (CH, d, $J_{C\text{-}C\text{-}F}$ 8.7 Hz), 144.8 (C), 159.3 (C), 159.8 (C, d, $J_{C\text{-}F}$ 255.5 Hz), 164.8 (C, d, $J_{C\text{-}C\text{-}C\text{-}F}$ 2.8 Hz); m/z (CI) 299.0828 (MH$^+$. $C_{16}H_{12}FN_2O_3$ requires 299.0832), 287 (10%), 255 (21), 147 (7), 127 (31), 113 (18).

tert-Butyl piperazine-1-carboxylate (205)[208]
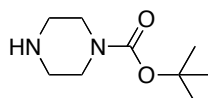
A solution of piperazine (**206**) (2.00 g, 23.2 mmol) in dichloromethane (50 mL) was cooled to 0 °C, and to this was added a solution of di-*tert*-butyl dicarbonate (**209**) (2.53 g, 11.6 mmol) in dichloromethane (25 mL) dropwise over a period of 0.5 h. The resultant suspension was stirred at 0 °C for 3 h, and then allowed to warm to ambient temperature. The organic layer was then washed with water (3 × 50 mL), dried (MgSO$_4$), filtered and concentrated *in vacuo* to give *tert*-butyl piperazine-1-carboxylate (**205**) (1.89 g, 88%) as a colourless solid, which was used without further purification. Mp 46–48°C (lit.,[208] mp 46–47 °C); v_{max}/cm^{-1} (neat) 3325 (NH), 2978 (CH), 1684 (CO), 1422, 1242, 1163, 1121, 1005; δ_H (400 MHz, CD$_3$OD) 1.48 (9H, s, O^{t}Bu), 2.75–2.79 (4H, m, 2 × NCH$_2$), 3.40 (4H, t, *J* 4.8 Hz, 2 × NCH$_2$); δ_C (101 MHz, CD$_3$OD) 28.6 (3 × CH$_3$), 45.1 (2 × br CH$_2$), 46.2 (2 × CH$_2$), 81.3 (C), 156.5 (C); *m/z* (EI) 187 (MH$^+$, 100%) 175 (83), 131 (95), 102 (11).

tert-Butyl 4-{2'-fluoro-5'-[(4'''-oxo-3'''*H*-phthalazin-1'''-yl)methyl]benzoyl}piperazine-1-carboxylate (200)[200]
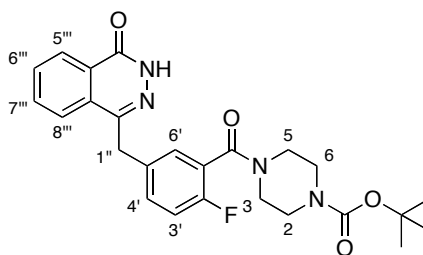
To a solution of 2-fluoro-5-[(4''-oxo-3''*H*-phthalazin-1''-yl)methyl]benzoic acid (**201**) (0.500 g, 1.68 mmol) in *N,N'*-dimethylformamide (50 mL) was added triethylamine (0.350 mL, 2.51 mmol) followed by *O*-benzotriazole-*N,N,N',N'*-tetramethyluroniumhexafluorophosphate (0.699 g, 1.84 mmol). The reaction mixture was stirred at ambient temperature for 1 h, after which it was heated to 50 °C and *tert*-butyl piperazine-1-carboxylate (**205**) (0.312 g, 1.68 mmol) added. After stirring for a further 72 h, water (50 mL) was added and the mixture stirred for a further 2 h before being cooled to 0 °C. The resultant precipitate was collected by vacuum filtration and stringently washed with water (2 × 25 mL), diethyl ether (2 × 25 mL) and isopropan-2-ol (2 × 25 mL) to

afford *tert*-butyl 4-{2'-fluoro-5'-[(4'''-oxo-3'''*H*-phthalazin-1'''-yl)methyl]benzoyl}piperazine-1-carboxylate (**200**) (0.533 g, 68%) as a pale yellow solid. Mp 215–216 °C; ν_{max}/cm^{-1} (neat) 3206 (NH), 2976 (CH), 1640 (CO), 1495, 1410, 1364, 1248, 1163, 1013; δ_H (400 MHz, CDCl$_3$) 1.47 (9H, s, O^{t}Bu), 3.27 (2H, br s, NCH$_2$), 3.38 (2H, t, *J* 4.8 Hz, NCH$_2$), 3.51 (2H, br s, NCH$_2$), 3.75 (2H, br s, NCH$_2$), 4.27 (2H, s, 1''-H$_2$), 7.04 (1H, t, *J* 9.2 Hz, ArH), 7.27–7.37 (2H, m, 2 × ArH), 7.68–7.79 (3H, m, 3 × ArH), 8.44–8.48 (1H, m, ArH), 9.69 (1H, s, NH); δ_C (101 MHz, CDCl$_3$) 28.4 (3 × CH$_3$), 37.7 (CH$_2$), 42.0 (2 × CH$_2$), 46.9 (2 × CH$_2$), 80.4 (C), 116.2 (CH, d, J_{C-C-F} 22.3 Hz), 123.9 (C, d, J_{C-C-F} 17.3 Hz), 125.1 (CH), 127.2 (CH), 128.3 (C), 129.2 (CH, d, $J_{C-C-C-F}$ 3.5 Hz), 129.5 (C), 131.6 (CH, d, $J_{C-C-C-F}$ 8.3 Hz), 131.7 (CH), 133.7 (CH), 134.3 (C, d, $J_{C-C-C-F}$ 3.8 Hz), 145.6 (C), 154.5 (C), 157.0 (C, d, J_{C-F} 247.8 Hz), 160.4 (C), 165.1 (C); *m/z* (EI) 466.2018 (M$^+$. C$_{25}$H$_{27}$FN$_4$O$_4$ requires 466.2016), 393 (12%), 366 (38), 281 (100), 254 (33), 196 (13), 166 (40), 91 (90).

4-[4''-Fluoro-3''-(piperazine-1'''-carbonyl)benzyl]-2*H*-phthalazin-1-one (199)[200]
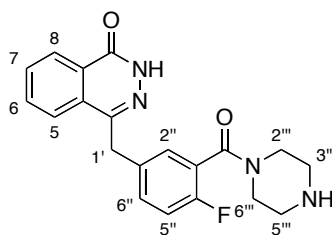
To a suspension of *tert*-butyl 4-{2'-fluoro-5'-[(4'''-oxo-3'''*H*-phthalazin-1'''-yl)methyl]benzoyl}piperazine-1-carboxylate (**200**) (0.533 g, 1.14 mmol) in ethanol (15 mL) was added a 6 M hydrochloric acid solution (30 mL), and the resultant reaction mixture stirred vigorously at ambient temperature for 18 h. The ethanol was removed *in vacuo* and the aqueous layer made alkaline (pH ~10) by the dropwise addition of a 4 M sodium hydroxide solution. The product was extracted using dichloromethane (3 × 50 mL) and the combined organic layer dried (MgSO$_4$), filtered and concentrated *in vacuo*. Purification by trituration using a 1:1 diethyl ether/petroleum ether mixture gave 4-[4''-fluoro-3''-(piperazine-1'''-carbonyl)benzyl]-2*H*-phthalazin-1-one (**199**) (0.294 g, 70%) as a white solid. Mp 193–195 °C; ν_{max}/cm^{-1} (neat) 3468 (NH), 2942 (CH), 1628 (CO), 1466, 1437, 1354, 1227, 1022, 770; δ_H (400 MHz, CDCl$_3$) 2.07 (1H, br s, NH), 2.81 (2H, br s, NCH$_2$), 2.95 (2H, t, *J* 4.4 Hz, NCH$_2$), 3.28 (2H, br s, NCH$_2$), 3.77 (2H, br s, NCH$_2$), 4.29 (2H, s, 1'-H$_2$), 7.02 (1H, t, *J* 8.8 Hz, ArH), 7.26–7.37 (2H, m, 2 × ArH), 7.70–7.80 (3H, m, 3 × ArH), 8.45–8.50 (1H, m, ArH), 11.46 (1H, br s, NH); δ_C (101 MHz,

CDCl$_3$) 37.7 (CH$_2$), 43.1 (CH$_2$), 45.7 (CH$_2$), 46.2 (CH$_2$), 48.2 (CH$_2$), 116.1 (CH, d, J_{C-C-F} 22.1 Hz), 124.3 (C, d, J_{C-C-F} 18.2 Hz), 125.1 (CH), 127.1 (CH), 128.3 (C), 129.1 (CH, d, $J_{C-C-C-F}$ 3.7 Hz), 129.6 (C), 131.2 (CH, d, $J_{C-C-C-F}$ 8.1 Hz), 131.6 (CH), 133.6 (CH), 134.2 (C, d, $J_{C-C-C-C-F}$ 3.1 Hz), 145.6 (C), 157.0 (C, d, J_{C-F} 247.6 Hz), 160.8 (C), 165.0 (C); *m/z* (EI) 366.1486 (M$^+$. C$_{20}$H$_{19}$FN$_4$O$_2$ requires 366.1492), 325 (13%), 298 (27), 281 (100), 254 (29), 85 (17).

4-{3''-[4'''-(4'''''-Fluorobenzyl)piperazine-1'''-carbonyl]-4''-fluorobenzyl}-2*H*-phthalazin-1-one (216)
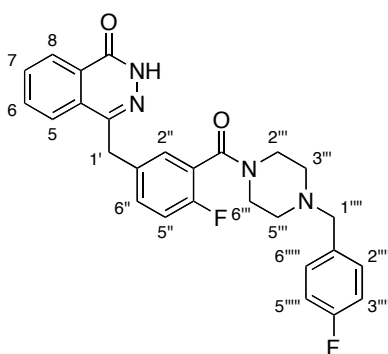
To a stirred solution of 4-[4''-fluoro-3''-(piperazine-1'''-carbonyl)benzyl]-2*H*-phthalazin-1-one (**199**) (0.023 g, 0.063 mmol) in dichloromethane (3 mL) was added 4-fluorobenzyl chloride (7.9 μL, 0.066 mmol) followed by *N,N'*-diisopropylethylamine (21.9 μL, 0.126 mmol). The resultant reaction mixture was stirred at ambient temperature for 12 h, and then water (5 mL) was added. The mixture was washed with water (2 × 5 mL) and the organic layer dried (MgSO$_4$), filtered and concentrated *in vacuo*. Purification using flash column chromatography (methanol/dichloromethane, 1:9) afforded 4-{3''-[4'''-(4'''''-fluorobenzyl)piperazine-1'''-carbonyl]-4''-fluorobenzyl}-2*H*-phthalazin-1-one (**216**) (0.011 g, 38%) as an off-white solid. Mp 109–111 °C; ν_{max}/cm^{-1} (neat) 3185 (NH), 2916 (CH), 1637 (CO), 1508, 1437, 1348, 1221, 1148, 999; δ_H (400 MHz, CDCl$_3$) 2.34 (2H, br s, NCH$_2$), 2.50 (2H, t, *J* 5.2 Hz, NCH$_2$), 3.28 (2H, br s, NCH$_2$), 3.48 (2H, s, 1'''''-H$_2$), 3.75–3.82 (2H, m, NCH$_2$), 4.28 (2H, s, 1'-H$_2$), 6.96–7.04 (3H, m, 3 × ArH), 7.24–7.34 (4H, m, 4 × ArH), 7.69–7.78 (3H, m, 3 × ArH), 8.44–8.50 (1H, m, ArH), 10.86 (1H, s, NH); δ_C (101 MHz, CDCl$_3$) 37.8 (CH$_2$), 42.0 (CH$_2$), 47.1 (CH$_2$), 52.5 (CH$_2$), 53.0 (CH$_2$), 62.0 (CH$_2$), 115.2 (2 × CH, d, J_{C-C-F} 21.2 Hz), 116.1 (CH, d, J_{C-C-F} 21.8 Hz), 124.3 (C, d, J_{C-C-F} 18.3 Hz), 125.1 (CH), 127.2 (CH), 128.3 (C), 129.1 (CH, d, $J_{C-C-C-F}$ 3.8 Hz), 129.6 (C), 130.5 (2 × CH, d, $J_{C-C-C-F}$ 7.9 Hz), 131.2 (CH, d, $J_{C-C-C-F}$ 7.9 Hz), 131.6 (CH), 133.3

(C, d, $J_{C-C-C-C-F}$ 3.0 Hz), 133.7 (CH), 134.1 (C, d, $J_{C-C-C-C-F}$ 3.4 Hz), 145.6 (C), 157.0 (C, d, J_{C-F} 247.7 Hz), 160.5 (C), 162.1 (C, d, J_{C-F} 245.0 Hz), 164.8 (C); *m/z* (ESI) 475.1929 (MH$^+$. $C_{27}H_{25}F_2N_4O_2$ requires 475.1940).

4-{3''-[4'''-(4'''''-Fluorobenzoyl)piperazine-1'''-carbonyl]-4''-fluorobenzyl}-2*H*-phthalazin-1-one (217)
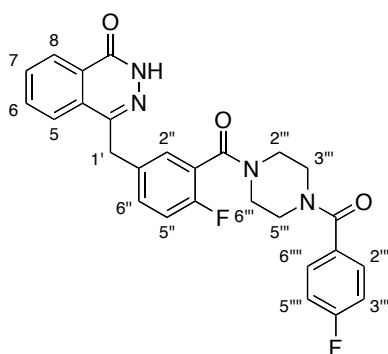
To a solution of 4-fluorobenzoic acid (0.029 g, 0.21 mmol) in dichloromethane (5 mL) was added *N,N'*-diisopropylethylamine (60.8 μL, 0.349 mmol) followed by *O*-benzotriazole-*N,N,N',N'*-tetramethyluroniumhexafluorophosphate (0.080 g, 0.21 mmol). The resultant reaction mixture was stirred vigorously under reflux for 1 h, after which a solution of 4-[4''-fluoro-3''-(piperazine-1'''-carbonyl)benzyl]-2*H*-phthalazin-1-one (**199**) (0.064 g, 0.17 mmol) in dichloromethane (5 mL) was added dropwise, and stirred for a further 24 h. On cooling to ambient temperature, water (5 mL) was added and the organic layer washed with water (3 × 10 mL) and a saturated sodium bicarbonate solution (10 mL), dried (MgSO$_4$), filtered and concentrated *in vacuo*. Purification using flash column chromatography (methanol/dichloromethane, 3:97) afforded 4-{3''-[4'''-(4'''''-fluorobenzoyl)piperazine-1'''-carbonyl]-4''-fluorobenzyl}-2*H*-phthalazin-1-one (**217**) (0.064 g, 75%) as a white solid. Mp 166–168 °C; ν_{max}/cm^{-1} (neat) 3202 (NH), 2922 (CH), 1629 (CO), 1425, 1285, 1223, 1152, 1005, 847; δ_H (400 MHz, CDCl$_3$) 3.20–4.05 (8H, m, 4 × NCH$_2$), 4.29 (2H, s, 1'-H$_2$), 6.98–7.14 (3H, m, 3 × ArH), 7.30–7.45 (4H, m, 4 × ArH), 7.68–7.79 (3H, m, 3 × ArH), 8.45–8.49 (1H, m, ArH), 11.37 (1H, s, NH); δ_C (101 MHz, CDCl$_3$) 37.7 (CH$_2$), 42.1 (2 × CH$_2$), 47.0 (2 × CH$_2$), 115.8 (2 × CH, d, J_{C-C-F} 21.9 Hz), 116.2 (CH, d, J_{C-C-F} 22.0 Hz), 123.6 (C, d, J_{C-C-F} 17.8 Hz), 125.0 (CH), 127.2 (CH), 128.3 (C), 129.3 (CH, d, $J_{C-C-C-F}$ 3.5 Hz), 129.5 (2 × CH, d, $J_{C-C-C-F}$ 8.7 Hz), 131.1 (C, d, $J_{C-C-C-C-F}$ 3.5 Hz), 131.6 (CH), 131.8 (CH, d, $J_{C-C-C-F}$ 8.0 Hz), 133.7 (CH), 134.5 (C, d, $J_{C-C-C-C-F}$ 3.5

Hz), 145.5 (C), 157.0 (C, d, J_{C-F} 247.4 Hz), 160.8 (2 × C), 163.6 (C, d, J_{C-F} 250.7 Hz), 165.2 (C), 169.7 (C); *m/z* (ESI) 511.1547 (MNa$^+$. $C_{27}H_{22}F_2N_4NaO_3$ requires 511.1552).

4-{3''-[4'''-(2'''''-Fluorobenzoyl)piperazine-1'''-carbonyl]-4''-fluorobenzyl}-2*H*-phthalazin-1-one (218)

4-{3''-[4'''-(2'''''-Fluorobenzoyl)piperazine-1'''-carbonyl]-4''-fluorobenzyl}-2*H*-phthalazin-1-one (**218**) was synthesised as described above for 4-{3''-[4'''-(4''''-fluorobenzoyl)piperazine-1'''-carbonyl]-4''-fluorobenzyl}-2*H*-phthalazin-1-one (**217**) using 2-fluorobenzoic acid (0.047 g, 0.34 mmol), *N,N'*-diisopropylethylamine (97.0 μL, 0.557 mmol), *O*-benzotriazole-*N,N,N',N'*-tetramethyluroniumhexafluorophosphate (0.127 g, 0.334 mmol) and 4-[4''-fluoro-3''-(piperazine-1'''-carbonyl)benzyl]-2*H*-phthalazin-1-one (**199**) (0.102 g, 0.278 mmol) in dichloromethane (10 mL). Purification using flash column chromatography (methanol/dichloromethane, 3:97) afforded 4-{3''-[4'''-(2''''-fluorobenzoyl)piperazine-1'''-carbonyl]-4''-fluorobenzyl}-2*H*-phthalazin-1-one (**218**) (0.072 g, 53%) as a white solid. NMR spectra showed a 56:44 mixture of rotamers, of which only the signals for one rotamer is recorded. Mp 246–248 °C; v_{max}/cm^{-1} (neat) 3043 (CH), 1684, 1641 (CO), 1464, 1433, 1289, 1251, 1007, 749; δ_H (CDCl$_3$, 400 MHz) 3.20–4.10 (8H, m, 4 × NCH$_2$), 4.30 (2H, s, 1'-H$_2$), 6.96–7.50 (7H, m, 7 × ArH), 7.67–7.81 (3H, m, 3 × ArH), 8.42–8.49 (1H, m, ArH), 10.17 (1H, s, NH); δ_C (CDCl$_3$, 101 MHz) 37.7 (CH$_2$), 41.8 (CH$_2$), 42.2 (CH$_2$), 46.8 (CH$_2$), 47.4 (CH$_2$), 115.9 (CH, d, J_{C-C-F} 21.4 Hz), 116.1 (CH, d, J_{C-C-F} 20.4 Hz), 123.4 (C, d, J_{C-C-F} 17.8 Hz), 123.7 (C, d, J_{C-C-F} 18.3 Hz), 125.0 (br CH), 125.0 (CH), 127.3 (CH), 128.4 (C), 129.3 (br CH), 129.5 (C), 131.7 (br CH), 131.8 (br CH), 131.9 (br CH), 133.7 (2 × CH), 134.4 (C, d, $J_{C-C-C-C-F}$ 2.9 Hz), 145.5 (C), 157.1 (C, d, J_{C-F} 247.5 Hz), 158.1 (C, d, J_{C-F} 247.8 Hz), 160.3 (C), 165.2 (C), 165.5 (C); *m/z* (ESI) 511.1545 (MNa$^+$. $C_{27}H_{22}F_2N_4NaO_3$ requires 511.1552).
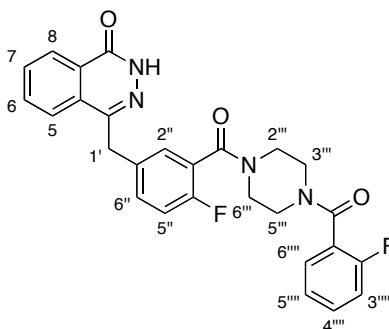
4-{3''-[4'''-(4'''''-Fluoro-2'''''-methylbenzoyl)piperazine-1'''-carbonyl]-4''-fluorobenzyl}-2H-phthalazin-1-one (219)
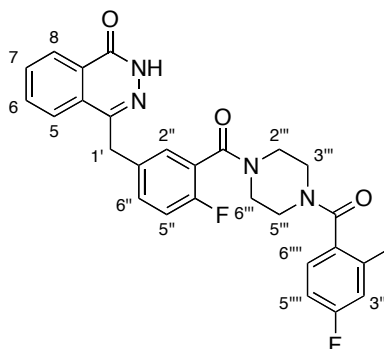
To a solution of 4-fluoro-2-methylbenzoic acid (0.042 g, 0.27 mmol) in dichloromethane (5 mL) was added ethyl 3-(3-dimethylaminopropyl)carbodiimide hydrochloride (0.052 g, 0.27 mmol) and the reaction mixture stirred at ambient temperature for 0.5 h. 4-(Dimethylamino)pyridine (0.017 g, 0.14 mmol) was then added and the mixture stirred for a further 0.5 h. A solution of 4-[4''-fluoro-3''-(piperazine-1'''-carbonyl)benzyl]-2H-phthalazin-1-one (**199**) (0.100 g, 0.273 mmol) in dichloromethane (5 mL) was then added dropwise and the resultant reaction mixture stirred vigorously under reflux for 24 h. On cooling to ambient temperature, water (5 mL) was added and the organic layer washed with water (3 × 5 mL) and a saturated sodium bicarbonate solution (5 mL), dried (MgSO$_4$), filtered and concentrated *in vacuo*. Purification using flash column chromatography (methanol/dichloromethane, 2:98) afforded 4-{3''-[4'''-(4'''''-fluoro-2'''''-methylbenzoyl)piperazine-1'''-carbonyl]-4''-fluorobenzyl} -2H-phthalazin-1-one (**219**) (0.043 g, 31%) as a white solid. NMR spectra showed a 59:41 mixture of rotamers, of which only the signals for one rotamer is recorded. Mp 175–177 °C; ν_{max}/cm^{-1} (neat) 3188 (NH), 2926 (CH), 1632 (CO), 1462, 1429, 1256, 1159, 1063, 1003; δ_H (400 MHz, CDCl$_3$) 2.32 (3H, s, CH$_3$), 3.15–3.45 (4H, m, 2 × NCH$_2$), 3.55–4.10 (4H, m, 2 × NCH$_2$), 4.30 (2H, s, 1'-H$_2$), 6.85–7.18 (4H, m, 4 × ArH), 7.26–7.39 (2H, m, 2 × ArH), 7.67–7.81 (3H, m, 3 × ArH), 8.43–8.50 (1H, m, ArH), 10.30 (1H, s, NH); δ_C (126 MHz, CDCl$_3$) 19.2 (CH$_3$), 37.7 (CH$_2$), 41.8 (CH$_2$), 42.4 (CH$_2$), 46.5 (CH$_2$), 46.9 (CH$_2$), 113.2 (CH, d, J_{C-C-F} 21.5 Hz), 116.3 (CH, d, J_{C-C-F} 20.6 Hz), 117.5 (CH, d, J_{C-C-F} 21.1 Hz), 123.6 (C, d, J_{C-C-F} 17.0 Hz), 125.0 (CH), 127.2 (CH), 127.8 (CH, d, $J_{C-C-C-F}$ 8.6 Hz), 128.3 (C), 129.3 (CH, d, $J_{C-C-C-F}$ 3.2 Hz), 129.6 (C), 131.5 (C, d, $J_{C-C-C-F}$ 7.3 Hz), 131.6 (CH), 131.8 (CH), 133.7 (CH), 134.5 (C, d, $J_{C-C-C-F}$ 3.4 Hz), 137.4 (C, d, $J_{C-C-C-F}$ 8.1 Hz), 145.5 (C), 157.0 (C, d, J_{C-F} 246.4 Hz), 160.7 (C), 162.9 (C, d, J_{C-F} 248.8 Hz), 165.3 (C), 169.6 (C); *m/z* (ESI) 525.1699 (MNa$^+$. C$_{28}$H$_{24}$F$_2$N$_4$NaO$_3$ requires 525.1709).

4-(3''-{4'''-[(4''''''-Fluorophenyl)acetyl]piperazine-1'''-carbonyl}-4''-fluorobenzyl)-2*H*-phthalazin-1-one (220)
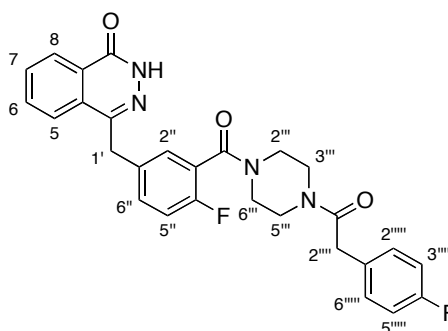
To a solution of 4-fluorophenylacetic acid (0.043 g, 0.28 mmol) in *N,N'*-dimethylformamide (5 mL) was added *N,N'*-diisopropylethylamine (93.4 µL, 0.546 mmol) followed by *O*-benzotriazole-*N,N,N',N'*-tetramethyluroniumhexafluorophosphate (0.105 g, 0.277 mmol), and the reaction mixture stirred vigorously at ambient temperature for 1 h. A solution of 4-[4''-fluoro-3''-(piperazine-1'''-carbonyl)benzyl]-2*H*-phthalazin-1-one (**199**) (0.100 g, 0.273 mmol) in *N,N'*-dimethylformamide (5 mL) was then added dropwise, and the resultant reaction mixture heated to and stirred at 50 °C for a further 24 h. On cooling to ambient temperature, dichloromethane was added (10 mL) and the organic layer washed with water (3 × 10 mL) and a saturated sodium bicarbonate solution (10 mL), dried (MgSO$_4$), filtered and concentrated *in vacuo*. Purification using flash column chromatography (methanol/dichloromethane, 4:96) afforded 4-(3''-{4'''-[(4''''''-fluorophenyl)acetyl]piperazine-1'''-carbonyl}-4''-fluorobenzyl)-2*H*-phthalazin-1-one (**220**) (0.063 g, 46%) as white solid. NMR spectra showed a 57:43 mixture of rotamers, of which only the signals for one rotamer is recorded. Mp 216–218 °C; v_{max}/cm^{-1} (neat) 2899 (CH), 2346, 1636 (CO), 1586 (C=C), 1508, 1431, 1219, 1157, 1011; δ_H (400 MHz, CDCl$_3$) 3.03–3.85 (10H, m, 4 × NCH$_2$ and 2''''-H$_2$), 4.28 (2H, br s, 1'-H$_2$), 6.95–7.07 (3H, m, 3 × ArH), 7.13–7.24 (2H, m, 2 × ArH), 7.27–7.36 (2H, m, 2 × ArH), 7.66–7.79 (3H, m, 3 × ArH), 8.44–8.49 (1H, m, ArH), 11.01 (1H, s, NH); δ_C (101 MHz, CDCl$_3$) 37.7 (CH$_2$), 39.9 (CH$_2$), 42.0 (2 × CH$_2$), 45.7 (CH$_2$), 46.7 (CH$_2$), 115.7 (2 × CH, d, J_{C-C-F} 21.4 Hz), 116.2 (CH, d, J_{C-C-F} 22.0 Hz), 123.5 (C, d, J_{C-C-F} 17.6 Hz), 125.0 (CH), 127.2 (CH), 128.3 (C), 129.2 (CH, d, $J_{C-C-C-F}$ 2.3 Hz), 129.5 (C), 130.2 (C), 130.2 (2 × CH, d, J_{C-C-F} 7.9 Hz), 131.6 (CH), 131.8 (CH, d, $J_{C-C-C-F}$ 8.1 Hz), 133.7 (CH), 134.5 (C, d, $J_{C-C-C-C-F}$ 3.4 Hz), 145.5 (C), 157.0 (C, d, J_{C-F} 247.6 Hz), 160.8 (C), 161.9 (C, d, J_{C-F} 247.6 Hz), 165.2 (C), 169.6 (C); *m/z* (ESI) 525.1705 (MNa$^+$. C$_{28}$H$_{24}$F$_2$N$_4$NaO$_3$ requires 525.1709).

4-(3''-{4'''-[(4'''''-Fluorophenyl)butane-1'''',4''''-dione]piperazine-1'''-carbonyl}-4''-fluorobenzyl)-2*H*-phthalazin-1-one (221)
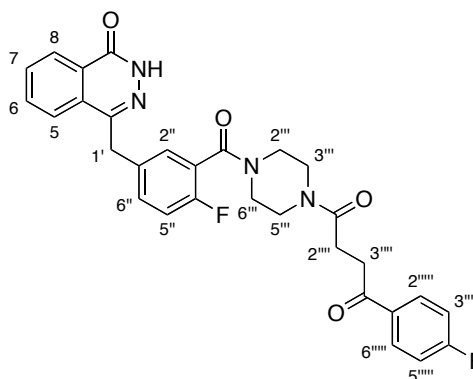

To a solution of 3-(4-fluorobenzoyl)propionic acid (0.053 g, 0.27 mmol) in dichloromethane (5 mL) was added ethyl 3-(3-dimethylaminopropyl)carbodiimide hydrochloride (0.052 g, 0.27 mmol) and the reaction mixture stirred at ambient temperature for 0.5 h. 4-(Dimethylamino)pyridine (0.017 g, 0.14 mmol) was then added and the mixture stirred for a further 0.5 h. A solution of 4-[4''-fluoro-3''-(piperazine-1'''-carbonyl)benzyl]-2*H*-phthalazin-1-one (**199**) (0.100 g, 0.273 mmol) in dichloromethane (5 mL) was then added dropwise and the resultant reaction mixture stirred vigorously under reflux for 24 h. On cooling to ambient temperature, water (5 mL) was added and the organic layer washed with water (3 × 5 mL) and a saturated sodium bicarbonate solution (5 mL), dried (MgSO$_4$), filtered and concentrated *in vacuo*. Purification using flash column chromatography (methanol/dichloromethane, 4:96) gave 4-(3''-{4'''-[(4'''''-fluorophenyl)butane-1'''',4''''-dione]piperazine-1'''-carbonyl}-4''-fluorobenzyl)-2*H*-phthalazin-1-one (**221**) (0.050 g, 34%) as a pale yellow solid. NMR spectra showed a 56:44 mixture of rotamers, of which only the signals for one rotamer is recorded. Mp 128–130 °C; ν_{max}/cm^{-1} (neat) 3208 (NH), 2909 (CH), 1636 (CO), 1595 (C=C), 1433, 1356, 1225, 1155, 1011; δ_H (400 MHz, CDCl$_3$) 2.82 (2H, t, *J* 6.4 Hz, 2''''-H$_2$), 3.24–3.46 (4H, m, NCH$_2$ and 3''''-H$_2$), 3.50–3.98 (6H, m, 3 × NCH$_2$), 4.28 (2H, s, 1'-H$_2$), 7.05 (1H, t, *J* 8.8 Hz, ArH), 7.10–7.16 (2H, m, 2 × ArH), 7.30–7.39 (2H, m, 2 × ArH), 7.68–7.81 (3H, m, 3 × ArH), 8.00–8.06 (2H, m, 2 × ArH), 8.44–8.49 (1H, m, ArH), 10.33 (1H, s, NH); δ_C (101 MHz, CDCl$_3$) 27.0 (CH$_2$), 33.4 (CH$_2$), 37.7 (CH$_2$), 42.0 (CH$_2$), 42.1 (CH$_2$), 45.1 (CH$_2$), 46.8 (CH$_2$), 115.7 (2 × CH, d, J_{C-C-F} 21.8 Hz), 116.2 (CH, d, J_{C-C-F} 21.9 Hz), 123.7 (C, d, J_{C-C-F} 17.6 Hz), 125.0 (CH), 127.2 (CH), 128.3 (C), 129.2 (CH, d, $J_{C-C-C-F}$ 3.0 Hz), 129.6 (C), 130.8 (2 × CH, d, $J_{C-C-C-F}$ 9.4 Hz), 131.6 (CH), 131.7 (CH, d, $J_{C-C-C-F}$ 8.0 Hz), 133.2 (C), 133.6 (CH), 134.5 (C, d, $J_{C-C-C-C-F}$ 3.3 Hz), 145.5 (C), 157.0 (C, d, J_{C-F} 247.4

Hz), 160.7 (C), 165.3 (C), 165.8 (C, d, $J_{\text{C-F}}$ 254.8 Hz), 170.5 (C), 197.4 (C); *m/z* (ESI) 567.1814 (MNa$^+$. $C_{30}H_{26}F_2N_4NaO_4$ requires 567.1796).

4-{4''-Fluoro-3''-[4'''-(4'''''-methoxybenzyl)piperazine-1'''-carbonyl]benzyl}-2*H*-phthalazin-1-one (222)
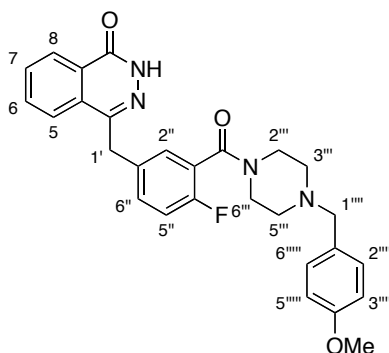
To a solution of 4-[4''-fluoro-3''-(piperazine-1'''-carbonyl)benzyl]-2*H*-phthalazin-1-one (**199**) (0.034 g, 0.093 mmol) in dichloromethane (3 mL) was added 4-methoxybenzyl chloride (13.3 μL, 0.0977 mmol) followed by *N,N'*-diisopropylethylamine (32.3 μL, 0.185 mmol). The resultant reaction mixture was stirred at ambient temperature for 24 h, and then diluted by the addition of water (5 mL). The organic layer was separated, dried (MgSO$_4$), filtered and concentrated *in vacuo*. Purification using flash column chromatography (methanol/dichloromethane, 4:96) afforded 4-{4''-fluoro-3''-[4'''-(4'''''-methoxybenzyl)piperazine-1'''-carbonyl]benzyl}-2*H*-phthalazin-1-one (**222**) (0.019 g, 42%) as a white solid. Mp 96–97 °C; ν_{max}/cm^{-1} (neat) 3171 (NH), 2913 (CH), 1636 (CO), 1613 (C=C), 1512, 1246, 1229, 1026, 997; δ_H (400 MHz, CDCl$_3$) 2.32 (2H, br s, NCH$_2$), 2.48 (2H, t, *J* 4.8 Hz, NCH$_2$), 3.27 (2H, br s, NCH$_2$), 3.46 (2H, s, 1'''''-H$_2$), 3.74–3.81 (5H, m, NCH$_2$ and OCH$_3$), 4.26 (2H, s, 1'-H$_2$), 6.83–6.88 (2H, m, 2 × ArH), 7.01 (1H, t, *J* 9.2 Hz, ArH), 7.19–7.25 (2H, m, 2 × ArH), 7.26–7.32 (2H, m, 2 × ArH), 7.68–7.78 (3H, m, 3 × ArH), 8.43–8.47 (1H, m, ArH), 9.85 (1H, s, NH); δ_C (101 MHz, CDCl$_3$) 37.8 (CH$_2$), 42.0 (CH$_2$), 47.1 (CH$_2$), 52.5 (CH$_2$), 53.0 (CH$_2$), 55.3 (CH$_3$), 62.2 (CH$_2$), 113.7 (2 × CH), 116.1 (CH, d, $J_{\text{C-C-F}}$ 22.0 Hz), 124.4 (C, d, $J_{\text{C-C-F}}$ 18.3 Hz), 125.1 (CH), 127.2 (CH), 128.4 (C), 129.1 (CH, d, $J_{\text{C-C-C-F}}$ 3.8 Hz), 129.6 (2 × C), 130.3 (2 × CH), 131.2 (CH, d, $J_{\text{C-C-C-F}}$ 8.0 Hz), 131.6 (CH), 133.6 (CH), 134.1 (C, d, $J_{\text{C-C-C-C-F}}$ 3.6 Hz), 145.6 (C), 157.1 (C, d, $J_{\text{C-F}}$ 247.6 Hz), 158.9 (C), 160.3 (C), 164.8 (C); *m/z* (EI) 486.2057 (M$^+$. $C_{28}H_{27}FN_4O_3$ requires 486.2067), 445 (9%), 365 (36), 340 (14), 281 (80), 121 (100), 105 (25).

4-{4''-Fluoro-3''-[4''''-(3'''''-Methoxybenzoyl)piperazine-1''''-carbonyl]benzyl}-2*H*-phthalazin-1-one (223)
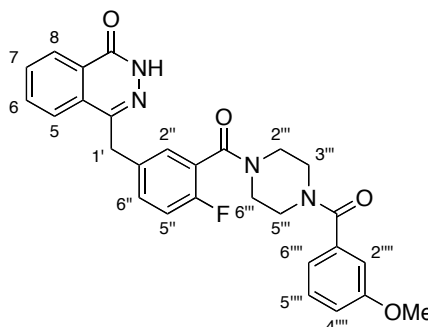
To a solution of 3-methoxybenzoic acid (0.032 g, 0.21 mmol) in *N*,*N'*-dimethylformamide (5 mL) was added *N*,*N'*-diisopropylethylamine (71.0 μL, 0.415 mmol) followed by *O*-benzotriazole-*N*,*N*,*N'*,*N'*-tetramethyluroniumhexafluorophosphate (0.080 g, 0.21 mmol), and the reaction mixture stirred vigorously at ambient temperature for 1 h. A solution of 4-[4''-fluoro-3''-(piperazine-1''''-carbonyl)benzyl]-2*H*-phthalazin-1-one (**199**) (0.076 g, 0.21 mmol) in *N*,*N'*-dimethylformamide (5 mL) was then added dropwise, and the resultant reaction mixture heated to 50 °C and stirred for a further 24 h. On cooling to ambient temperature, dichloromethane (10 mL) was added and the organic layer washed with water (3 × 10 mL) and a saturated sodium bicarbonate solution (10 mL), dried (MgSO₄), filtered and concentrated *in vacuo*. Purification using flash column chromatography (methanol/dichloromethane, 4:96) afforded 4-{4''-fluoro-3''-[4''''-(3'''''-methoxybenzoyl)piperazine-1''''-carbonyl]benzyl}-2*H*-phthalazin-1-one (**223**) (0.041 g, 40%) as a pale yellow solid. Mp 143–145 °C; ν_{max}/cm^{-1} (neat) 3202 (NH), 2900 (CH), 1632 (CO), 1464, 1431, 1288, 1225, 1149, 1008; δ_H (400 MHz, CDCl₃) 3.15–4.00 (11H, m, 4 × NCH₂ and OCH₃), 4.28 (2H, s, 1'-H₂), 6.88–7.12 (4H, m, 4 × ArH), 7.27–7.38 (3H, m, 3 × ArH), 7.68–7.82 (3H, m, 3 × ArH), 8.42–8.50 (1H, m, ArH), 9.92 (1H, s, NH); δ_C (101 MHz, CDCl₃) 37.7 (CH₂), 42.2 (2 × br CH₂), 47.0 (2 × br CH₂), 55.4 (CH₃), 112.6 (CH), 115.9 (CH), 116.2 (CH, d, J_{C-C-F} 22.3 Hz), 119.0 (CH), 123.7 (C, d, J_{C-C-F} 17.9 Hz), 125.0 (CH), 127.2 (CH), 128.4 (C), 129.3 (CH, d, $J_{C-C-C-F}$ 3.5 Hz), 129.6 (C), 129.8 (CH), 131.6 (CH), 131.7 (CH, d, $J_{C-C-C-F}$ 8.1 Hz), 133.7 (CH), 134.5 (C, d, $J_{C-C-C-C-F}$ 3.4 Hz), 136.4 (C), 145.5 (C), 157.0 (C, d, J_{C-F} 247.3 Hz), 159.8 (C), 160.6 (C), 165.2 (C), 170.4 (C); *m/z* (ESI) 523.1743 (MNa⁺. C₂₈H₂₅FN₄NaO₄ requires 523.1752).

4-(4''-Fluoro-3''-{4'''-[(3''''''-methoxyphenyl)acetyl]piperazine-1'''-carbonyl}benzyl)-2*H*-phthalazin-1-one (224)

4-(4''-Fluoro-3''-{4'''-[(3''''''-methoxyphenyl)acetyl]piperazine-1'''-carbonyl}benzyl)-2*H*-phthalazin-1-one (**224**) was synthesised as described above for 4-{4''-fluoro-3''-[4'''-(3''''''-methoxybenzoyl)piperazine-1'''-carbonyl]benzyl}-2*H*-phthalazin-1-one (**223**) using 3-methoxyphenylacetic acid (0.023 g, 0.14 mmol), *N,N'*-diisopropylethylamine (46.7 μL, 0.273 mmol), *O*-benzotriazole-*N,N,N',N'*-tetramethyluroniumhexafluorophosphate (0.052 g, 0.14 mmol) and 4-[4''-fluoro-3''-(piperazine-1'''-carbonyl)benzyl]-2*H*-phthalazin-1-one (**199**) (0.050 g, 0.14 mmol) in *N,N'*-dimethylformamide (5 mL). Purification using flash column chromatography (methanol/dichloromethane, 4:96) gave 4-(4''-fluoro-3''-{4'''-[(3''''''-methoxyphenyl)acetyl]piperazine-1'''-carbonyl}benzyl)-2*H*-phthalazin-1-one (**224**) (0.045 g, 64%) as an off-white solid. NMR spectra showed a 60:40 mixture of rotamers, of which only the signals for the major rotamer is recorded. Mp 108–110 °C; ν_{max}/cm^{-1} (neat) 3192 (NH), 2915 (CH), 1638 (CO), 1491, 1431, 1258, 1150, 1013, 843; δ_H (400 MHz, CDCl$_3$) 3.00–3.82 (13H, m, 4 × NCH$_2$, 2''''''-H$_2$ and OCH$_3$), 4.27 (2H, s, 1'-H$_2$), 6.75–6.85 (3H, m, 3 × ArH), 6.97–7.08 (1H, m, ArH), 7.19–7.25 (1H, m, ArH), 7.27–7.35 (2H, m, 2 × ArH), 7.67–7.72 (1H, m, ArH), 7.74–7.79 (2H, m, 2 × ArH), 8.43–8.49 (1H, m, ArH), 9.88 (1H, s, NH); δ_C (101 MHz, CDCl$_3$) 37.7 (CH$_2$), 41.2 (CH$_2$), 42.0 (2 × CH$_2$), 45.8 (CH$_2$), 46.7 (CH$_2$), 55.2 (CH$_3$), 112.4 (CH), 114.3 (CH), 116.2 (CH, d, $J_{\text{C-C-F}}$ 22.1 Hz), 120.8 (CH), 123.6 (C, d, $J_{\text{C-C-F}}$ 18.1 Hz), 125.0 (CH), 127.2 (CH), 128.3 (C), 129.2 (CH, d, $J_{\text{C-C-C-F}}$ 2.6 Hz), 129.5 (C), 129.9 (CH), 131.6 (CH), 131.7 (CH, d, $J_{\text{C-C-C-F}}$ 7.3 Hz), 133.7 (CH), 134.5 (C, d, $J_{\text{C-C-C-C-F}}$ 3.5 Hz), 136.1 (C), 145.5 (C), 157.0 (C, d, $J_{\text{C-F}}$ 246.5 Hz), 160.0 (C), 160.8 (C), 165.2 (C), 169.7 (C); *m/z* (ESI) 537.1903 (MNa$^+$. C$_{29}$H$_{27}$FN$_4$NaO$_4$ requires 537.1909).

(4-Methoxyphenyl)acetyl chloride (227)[210]

To a solution of 4-methoxyphenylacetic acid (**226**) (0.500 g, 3.01 mmol) in toluene (25 mL) was added thionyl chloride (2.19 mL, 30.1 mmol), and the resultant solution stirred vigorously under reflux for 48 h. On cooling to ambient temperature, the toluene was removed *in vacuo* and excess thionyl chloride removed by azeotroping with additional aliquots of toluene (3 × 25 mL). The resultant reside was washed with hexane (3 × 25 mL) and the organic layer concentrated *in vacuo* to afford (4-methoxyphenyl)acetyl chloride (**227**) (0.502 g, 90%) as a yellow oil, which was used without further purification. ν_{max}/cm^{-1} (neat) 2938 (CH), 1692 (CO), 1613, 1514, 1406, 1238, 1179, 1024, 816; δ_H (500 MHz, CDCl$_3$) 3.81 (3H, s, OCH$_3$), 4.08 (2H, s, CH$_2$), 6.88–6.91 (2H, m, 2 × ArH), 7.17–7.21 (2H, m, 2 × ArH); δ_C (126 MHz, CDCl$_3$) 52.3 (CH$_2$), 55.3 (CH$_3$), 114.4 (2 × CH), 123.3 (C), 130.7 (2 × CH), 159.5 (C), 172.3 (C).

4-(4''-Fluoro-3''-{4'''-[(4''''''-methoxyphenyl)acetyl]piperazine-1'''-carbonyl}benzyl)-2*H*-phthalazin-1-one (225)
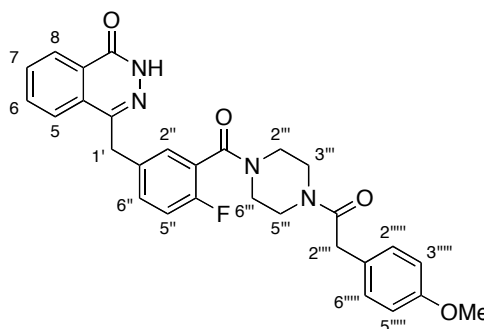
To a solution of 4-[4''-fluoro-3''-(piperazine-1'''-carbonyl)benzyl]-2*H*-phthalazin-1-one (**199**) (0.050 g, 0.14 mol) in dichloromethane (5 mL) was added (4-methoxyphenyl)acetyl chloride (**227**) (0.030 g, 0.16 mmol) followed by *N*,*N'*-diisopropylethylamine (47.5 μL, 0.273 mmol) dropwise. The resultant solution was stirred at ambient temperature for 24 h, and then diluted by the addition of water (5 mL). The organic layer was then washed with water (2 × 5 mL), dried (MgSO$_4$), filtered and concentrated *in vacuo*. Purification using flash column chromatrography (methanol/dichloromethane, 1:99) afforded 4-(4''-fluoro-3''-{4'''''-[(4''''''-methoxyphenyl)acetyl]piperazine-1'''-carbonyl}benzyl)-2*H*-phthalazin-

1-one (**225**) (0.037 g, 53%) as a white solid. NMR spectra showed a 53:47 mixture of rotamers, of which only the signals for one rotamer is recorded. Mp decomp >280 °C; ν_{max}/cm^{-1} (neat) 3188 (NH), 2918 (CH), 1634 (CO), 1611 (C=C), 1512, 1429, 1244, 1175, 1011; δ_H (400 MHz, CDCl$_3$) 3.00–3.83 (13H, m, 4 × NCH$_2$, 2''''-H$_2$ and OCH$_3$), 4.27 (2H, s, 1'-H$_2$), 6.87 (2H, d, J 8.6 Hz, 2 × ArH), 6.97–7.08 (1H, m, ArH), 7.16 (2H, d, J 8.6 Hz, 2 × ArH), 7.27–7.35 (2H, m, 2 × ArH), 7.67–7.79 (3H, m, 3 × ArH), 8.43–8.49 (1H, m, ArH), 10.33 (1H, s, NH); δ_C (101 MHz, CDCl$_3$) 37.7 (CH$_2$), 40.2 (CH$_2$), 41.9 (CH$_2$), 42.0 (CH$_2$), 45.7 (CH$_2$), 46.7 (CH$_2$), 55.3 (CH$_3$), 114.4 (2 × CH), 116.2 (CH, d, J_{C-C-F} 22.2 Hz), 123.6 (C, d, J_{C-C-F} 17.9 Hz), 125.0 (CH), 126.5 (C), 127.2 (CH), 128.3 (C), 129.2 (CH, d, $J_{C-C-C-F}$ 3.7 Hz), 129.6 (2 × CH and C), 131.6 (CH), 131.7 (CH, d, $J_{C-C-C-F}$ 7.9 Hz), 133.7 (CH), 134.4 (C, d, $J_{C-C-C-C-F}$ 3.3 Hz), 145.5 (C), 157.0 (C, d, J_{C-F} 248.0 Hz), 158.6 (C), 160.7 (C), 165.2 (C), 170.1 (C); m/z (ESI) 537.1892 (MNa$^+$. C$_{29}$H$_{27}$FN$_4$NaO$_4$ requires 537.1909).

3-Fluoropropyl-4'-methylbenzenesulfonate (230)[211]
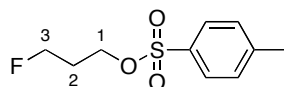
To a solution of 3-fluoropropan-1-ol (**229**) (96.2 μL, 1.28 mmol) in dichloromethane (5 mL) was added triethylamine (0.357 mL, 2.56 mmol) dropwise. The solution was cooled to 0 °C and *p*-toluenesulfonyl chloride (0.269 g, 1.41 mmol) added in small portions. The resultant mixture was allowed to warm to ambient temperature and stirred for 48 h. Water (15 mL) was added to quench the reaction and the crude product extracted using dichloromethane (3 × 20 mL). The organic layer was dried (MgSO$_4$), filtered and concentrated *in vacuo*. Purification using flash column chromatography (ethyl acetate/hexane, 15:85) gave 3-fluoropropyl-4'-methylbenzenesulfonate (**230**) (0.244 g, 82%) as a colourless oil. ν_{max}/cm^{-1} (neat) 3213, 2907 (CH), 1635 (C=C), 1496, 1429, 1255, 1159 (SO$_2$), 1004, 772; δ_H (400 MHz, CDCl$_3$) 2.04 (2H, dquint, J 26.1, 5.6 Hz, 2-H$_2$), 2.46 (3H, s, CH$_3$), 4.16 (2H, t, J 6.1 Hz, 1-H$_2$), 4.48 (2H, dt, J 46.9, 5.6 Hz, 3-H$_2$), 7.33–7.38 (2H, m, 2 × ArH), 7.78–7.82 (2H, m, 2 × ArH); δ_C (101 MHz, CDCl$_3$) 21.7 (CH$_3$), 30.0 (CH$_2$, d, J_{C-C-F} 20.1 Hz), 66.1 (CH$_2$, d, $J_{C-C-C-F}$ 4.8 Hz), 79.5 (CH$_2$, J_{C-F} 166.0 Hz), 127.9 (2 × CH), 129.9 (2 × CH), 132.8 (C), 145.0 (C); m/z (EI) 232.0565 (M$^+$. C$_{10}$H$_{13}$FO$_3$S requires 232.0569), 173 (39%), 155 (100), 84 (68), 65 (21).

5.9 Crispine C Experimental

(1'*E*)-1,2-Dimethoxy-4-(2'-nitrovinyl)benzene (248)[224]
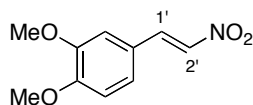
To a solution of 3,4-dimethoxybenzaldehyde (**249**) (1.00 g, 6.02 mmol) in toluene (30 mL) was added nitromethane (1.63 mL, 30.1 mmol) and ammonium acetate (0.464 g, 6.02 mmol). The resultant solution was stirred under reflux for 18 h. After cooling to ambient temperature, the reaction mixture was washed with water (2 × 30 mL) followed by brine (2 × 30 mL). The organic layer was dried (MgSO$_4$), filtered and concentrated *in vacuo* to give (1'*E*)-1,2-dimethoxy-4-(2'-nitrovinyl)benzene (**248**) (1.25 g, 100%) as a yellow solid, which was used without further purification. Mp 140–141 °C (lit.,[224] Mp 140–141 °C); ν_{max}/cm^{-1} (neat) 3127, 2999 (CH), 1627 (C=C), 1598 (NO), 1488, 1336 (NO), 1260, 1140, 1033; δ_H (400 MHz, CDCl$_3$) 3.93 (3H, s, OCH$_3$), 3.95 (3H, s, OCH$_3$), 6.92 (1H, d, *J* 8.4 Hz, ArH), 7.01 (1H, d, *J* 2.0 Hz, ArH), 7.18 (1H, dd, *J* 8.4, 2.0 Hz, ArH), 7.53 (1H, d, *J* 13.6 Hz, 2'-H), 7.97 (1H, d, *J* 13.6 Hz, 1'-H); δ_C (101 MHz, CDCl$_3$) 56.0 (CH$_3$), 56.1 (CH$_3$), 110.3 (CH), 111.4 (CH), 122.8 (C), 124.6 (CH), 135.2 (CH), 139.3 (CH), 149.6 (C), 152.8 (C); *m/z* (CI) 210.0763 (MH$^+$. C$_{10}$H$_{12}$NO$_4$ requires 210.0766), 180 (15%), 167 (21), 151 (7).

(±)-1,2-Dimethoxy-4-(1'-methoxy-2'-nitroethyl)benzene (247)[224]
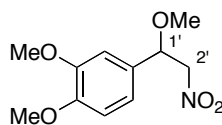
To a suspension of (1*E*)-1,2-dimethoxy-4-(2'-nitrovinyl)benzene (**248**) (4.54 g, 21.7 mmol) in methanol (100 mL) was added a commercially prepared solution of 25% sodium methoxide in methanol (10 mL) dropwise. The resultant reaction mixture was stirred at ambient temperature for 3.5 h, after which acetic acid (5 mL) was added dropwise. The mixture was stirred for a further 1.5 h and then concentrated *in vacuo*. The residue was reconstituted in toluene (100 mL) and washed with water (3 × 100 mL), and the organic layer dried (MgSO$_4$), filtered and concentrated *in vacuo*. Purification using flash column

chromatography (ethyl acetate/petroleum ether, 1:1) afforded (±)-1,2-dimethoxy-4-(1'-methoxy-2'-nitroethyl)benzene (**247**) (2.62 g, 50%) as a yellow solid. Mp 97–98 °C (lit.,[224] Mp 104–106 °C); ν_{max}/cm^{-1} (neat) 2999 (CH), 1683, 1597 (C=C), 1587 (NO), 1571, 1424, 1260, 1137, 1017; δ_H (400 MHz, CDCl$_3$) 3.26 (3H, s, OCH$_3$), 3.89 (3H, s, OCH$_3$), 3.90 (3H, s, OCH$_3$), 4.38 (1H, dd, J 12.4, 3.2 Hz, 2'-*H*H), 4.61 (1H, dd, J 12.4, 10.0 Hz, 2'-H*H*), 4.89 (1H, dd, J 10.0, 3.2 Hz, 1'-H), 6.85–6.93 (3H, m, 3 × ArH); δ_C (101 MHz, CDCl$_3$) 56.0 (CH$_3$), 56.0 (CH$_3$), 57.0 (CH$_3$), 79.9 (CH), 80.6 (CH$_2$), 109.1 (CH), 111.3 (CH), 119.6 (CH), 128.3 (C), 149.6 (2 × C); m/z (CI) 242.1029 (MH$^+$. C$_{11}$H$_{16}$NO$_5$ requires 242.1028), 228 (67%), 210 (100), 181 (51), 167 (24), 128 (6).

4-(Benzyloxycarbonylamino)butanoic acid (250)[229]
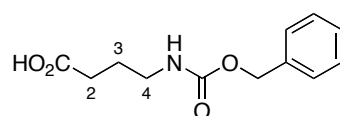
To a stirred 2 M sodium hydroxide solution (15.0 mL, 30.0 mmol) was added γ-aminobutyric acid (**251**) (3.00 g, 29.1 mmol). To this was added a further aliquot of 2 M sodium hydroxide solution (15.0 mL, 30.0 mmol) and benzyl chloroformate (4.40 mL, 30.8 mmol) simultaneously. The reaction mixture was vigorously stirred at 0–5 °C for 1 h, and then at ambient temperature for a further 1 h. The reaction mixture was extracted into diethyl ether (3 × 50 mL), and the aqueous layer acidified by the addition of concentrated hydrochloric acid solution (pH 3). After cooling in an ice bath, the resultant crystals were removed by filtration and air dried to yield the desired product (**250**) (4.82 g, 70%) as a white solid, which was used without further purification. Spectroscopic data in accordance with the literature.[229] Mp 61–62 °C (lit.,[229] mp 64–65 °C); δ_H (500 MHz, CDCl$_3$) 1.84 (2H, quint, J 7.0 Hz, 3-H$_2$), 2.40 (2H, t, J 7.0 Hz, 2-H$_2$), 3.26 (2H, q, J 7.0 Hz, 4-H$_2$), 4.92 (1H, br s, NH), 5.09 (2H, s, C*H*$_2$Ph), 5.80 (1H, br s, OH), 7.30–7.36 (5H, m, 5 × ArH); δ_C (125 MHz, CDCl$_3$) 25.0 (CH$_2$), 31.1 (CH$_2$), 40.2 (CH$_2$), 66.8 (CH$_2$), 128.1 (CH), 128.2 (2 × CH), 128.6 (2 × CH), 136.4 (C), 156.6 (C), 178.2 (C); m/z (EI) 237.0997 (M$^+$. C$_{12}$H$_{15}$NO$_4$ requires 237.1001), 219 (5%), 188 (6), 146 (4), 108 (98), 91 (100), 82 (55), 65 (53), 49 (48).

(±)-*N*-[2-(3',4'-Dimethoxyphenyl)-2-methoxyethyl]-4''-(benzyloxycarbonylamino) butanamide (245)
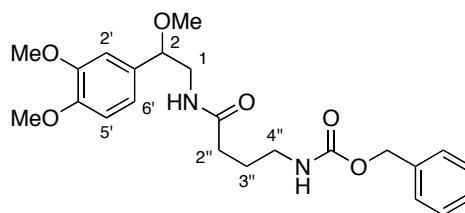
To a solution of (±)-1,2-dimethoxy-4-(1'-methoxy-2'-nitroethyl)benzene (**247**) (0.295 g, 1.22 mmol) in diethyl ether (10 mL) was added dropwise, a lithium aluminium hydride suspension (1.0 M in diethyl ether) (3.69 mL, 3.67 mmol). The resultant solution was stirred vigorously under reflux for 2 h, and then cooled to ambient temperature. Excess lithium aluminium hydride was carefully quenched by the dropwise addition of water (2.5 mL). The organic layer was separated and concentrated *in vacuo* to afford the (±)-2-(3',4'-dimethoxyphenyl)-2-methoxyethanamine (**246**) (0.078 g, 30%) as a light green oil, which was used immediately in the next step without further purification. A solution of (±)-2-(3',4'-dimethoxyphenyl)-2-methoxyethanamine (**246**) (0.078 g, 0.37 mmol) in dichloromethane (10 mL) was cooled to 0 °C, and to this was added 4-(benzyloxycarbonylamino)butanoic acid (**250**) (0.092 g, 0.39 mmol), 4-(dimethylamino)pyridine (0.005 g, 0.041 mmol) and ethyl 3-(3-dimethylaminopropyl)carbodiimide hydrochloride (0.071 g, 0.37 mmol). The resultant reaction mixture was stirred at 0 °C for 2 h, and then allowed to gradually warm to ambient temperature and stirred for 15 h. After concentration *in vacuo*, the crude reaction mixture was reconstituted in ethyl acetate (20 mL) and washed with water (3 × 20 mL). The organic layer was dried (MgSO$_4$), filtered and concentrated *in vacuo*. Purification using flash column chromatography (methanol/dichloromethane, 1:9) afforded (±)- *N*-[2-(3',4'-dimethoxyphenyl)-2-methoxyethyl]-4''-(benzyloxycarbonylamino) butanamide (**245**) (0.127 g, 79%) as a colourless oil. ν_{max}/cm^{-1} (neat) 3325 (NH), 2940 (CH), 1705 (CO), 1512, 1451, 1250, 1134, 1026, 741; δ_H (400 MHz, CDCl$_3$) 1.83 (2H, quint, *J* 6.8 Hz, 3''-H$_2$), 2.23 (2H, t, *J* 6.8 Hz, 2''-H$_2$), 3.15–3.28 (6H, m, OCH$_3$, 4''-H$_2$ and 1-*H*H), 3.60–3.70 (1H, m, 1-H*H*), 3.86 (6H, s, 2 × OCH$_3$), 4.19 (1H, dd, *J* 8.8, 4.0 Hz, 2-H), 5.09 (2H, s, OC*H*$_2$Ph), 5.14 (1H, br s, NH), 6.21 (1H, br s, NH), 6.80–6.85 (3H, m, 3 × ArH), 7.28–7.37 (5H, m, 5 × ArH); δ_C (101 MHz, CDCl$_3$) 26.0 (CH$_2$), 33.7 (CH$_2$), 40.4 (CH$_2$), 45.7 (CH$_2$), 55.9 (2 × CH$_3$), 56.7 (CH$_3$), 66.7 (CH$_2$), 82.1 (CH), 109.3 (CH), 111.0 (CH), 119.3 (CH), 128.1 (2 × CH), 128.5 (3 × CH), 131.5 (C), 136.6 (C), 148.9 (C), 149.2

(C), 156.8 (C), 172.6 (C); *m/z* (FAB) 431.2171 (MH$^+$. C$_{23}$H$_{31}$N$_2$O$_6$ requires 431.2182), 270 (40%), 181 (100), 180 (22), 151 (8), 91 (43).

(±)-1-(3',4'-Dimethoxyphenyl)-2-nitroethanol (256)[236]
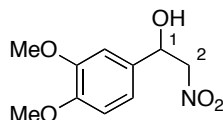
To a solution of 3,4-dimethoxybenzaldehyde (**249**) (1.50 g, 9.03 mmol) in dimethyl sulfoxide (10 mL) was added nitromethane (4.89 mL, 90.3 mmol) and 4Å molecular sieves. The reaction mixture was stirred at ambient temperature for 48 h then diluted by the addition of water (50 mL) and extracted with ethyl acetate (200 mL). The organic layer was stringently washed with water (5 × 100 mL), dried (MgSO$_4$), filtered and concentrated *in vacuo*. Purification using flash column chromatography (ethyl acetate/hexane, 1:4) afforded (±)-1-(3',4'-dimethoxyphenyl)-2-nitroethanol (**256**) (1.74 g, 85%) as a yellow solid. Spectroscopic data in accordance with the literature.[236] Mp 89–91 °C (lit.,[236] mp 91–92 °C); v_{max}/cm^{-1} (neat) 3497 (OH), 2840 (CH), 1680, 1541, 1512, 1423, 1374, 1256, 1232; δ_H (500 MHz, CDCl$_3$) 2.76 (1H, d, *J* 3.2 Hz, OH), 3.88 (3H, s, OCH$_3$), 3.90 (3H, s, OCH$_3$), 4.49 (1H, dd, *J* 13.5, 3.2 Hz, 2-*H*H), 4.61 (1H, dd, *J* 13.5, 10.0 Hz, 2-H*H*), 5.42 (1H, dt, *J* 10.0, 3.2 Hz, 1-H), 6.86–6.89 (1H, m, ArH), 6.91–6.94 (2H, m, 2 × ArH); δ_C (126 MHz, CDCl$_3$) 56.0 (CH$_3$), 56.0 (CH$_3$), 70.9 (CH), 81.3 (CH$_2$), 108.9 (CH), 111.4 (CH), 118.4 (CH), 130.7 (2 × C), 149.5 (C); *m/z* (CI) 228.0875 (MH$^+$. C$_{10}$H$_{14}$NO$_5$ requires 228.0872), 210 (77%), 181 (32), 167 (98), 165 (31), 113 (4), 85 (6), 73 (12).

(±)-1-(3',4'-Dimethoxyphenyl)-2-aminoethanol (255)[236]
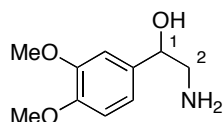
A solution of (±)-1-(3',4'-dimethoxyphenyl)-2-nitroethanol (**256**) (1.22 g, 5.37 mmol) in methanol (10 mL) was added dropwise to a suspension of 10% palladium on activated carbon (0.25 g) in methanol (10 mL) with constant stirring. The resultant reaction mixture was stirred under an atmosphere of H$_2$ at ambient temperature for 24 h. After filtering through a pad of Celite® and washing with methanol (150 mL), the solution was

concentrated *in vacuo* to afford (±)-1-(3',4'-dimethoxyphenyl)-2-aminoethanol (**255**) (1.06 g, 100%) as a pale yellow oil which was used without further purification. ν_{max}/cm^{-1} (neat) 3356 (NH/OH), 2940 (CH), 2839, 1589 (C=C), 1512, 1458, 1258, 1234, 1134; δ_H (400 MHz, CDCl$_3$) 2.79 (1H, dd, *J* 12.4, 7.6 Hz, 2-*H*H), 2.95 (1H, dd, *J* 12.4, 3.2 Hz, 2-H*H*), 3.45 (1H, br s, OH), 3.86 (3H, s, OCH$_3$), 3.87 (3H, s, OCH$_3$), 4.56–4.60 (1H, m, 1-H), 6.80–6.87 (2H, m, 2 × ArH), 6.90 (1H, br s, ArH); δ_C (101 MHz, CDCl$_3$) 49.3 (CH$_2$), 55.9 (2 × CH$_3$), 74.2 (CH), 109.0 (CH), 111.0 (CH), 118.1 (CH), 135.2 (C), 148.4 (C), 149.0 (C); *m/z* (CI) 198 (MH$^+$, 100%), 180 (98), 167 (95), 139 (7), 85 (3), 69 (4).

(±)-*N*-[2-(3',4'-Dimethoxyphenyl)-2-hydroxyethyl]-4''-(benzyloxycarbonylamino) butanamide (257)
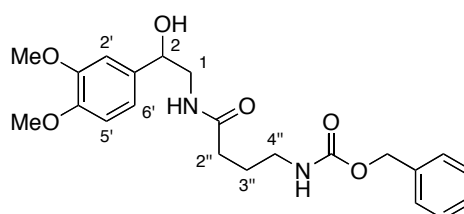
A solution of 4-(benzyloxycarbonylamino)butanoic acid (**250**) (0.518 g, 2.18 mmol) and ethyl 3-(3-dimethylaminopropyl)carbodiimide hydrochloride (0.399 g, 2.08 mmol) in dichloromethane (10 mL) was stirred at 0 °C for 0.2 h. 4-(Dimethylamino)pyridine (0.025 g, 0.20 mmol) was added and the solution stirred for a further 0.2 h. A solution of (±)-1-(3',4'-dimethoxyphenyl)-2-aminoethanol (**255**) (0.410 g, 2.08 mmol) in dichloromethane (10 mL) was then added dropwise to the reaction mixture and stirred for 2 h at 0 °C. The reaction mixture was then allowed to gradually warm to ambient temperature and stirred for a further 16 h. The mixture was diluted with dichloromethane (50 mL) and washed with water (3 × 50 mL). The organic layer was dried (MgSO$_4$), filtered and concentrated *in vacuo*. Purification using flash column chromatography (methanol/dichloromethane, 1:99) afforded (±)-*N*-[2-(3',4'-dimethoxyphenyl)-2-hydroxyethyl]-4''-(benzyloxycarbonylamino) butanamide (**257**) (0.680 g, 79%) as a brown oil. ν_{max}/cm^{-1} (neat) 3308 (OH/NH), 2938 (CH), 1699 (CO), 1645 (C=C), 1514, 1256, 1234, 1138, 1024; δ_H (400 MHz, CDCl$_3$) 1.70–1.86 (2H, m, 3''-H$_2$), 2.18 (2H, t, *J* 6.8 Hz, 2''-H$_2$), 3.10–3.29 (3H, m, 4''-H$_2$ and 1-*H*H), 3.56–3.65 (1H, m, 1-H*H*), 3.82 (3H, s, OCH$_3$), 3.83 (3H, s, OCH$_3$), 4.74 (1H, dd, *J* 8.4, 2.8 Hz, 2-H), 5.04 (2H, s, OC*H*$_2$Ph), 5.31 (1H, t, *J* 6.0 Hz, NH), 6.60 (1H, t, *J* 5.6 Hz, NH), 6.77–6.92 (3H, m, 3 × ArH), 7.27–7.32 (5H, m, 5 × ArH); δ_C (101 MHz, CDCl$_3$) 26.2 (CH$_2$), 33.3 (CH$_2$), 40.1 (CH$_2$), 47.7 (CH$_2$), 55.9 (CH$_3$), 55.9

(CH$_3$), 66.8 (CH$_2$), 73.0 (CH), 109.1 (CH), 111.1 (CH), 118.1 (CH), 128.1 (2 × CH), 128.5 (3 × CH), 134.6 (C), 136.4 (C), 148.5 (C), 149.0 (C), 157.1 (C), 173.8 (C); *m/z* (FAB) 417.2023 (MH$^+$. C$_{22}$H$_{29}$N$_2$O$_6$ requires 417.2026), 389 (20%), 249 (20), 179 (33), 150 (12), 91 (100), 84 (75), 57 (28).

4-(1',3'-Dioxo-1',3'-dihydro-2'*H*-isoindolin-2'-yl)butanoic acid (259)[237]
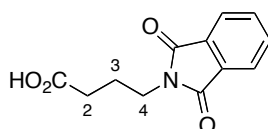
A neat mixture of γ-aminobutyric acid (**251**) (1.00 g, 9.70 mmol) and phthalic anhydride (**258**) (1.44 g, 9.70 mmol) were stirred at 170 °C for 5 h. After cooling to ambient temperature, the resulting solid was dissolved in dichloromethane (50 mL) and washed with 0.1 M hydrochloric acid (3 × 20 mL). The organic layer was dried (MgSO$_4$), filtered and concentrated under reduced pressure to yield 4-(1',3'-dioxo-1',3'-dihydro-2'*H*-isoindolin-2'-yl)butanoic acid (**259**) (2.11 g, 93%) as a white solid. Spectroscopic data in accordance with the literature.[237] Mp 111–113 °C (lit.,[237] mp 117 °C); ν$_{max}$/cm^{-1} (neat) 2940 (OH), 1766 (CO), 1696 (CO), 1469, 1436, 1312, 1284, 1120, 893; δ$_H$ (400 MHz, CDCl$_3$) 2.03 (2H, quint, *J* 7.0 Hz, 3-H$_2$), 2.43 (2H, t, *J* 7.0 Hz, 2-H$_2$), 3.77 (2H, t, *J* 7.0 Hz, 4-H$_2$), 7.70–7.75 (2H, m, 2 × ArH), 7.83–7.88 (2H, m, 2 × ArH); δ$_C$ (101 MHz, CDCl$_3$) 23.7 (CH$_2$), 31.0 (CH$_2$), 37.1 (CH$_2$), 123.3 (2 × CH), 132.0 (2 × C), 134.0 (2 × CH), 168.4 (2 × C), 177.0 (C); *m/z* (EI) 233.0691 (M$^+$. C$_{12}$H$_{11}$NO$_4$ requires 233.0688), 215 (40%), 187 (22), 174 (80), 160 (100), 130 (14), 104 (22), 76 (23), 49 (11).

(±)-*N*-[2-(3',4'-Dimethoxyphenyl)-2-hydroxyethyl]-4''-(1''',3'''-dioxo-1''',3'''-dihydro-2'''*H*-isoindolin-2'''-yl)butanamide (260)
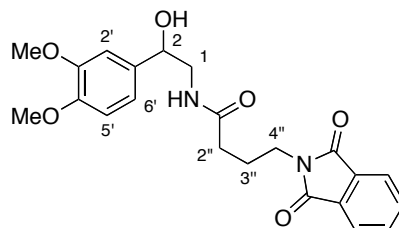
A solution of 4-(1',3'-dioxo-1',3'-dihydro-2'*H*-isoindolin-2'-yl)butanoic acid (**259**) (0.406 g, 1.74 mmol) and ethyl 3-(3-dimethylaminopropyl)carbodiimide hydrochloride (0.318 g,

1.66 mmol) in dichloromethane (10 mL) was stirred at 0 °C for 0.25 h. 4-(Dimethylamino)pyridine (0.020 g, 0.16 mmol) was added and the solution stirred for a further 0.25 h. A solution of (±)-1-(3',4'-dimethoxyphenyl)-2-aminoethanol (**255**) (0.327 g, 1.66 mmol) in dichloromethane (10 mL) was then added dropwise to the reaction mixture and stirred for 2 h at 0 °C. After gradually warming to ambient temperature, the mixture was stirred for a further 16 h before being diluted with dichloromethane (100 mL) and washed with water (3 × 100 mL). The organic layer was dried (MgSO$_4$), filtered and concentrated *in vacuo*. Purification using flash column chromatography (methanol/dichloromethane, 1:99) followed by trituration with diethyl ether afforded (±)-*N*-[2-(3',4'-dimethoxyphenyl)-2-hydroxyethyl]-4''-(1''',3'''-dioxo-1''',3'''-dihydro-2'''*H*-isoindolin-2'''-yl)butanamide (**260**) (0.512 g, 75%) as an off-white solid. Mp 120–123 °C; ν_{max}/cm^{-1} (neat) 3366 (NH/OH), 2938 (CH), 1769 (CO), 1703 (CO), 1515, 1396, 1259, 1232, 1023; δ_H (400 MHz, CDCl$_3$) 2.01–2.10 (2H, m, 3'-H$_2$), 2.16–2.33 (2H, m, 2'-H$_2$), 3.31 (1H, ddd, *J* 13.6, 8.4, 5.2 Hz, 1-*H*H), 3.54 (1H, br s, OH), 3.66–3.74 (3H, m, 4'-H$_2$ and 1-H*H*), 3.87 (3H, s, OCH$_3$), 3.89 (3H, s, OCH$_3$), 4.85 (1H, dd, *J* 8.4, 2.4 Hz, 2-H), 6.34 (1H, t, *J* 5.2 Hz, NH), 6.84–6.86 (1H, m, ArH), 6.89–6.96 (2H, m, 2 × ArH), 7.71–7.76 (2H, m, 2 × ArH), 7.83–7.87 (2H, m, 2 × ArH); δ_C (101 MHz, CDCl$_3$) 24.9 (CH$_2$), 33.5 (CH$_2$), 37.1 (CH$_2$), 47.8 (CH$_2$), 55.9 (CH$_3$), 56.0 (CH$_3$), 73.3 (CH), 109.0 (CH), 111.1 (CH), 118.0 (CH), 123.4 (2 × CH), 132.0 (2 × C), 134.2 (2 × CH), 134.4 (C), 148.6 (C), 149.1 (C), 168.8 (2 × C), 173.1 (C); *m/z* (FAB) 413.1711 (MH$^+$. C$_{22}$H$_{25}$N$_2$O$_6$ requires 413.1713), 395 (37%), 307 (100), 289 (56), 216 (18), 154 (79), 136 (68).

1-[3'-(1'',3''-Dioxo-1'',3''-dihydro-2''*H*-isoindolin-2''-yl)propyl]-6,7-dimethoxyisoquinoline (261)
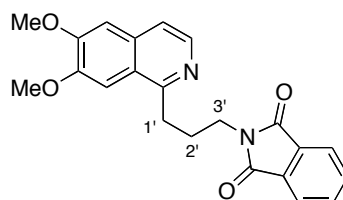
A solution of *N*-[2-(3',4'-dimethoxyphenyl)-2-hydroxyethyl]-4''-(1''',3'''-dioxo-1''',3'''-dihydro-2'''*H*-isoindolin-2'''-yl)butanamide (**260**) (2.05 g, 4.97 mmol) in toluene (15 mL) was stirred vigorously under reflux, and to this was added freshly distilled phosphorus oxychloride (1.16 mL, 12.4 mmol) dropwise. The reaction mixture was stirred for 18 h and then cooled to ambient temperature. After concentration *in vacuo*, the crude reaction

mixture was purified using flash column chromatography (methanol/dichloromethane, 1:99) to afford 1-[3'-(1'',3''-dioxo-1'',3''-dihydro-2''H-isoindolin-2''-yl)propyl]-6,7-dimethoxyisoquinoline (**261**) (1.23 g, 66%) as a light brown solid. Mp 125–127 °C; ν_{max}/cm^{-1} (neat) 3308, 2969 (CH), 2629, 1688 (CO), 1508, 1400, 1273, 1166, 1122; δ_H (500 MHz, CD$_3$OD) 2.38 (2H, quint, J 7.0 Hz, 2'-H$_2$), 3.52–3.57 (2H, m, 1'-H$_2$), 3.90 (2H, t, J 7.0 Hz, 3'-H$_2$), 4.05 (3H, s, OCH$_3$), 4.08 (3H, s, OCH$_3$), 7.47 (1H, s, ArH), 7.62 (1H, s, ArH), 7.77–7.79 (4H, m, 4 × ArH), 7.96 (1H, d, J 6.5 Hz, ArH), 8.17 (1H, d, J 6.5 Hz, ArH); δ_C (126 MHz, CD$_3$OD) 28.8 (CH$_2$), 29.9 (CH$_2$), 38.3 (CH$_2$), 57.1 (CH$_3$), 57.4 (CH$_3$), 105.6 (CH), 107.5 (CH), 123.1 (CH), 123.6 (C), 124.1 (2 × CH), 130.4 (CH), 133.1 (2 × C), 135.5 (2 × CH), 138.5 (C), 154.5 (C), 156.5 (C), 159.2 (C), 169.7 (2 × C); m/z (CI) 377.1503 (MH$^+$. C$_{22}$H$_{21}$N$_2$O$_4$ requires 377.1501), 279 (4%), 203 (3), 161 (5), 120 (11), 69 (8).

1-[3'-{*N,N'*-Bis(*tert*-butoxycarbonyl)guanidino}propyl]-6,7-dimethoxyisoquinoline (262)
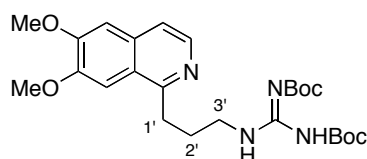
To a solution of 1-[3'-(1'',3''-dioxo-1'',3''-dihydro-2''H-isoindolin-2''-yl)propyl]-6,7-dimethoxyisoquinoline (**261**) (0.044 g, 0.12 mmol) in ethanol (10 mL) was added hydrazine monohydrate (12.9 μL, 0.266 mmol) and the resultant solution stirred under reflux for 20 h. After cooling to ambient temperature, the mixture was concentrated *in vacuo* and the crude residue reconstituted in methanol (10 mL). To this was added *N,N'*-bis(*tert*-butoxycarbonyl)-1H-pyrazole-1-carboxamidine (0.25 g, 0.80 mmol) followed by 4-dimethylaminopyridine (0.001 g, 0.008 mmol) and the reaction mixture stirred at ambient temperature for further 24 h. Concentration *in vacuo*, followed by purification using flash column chromatography (methanol/chloroform, 1:99) afforded 1-[3'-{*N,N'*-bis(*tert*-butoxycarbonyl)guanidino}propyl]-6,7-dimethoxyisoquinoline (**262**) (0.05 g, 82%) as a pale yellow oil. ν_{max}/cm^{-1} (neat) 3361 (NH), 2479, 2247, 2216, 2070, 1122, 1092, 973; δ_H (400 MHz, CD$_3$OD) 1.45 (9H, s, O^{t}Bu), 1.52 (9H, s, O^{t}Bu), 2.11 (2H, quint, J 6.8 Hz, 2'-H$_2$), 3.27–3.29 (2H, m, 1'-H$_2$), 3.51 (2H, q, J 6.8 Hz, 3'-H$_2$), 4.00 (3H, s, OCH$_3$), 4.01 (3H, s, OCH$_3$), 7.29 (1H, s, ArH), 7.47 (1H, s, ArH), 7.56 (1H, d, J 6.0 Hz, ArH), 8.15 (1H, d, J 6.0 Hz, ArH); δ_C (126 MHz, CD$_3$OD) 28.3 (3 × CH$_3$), 28.6 (3 × CH$_3$), 30.0 (CH$_2$),

33.1 (CH$_2$), 41.6 (CH$_2$), 56.5 (CH$_3$), 56.6 (CH$_3$), 80.3 (C), 84.4 (C), 104.7 (CH), 106.7 (CH), 120.2 (CH), 124.1 (C), 135.2 (C), 140.5 (CH), 152.0 (C), 154.8 (C), 157.6 (C), 159.8 (C), 164.5 (C); *m/z* (FAB) 489.2715 (MH$^+$. C$_{25}$H$_{37}$N$_4$O$_6$ requires 489.2713), 389 (4%), 289 (27), 230 (12), 205 (8), 149 (3), 58 (10).

1-(3'-Guanidinopropyl)-6,7-dimethoxyisoquinoline (Crispine C) (243)[214]
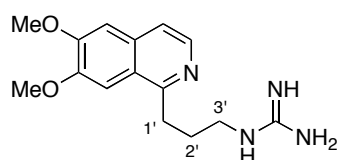
To a stirred solution of 1-[3'-{*N,N'*-bis(*tert*-butoxycarbonyl)guanidino}propyl]-6,7-dimethoxyisoquinoline (**262**) (0.050 g, 0.10 mmol) in dichloromethane (5 mL) was added trifluoroacetic acid (0.25 mL). The reaction mixture was stirred at ambient temperature for 2 h and then concentrated *in vacuo*. The crude residue was reconstituted in methanol (3 mL) and to this was added a few drops of concentrated hydrochloric acid. After stirring at ambient temperature for 0.5 h, the mixture was concentrated *in vacuo* to yield a crude residue, which upon trituration with dichloromethane afforded 1-(3'-guanidinopropyl)-6,7-dimethoxyisoquinoline (Crispine C) (**243**) (0.025 g, 73%) as a pale yellow solid. Mp 203–204 °C (lit.,[214] mp 208–210 °C); ν_{max}/cm^{-1} (neat) 3317 (NH), 3131, 1652, 1634, 1508, 1409, 1280, 1232, 1167; δ_H (500 MHz, CD$_3$OD) 2.18 (2H, quint, *J* 7.1 Hz, 2'-H$_2$), 3.43 (2H, t, *J* 7.1 Hz, 1'-H$_2$), 3.59–3.62 (2H, m, 3'-H$_2$), 4.12 (3H, s, OCH$_3$), 4.12 (3H, s, OCH$_3$), 7.66 (1H, s, ArH), 7.70 (1H, s, ArH), 8.12 (1H, d, *J* 6.6 Hz, ArH), 8.24 (1H, d, *J* 6.6 Hz, ArH); δ_C (126 MHz, CD$_3$OD) 29.5 (CH$_2$), 29.7 (CH$_2$), 41.8 (CH$_2$), 57.4 (CH$_3$), 57.5 (CH$_3$), 105.6 (CH), 107.6 (CH), 123.3 (CH), 123.8 (C), 130.4 (CH), 138.9 (C), 154.9 (C), 156.3 (C), 158.8 (C), 159.6 (C); *m/z* (FAB) 289.1662 (MH$^+$. C$_{15}$H$_{21}$N$_4$O$_2$ requires 289.1665), 242 (3%), 154 (100), 136 (63), 120 (11), 107 (20), 89 (15), 77 (13).

6 References

1   S. M. Ametamey, M. Honer and P. A. Schubiger, *Chem. Rev.*, 2008, **108**, 1501.

2   W. Semmler and M. Schwaiger, *Molecular Imaging I*, Springer, Berlin, 2008.

3   S. L. Pimlott and A. Sutherland, *Chem. Soc. Rev.*, 2011, **40**, 149.

4   S. Vallabhajosula, *Molecular Imaging: Radiopharmaceuticals for PET and SPECT*, Springer, Berlin, 2009.

5   R. N. Gibson, *Essential Medical Imaging*, Cambridge University Press, Cambridge, 2009.

6   P. W. Miller, N. J. Long, R. Vilar and A. D. Gee, *Angew. Chem. Int. Ed.*, 2008, **47**, 8998.

7   S. L. Kitson, V. Cuccurullo, A. Ciarmiello, D. Salvo and L. Mansi, *Curr. Radiopharm.*, 2009, **2**, 224.

8   A. K. Buck, S. Nekolla, S. Ziegler, A. Beer, B. J. Krause, K. Herrmann, K. Scheidhauer, H.-J. Wester, E. J. Rummeny, M. Schwaiger and A. Drzezga, *J. Nucl. Med.*, 2008, **49**, 1305.

9   W. Zhang, S. Oya, M.-P. Kung, C. Hou, D. L. Maier and H. F. Kung, *Nucl. Med. Biol.*, 2005, **32**, 799.

10   Parkinson's, www.parkinsons.org.uk/content/about-parkinsons, Accessed 20 August 2014.

11   J. L. Neumeyer, A. Campbell, S. Wang, Y. Gao, R. A. Milius, N. S. Kula, R. J. Baldessarini, Y. Zea-Ponce, R. M. Baldwin and R. B. Innis, *J. Med. Chem.*, 1994, **37**, 1558.

12   C. Braestrup, R. Albrechtsen and R. F. Squires, *Nature*, 1977, **269**, 702.

13   S. Taliani, I. Pugliesi and F. Da Settimo, *Curr. Topics Med. Chem.*, 2011, **11**, 860.

14   V. Papadopoulos, M. Baraldi, T. R. Guilarte, T. B. Knudsen, J.-J. Lacapère, P. Lindemann, M. D. Norenberg, D. Nutt, A. Weizman, M.-R. Zhang and M. Gavish, *Trends Pharmacol. Sci.*, 2006, **27**, 402.

15   R. Sprengel, P. Werner, P. H. Seeburg, A. G. Mukhin, M. R. Santi, D. R. Grayson, A. Guidotti and K. E. Krueger, *J. Biol. Chem.*, 1989, **264**, 20415.

16   B. Costa, A. Salvetti, L. Rossi, F. Spinetti, A. Lena, B. Chelli, M. Rechichi, E. Da Pozzo, V. Gremigni and C. Martini, *Mol. Pharmacol.*, 2006, **69**, 37.

17   P. Casellas, S. Galiegue and A. S. Basile, *Neurochem. Int.*, 2002, **40**, 475.

18   V. Papadopoulos, H. Amri, N. Boujrad, C. Cascio, M. Culty, M. Garnier, M. Hardwick, H. Li, B. Vidic, A. S. Brown, J. L. Reversa, J. M. Bernassau and K. Drieu, *Steroids*, 1997, **62**, 21.

19   A. M. Scarf and M. Kassiou, *J. Nucl. Med.*, 2011, **52**, 677.

20   A. S. C. Ching, B. Kuhnast, A. Damont, D. Roeda, B. Tavitian and F. Dollé, *Insights Imaging*, 2012, **3**, 111.

21   M. Gavish, I. Bachman, R. Shoukrun, Y. Katz, L. Veenman, G. Weisinger and A. Weizman, *Pharmacol. Rev.*, 1999, **51**, 629.

22   A. M. Scarf, L. M. Ittner and M. Kassiou, *J. Med. Chem.*, 2009, **52**, 581.

23   R. Rupprecht, V. Papadopoulos, G. Rammes, T. C. Baghai, J. Fan, N. Akula, G. Groyer, D. Adams and M. Schumacher, *Nat. Rev. Drug Discov.*, 2010, **9**, 971.

24   N. Boujrad, B. Vidic and V. Papadopoulos, *Endocrinology*, 1996, **137**, 5727.

25   D. M. Zisterer and D. C. Williams, *Gen. Pharmac.*, 1997, **29**, 305.

26   C. J. D. Austin, J. Kahlert, M. Kassiou and L. M. Rendina, *Int. J. Biochem. Cell Biol.*, 2013, **45**, 1212.

27   V. Papadopoulos, L. Lecanu, R. C. Brown, Z. Han and Z.-X. Yao, *Neuroscience*, 2006, **138**, 749.

28   S. Venneti, B. J. Lopresti and C. A. Wiley, *Prog. Neurobiol.*, 2006, **80**, 308.

29   A. Cagnin, M. Kassiou, S. R. Meikle and R. B. Banati, *Neurotherapeutics*, 2007, **4**, 443.

30   J. Gerhmann, Y. Matsumoto and G. W. Kreutzberg, *Brain Res. Rev.*, 1995, **20**, 269.

31   C. C. Chao, S. Hu, T. W. Molitor, E. G. Shaskan and P. K. Peterson, *J. Immunol.*, 1992, **149**, 2736.

32   C. C. Chao, S. Hu and P. K. Peterson, *J. Leukocyte Biol.*, 1995, **58**, 65.

33   A. H. Jacobs and B. Tavitian, *J. Cereb. Blood Flow Metab.*, 2012, **32**, 1393.

34   K. Nakajima and S. Kohsaka, *J. Biochem.*, 2001, **130**, 169.

35   J. Bauer, T. Sminia, F. G. Wouterlood and C. D. Dijkstra, *J. Neurosci. Res.*, 1994, **38**, 365.

36   A. Gerhard, N. Pavese, G. Hotton, F. Turkheimer, M. Es, A. Hammers, K. Eggert, W. Oertel, R. B. Banati and D. J. Brooks, *Neurobiol. Dis.*, 2006, **21**, 404.

37   H. Mühleisen, J. Gehrmann and R. Meyermann, *Neuropath. App. Neurobiol.*, 1995, **21**, 505.

38   F. Dollé, C. Luus, A. Reynolds and M. Kassiou, *Curr. Med. Chem.*, 2009, **16**, 2899.

39   M. E. Van Dort, B. J. Ciliax, D. L. Gildersleeve, P. S. Sherman, K. C. Rosenspire, A. B. Young, L. Junck and D. M. Wieland, *J. Med. Chem.*, 1988, **31**, 2081.

40   D. R. Turton, V. W. Pike, M. Cartoon and D. A. Widdowson, *J. Labelled Compd. Radiopharm.*, 1984, **21**, 1209.

41   L. Junck, J. M. M. Olson, B. J. Ciliax, R. A. Koeppe, G. L. Watkins, D. M. Jewett, P. E. McKeever, D. M. Wieland, M. R. Kilbourn, S. Starosta-Rubinstein, W. R. Mancini, D. E. Kuhl, H. S. Greenberg and A. B. Young, *Ann. Neurol.*, 1989, **26**, 752.

42   P. J. Schweitzer, B. A. Fallon, J. J. Mann and J. S. D. Kumar, *Drug Discov. Today*, 2010, **15**, 933.

43   A. Cagnin, A. Gerhard and R. B. Banati, *Eur. Neuropsychopharmacol.*, 2002, **12**, 581.

44   A. Cappelli, P. G. Mohr, A. Gallelli, G. Giuliani, M. Anzini, S. Vomero, M. Fresta, P. Porcu, E. Maciocco, A. Concas, G. Biggio and A. Donati, *J. Med. Chem.*, 2003, **46**, 3568.

45   L. Stevenson, S. L. Pimlott and A. Sutherland, *Tetrahedron Lett.*, 2007, **48**, 7137.

46   Y. L. Janin, E. Roulland, A. Beurdeley-Thomas, D. Decaudin, C. Monneret and M.-F. Poupon, *J. Chem. Soc., Perkin Trans. 1*, 2002, 529.

47   H. C. Manning, T. Goebel, J. N. Marx and D. J. Bornhop, *Org. Lett.*, 2002, **4**, 1075.

48   R. Camsonne, C. Crouzel, D. Comar, M. Mazière, C. Prenant, J. Sastre, M. A. Moulin and A. Syrota, *J. Labelled Compd. Radiopharm.*, 1984, **21**, 985.

49   P. Charbonneau, A. Syrota, C. Crouzel, J. M. Valois and C. Prenant, *Circulation*, 1986, **73**, 476.

50   F. Shah, S. P. Hume, V. W. Pike, S. Ashworth and J. McDermott, *Nucl. Med. Biol.*, 1994, **21**, 573.

51   O. Rahman, T. Kihlberg and B. Langström, *J. Chem. Soc., Perkin Trans. 1*, 2002, 2699.

52   S. L. Pimlott, L. Stevenson, D. J. Wyper and A. Sutherland, *Nucl. Med. Biol.*, 2008, **35**, 537.

53   W. Yu, E. Wang, R. J. Voll, A. H. Miller and M. M. Goodman, *Bioorg. Med. Chem.*, 2008, **16**, 6145.

54   J. L. Hughes, P. S. Jones, J. S. Beech, D. Wang, D. K. Menon, F. I. Aigbirhio, T. D. Fryer and J. C. Baron, *NeuroImage*, 2012, **59**, 2007.

55   P. Gunnarsson, L. Levander, P. Pahlsson and M. Grenegard, *FASEB J.*, 2007, **21**, 4059.

56   A. P. Kozikowski, D. Ma, J. Brewer, S. Sun, E. Costa, E. Romeo and A. Guidotti, *J. Med. Chem.*, 1993, **36**, 2908.

57   E. Romeo, S. Cavallaro, A. Korneyev, A. P. Kozikowski, D. Ma, A. Polo, E. Costa and A. Guidotti, *J. Pharmacol. Exp. Ther.*, 1993, **267**, 462.

58   E. Romeo, J. Auta, A. P. Kozikowski, D. Ma, V. Papadopoulos, G. Puia, E. Costa and A. Guidotti, *J. Pharmacol. Exp. Ther.*, 1992, **262**, 971.

59   V. Vin, N. Leducq, F. Bono and J. M. Herbert, *Biochem. Biophys. Res. Commun.*, 2003, **310**, 785.

60   I. Bennacef, C. N. Haile, A. Schmidt, A. O. Koren, J. P. Seibyl, J. K. Staley, F. Bois, R. M. Baldwin and G. Tamagnan, *Bioorg. Med. Chem.*, 2006, **14**, 7582.

61   F. Chauveau, H. Boutin, N. Van Camp, F. Dollé and B. Tavitian, *Eur. J. Nucl. Med. Mol. Imaging*, 2008, **35**, 2304.

62   B. Gulyás, A. Vas, C. Halldin, J. Sovago, J. Sandell, H. Olsson, A. Fredriksson, S. Stone-Elander and L. Farde, *Nucl. Med. Biol.*, 2002, **29**, 753.

63   A. Vas, Y. Shchukin, Z. Karrenbauer, K. Cselényi, J. Kostulas, I. Hillert, A. Savic, C. Takano, C. Halldin and B. Gulyás, *J. Neurol. Sci.*, 2008, **264**, 9.

64   A. Kita, H. Kohayakawa, T. Kinoshita, Y. Ochi, K. Nakamichi, S. Kurumiya, K. Furukawa and M. Oka, *Br. J. Pharmacol.*, 2004, **142**, 1059.

65   K. Yanamoto, M.-R. Zhang, K. Kumata, A. Hatori, M. Okada and K. Suzuki, *Neurosci. Lett.*, 2007, **428**, 59.

66   S. Z. Langer, S. Arbilla, J. Benavides and B. Scatton, *Adv. Biochem. Pyschopharmacol.*, 1990, **46**, 61.

67   A. Trapani, C. Palazzo, M. de Candia, F. M. Lasorsa and G. Trapani, *Bioconj. Chem.*, 2013, **24**, 1415.

68   C. J. R. Fookes, T. Q. Pham, F. Mattner, I. Greguric, C. Loc'h, X. Liu, P. Berghofer, R. Shepherd, M.-C. Gregoire and A. Katsifis, *J. Med. Chem.*, 2008, **51**, 3700.

69   S. Selleri, F. Bruni, C. Costagli, A. Costanzo, G. Guerrini, G. Ciciani, B. Costa and C. Martini, *Bioorg. Med. Chem.*, 2001, **9**, 2661.

70   S. Selleri, P. Gratteri, C. Costagli, C. Bonaccini, A. Costanzo, F. Melani, G. Guerrini, G. Ciciani, B. Costa, F. Spinetti, C. Martini and F. Bruni, *Bioorg. Med. Chem.*, 2005, **13**, 4821.

71   M. L. James, R. R. Fulton, D. J. Henderson, S. Eberl, S. R. Meikle, S. Thomson, R. D. Allan, F. Dolle, M. J. Fulham and M. Kassiou, *Bioorg. Med. Chem.*, 2005, **13**, 6188.

72   C. Thominiaux, F. Dollé, M. L. James, Y. Bramoullé, H. Boutin, L. Besret, M. C. Grégoire, H. Valette, M. Bottlaender, B. Tavitian, P. Hantraye, S. Selleri and M. Kassiou, *Appl. Radiat. Isot.*, 2006, **64**, 570.

73   M. L. James, R. R. Fulton, J. Vercoullie, D. J. Henderson, L. Garreau, S. Chalon, F. Dolle, S. Selleri, D. Guilloteau and M. Kassiou, *J. Nucl. Med.*, 2008, **49**, 814.

74   D. Tang, M. R. Hight, E. T. McKinley, A. Fu, J. R. Buck, R. A. Smith, M. N. Tantawy, T. E. Peterson, D. C. Colvin, M. S. Ansari, M. Nickels and H. C. Manning, *J. Nucl. Med.*, 2012, **53**, 287.

75   N. Arlicot, J. Vercouillie, M.-J. Ribeiro, C. Tauber, Y. Venel, J.-L. Baulieu, S. Maia, P. Corcia, M. G. Stabin, A. Reynolds, M. Kassiou and D. Guilloteau, *Nucl. Med. Biol.*, 2012, **39**, 570.

76   T. Okubo, R. Yoshikawa, S. Chaki, S. Okuyama and A. Nakazato, *Bioorg. Med. Chem.*, 2004, **12**, 423.

77   S. Okuyama, S. Chaki, R. Yoshikawa, S.-i. Ogawa, Y. Suzuki, T. Okubo, A. Nakazato, M. Nagamine and K. Tomisawa, *Life Sci.*, 1999, **64**, 1455.

78   M. Culty, P. Silver, A. Nakazato, M. Gazouli, H. Li, M. Muramatsu, S. Okuyama and V. Papadopoulos, *Drug Develop. Res.*, 2001, **52**, 475.

79   E. Briard, S. S. Zoghbi, F. G. Siméon, M. Imaizumi, J. P. Gourley, H. U. Shetty, S. Lu, M. Fujita, R. B. Innis and V. W. Pike, *J. Med. Chem.*, 2009, **52**, 688.

80   Y. Fujimura, Y. Kimura, F. G. Siméon, L. P. Dickstein, V. W. Pike, R. B. Innis and M. Fujita, *J. Nucl. Med.*, 2010, **51**, 145.

81   M. Wang, M. Gao, K. D. Miller and Q.-H. Zheng, *Steroids*, 2011, **76**, 1331.

82   L. P. Dickstein, S. S. Zoghbi, Y. Fujimura, M. Imaizumi, Y. Zhang, V. W. Pike, R. B. Innis and M. Fujita, *Eur. J. Nucl. Med. Mol. Imaging*, 2011, **38**, 352.

83   D. R. Owen, O. W. Howell, S.-P. Tang, L. A. Wells, I. Bennacef, M. Bergstrom, R. N. Gunn, E. A. Rabiner, M. R. Wilkins, R. Reynolds, P. M. Matthews and C. A. Parker, *J. Cereb. Blood Flow Metab.*, 2010, **30**, 1608.

84   D. R. J. Owen, R. N. Gunn, E. A. Rabiner, I. Bennacef, M. Fujita, W. C. Kreisl, R. B. Innis, V. W. Pike, R. Reynolds, P. M. Matthews and C. A. Parker, *J. Nucl. Med.*, 2011, **52**, 24.

85   D. R. Owen, A. J. Yeo, R. N. Gunn, K. Song, G. Wadsworth, A. Lewis, C. Rhodes, D. J. Pulford, I. Bennacef, C. A. Parker, P. L. StJean, L. R. Cardon, V. E. Mooser, P. M. Matthews, E. A. Rabiner and J. P. Rubio, *J. Cereb. Blood Flow Metab.*, 2012, **32**, 1.

86   S. Venneti, B. J. Lopresti and C. A. Wiley, *Glia*, 2013, **61**, 10.

87   R. H. Bradbury, C. P. Allott, M. Dennis, E. Fisher, J. S. Major, B. B. Masek, A. A. Oldham, R. J. Pearce and N. Rankine, *J. Med. Chem.*, 1992, **35**, 4027.

88   L. Kürti and B. Czakó, *Strategic Applications of Named Reactions in Organic Synthesis*, Elsevier Academic Press, London, 2005.

89   L. Stevenson, A. A. S. Tavares, A. Brunet, F. I. McGonagle, D. Dewar, S. L. Pimlott and A. Sutherland, *Bioorg. Med. Chem. Lett.*, 2010, **20**, 954.

90   N. Miyaura and A. Suzuki, *J. Chem. Soc., Chem Commun.*, 1979, 866.

91   A. Suzuki, *Angew. Chem. Int. Ed.*, 2011, **50**, 6722.

92   N. Miyaura and A. Suzuki, *Chem. Rev.*, 1995, **95**, 2457.

93   A. L. Casado and P. Espinet, *Organometallics*, 1998, **17**, 954.

94   K. Matos and J. A. Soderquist, *J. Org. Chem.*, 1998, **63**, 461.

95   S. Guillou and Y. L. Janin, *J. Heterocyclic Chem.*, 2008, **45**, 1377.

96   R. Nakao, H. Rhee and Y. Uozumi, *Org. Lett.*, 2004, **7**, 163.

97   T. D. Sheppard, *Org. Biomol. Chem.*, 2009, **7**, 1043.

98   S. H. Yang, C. S. Li and C. H. Cheng, *J. Org. Chem.*, 1987, **52**, 691.

99   A. A. Cant, R. Bhalla, S. L. Pimlott and A. Sutherland, *Chem. Commun.*, 2012, **48**, 3993.

100   I. Cepanec, *Synthesis of Biaryls*, Elsevier, Oxford, 2004.

101   A. Klapars and S. L. Buchwald, *J. Am. Chem. Soc.*, 2002, **124**, 14844.

102   A. Fürstner and J. W. J. Kennedy, *Chem. Eur. J.*, 2006, **12**, 7398.

103   F. R. Leroux and H. Mettler, *Adv. Synth. Catal.*, 2007, **349**, 323.

104   R. Bolton, *J. Labelled Comp. Radiopharm.*, 2002, **45**, 485.

105   R. H. Seevers and R. E. Counsell, *Chem. Rev.*, 1982, **82**, 575.

106   B. Biasotti, S. Dallavalle, L. Merlini, C. Farina, S. Gagliardi, C. Parini and P. Belfiore, *Bioorg. Med. Chem.*, 2003, **11**, 2247.

107   L. Lunazzi, M. Mancinelli, A. Mazzanti, S. Lepri, R. Ruzziconi and M. Schlosser, *Org. Biomol. Chem.*, 2012, **10**, 1847.

108   W. A. Volkert and T. J. Hoffman, *Chem. Rev.*, 1999, **99**, 2269.

109   T. Sandmeyer, *Chem. Ber.*, 1884, **17**, 1633.

110   F. D. Bellamy and K. Ou, *Tetrahedron Lett.*, 1984, **25**, 839.

111   E. A. Krasnokutskaya, N. I. Semenischeva, V. D. Filimonov and P. Knochel, *Synthesis*, 2007, 81.

112   A. A. Cant, S. Champion, R. Bhalla, S. L. Pimlott and A. Sutherland, *Angew. Chem. Int. Ed.*, 2013, **52**, 7829.

113   J. E. Pickett, K. Nagakura, A. R. Pasternak, S. G. Grinnell, S. Majumdar, J. S. Lewis and G. W. Pasternak, *Bioorg. Med. Chem. Lett.*, 2013, **23**, 4347.

114   X. Li, Z. Mao, Y. Wang, W. Chen and X. Lin, *Tetrahedron*, 2011, **67**, 3858.

115   H. Huang, H. Jiang, K. Chen and H. Liu, *J. Org. Chem.*, 2009, **74**, 5476.

116   Z. Shao, J. Wang, K. Ding and A. S. C. Chan, *Adv. Synth. Catal.*, 2007, **349**, 2375.

117   A. M. Palmer, *Neurobiol. Dis.*, 2010, **37**, 3.

118   J. M. Scherrmann, *Vasc. Pharmacol.*, 2002, **38**, 349.

119   N. J. Abbott, A. A. K. Patabendige, D. E. M. Dolman, S. R. Yusof and D. J. Begley, *Neurobiol. Dis.*, 2010, **37**, 13.

120   N. J. Abbott, L. Ronnback and E. Hansson, *Nat. Rev. Neurosci.*, 2006, **7**, 41.

121   L. Di, H. Rong and B. Feng, *J. Med. Chem.*, 2012, **56**, 2.

122   R. Gabathuler, *Neurobiol. Dis.*, 2010, **37**, 48.

123   A. Leo, C. Hansch and D. Elkins, *Chem. Rev.*, 1971, **71**, 525.

124   C. Giaginis and A. Tsantili-Kakoulidou, *J. Pharm. Sci.*, 2008, **97**, 2984.

125   J. T. Goodwin and D. E. Clark, *J. Pharmacol. Exp. Ther.*, 2005, **315**, 477.

126   K. Valko, *LCGC North America*, 2007, **25**, 284.

127   S. Ong, H. Liu and C. Pidgeon, *J. Chromatogr. A*, 1996, **728**, 113.

128   C. Y. Yang, S. J. Cai, H. Liu and C. Pidgeon, *Adv. Drug Deliv. Rev.*, 1996, **23**, 229.

129   C. Pidgeon, S. Ong, H. Liu, X. Qiu, M. Pidgeon, A. H. Dantzig, J. Munroe, W. J. Hornback and J. S. Kasher, *J. Med. Chem.*, 1995, **38**, 590.

130   K. Valkó, *J. Chromatogr. A*, 2004, **1037**, 299.

131   K. Valko, S. Nunhuck, C. Bevan, M. H. Abraham and D. P. Reynolds, *J. Pharm. Sci.*, 2003, **92**, 2236.

132   R. N. Waterhouse, *Mol. Imaging Biol.*, 2003, **5**, 376.

133   A. A. S. Tavares, J. Lewsey, D. Dewar and S. L. Pimlott, *Nucl. Med. Biol.*, 2012, **39**, 127.

134   R. A. Frank, B. Långström, G. Antoni, M. C. Montalto, E. D. Agdeppa, M. Mendizabal, I. A. Wilson and J.-L. Vanderheyden, *J. Labelled Compd. Radiopharm.*, 2007, **50**, 746.

135   Tocris Bioscience, www.tocris.com/pharmacologicalGlossary.php, Accessed 4 August 2014.

136   C. Yung-Chi and W. H. Prusoff, *Biochem. Pharmacol.*, 1973, **22**, 3099.

137   A. Cappelli, M. Anzini, S. Vomero, P. G. De Benedetti, M. C. Menziani, G. Giorgi and C. Manzoni, *J. Med. Chem.*, 1997, **40**, 2910.

138   M. Anzini, A. Cappelli, S. Vomero, M. Seeber, M. C. Menziani, T. Langer, B. Hagen, C. Manzoni and J.-J. Bourguignon, *J. Med. Chem.*, 2001, **44**, 1134.

139   J. Marco-Contelles, E. Pérez-Mayoral, A. Samadi, M. d. C. Carreiras and E. Soriano, *Chem. Rev.*, 2009, **109**, 2652.

140   S. V. Ryabukhin, D. M. Volochnyuk, A. S. Plaskon, V. S. Naumchik and A. A. Tolmachev, *Synthesis*, 2007, 1214.

141   T. K. Hayes, R. Villani and S. M. Weinreb, *J. Am. Chem. Soc.*, 1988, **110**, 5533.

142   M. Mizuno, M. Yamashita, Y. Sawai, K. Nakamoto and M. Goto, *Tetrahedron*, 2006, **62**, 8707.

143   S. Asghari, M. Qandalee, Z. Naderi and Z. Sobhaninia, *Mol. Diversity*, 2010, **14**, 569.

144   T. Chanda, R. K. Verma and M. S. Singh, *Chem. Asian J.*, 2012, **7**, 778.

145   M. Anzini, A. Cappelli and S. Vomero, *Heterocycles*, 1994, **38**, 103.

146   R. Teodoro, R.-P. Moldovan, C. Lueg, R. Günther, C. Donat, F.-A. Ludwig, S. Fischer, W. Deuther-Conrad, B. Wünsch and P. Brust, *Org. Med. Chem. Lett.*, 2013, **3**, 1.

147   E. M. F. Billaud, L. Rbah-Vidal, A. Vidal, S. Besse, S. Tarrit, S. Askienazy, A. Maisonial, N. Moins, J.-C. Madelmont, E. Miot-Noirault, J.-M. Chezal and P. Auzeloux, *J. Med. Chem.*, 2013, **56**, 8455.

148   A. Cappelli, M. Matarrese, R. M. Moresco, S. Valenti, M. Anzini, S. Vomero, E. A. Turolla, S. Belloli, P. Simonelli, M. A. Filannino, M. Lecchi and F. Fazio, *Bioorg. Med. Chem.*, 2006, **14**, 4055.

149   S. J. Blanksby and G. B. Ellison, *Acc. Chem. Res.*, 2003, **36**, 255.

150   D. O'Hagan, *Chem. Soc. Rev.*, 2008, **37**, 308.

151   J. Sóvágó, D. S. Dupuis, B. Gulyás and H. Hall, *Brain Res. Rev.*, 2001, **38**, 149.

152   S. Kar and C. Hawkes, *Handbook of Neurochemistry and Molecular Neurobiology. Practical Neurochemistry Methods*, Springer, New York, 2007.

153   N. Vasdev, D. E. Green, D. C. Vines, K. McLarty, P. N. McCormick, M. D. Moran, S. Houle, A. A. Wilson and R. M. Reilly, *Cancer Biother. Radio.*, 2013, **28**, 254.

154   Y. Katz, A. Eitan, Z. Amiri and M. Gavish, *Eur. J. Pharmacol.*, 1988, **148**, 483.

155   A. Batarseh and V. Papadopoulos, *Mol. Cell. Endocrinol.*, 2010, **327**, 1.

156   M. Hardwick, D. Fertikh, M. Culty, H. Li, B. Vidic and V. Papadopoulos, *Cancer Res.*, 1999, **4**, 831.

157   S. K. Singh, C. Hawkins, I. D. Clarke, J. A. Squire, J. Bayani, T. Hide, R. M. Henkelman, M. D. Cusimano and P. B. Dirks, *Nature*, 2004, **432**, 396.

158   M. Koenig, J. B. Schofield, B. F. Warren and N. A. Shepherd, *Histopathology*, 2009, **55**, 214.

159   J. A. Brown and R. B. Marala, *J. Pharmacol. Toxicol.*, 2002, **47**, 137.

160   V. Cepeda, M. A. Fuertes, J. Castilla, C. Alonso, C. Quevedo, M. Soto and J. M. Pérez, *Recent Pat. Anti-Canc.*, 2006, **1**, 39.

161   J. H. J. Hoeijmakers, *New Engl. J. Med.*, 2009, **361**, 1475.

162   A. J. Chalmers, *Brit. Med. Bull.*, 2009, **89**, 23.

163 D. D'Amours, S. Desnoyers, I. D'Silva and G. G. Poirier, *Biochem. J.*, 1999, **342**, 249.

164 A. Bürke, *FEBS J.*, 2005, **272**, 4576.

165 J.-X. He, C.-H. Yang and Z.-H. Miao, *Acta Pharm. Sinic.*, 2010, **31**, 1172.

166 Z. Wang, F. WAng, T. Tang and C. Guo, *Front. Med.*, 2012, **6**, 156.

167 J. C. Ame, V. Rolli, V. Schreiber, C. Niedergang, F. Apiou, P. Decker, S. Muller, T. Höger, J. Ménissier de Murcia and G. de Murcia, *J. Biol. Chem.*, 1999, **274**, 17860.

168 M. Miwa and M. Masutani, *Caner Sci.*, 2007, **98**, 1528.

169 M. Rouleau, A. Patel, M. J. Hendzel, S. H. Kaufmann and G. G. Poirier, *Nat. Rev. Cancer*, 2010, **10**, 293.

170 M. F. Langelier, K. M. Servent, E. E. Rogers and J. M. Pascal, *J. Biol. Chem.*, 2008, **283**, 4105.

171 G. de Murcia and J. Ménissier de Murcia, *Trends Biochem. Sci*, 1994, **19**, 172.

172 Z. Tao, P. Gao and H. W. Liu, *J. Am. Chem. Soc.*, 2009, **131**, 14258.

173 D. V. Ferraris, *J. Med. Chem.*, 2010, **53**, 4561.

174 N. Ogata, K. Ueda, H. Kagamiyama and O. Hayaishi, *J. Biol. Chem.*, 1980, **255**, 7616.

175 M. Masson, C. Niedergang, V. Schreiber, S. Muller, J. M. de Murcia and G. de Murcia, *Mol. Cell Biol.*, 1998, **18**, 3563.

176 J. B. Clark, G. M. Ferris and S. Pinder, *Biochim. Biophys. Acta*, 1971, **238**, 82.

177 A. Ruf, J. Ménissier De Murcia, G. M. Ménissier De Murcia and G. E. Schulz, *Proc. Natl. Acad. Sci*, 1996, **93**, 7481.

178 A. Ruf, G. de Murcia and G. E. Schulz, *Biochemistry*, 1998, **37**, 3893.

179 P. Jones, *Nat. Biotechnol.*, 2012, **30**, 249.

180 C. M. Annunziata and J. O'Shaughnessy, *Clin. Cancer Res.*, 2010, **16**, 4517.

181 M. Ljungman, *Chem. Rev.*, 2009, **109**, 2929.

182 N. J. Curtin, *Expert Rev. Mol. Med.*, 2005, **7**, 1.

183 H. E. Bryant, N. Schultz, H. D. Thomas, K. M. Parker, D. Flower, E. Lopez, S. Kyle, M. Meuth, N. J. Curtin and T. Helleday, *Nature*, 2005, **434**, 913.

184 H. Farmer, N. McCabe, C. J. Lord, A. N. J. Tutt, D. A. Johnson, T. B. Richardson, M. Santarosa, K. J. Dillon, I. Hickson, C. Knights, N. M. B. Martin, S. P. Jackson, G. C. M. Smith and A. Ashworth, *Nature*, 2005, **434**, 917.

185 N. J. Curtin, *Drug Discov. Today*, 2012, **9**, e51.

186   K. A. Gelmon, M. Tischkowitz, H. Mackay, K. Swenerton, A. Robidoux, K. Tonkin, H. Hirte, D. Huntsman, M. Clemons, B. Gilks, R. Yerushalmi, E. Macpherson, J. Carmichael and A. Oza, *Lancet Oncol.*, 2011, **12**, 852.

187   R. Plummer, P. Lorigan, N. Steven, L. Scott, M. Middleton, R. Wilson, E. Mulligan, N. Curtin, D. Wang, R. Dewji, A. Abbattista, J. Gallo and H. Calvert, *Cancer Chemoth. Pharm.*, 2013, **71**, 1191.

188   S. Kummar, A. Chen, J. Ji, Y. Zhang, J. M. Reid, M. Ames, L. Jia, M. Weil, G. Speranza, A. J. Murgo, R. Kinders, L. Wang, R. E. Parchment, J. Carter, H. Stotler, L. Rubinstein, M. Hollingshead, G. Melillo, Y. Pommier, W. Bonner, J. E. Tomaszewski and J. H. Doroshow, *Cancer Res.*, 2011, **71**, 5626.

189   T. A. Yap, S. K. Sandhu, C. P. Carden and J. S. de Bono, *CA-Cancer J. Clin.*, 2011, **61**, 31.

190   Z. Tu, W. Chu, J. Zhang, C. S. Dence, M. J. Welch and R. H. Mach, *Nucl. Med. Biol.*, 2005, **32**, 437.

191   D. Zhou, W. Chu, J. Xu, L. A. Jones, X. Peng, S. Li, D. L. Chen and R. H. Mach, *Bioorg. Med. Chem.*, 2014, **22**, 1700.

192   T. Reiner, E. J. Keliher, S. Earley, B. Marinelli and R. Weissleder, *Angew. Chem. Int. Ed.*, 2011, **50**, 1922.

193   T. Reiner, S. Earley, A. Turetsky and R. Weissleder, *Chem. Bio. Chem*, 2010, **11**, 2374.

194   G. M. Thurber, K. S. Yang, T. Reiner, R. H. Kohler, P. Sorger, T. Mitchison and R. Weissleder, *Nat. Commun.*, 2013, **4**, 1504.

195   E. J. Keliher, T. Reiner, A. Turetsky, S. A. Hilderbrand and R. Weissleder, *Chem. Med. Chem.*, 2011, **6**, 424.

196   X.-L. Cockcroft, K. J. Dillon, L. Dixon, J. Drzewiecki, F. Kerrigan, V. M. Loh Jr, N. M. B. Martin, K. A. Menear and G. C. M. Smith, *Bioorg. Med. Chem. Lett.*, 2006, **16**, 1040.

197   V. M. Loh Jr, X.-L. Cockcroft, K. J. Dillon, L. Dixon, J. Drzewiecki, P. J. Eversley, S. Gomez, J. Hoare, F. Kerrigan, I. T. W. Matthews, K. A. Menear, N. M. B. Martin, R. F. Newton, J. Paul, G. C. M. Smith, J. Vile and A. J. Whittle, *Bioorg. Med. Chem. Lett.*, 2005, **15**, 2235.

198   K. J. Dillon, G. C. M. Smith and N. M. B. Martin, *J. Biomol. Screen.*, 2003, **8**, 347.

199   T. Kinoshita, I. Nakanishi, M. Warizaya, A. Iwashita, Y. Kido, K. Hattori and T. Fujji, *FEBS Lett.*, 2004, **556**, 43.

200   K. A. Menear, C. Adcock, R. Boulter, X.-l. Cockcroft, L. Copsey, A. Cranston, K. J. Dillon, J. Drzewiecki, S. Garman, S. Gomez, H. Javaid, F. Kerrigan, C. Knights,

A. Lau, V. M. Loh, I. T. W. Matthews, S. Moore, M. J. O'Connor, G. C. M. Smith and N. M. B. Martin, *J. Med. Chem.*, 2008, **51**, 6581.

201   K. A. Menear, A. P. Ottridge, D. J. Londesbrough, M. R. Hallett, K. R. Mullholland, J. D. Pittam, D. D. P. Laffan, I. W. Ashworth, M. F. Jones and J. H. Cherryman, in *WO 2008/047082 (A2)*, 2008.

202   L. Horner, H. Hoffmann and H. G. Wippel, *Chem. Ber.*, 1958, **91**, 61.

203   W. S. Wadsworth and W. D. Emmons, *J. Am. Chem. Soc.*, 1961, **83**, 1733.

204   B. E. Maryanoff and A. B. Reitz, *Chem. Rev.*, 1989, **89**, 863.

205   W. C. Still and C. Gennari, *Tetrahedron Lett.*, 1983, **24**, 4405.

206   Y. Schmidt and B. Breit, *Chem. Eur. J.*, 2011, **17**, 11780.

207   S. E. Denmark and J. Amburgey, *J. Am. Chem. Soc.*, 1993, **115**, 10386.

208   S. Sengmany, E. Le Gall, C. Le Jean, M. Troupel and J.-Y. Nédélec, *Tetrahedron*, 2007, **63**, 3672.

209   E. Valeur and M. Bradley, *Chem. Soc. Rev.*, 2009, **38**, 606.

210   M. Drąg, J. Grembecka, M. Pawełczak and P. Kafarski, *Eur. J. Med. Chem.*, 2005, **40**, 764.

211   M. Fujinaga, T. Yamasaki, J. Yui, A. Hatori, L. Xie, K. Kawamura, C. Asagawa, K. Kumata, Y. Yoshida, M. Ogawa, N. Nengaki, T. Fukumura and M.-R. Zhang, *J. Med. Chem.*, 2012, **55**, 2342.

212   United States Department of Agriculture, http://www.ars-grin.gov/cgi-bin/npgs/html/taxon.pl?316602, Accessed 25 March 2014.

213   Suffolk Wildlife Trust, www.suffolkwildlifetrust.org/node/12618, Accessed 27 March 2014.

214   Q. Zhang, G. Tu, Y. Zhao and T. Cheng, *Tetrahedron*, 2002, **58**, 6795.

215   Plants for a Future, www.pfaf.org/user/Plant.aspx?LatinName=carduus+crispus, Accessed 27 March 2014.

216   Seasonal Wild Flowers, www.seasonalwildflowers.com/june/welted-thistle.html, Accessed 26 March 2014.

217   H.-J. Knölker and S. Agarwal, *Tetrahedron Lett.*, 2005, **46**, 1173.

218   F. D. King, *Tetrahedron*, 2007, **63**, 2053.

219   S. C. K. Rotte, A. G. Chittiboyina and I. A. Khan, *Eur. J. Org. Chem.*, 2013, 6355.

220   S. Saha, C. Venkata Ramana Reddy and B. Patro, *Tetrahedron Lett.*, 2011, **52**, 4014.

221   S. M. Allin, S. N. Gaskell, J. M. R. Towler, P. C. B. Page, B. Saha, M. J. McKenzie and W. P. Martin, *J. Org. Chem.*, 2007, **72**, 8972.

222   R. Sánchez-Obregón, B. Ortiz, V. M. Mastranzo, F. Yuste and J. L. G. Ruano, *Tetrahedron Lett.*, 2013, **54**, 1893.

223   S. J. Czarnocki, K. Wojtasiewicz, A. P. Jóźwiak, J. K. Maurin, Z. Czarnocki and J. Drabowicz, *Tetrahedron*, 2008, **64**, 3176.

224   K. A. Walker, M. R. Boots, J. F. Stubbins, M. E. Rogers and C. W. Davis, *J. Med. Chem.*, 1983, **26**, 174.

225   A. T. Nielsen, *J. Org. Chem.*, 1962, **27**, 1998.

226   H. H. Wasserman, M. J. Hearn, B. Haveaux and M. Thyes, *J. Org. Chem.*, 1976, **41**, 153.

227   J. O. Osby and B. Ganem, *Tetrahedron Lett.*, 1985, **26**, 6413.

228   S. Ram and R. E. Ehrenkaufer, *Tetrahedron Lett.*, 1984, **25**, 3415.

229   R. L. Blankespoor, A. N. K. Lau and L. L. Miller, *J. Org. Chem.*, 1984, **49**, 4441.

230   J. A. Joule and K. Mills, *Heterocyclic Chemistry*, Blackwell Science Ltd, Oxford, 2000.

231   X. Zhao and X. Wan, *Org. Prep. Proced. Int.*, 1995, **27**, 513.

232   F. A. Carey and R. J. Sundberg, *Advanced Organic Chemistry. Part A: Structure and Mechanisms*, Springer, New York, 2000.

233   Y. Mi and E. J. Corey, *Tetrahedron Lett.*, 2006, **47**, 2515.

234   J. S. Yadav, B. V. S. Reddy, P. Vishnumurthy and C. J. Chary, *Tetrahedron Lett.*, 2007, **48**, 5915.

235   Y. Zhou, J. Dong, F. Zhang and Y. Gong, *J. Org. Chem.*, 2010, **76**, 588.

236   T. Yasuhara, N. Zaima, S. Hashimoto, M. Yamazaki and O. Muraoka, *Heterocycles*, 2009, **77**, 1397.

237   E. Guénin, M. Monteil, N. Bouchemal, T. Prangé and M. Lecouvey, *Eur. J. Org. Chem.*, 2007, 3380.

238   M. S. Bernatowicz, Y. Wu and G. R. Matsueda, *J. Org. Chem.*, 1992, **57**, 2497.

239   M. S. Bernatowicz, Y. Wu and G. R. Matsueda, *Tetrahedron Lett.*, 1993, **34**, 3389.

240   B. Riegel, C. J. Albisetti Jr., G. R. Lappin and R. H. Baker, *J. Am. Chem. Soc.*, 1946, **68**, 2685.

241   C. E. Kaslow and M. M. Marsh, *J. Org. Chem.*, 1947, **12**, 456.

242   Y. Itzhak, L. Baker and M. D. Norenberg, *Glia*, 1993, **9**, 211.

243   D. R. Gehlert, D. T. Stephenson, D. A. Schober, K. Rash and J. A. Clemens, *Neurochem.*, 1997, **31**, 705.